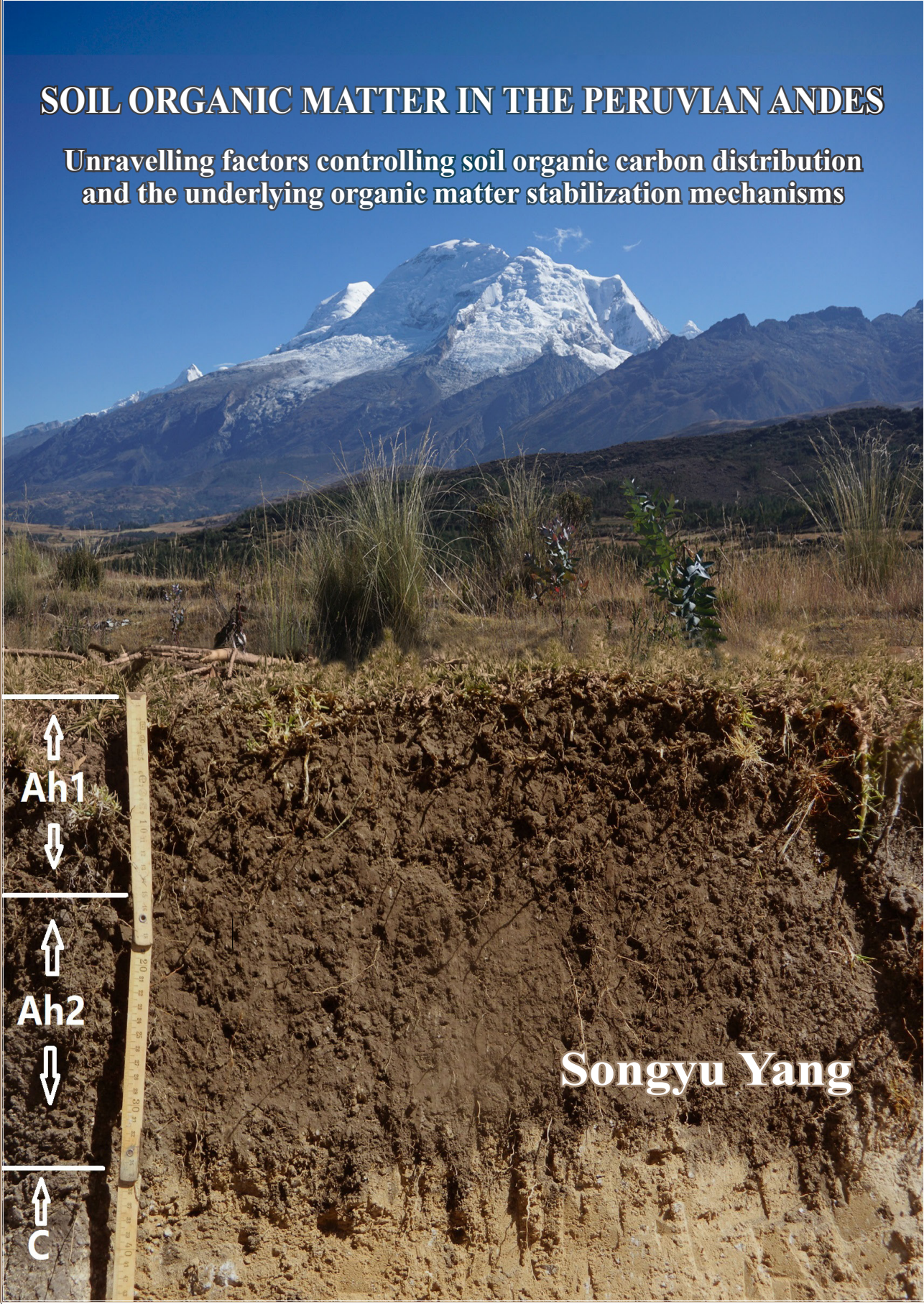
SOIL ORGANIC MATTER IN THE PERUVIAN ANDES

Unravelling factors controlling soil organic carbon distribution and the underlying organic matter stabilization mechanisms



Songyu Yang

SOIL ORGANIC MATTER IN THE PERUVIAN ANDES

Unravelling factors controlling soil organic carbon distribution and the underlying organic matter stabilization mechanisms

Songyu Yang

ISBN: 978-94-91407-83-3

Printed by: ProefschriftMaken

Cover design: Jiajia Gao & Songyu Yang

Copyright © Songyu Yang 2020

All rights reserved.

SOIL ORGANIC MATTER IN THE PERUVIAN ANDES

Unravelling factors controlling soil organic carbon distribution and the underlying organic matter stabilization mechanisms

ACADEMISCH PROEFSCHRIFT

ter verkrijging van de graad van doctor

aan de Universiteit van Amsterdam

op gezag van de Rector Magnificus

prof. dr. ir. K.I.J. Maex

ten overstaan van een door het College voor Promoties ingestelde commissie,

in het openbaar te verdedigen in de Agnietenkapel

op woensdag 1 april 2020, te 10.00 uur

door

Songyu Yang

geboren te Guizhou

Promotiecommissie:

Promotores:	Dr. E. L. H. Cammeraat	Universiteit van Amsterdam
	Dr. B. Jansen	Universiteit van Amsterdam
Copromotores:	Prof. dr. K. Kalbitz	Universiteit van Amsterdam
	Prof. dr. F. T. de Vries	Universiteit van Amsterdam
Overige leden:	Prof. dr. I. Kögel-Knabner	Technische Universität München
	Prof. dr. B. van Wesemael	Université Catholique de Louvain
	Prof. dr. ir. W. Bouten	Universiteit van Amsterdam
	Dr. A. Tietema	Universiteit van Amsterdam
	Dr. W. D. Gosling	Universiteit van Amsterdam

Faculteit der Natuurwetenschappen, Wiskunde en Informatica

This research was carried out at the Institute for Biodiversity and Ecosystem Dynamics (IBED), Faculty of Science, University of Amsterdam (Amsterdam, The Netherlands). This research was financially supported by China Scholarship Council (CSC) and by IBED, University of Amsterdam.

Table of Contents

Summary 7

Samenvatting 11

摘要 17

Chapter 1

General Introduction 21

Chapter 2

Soil organic carbon stocks controlled by lithology and soil depth in a Peruvian alpine grassland of the Andes 35

Chapter 3

Lithology controlled soil organic carbon stabilization in an alpine grassland of the Peruvian Andes 59

Chapter 4

Lithology and climate controlled soil aggregate size distribution and organic carbon stability in the Peruvian Andes 83

Chapter 5

Selective stabilization of soil fatty acids related to their carbon chain length and presence of double bonds in the Peruvian Andes 107

Chapter 6

Synthesis 129

Appendices 139

References 155

List of Abbreviations 170

Publications and Author Contributions 171

Acknowledgements 172



Summary

Soil contains the largest terrestrial carbon (C) pool and plays an important role in global C dynamics. Alpine grasslands of the Neotropical Peruvian Andes have large soil organic carbon (SOC) stocks, which are crucial to food production and water provision for the surrounding areas. With regard to the high vulnerability of the grasslands under climate change, it is important to have insight into the persistence and vulnerability of the SOC stocks and the underlying stabilization mechanisms. However, alpine grassland soils in the Peruvian Andes are less-studied with regard to SOC stocks, and especially with regard to the mechanisms controlling SOC storage and Soil Organic Matter (SOM) composition at the molecular level. The objectives of this thesis were: (1) to quantify the SOC stocks and to find key factors controlling the SOC spatial patterns, (2) to have insights into the underlying mechanisms of soil organic matter stabilization, (3) to investigate SOM stabilization controlled by soil aggregation as affected by lithology and precipitation, and (4) to investigate potential relationships between SOM molecular composition and SOM stabilization in the studied alpine grasslands of the Peruvian Andes.

Chapter 1 provides the background of the research topic and general information of the sampling sites in the alpine grasslands of the Peruvian Andes. Briefly, in this chapter we summarized recent research progress in SOM stabilization mechanisms and proposed how to apply the knowledge of SOM stabilization for the soils of the Peruvian Andes under the background of global change.

In Chapter 2 the spatial distribution of SOC stocks was investigated over a variety of different bedrocks, land use types, grazing intensities and topographical positions. Soil samples were collected from 69 plots to estimate the SOC stocks of the entire soil profiles for the study area near Cajamarca (the wet site). In addition, multiple linear models were applied to identify significant soil formation and environmental factors controlling the distribution of SOC. The SOC stocks of the studied area were 215±21 Mg ha^{-1}, which is higher compared to the global average level but lower compared to comparable ecosystems in the Ecuadorian Andes. The spatial variation of the total SOC stocks was predicted by soil depth and soil moisture. When soil depth and soil moisture were controlled as conditional variables, lithology was the key factor controlling the distribution of

SOC stocks. Different from the total SOC stocks, SOC stocks of the upper 10 cm were predicted by soil moisture, lithology, grazing intensity and altitude. Most studies estimate SOC stocks by sampling to a limited constant depth. However, our results suggest that SOC stocks should be estimated using the entire soil profiles, because sampling to a limited constant depth results in underestimations of SOC stocks and overestimations of the effects of soil formation and environmental factors on the SOC stock distribution.

In Chapter 3 the effects of lithology on SOC stocks and SOM stabilization were investigated. Samples were collected from limestone soils (LSs) and acid igneous rock soils (ASs) in the wet site. SOM stabilization mechanisms were investigated using a selective extraction method to isolate active Fe, Al and Ca fractions. The results showed that the LSs had significantly higher SOC stocks than the ASs. In both LSs and ASs, SOM was stabilized by complexation with and/or adsorption on Fe- and Al-oxides. Exclusively in the LSs, the formation of Ca^{2+} bridges between OM and mineral surfaces also contributed to SOM stabilization. The Ca-induced SOM stabilization gives a potential explanation for the higher SOC stocks in the LSs. In contrast, no evidence was found that OM stabilization was controlled by crystalline Fe oxides, clay contents, allophones, Al toxicity or aggregate stability. The results suggest a shift in SOM stabilization dominated by Fe- and Al- oxides to that with the presence of Ca^{2+} bridges with increasing pH values driven by lithology.

In Chapter 4 the effects of precipitation and lithology on soil aggregate-size distribution and SOC stability were investigated. A wet-sieving method was applied to determine aggregate-size distribution, whereas a 76-day incubation of intact and crushed soil aggregates was applied to estimate SOC stability and aggregate-controlled SOM stabilization. Aggregate-size distribution was mainly controlled by lithology rather than precipitation, as indicated by larger aggregates for the LSs compared to the ASs. SOC stability declined with precipitation in the LSs, but had no significant change in the ASs. SOM occluded in aggregates played a limited role in SOM stabilization, as indicated by: (1) limited changes in SOC mineralization rates between intact and crushed aggregates, and (2) inconsistent patterns of aggregate-size distribution and patterns of SOC mineralization. Thus, SOM adsorption on mineral surfaces was the major stabilization mechanism. The results suggest that SOC stability was controlled by the interaction between lithology and precipitation, which is further controlled by

soil mineralogy in relation to SOM input.

In Chapter 5 the molecular composition of SOM in relation to its stability against decomposition was investigated. For this, pyrolysis-gas chromatography/mass spectrometry (GC/MS) analyses assisted by tetramethylammonium hydroxide (TMAH) were applied using samples from the 76-day soil incubation with aggregates intact and crushed as described in Chapter 4. Potential changes in SOM molecular composition before and after incubation were used to estimate SOM stability and the microbial transformation of SOM molecules. Differences in SOM molecular composition after the incubation between intact and crushed aggregates were used to estimate the SOM protected by occlusion in aggregates. The results showed large relative abundances of compounds derived from fatty acids (FAs), with a major contribution of free FAs. The presence of double bonds (unsaturated vs. saturated FAs) and carbon chain length were key factors controlling the FA stability. Unsaturated FAs were more depleted after the incubation compared to saturated FAs and positively associated with soil organic carbon mineralization rates. The depletion of unsaturated FAs is likely to be explained by their easier degradation compared to saturated FAs and further attributed to their less stabilization controlled by association with mineral surfaces and/or chemical properties. Instead, it is unlikely explained by the stabilization controlled by occlusion in aggregates. Long-chain FAs were more depleted than short-chain FAs after the incubation and a possible explanation for this is that short-chain FAs received more protection by occluded in aggregate. Although we observed the microbial transformation of FAs during the incubation, it had limited effects on the prediction of FA stability using double bonds and carbon chain length. Finally, soil types and horizons also influenced the effects of double bonds and carbon chain length on FA stability. This suggests that more studies are required before generalizing our findings to other soils. The results give the evidence to show that the inherent properties of soil FAs control their interactions with the soil matrix and indirectly govern their stabilization and persistence in the Peruvian Andean soils under study.

Chapter 6 gives a synthesis of the major findings in this Thesis. The major findings were that: (1) Lithology is the key factor controlling SOC stocks and stability; (2) SOM stabilization is controlled by Fe- and Al-oxides in the wet-ASs, and is promoted by Ca^{2+} bridges in addition to the Fe- and Al-oxides in the wet-LSs; (3) SOC stability decreases with precipitation in the LSs but has limited

differences in the ASs, which can be explained by soil mineralogy in relation to SOM input; and (4) the presence of double bonds and carbon chain length control the stability of fatty acids through the interactions with the soil matrix.

Implications of the findings were also discussed in Chapter 6. With regard to the SOM molecular composition, the results agree with the studies that found lipid-rich and lignin-depleted soils in the Andean grasslands of Ecuador. However, this is not common in soils from other areas. Further studies can focus on the underlying mechanisms of the large lipid fraction. With regard to SOM stabilization in general, the results gave evidence that SOM chemical composition affects SOM stability and their interactions with the soil matrix. Since the results are insufficient to explain whether the differences in stability between unsaturated and saturated FAs are attributed to chemical recalcitrance or interactions with mineral surfaces, more studies are required to investigate the affinity of unsaturated and saturated fatty acids to absorbed on mineral surfaces against microbial decomposition. With regard to the implications for ecosystem management, the results indicated the importance of the interaction between lithology and precipitation in relation to the OM input. Future research could focus on potential applications of the knowledge highlighted in this thesis to improve soil quality and to sustain ecosystem services of the Andean grasslands.

Samenvatting

De bodem bevat de grootste terrestrische koolstof (C) voorraad en speelt een belangrijke rol in de wereldwijde C-dynamiek. Alpiene graslanden van de Neotropische Peruviaanse Andes hebben grote voorraden bodem organische koolstof in de bodem (SOC), die cruciaal zijn voor voedselproductie en watervoorziening van omliggende gebieden. Aangezien deze graslanden zeer gevoelig zijn voor klimaatverandering is het essentieel om inzicht te krijgen in de persistentie en kwetsbaarheid van de SOC-voorraden en de onderliggende stabilisatiemechanismen van SOC. Alpiene graslandgronden in de Peruaanse Andes zijn maar in zeer beperkte mate bestudeerd met betrekking tot hun SOC voorraad, vooral voor wat betreft de controlemechanismen die de SOC voorraad bepalen en daarnaast ook de samenstelling van bodem organische stof (SOM) op moleculair niveau. De doelstellingen van dit proefschrift zijn: (1) om de SOC voorraad te kwantificeren en om sleutelfactoren te vinden die de ruimtelijke SOC patronen bepalen, (2) om inzicht te verkrijgen in de onderliggende mechanismen van bodem organische stof stabilisatie, (3) om de stabilisatie van bodem organische stof door bodemaggregaatvorming onder gecontroleerde omstandigheden te onderzoeken in relatie tot lithologie en neerslag, en (4) om mogelijke relaties tussen de moleculaire samenstelling en de stabilisatie van bodem organische stof in de bestudeerde alpiene graslanden van de Peruaanse Andes nader te onderzoeken.

Hoofdstuk 1 presenteert de achtergrond van het onderzoek en daarnaast ook algemene informatie over de bemonsteringslocaties in de alpiene graslanden van de Peruaanse Andes. Kort samengevat hebben we in dit hoofdstuk de recente wetenschappelijk stand van zaken ten aanzien van SOM samengevat en geven we aan hoe de kennis van SOM-stabilisatie kan worden toegepast voor de bodem van de Peruaanse Andes tegen de achtergrond van ‘global change’.

In hoofdstuk 2 wordt de ruimtelijke verdeling van SOC-voorraden onderzocht in relatie tot gesteente soort, landgebruikstype, begrazingsintensiteit en topografische positie. Bodemmonsters werden verzameld van 69 locaties om de SOC-voorraden, gebaseerd op het complete bodemprofiel, te bepalen voor het studiegebied bij Cajamarca (het “natte” studiegebied). Bovendien werden

meerdere lineaire modellen toegepast om bodemvormings- en omgevingsfactoren te identificeren die de ruimtelijke verdeling van SOC bepalen. De SOC-voorraad van het bestudeerde gebied was 215 ± 21 Mg ha^{-1}, wat hoger is dan het wereldwijde gemiddelde niveau, maar lager dan in vergelijkbare ecosystemen in de Ecuadoriaanse Andes. De ruimtelijke variatie van de totale SOC-voorraad kon worden voorspeld door bodemdiepte en bodemvocht. Met bodemdiepte en bodemvocht als voorwaardelijke variabelen, wordt lithologie de sleutelfactor die de ruimtelijke verdeling van SOC-voorraad bepaalt. In tegenstelling tot de totale SOC-voorraad, wordt de SOC-voorraad van de bovenste 10 cm voorspeld door bodemvocht, lithologie, begrazingsintensiteit en hoogte. De meeste onderzoeken naar SOC schatten de SOC-voorraad door bemonstering tot een constante, maar beperkte diepte. Onze resultaten laten echter zien dat de SOC-voorraad moet worden bepaald aan de volledige bodemprofielen, omdat bemonstering tot een beperkte constante diepte resulteert in een onderschatting van de SOC-voorraad en een overschatting van de effecten van bodemvorming en omgevingsfactoren op de verdeling van de SOC-voorraad.

In hoofdstuk 3 worden de effecten van de lithologie op SOC-voorraden en SOM-stabilisatie onderzocht. Monsters werden verzameld van bodems op kalksteen (LS's) en bodems op zure stollingsgesteente (AS's) afkomstig van de natte onderzoekslocatie. SOM-stabilisatiemechanismen werden onderzocht met behulp van een selectieve extractiemethode om actieve Fe-, Al- en Ca-fracties te isoleren. De resultaten toonden aan dat de LS's aanzienlijk hogere SOC-voorraden hadden dan de AS's. In zowel LS's als AS's werd SOM gestabiliseerd door complexering met en / of adsorptie aan Fe- en Al-oxiden. Alleen in de LS droeg de vorming van Ca^{2+} -bruggen tussen OM en mineraaloppervlakken ook bij aan SOM-stabilisatie. De Ca-gerelateerde SOM-stabilisatie geeft een mogelijke verklaring voor de hogere SOC-voorraden in de LS. Daarentegen werd geen bewijs gevonden dat de OM-stabilisatie werd geregeld door kristallijne Fe-oxiden, klei-gehalte, allofanen, Al-toxiciteit of aggregaatstabiliteit. De resultaten suggereren een verschuiving van SOM-stabilisatie gedomineerd door Fe- en Al-oxiden naar die met de aanwezigheid van Ca^{2+} -bruggen met toenemende pH-waarden, en is lithologie bepaald.

In hoofdstuk 4 werden de effecten van neerslag en lithologie op de verdeling van de bodemaggregaatgrootte en SOC-stabiliteit onderzocht. De natte zeefmethode werd toegepast om de aggregaatgrootteverdeling te bepalen, terwijl een 76-daagse incubatie van intacte en gemalen bodemaggregaten werd toegepast om de SOC-stabiliteit en aggregaat-gecontroleerde SOM-stabilisatie te bepalen. De aggregaatgrootteverdeling werd hoofdzakelijk bepaald door de lithologie in plaats van door neerslag, wat te zien is aan grotere aggregaten voor de LS's in vergelijking tot die van de AS's. De SOC-stabiliteit nam af met neerslag in de LS's, maar had geen significante verandering in de AS's. In aggregaten ingesloten SOM speelt een beperkte rol in SOM-stabilisatie, wat zich uit in: (1) beperkte veranderingen in SOC-mineralisatiesnelheden tussen intacte en gemalen aggregaten, en (2) inconsistente patronen van de aggregaat grootteverdeling, en in de patronen van SOC-mineralisatie. SOM-adsorptie op mineraaloppervlakken was dus het belangrijkste gevonden stabilisatiemechanisme. De resultaten suggereren dat SOC-stabiliteit word gecontroleerd door de interactie tussen lithologie en neerslag, die verder wordt geregeld door bodemmineralogie in relatie tot de input van SOM.

In hoofdstuk 5 werd de moleculaire samenstelling van SOM onderzocht in relatie tot zijn stabiliteit ten aanzien van decompositie. Hiervoor werden pyrolyse-gaschromatografie / massaspectrometrie (GC / MS) -analyses met behulp van tetramethylammoniumhydroxide (TMAH) uitgevoerd aan monsters van de 76-daagse bodemincubatie met intacte en vermalen aggregaten zoals beschreven in hoofdstuk 4. Mogelijke veranderingen in moleculaire samenstelling van SOM voor en na incubatie werden gebruikt om de stabiliteit van SOM en de microbiële transformatie van SOM-moleculen te bepalen. Verschillen in moleculaire samenstelling van SOM, na incubatie tussen intacte en gemalen aggregaten werden gebruikt om de door occlusie beschermde SOM in aggregaten te bepalen. De resultaten toonden grote relatieve hoeveelheden verbindingen die afgeleid zijn van vetzuren (FA's), waaronder een belangrijke bijdrage van vrije FA's. De aanwezigheid van dubbele bindingen (onverzadigde versus verzadigde FA's) en koolstofketenlengte waren sleutelfactoren die de FA-stabiliteit bepaalden. Onverzadigde FA's waren na de incubatie minder aanwezig in vergelijking tot verzadigde FA's, en ze waren positief geassocieerd met de mineralisatiegraad van de SOC in de bodem. De verminderde aanwezigheid van onverzadigde FA's

wordt zeer waarschijnlijk verklaard door hun gemakkelijkere afbraak in vergelijking tot verzadigde FA's, en wordt verder toegeschreven aan een verminderde stabilisatie, die wordt bepaald door associatie met mineraal oppervlakken en / of chemische eigenschappen. Het is daarnaast onwaarschijnlijk dat dit verklaard kan worden door occlusie van organische stof in aggregaten. De aanwezigheid van lange-keten FA's was na incubatie sterker verminderd dan die voor korte-keten FA's, en een mogelijke verklaring hiervoor is dat korte-keten FA's beter beschermd waren doordat ze totaal werden afgesloten binnen de aggregaten. Alhoewel we microbiële transformatie van FA's tijdens de incubatie hebben waargenomen, had het een beperkte effect op de voorspelling van de stabiliteit van FA's voor wat betreft dubbele bindingen en koolstofketenlengte. Tenslotte beïnvloedden de bodemsoort en de horizonten ook de effecten van dubbele bindingen en koolstofketenlengte op de stabiliteit van FA's. Dit suggereert dat meer studie nodig is voordat onze bevindingen naar andere bodems kunnen worden gegeneraliseerd. De resultaten tonen aan dat de inherente eigenschappen van FA's in de bodem de interacties met de bodemmatrix beheersen en indirect hun stabilisatie en persistentie regelen in de onderzochte bodems van de Peruaanse Andes.

Hoofdstuk 6 geeft een synthese van de belangrijkste bevindingen in dit proefschrift. De belangrijkste bevindingen waren dat: (1) Lithologie de sleutelfactor is voor het beheersen van de SOC-voorraad en -stabiliteit; (2) Stabilisatie van SOM wordt bepaald door Fe- en Al-oxiden in AS bodems in de natte onderzoekslocatie, en daar in de LS bodems ook wordt bevorderd door Ca^{2+} -bruggen naast de Fe- en Al-oxiden; (3) Stabiliteit van SOC neemt af met neerslag in de LS's maar heeft beperkte invloed in de AS's, wat kan worden verklaard door de bodemmineralogie en de input van SOM; en (4) de aanwezigheid van dubbele bindingen en koolstofketenlengte regelen de stabiliteit van vetzuren door de interacties met de bodemmatrix. De implicaties van de bevindingen worden ook besproken in hoofdstuk 6. Met betrekking tot de moleculaire samenstelling van SOM komen de resultaten overeen met studies aan lipide-rijke en lignine-arme bodems in de Andes-graslanden van Ecuador. Dit is echter niet een algemeen voorkomend patroon in bodems uit andere gebieden. Vervolgstudies zouden zich kunnen richten op de onderliggende mechanismen van de stabilisatie van de grote lipidenfractie. Wat betreft de stabilisatie van SOM in het algemeen, gaven de resultaten aan dat de chemische samenstelling van SOM, de stabiliteit van de SOM en de interactie met de bodemmatrix beïnvloedt. Omdat de resultaten niet

kunnen verklaren of de verschillen in stabiliteit tussen onverzadigde en verzadigde FA's kunnen worden toegeschreven aan chemische recalcitrantie of interacties met mineraaloppervlakken, zijn er meer studies nodig naar de voorkeur van onverzadigde en verzadigde vetzuren voor absorptie aan mineraaloppervlakken, en de bescherming tegen microbiële decompositie. De bevindingen van deze studie voor ecosysteembeheer, wijzen op het belang van de interactie tussen lithologie en neerslag in relatie tot OM-input. Toekomstig onderzoek zou zich kunnen richten op mogelijke toepassingen van de kennis die in dit proefschrift wordt benadrukt om de bodemkwaliteit te verbeteren en de ecosysteemdiensten van de Andes-graslanden in stand te houden.

摘要

土壤作为最大的陆地碳库在全球碳循环中扮演重要角色。位于新热带的秘鲁安第斯高山草原拥有丰富的土壤碳库，并在为周边地区供水及食物生产上起到重要作用。鉴于安第斯高山草原在全球变化背景下的脆弱性，深入研究其土壤有机碳库的稳定性和脆弱性及其相关机制显得尤为重要。目前关于秘鲁安第斯高山草原土壤有机碳储量的研究相对较少，特别是涉及控制有机碳稳定性的机制和在分子水平上分析有机质组成的研究更为缺乏。因此本文研究目标主要涵盖：(1) 测定与计算秘鲁安第斯高山草原土壤有机碳储量并寻找控制土壤有机碳空间格局的关键因素；(2) 深入研究控制土壤有机质稳定性的机制；(3) 研究降水和成土母质对土壤团聚体控制下有机质稳定性机制的作用；(4)探究有机质分子结构与其稳定性间的潜在联系。

第一章介绍了研究背景以及研究涉及的秘鲁安第斯高山草原概况。具体而言，本章总结了近来关于土壤有机质稳定性机制的研究进展，特别是在全球变化的背景下，如何利用土壤有机质稳定机制开展针对秘鲁安第斯高山土壤的研究。

第二章研究了在不同成土母质、土地利用类型、放牧强度及地形因子的条件下，土壤有机碳储量的空间分布格局。土样采自卡哈马卡市附近（湿润样地）的 69 个样点，并用来计算整个土壤剖面的有机碳储量。研究利用多元线性模型来确定对土壤有机碳空间分布格局有显著影响的环境及成土因子。结果显示研究区域的土壤有机碳总储量为 215±21 Mg ha^{-1}，明显高于全球平均水平但低于厄瓜多尔的类似生态系统。土壤深度和含水率是控制有机碳总储量空间格局的关键因素。当土壤深度和含水率作为协变量被控制时，成土母质成为影响有机碳总储量空间分布的关键因素。与有机碳总储量不同，表层有机碳储量（10cm）的控制因素有土壤含水率，成土母质，放牧强度和海拔。目前多数研究仅利用有限的固定深度来估算土壤有机碳储量，本研究表明这样的估算方法会造成对有机碳储量的低估以及环境及对成土因子对土壤有机碳储量作用程度的高估。因此，研究结果揭示了利用完整土壤剖面估算土壤有机碳储量空间分布的重要性。

第三章进一步研究了成土母质对土壤有机碳储量及有机质稳定机制的作用。土样采自湿润样地中发育自石灰岩和酸性火成岩的土壤。研究采用选

择性提取法分离铁、铝和钙组分以研究土壤有机质稳定机制。结果显示石灰岩土有机碳储量显著高于酸性火成岩土。在两种土壤中，有机质与铁铝螯合或吸附于铁铝氧化物表面提高了有机质的稳定性。在石灰岩土中，钙阳离子桥促进了有机质与矿物表面的吸附并提高有机质的稳定性。此外，与钙阳离子桥相关的稳定机制解释了石灰岩土较高的有机碳储量。研究并未发现关于结晶态铁氧化物、粘土、水铝英石、铝毒性及团聚体稳定性促进土壤有机质稳定的证据。最后，研究结果显示了土壤有机质稳定机制随 pH 值升高而从铁铝（氧化物）控制到钙阳离子桥控制的变化趋势。

第四章研究了降水和成土母质对土壤团聚体粒径分布和土壤有机碳稳定性的作用。实验用干筛法测定团聚体粒径分布，并通过对比培养 76 天完整团聚体和破碎团聚体的 CO_2 释放结果来估算有机碳稳定性和其中团聚体控制的部分。团聚体粒径分布的控制因素是成土母质而非降水：石灰岩土的团聚体粒径大于酸性火成岩土。有机碳稳定性在石灰岩土中随降水减少而降低，但在酸性火成岩土中则无明显变化。团聚体包裹对有机质稳定的作用有限，主要由于：(1) 有机碳矿化速率在完整团聚体和破碎团聚体中的差别不明显；(2) 团聚体粒径分布与有机碳矿化速率并不吻合。因此，矿物表面对有机质的吸附才是促进其稳定的主要原因。结果显示，有机碳稳定性主要受控于降水与成土母质的交互作用，这种交互作用进一步受土壤矿物组成及有机质输入的影响。

第五章探究了有机质分子结构对其稳定性的影响。研究使用添加了氢氧化四甲铵 (TMAH) 的热解气相色谱/质谱技术 (GC/MS)，探究第四章中 76 天培养实验前后完整团聚体和破碎团聚体中有机质分子结构的变化。培养前后分子结构变化用来表征不同分子的稳定性及微生物对有机质分子结构的转化，完整及破碎团聚间的差别用来研究团聚体对有机质分子的保护作用。结果显示热解后的来源于脂肪酸的物质有着较大的相对丰度，其中游离态脂肪酸可能有较大贡献。脂肪酸的稳定性取决于不饱和双键（饱和与不饱和脂肪酸）和碳链长度。与饱和脂肪酸相比，不饱和脂肪酸的相对丰度在培养后明显降低，并与土壤有机碳矿化速率显著正相关。微生物分解极可能是不饱和脂肪酸相对丰度降低的原因。不饱和脂肪酸与饱和脂肪酸之间的差别可能是由于矿物表面吸附或分子结构的不同，但不能用与团聚体包裹控制的有机质稳定性机制加以解释。长链脂肪酸相较短链脂肪酸在培养后明显减少，可能的原因是短链脂肪酸可以得到团聚体更有效的保护。尽

管实验观察到微生物对脂肪酸的转换作用，但这种转化对利用双键和碳链长度对脂肪酸稳定性预测的影响相对有限。此外，双键和碳链长度对脂肪酸稳定性的影响会随土壤类型和土层的不同而改变。因此，在把本章结论推广到其它土壤前需要开展更多的研究。本章结果为在秘鲁安第斯高山草原，土壤脂肪酸的分子结构影响其与土壤基质相互作用并间接影响其稳定性的假设提供了证据支持。

第六章总结了论文的主要发现：(1) 成土母质是影响土壤有机碳储量及稳定性的主要因素；(2) 在湿润样地，酸性火成岩土中有机质稳定性主要受控于铁铝（氧化物），石灰岩土中钙阳离子桥则起到了额外的作用；(3) 石灰岩土中有机碳稳定性随降水减少而降低，酸性火成岩土中降水作用不明显，此过程可能受土壤矿物及有机质输入的作用；(4) 土壤中重要组分脂肪酸的稳定性受不饱和双键及碳链长度影响。

第六章对论文的应用前景展开讨论。对于有机质分子结构，结果显示了大量的脂质（或脂肪酸）组分，而木质素与多糖类物质较少。这样的结果与厄瓜多尔安第斯高山土壤相吻合，但与其余地区一般性的结果不一致。未来研究可深入探究该地区的土壤有机质组成的相关机制。对于有机质稳定机制而言，结果揭示了有机质分子结构会影响其与土壤基质的作用并进一步影响其稳定性。但本论文研究结果不足以解释饱和脂肪酸与不饱和脂肪酸之间的稳定性差异是由于其化学稳定性差异或是与矿物表面亲和性差异，因此进一步研究可关注饱和与不饱和脂肪酸对土壤矿物表面吸附的亲和性及对抗微生物分解存在的潜在差异。在生态系统管理方面，结果揭示了降水与成土母质作用及有机质输入的重要性。此外，未来研究可致力于将此论文的发现应用于为安第斯高山草原提高土壤质量及维持生态系统服务功能的实践中。



Chapter 1

General Introduction

Soil organic carbon (SOC) is a large terrestrial carbon (C) pool and plays an important role in global C dynamics. SOC stocks are large in alpine grasslands of the Peruvian Andes and contribute to ecosystem services such as agricultural production and water provision. The alpine grasslands of the Peruvian Andes are vulnerable against climate change, and the SOC stocks there act as a potential C sink or source for atmospheric CO_2. Studies on SOC stocks and stabilization in the Andes have mostly been conducted on volcanic ash soils in Ecuador. In contrast, soils developed on other substrates in the Peruvian Andes have been less-studied. Furthermore, the heterogeneity in climate in the Peruvian Andean can potentially introduce spatial variability in SOC storage and stability. Also in this respect, relevant studies are rare.

SOC stocks are largely controlled by the stabilization of soil organic matter (SOM). Recently, we have seen a shift from traditional views of SOM stabilization based on the 'humification' model and molecular recalcitrance to a new paradigm based on the protection of SOM by the soil matrix against decomposers. In this emerging new view, SOM is stabilized by adsorption on mineral surfaces and occlusion in aggregates, whereas molecular composition is less important in long-term SOM stabilization (Lehmann and Kleber, 2015; Schmidt et al., 2011). Applying the new paradigm of SOM stabilization will help to gain insights into the underlying mechanisms for the storage and stability of SOC stocks in the Peruvian Andes.

The objectives of this thesis were to investigate SOC stocks and the underlying mechanisms controlling SOC persistence in the Peruvian Andes. The first step was to estimate SOC stocks of the study area and to identify key factors controlling the SOC spatial pattern. Afterward, soil samples were collected based on the key factor(s) previously identified plus two contrasting precipitation levels. SOM stabilization mechanisms based on the new paradigm were investigated using a combination of selective extraction methods, aggregate-size fractionation and an incubation experiment of intact versus crushed aggregates. Finally, we paid special attention to SOM molecular composition in relation to microbial

decomposition to gain insights into relationships between molecular composition and SOM stabilization.

1.1. Background

1.1.1. Importance of soil organic carbon

Soil is a large terrestrial C pool (2500 Gt), which is much larger than the sum of the atmospheric C pool and the vegetation C pool together (Lal, 2004). This soil C pool is comprised of SOC (1550 Gt) and soil inorganic carbon (950 Gt). Studies on global change indicate that the climate will be consistently warming in the 21st century (Field, 2014). On one hand, global warming can induce the loss of SOC storage and further stimulate the emission of greenhouse gases (e.g. CO_2 and CH_4). On the other hand, global warming can be alleviated by SOC sequestration that stores greenhouse gases in the form of SOM (Lal, 2004). Based on the Paris Climate Agreement, increasing global SOC stocks by 0.4% per year (2.5 Gt C year^{-1}) can potentially offset 30% of the global greenhouse gas emissions (Minasny et al., 2017). Given the importance of SOC for global warming, it is important to understand the impacts of global change on the SOC stock and its stability, as well as the underlying mechanisms of SOC stabilization.

1.1.2. Persistence of soil organic matter

SOC stocks and persistence are largely controlled by SOM stabilization. Traditional theories assume that the persistence of SOM is dependent on the chemical recalcitrance of macromolecules formed by the "humification" process (Stevenson, 1994). However, recent studies show that compounds previously considered to be recalcitrant against decomposition (e.g. lignin) can be decomposed rapidly in soils. In contrast, compounds previously considered to be decomposed very fast (e.g. polysaccharides and proteins) can persist against microbial degradation for a long period in soils (Lehmann and Kleber, 2015; Schmidt et al., 2011). Furthermore, the macromolecules previously assumed to be important in the "humification" model have been shown to be self-assembled formations of small molecules (Myneni et al., 1999). Since the "humification" model and relevant concepts receive an increasing criticism, new emergent views argued that SOM degradation is a progressive decomposition and transformation

of plant- and microbe-derived OM. For the decomposition and transformation, the accessibility of SOM to microbial decomposition and the surrounding environment is now thought to play an important role (Lehmann and Kleber, 2015). In general, SOM is protected against decomposition by interacting with the soil matrix. The underlying mechanisms are: (1) interactions of SOM with mineral surfaces and metal ions, (2) physical occlusion of SOM by soil aggregates, and (3) chemical recalcitrance of SOM (Lützow et al., 2006).

The formation of organo-mineral associations promotes long-term SOM stabilization as it strongly reduces the biological availability of mineral-associated OM. Literature reports lower mineralization rates for SOM associated with mineral as compared to other SOM fractions (Chenu et al., 2002; Schrumpf et al., 2013). Generally, SOM stabilized by mineral surfaces is characterized by lower C/N ratios, higher microbial-origin and longer resident time compared to bulk SOM and other SOM fractions (Kleber et al., 2015; Kögel-Knabner et al., 2008). Mineral-controlled SOM stabilization is dependent on soil pH values. In acid soils, SOM interacts with Fe, Al and Mn oxides via ligand exchange, whereas in alkaline and neutral soils, polyvalent cation bridges (e.g. Ca^{2+}) are considered crucial to the interactions between SOM and mineral surfaces (Lützow et al., 2006; Rowley et al., 2018). Kleber et al. (2007) created a conceptual model in which the formation of OM-mineral association is explained as a self-organized process. In this model, amphiphilic compounds and proteins are adsorbed on mineral surfaces via strong interactions forming the stable inner layer, whereas other compounds are retained loosely outside the inner layer forming the kinetic zone via weak interactions (Kleber et al., 2007). The OM-mineral fraction is usually separated from the bulk SOM using density fractionation because the OM-mineral associations have higher densities than other OM fractions (Cerli et al., 2012; Moni et al., 2012). In general, the mineral-associated OM is the major fraction of bulk SOM. In addition to the OM-mineral associations, SOM can also be stabilized by complexed with metal ions (e.g Fe^{3+} and Al^{3+}) in acidic soils, especially soils of volcanic origin (Lützow et al., 2006).

SOM can be stabilized by occlusion in aggregates due to their physical inaccessibility to decomposers (Lützow et al., 2006). Compared to unprotected OM and mineral-associated OM, aggregate-occluded OM is characterized by an intermediate residential time, C/N ratios and the presence of microbial-derived OM (Schrumpf et al., 2013; Wagai et al., 2009). Microaggregates (<0.25mm) in

macroaggregates (>0.25mm) play an important role in stabilizing SOM (Six et al., 2000). Macroaggregates act as the habitat for microorganisms, in which plant-derived SOM is decomposed. The SOM decomposition in macroaggregates controls the formation of microaggregates and further determines the turnover and stabilization of microaggregate-protected SOM (Six et al., 2000; Six and Paustian, 2014). Similarly, Wagai et al. (2009) suggested dividing aggregate-occluded SOM into two fractions, which are similar to the two SOM fractions protected by macroaggregates and by microaggregates. SOM occluded in aggregates can be separated using a combination of density fractionation and ultrasonic. First, a density fractionation without an ultrasonic treatment is conducted to isolate free light (unprotected) OM from other OM fractions. Afterward, the ultrasonic treatment is applied to release occluded OM, followed by another density fractionation to separate occluded OM from mineral-associated OM (Cerli et al., 2012; Kaiser and Berhe, 2014).

Although recent studies indicate that molecular composition is less important in controlling SOM persistence than previously thought (Lehmann and Kleber, 2015; Schmidt et al., 2011), a consensus is still absent for the importance of SOM molecular composition on SOM persistence. An important reason for this is that the effects of SOM molecular composition on interactions between SOM and the soil matrix are not well understood. In general, microbial-derived SOM is considered to be preferentially stabilized by mineral surfaces (Moni et al., 2012). However, plant-derived SOM can also be protected by mineral surfaces. With regard to aggregate-controlled SOM stabilization, some studies reported that fire-induced aromatic compounds are preferentially stabilized by occlusion in aggregates. Furthermore, Angst et al. (2018a) reported that soil lipids with different origins are selectively stabilized by different-sized aggregates. In contrast, Wagai et al. (2009) summarized that aggregate-occluded SOM has a large range of molecular characteristics. Thus, further research is needed for a better understanding of the molecular composition of SOM and how this affects its stabilization.

1.1.3. Factors controlling soil organic matter persistence

The persistence and turnover of SOM are largely controlled by soil formation and environmental (SFE) factors. Climate factors, especially precipitation and temperature, act as primary drivers for the persistence and turnover of SOM. In

general, soils with cool and humid climate accumulate more OM compared to soils under warm and dry climate (Wiesmeier et al., 2019). Precipitation regulates not only primary productivity and SOM input but also SOM decomposition through affecting soil water availability. Temperature can potentially constrain SOC storage because the microbial decomposition of SOM is stimulated under warm conditions (Chaplot et al., 2010; Wiesmeier et al., 2019). In addition, climate factors can also change soil mineralogy by controlling weathering processes and further govern SOM stabilization via mineral surfaces (Doetterl et al., 2018, 2015b). Vegetation plays an important role in controlling the input and decomposition of SOM, especially at the regional scale. However, the effects of vegetation decrease with soil depth and are largely controlled by climate factors (Wiesmeier et al., 2019). Lithology (or parent material) is also an important predictor for SOM persistence as reported by different studies (Angst et al., 2018a; Hobley et al., 2015; Wagai et al., 2008). This can be explained by the close relationships between lithology and soil mineralogy that controls SOM stabilization. However, the relative importance of lithology is also dependent on the scale and the interactions with other factors (Wiesmeier et al., 2019). Furthermore, topographical factors (e.g. slope angle and aspect) can also impact SOM accumulation through the controls of soil wetness, soil erosion, redox status and soil formation process (Wang et al., 2014; Wiesmeier et al., 2019).

Human activities also have crucial impacts on SOC storage and decomposition. Land use (change) has important effects on the stability and storage of SOM. In general, SOC stocks are higher in grassland and forest soils compared to cultivated soils (Guo and Gifford, 2002). Land use change that shifts from grassland or forest to cultivation causes depletion of SOC, whereas cropland abandonment and afforestation stimulate SOC storage (Poeplau et al., 2011). Furthermore, land use change also induces changes in SOM fractions and in SOM stabilization (Hamkalo and Bedernichek, 2014; Rolando et al., 2017a). Grazing in grasslands is reported having positive, negative and no obvious effects on SOC stocks and stability. This might be attributed to the interactions between grazing and other factors (McSherry and Ritchie, 2013). Nevertheless, overgrazing has significantly negative effects on SOC sequestration in the Andes (Podwojewski et al., 2002). The loss of SOC stocks related to land use change and overgrazing can be attributed to declined C input, soil erosion and SOM destabilization caused by aggregate destruction (Wiesmeier et al., 2019).

1.2. Soil organic carbon in alpine grasslands of the Andes

1.2.1. General information

Tropical alpine grasslands occur between the upper forest line and the snow line, with altitudes ranging from 3400m to 5000m. The Andes have the largest area of the tropical alpine grasslands, known as páramo, jalca and puna, depending on vegetation and precipitation (Buytaert et al., 2011). Although these grasslands cover limited areas, they provide important ecosystem services including biodiversity conservation, carbon sequestration, water provision and food production (Buytaert et al., 2011; Rolando et al., 2017b). Also, these grasslands are disturbed by human activities including cultivation, grazing, tree plantation and mining activities (Rolando et al., 2017b).

Alpine grassland ecosystems are highly vulnerable to climate change, which potentially threatens the ecosystem services they deliver (Field, 2014; Rolando et al., 2017b). Changes in precipitation and temperature can potentially cause shifts in species range, distribution of vegetation zones and fragmentation of the habitat (Buytaert et al., 2011). If the alpine grasslands receive less precipitation, water provision for the lowland with dry climate will decline. When the climate becomes warmer, the Andean grassland ecosystems tend to shift to higher elevation due to an upper shift of the cloud forest and degradation of the glacier. In addition, agriculture activities like cultivation and grazing will also move to higher altitudes. Furthermore, glacier melting due to warming can cause severe water scarcity for the adjacent populated areas (Chevallier et al., 2011; Rolando et al., 2017b).

1.2.2. SOC stocks and stability

Alpine grasslands of the Andes are characterized by their high SOC storage compared to other ecosystems (Buytaert et al., 2011; Tonneijck et al., 2010; Yang et al., 2018). These large SOC stocks act as a potential source of C loss to the atmosphere as CO_2 under global change and are crucial to the ecosystem services including water provision and food production (Buytaert et al., 2011; Rolando et al., 2017b). Precipitation is an important driver for the spatial distribution of SOC stocks in alpine grasslands of the Andes. SOC stocks decrease from up to 530±40 Mg ha^{-1} in the Ecuadorian humid páramo grassland (Farley et al., 2004; Tonneijck et al., 2010) to a level between118±15 and 136±4 Mg ha^{-1} in the Peruvian dry

puna grassland (Muñoz-García and Faz-Cano, 2012; Rolando et al., 2017a; Zimmermann et al., 2009). Surprisingly, spatial distributions of SOC stocks are not clearly controlled by vegetation in Andean grasslands (Nierop et al., 2007; Tonneijck et al., 2010; Zimmermann et al., 2009). In addition, land use except for overgrazing also has limited impact on SOC stocks in this region (Podwojewski et al., 2002; Rolando et al., 2017a; Yang et al., 2018).

SOM stabilization mechanisms are little studied in the Andean grasslands. Buytaert et al. (2006b) and Tonneijck et al. (2010) reported that SOM is stabilized by interacting with mineral surfaces and/or complexed with Fe and Al in volcanic ash soils in the Ecuadorian Andes. Rolando et al. (2017b) reported that SOM is stabilized by adsorption on mineral surfaces and occluded in aggregates in the wet puna of Central Peru. In addition, alleviated SOM degradation due to the cold and humid environment and Al toxicity due to the low pH of volcanic-ash soils can also be potential factors promoting SOM accumulation in the Andes (Hribljan et al., 2016). For the Southern Andes in Chile, Doetterl et al. (2015) conducted a study on SOC stabilization in grassland through a 4000-km-long transect with a wide range of climate and geological conditions. Their results showed that soils with mild and wet climate had the largest SOC stocks and the SOM stabilization was largely controlled by interactions between climate and soil mineralogy (Doetterl et al., 2015).

1.2.3. What is unknown

It is important to understand the underlying mechanisms for the large SOC stocks in the alpine grasslands of the Andes. Studies on SOC storage and stabilization in the Andes were mostly conducted in Ecuadorian Páramo, where soils are generally developed on volcanic ash. However, soils in the jalca or wet puna in Northern Peru are rich in SOC but developed from substrate other than volcanic ash. These soils have been less studied, especially with regard to the SOM stabilization related to OM-mineral interaction, soil aggregation and OM molecular composition. Furthermore, alpine grasslands of the Peruvian Andes are characterized by heterogeneity in climate conditions (Merkel, 2017). As climate factors are primary drivers controlling SOC distribution by regulating OM input and weathering processes, it is important to know the effects of climate factors (e.g. precipitation) in the Peruvian Andes. However, relevant studies were rare in the Peruvian Andes based on the knowledge of the author.

1.3. Aim and objectives

Given the importance of the alpine grasslands of the Peruvian Andes for ecosystem services and the vulnerability of the ecosystem to global change, it is important to having insights into the factors that drive SOC stocks and the underlying mechanisms of SOM stabilization in these areas. The objectives of the research were to quantify SOC stocks and the underlying mechanisms controlling SOC persistence in the alpine grassland of the Peruvian Andes.

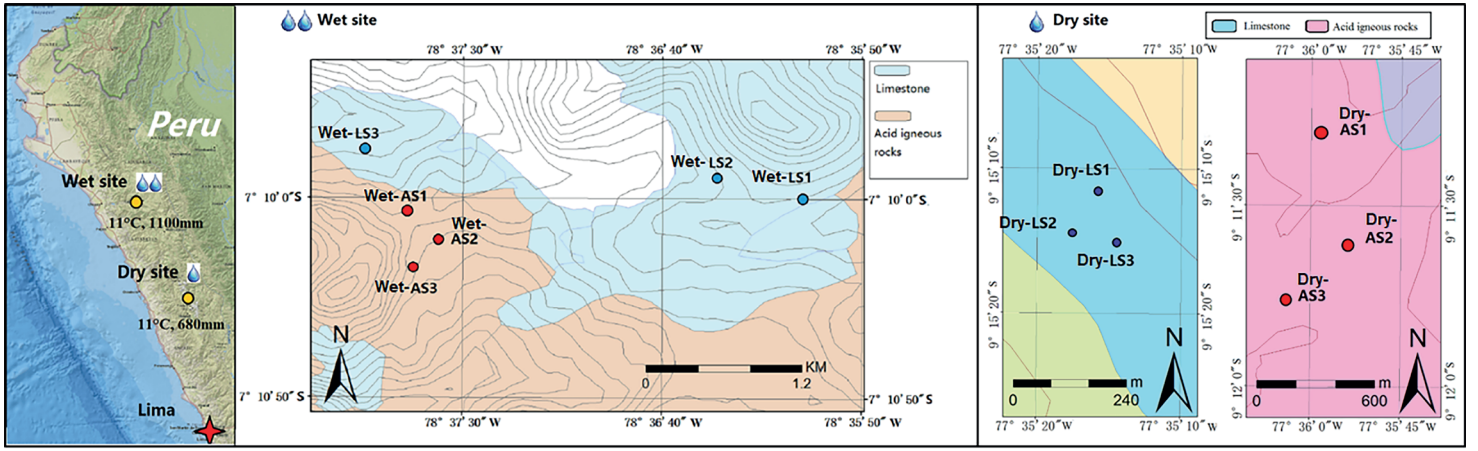
The following specific objectives were formulated:

- To estimate SOC stocks of the study area and to identify key factors controlling the spatial pattern of SOC distribution (Chapter 2).
- To determine SOM stabilization controlled by adsorption on mineral surfaces in soils developed on contrasting bedrocks (Chapter 3).
- To investigate the effects of precipitation and lithology on SOC stocks and stability, as well as to what extent soil aggregation contribute to stabilizing SOM (Chapter 4).
- To gain insights into relationships between SOM molecular composition and SOM stabilization controlled by the soil matrix (Chapter 5).

1.4. Description of the study area

1.4.1. Site description

The study area is located in the Peruvian Andes and belongs to the Neotropical alpine grasslands, namely wet puna or jalca, which are considered as a transition between the páramo and the dry puna (Sánchez Vega et al., 2005). This region is also subject to disturbance including cultivation and grazing as a result of human activities. In addition, plantation of pine trees and eucalypt trees is also common in the study area (Rolando et al., 2017b). Precipitation decreases from the north to the south, whereas temperature has almost no changes through the latitude gradient. However, the climate has large temporal and spatial heterogeneity in this region (Merkel, 2017; Rolando et al., 2017b).



Site	Wet site					Dry site				
	Parent material	Altitude	Soil depth	Ave. depth	Gravels in LM fractions	Parent material	Altitude	Soil depth	Ave. depth	Gravels in LM fractions
		m	cm		%		m	cm		%
LS1	Limestone	3716	57		6.86	Limestone	3573	56		8.70
LS2	Limestone	3717	66	61	3.13	Limestone	3532	54	61	5.42
LS3	Limestone	3517	60		0.16	Limestone	3560	73		13.01
AS1	Granite/ignimbrite	3583	68		10.86	Granodiorite	3667	44		50.28
AS2	Granite/ignimbrite	3585	45	49	14.12	Granodiorite-rich glacier materials	3521	60	51	39.57
AS3	Granite/ignimbrite	3586	35		28.60	Granodiorite-rich glacier materials	3495	50		61.05

Fig. 1.1 Sampling site description. LS: limestone soil, AS: acid igneous rock soil, LM: large macroaggregates (>2 mm). The ArcGIS Online World Topographic Map basemap (Esri., 2013) was used for the map of Peru on the left, whereas the data for the contour lines in the maps of the wet site and the dry site was derived from Geo GPS Perú, (2014).

1.4.2. Sampling plots

Soil samples were collected from two separate sites with similar altitudes and temperatures but with different precipitation levels, the wet site and the dry site, respectively. Fig. 1.1 gives the locations of the wet site and the dry site, whereas Table A1.1 presents detailed information in sampling sites and soil profiles.

The wet site is located on the continental divide between the Pacific and the Atlantic Ocean, which is to the west of the city of Cajamarca (7° 11' S, 78° 35' W) in the Peruvian Andes. The sampling area has altitudes between 3400 m asl and 3900 m asl. The annual average temperature is estimated as 11 °C, with large daily variation and minor seasonal change. The area receives 1100 mm precipitation per year, which mainly occurs between October and April (Merkel, 2017; Sánchez Vega et al., 2005). The geology is comprised of a basement of folded Cretaceous sedimentary formations and a layer of igneous materials that are partially-overlying the basement. The basement, which belongs to the Formations of Cajamarca, Chulec-Calizas, Pariatambo, Farrat and Yumagual, consists of bedrocks such as limestones, marls, shales and quartzites. The igneous materials belong to the San Pablo Formation, and consist of ignimbrite and granite (Geo GPS Perú, 2014; Reyes-Rivera, 1980). Soil types of this region are dependent on topography and lithology. For topography, shallow and less-developed soils (e.g. Leptosols and Regosols) are distributed at the mountain top, whereas soils rich in SOC in relation to humid soil conditions (e.g. Histosols and Gleysols) are common in the valley bottom. For lithology, soils developed on calcareous bedrocks are generally classified as Phaeozems due to their large SOC stocks and high base saturation, whereas soils formed on acid igneous rocks usually belong to Umbrisols or Andosols because of their low base saturation and volcanic bedrock types (WRB, 2014). The land use in the wet site is characterized by a rotation of cultivation, land abandonment and grazing that was applied in a period of 3-5 years, which is considered to sustain the fertility and the productivity of the soils.

The dry site is located on the west side of the Cordillera Blanca of the Andes, to the northeast of the city of Carhuaz (9°22' S, 77°59' W). Altitudes of the sampling sites are between 3490 m asl and 3700 m asl. Similar to the wet site, the annual average temperature is 11 °C. However, the annual precipitation is estimated as 680 mm in the dry site at an altitude of 3600 m (Merkel, 2017),

which is only 60% of that in the wet site. The batholith of the high mountain chain (>5000 m asl) of the Cordillera Blanca are comprised of Neogene intrusive igneous rocks, which have a major contribution of granodiorite. The western foot slopes of the high mountain chain are partially covered by fluvio-glacial sediments, which contain a large proportion of granodiorite fragments. For the foot slope region not covered by the fluvio-glacial materials, extrusive igneous rocks such as ignimbrite are found in the Yungay Formation, whereas folded limestones, cherts and shales are distributed in the Carhuaz Formation and the Santa Formation (Coldwell et al., 2011; Geo GPS Perú, 2014). Similar to the wet site, soil classification of the dry site is also dependent on topography and lithology. For example, soils developed on limestone or shale are predominantly classified as Phaeozems or Umbrisols, whereas soils developed on granodiorite and ignimbrite generally belong to Umbrisols or Andosols. In addition, Histosols and Gleysols are often found on sub-glacial or alluvial materials located in the valley bottom (WRB, 2014). The typical land use type is grassland with shrub patches. Cultivation and grazing are common human activities in the dry site.

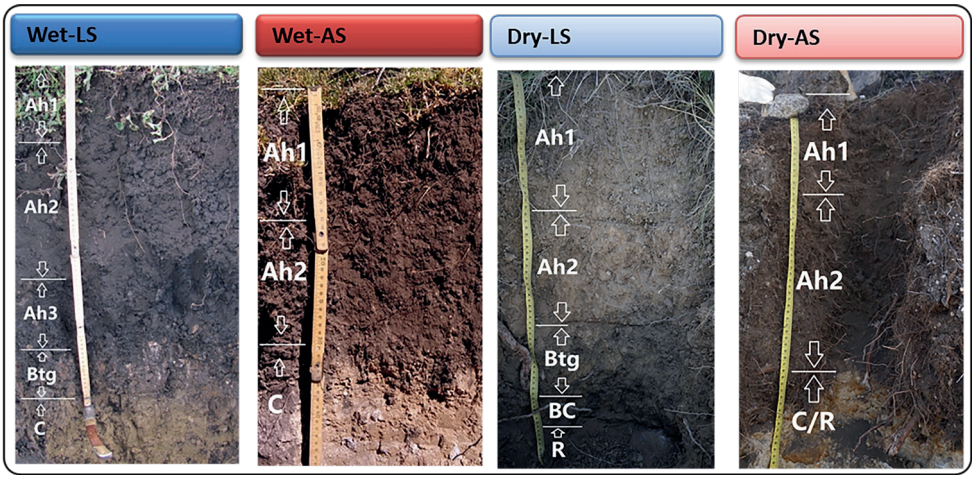


Fig 1.2 Typical soil profiles from the sampling sites with the combination of each precipitation level and bedrock type. Wet: the wet site, dry: they dry site, LS: limestone soil, AS: acid igneous rock soil.

1.5. Research outline and structure

In **Chapter 1**, a general introduction to the topic and a description of the study area are provided. A literature review on SOC stock and stabilization including

current knowledge gaps is conducted in this chapter. Base on the knowledge gaps, the objectives and the outline of this thesis are presented.

In **Chapter 2**, we quantified SOC stocks of the study area and identified the key factors controlling the distribution of SOC stocks. For this, soil samples were collected from 69 sampling plots in the wet site and SOC stocks were assessed to C or R horizons. Significant predictors for SOC stock patterns were selected from environmental factors and soil properties, namely lithology, land use, grazing intensity, slope position, slope angle, altitude, soil moisture and soil depth, using linear models.

In **Chapter 3**, soils developed on limestone and acid igneous rocks in the wet site were collected to investigate potential differences in SOC stocks and underlying stabilization mechanisms. We applied a selective extraction method to separate active Fe, Al and Ca fractions that explain OM stabilization governed by interacting with mineral surfaces.

In **Chapter 4**, the objectives were to investigate the potential controls of lithology and precipitation in soil aggregation and OM stabilization by occluded in aggregates. Soil samples were collected from both limestone and acids igneous rocks in two sampling sites with two different precipitation levels. A dry-sieving method was applied to determine soil aggregate-size distribution, and a 76-day incubation was used to estimate SOC stability against microbial decomposition. Furthermore, intact aggregates and crushed aggregates were incubated to estimate SOC protected by occlusion in soil aggregates.

In **Chapter 5**, we aimed to investigate potential controls of SOM molecular composition on their persistence to microbial degradation. For this, a combination of an incubation experiment of intact versus crushed aggregates and pyrolysis-GC/MS analyses were applied. Specifically, the objectives included: (1) to assess whether inherent properties of OM control OM stability against decomposition, and (2) to assess whether the potential controls of OM stability can be explained by OM stabilization by soil matrix.

In **Chapter 6**, the major findings of this thesis are synthesized and integrated. In addition, discussions are made for the implications of the findings for the management of the Andean grasslands and for SOM stabilization in general.



- SOC stocks controlled by lithology and soil depth

Chapter 2

Soil organic carbon stocks controlled by lithology and soil depth in a Peruvian alpine grassland of the Andes

This chapter has been published as:

Yang, S., Cammeraat, E., Jansen, B., den Haan, M., van Loon, E., Recharte, J., 2018. Soil organic carbon stocks controlled by lithology and soil depth in a Peruvian alpine grassland of the Andes. Catena 171, 11–21. doi:10.1016/j.catena.2018.06.038

- SOC stocks controlled by lithology and soil depth

Abstract

The soil is the largest carbon (C) pool in the terrestrial ecosystem, and soil organic carbon (SOC) stocks play an important role in global C dynamics. Alpine grasslands of the Andes are characterized by high SOC stocks. Quantifying SOC stocks and unraveling key factors controlling SOC stocks, is necessary to obtain a better understanding of the dynamics of the large C stocks in this environment. However, most studies on C dynamics of the Andes focus on volcanic-ash soils, whereas information about non-volcanic ash soils in this region is scarce. Our objectives were: (1) to estimate SOC stocks in an alpine grassland of the Peruvian Andes (7°11'S, 78°35'W) with parent materials other than volcanic ash, and (2) to identify the underlying soil formation and environmental (SFE) factors and soil properties explaining observed patterns of SOC stocks. We sampled 69 plots up to the parent material to measure soil properties and to calculate SOC stocks, in relation to lithology, land use, grazing intensity, slope angle, slope position and altitude. We applied linear models to identify key factors controlling SOC stocks. Our results showed that total SOC stocks had a mean value of 215 ± 21 Mg ha^{-1}, whereas SOC stocks of the upper 10 cm and 40 cm comprised 29.3% and 80.0% of total SOC stocks respectively. The variation of the total SOC stocks was mainly explained by soil depth and soil moisture. When soil depth and soil moisture were controlled as conditional variables, lithology became the key factor controlling the total SOC stocks. For the SOC stocks of the upper 10 cm, soil moisture explained a large part of the variation, whereas lithology, grazing intensity and altitude were also significant predictors. Our results also show that when soils are sampled with limited depths instead of the entire soil profile, SOC stocks can be underestimated, and the effects of the SFE factors on SOC stocks can be overestimated

Keywords: Entire profile SOC stock; Soil moisture; Grazing; Topography; Linear model

2.1. Introduction

Soil is one of the largest terrestrial carbon (C) pools, and plays an important role in global terrestrial C dynamics (Lal, 2004; Luo et al., 2016). Within the global terrestrial C pools, neotropical alpine grass- lands of the Andes are characterized by high soil organic carbon (SOC) stocks (Buytaert et al., 2011; Sierra et al., 2007; Tonneijck et al., 2010). Previous studies of SOC in the Neotropical Andes focused on soils in recent volcanic-ash, especially being dominant in Ecuador (Farley et al., 2004; Minaya et al., 2016; Poulenard et al., 2003; Tonneijck et al., 2010). However, soils with parent materials other than volcanic ash also cover large areas of the Andean highland. In Peru about 27% of the Andean area is covered by Tertiary to Cretaceous volcanic rocks, mostly being ignimbrites in the northern half of Peru, and where active volcanism and recent ash deposits are absent (Buytaert et al., 2011; Geo GPS Perú, 2014). For these soils, only a limited number of studies have been reported (Muñoz-García and Faz-Cano, 2012; Segnini et al., 2011; Zimmermann et al., 2009). Apart from the importance with respect to the carbon cycle, Andean grasslands are characterized by their high soil water holding capacity, and act as water sources and regulate the provision of water to the arid coastal regions of the South American continent (Buytaert et al., 2011; Lineger et al., 1998). The high water holding capacity is partially attributed to the high SOC stocks (Buytaert et al., 2011). As such the management of these grasslands, including the soil, is crucial for maintaining ecosystems services especially for the western side of the Andean mountain range.

Soil formation and environmental (SFE) factors control SOC stocks and their persistence to a large degree, through complex interactions with organic matter (OM) and other factors, including mineralogy, physical properties, OM input and OM degradation (Luo et al., 2016; Schmidt et al., 2011). SOC stocks are to a large degree determined by the stabilization of OM, which is strongly affected by interactions between OM and soil minerals (Doetterl et al., 2015b; Lützow et al., 2006; Six et al., 2002). Contrasting mineralogical characteristics may cause differences in OM adsorption mechanisms on minerals, as well as physical stabilization related to the aggregate formation (Kögel-Knabner et al., 2008; Lützow et al., 2006; Percival et al., 2000). Lithology (parent material) determines soil mineralogy and as such plays a role in controlling SOC stocks. In addition to lithology, effects of land use (change) and grazing are reported to be important. Generally, cropland has lower SOC stocks than natural forest and grassland, and land use shifting from natural forest or grassland to cropland has negative effects

on SOC sequestration (Guo and Gifford, 2002; Poeplau et al., 2011). In addition, effects of land use (change) on SOC stocks are dependent on other factors (Leifeld et al., 2005; Powers et al., 2011), such as grazing. The effects of grazing on SOC stocks can be variable, ranging from positive to negative as summarized by Mcsherry and Ritchie (2013) and Piñeiro et al. (2010). This variability can be explained by the complex interaction between grazing, primary production, vegetation type and climate. Furthermore, topographic factors including altitude, slope angle and slope position, are also reported to have impacts on SOC accumulation, especially in mountainous regions (Ayoubi et al., 2012; Garcia-Pausas et al., 2007; Schwanghart and Jarmer, 2011).

SOC stocks are generally estimated using limited constant soil depths, generally with only the topsoil included (e.g. Sebastian Doetterl et al., 2015; Du et al., 2014; Fernández-Romero et al., 2014; Minaya et al., 2016). However, soil depths are not always constant, and the subsoil may contain large amounts of SOC (Batjes, 2014). In addition, the persistence and stabilization of SOC may also differ between the topsoil and the subsoil (Schmidt et al., 2011). Studies may run a risk of inaccurate estimations of the SOC stocks as well as effects of external factors controlling the SOC stocks, when only limited constant soil depths instead of the entire soil profiles are examined (Harrison et al., 2011; Tonneijck et al., 2010; Wiesmeier et al., 2012). Therefore, Wiesmeier et al. (2012) recommended including entire soil profiles rather than sampling soils with constant depths when estimating SOC stocks.

In the present study, soil samples were collected with the entire soil profiles, from an Andean high altitude grassland with parent materials other than volcanic ash. The study area is characterized by heterogeneous SFE factors including lithology, land use, grazing intensity and topographical factors. The objectives of the study were: (1) to make an estimate of SOC stocks assessed to the C or R horizon, (2) to identify key factors controlling SOC stocks from the SFE factors as well as soil properties.

2.2. Materials and methods

2.2.1. Site description

The study area is located approximately 10 km to the west of the city Cajamarca in Peru (7° 11’ S, 78° 35’ W, Fig. 2.1), on the broad South American continental

watershed between the Rio Jequetepeque (Pacific) and the Rio Cajamarca (Atlantic). The altitudes of the study area range from 3370 m to 3900 m above sea level. Mean annual temperatures were reported for two stations in or near the field area, based on 8–10 years of measurements: 8.2 - 10.8 °C for mean annual temperature, 12.0–14.7 °C for mean daily maximum temperature and 4.4 - 7.5 °C for mean daily minimum temperature for Porcon 2 (3510 masl) and Cumbe Mayo (3410 masl) stations. The temperature has small seasonal but large daily variations (Sánchez Vega and Dillon, 2006). The annual precipitations are between 616 and 1317 mm. The majority of precipitation falls in the wet season between October and April, but the amount is also strongly influenced by orographic effects (Sánchez Vega and Dillon, 2006).

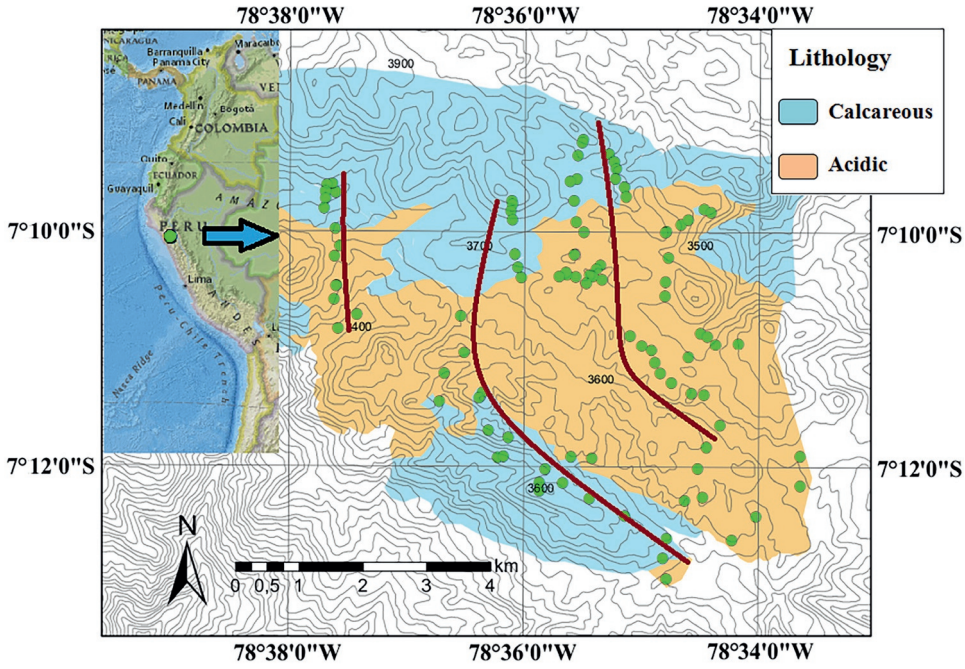


Fig. 2.1. Sampling sites in the study area. The picture on the left gives location of the study area, and green points on the main map indicate 69 sampling plots. The calcareous bedrocks are marked with blue background, and the acidic bedrocks are marked with yellow background. Bold red lines indicate transect lines. The distance between 2 adjacent contour lines is 50m.

The geological formations consist of a basement of folded Cretaceous marine sediments which are partly overlain or intruded by igneous bedrock. The sediments include the formations of Cajamarca, Chulec-Calizas, Pariatambo,

Farrat and Yumagual, with limestone, shale, marl and quartzite lithologies. The igneous bedrocks that belong to the San Pablo formation include intrusive bedrock of granite and extrusive bedrock of ignimbrites (Geo GPS Perú, 2014; Reyes-Rivera, 1980).

Soil types are directly related to the parent materials and slope position. Going from the top position to the valley bottom we find for the successive lithologies the following dominant soil types (WRB, 2006): on quartzites: Leptosols and Regosols; on limestones and marls: Leptosols, Phaeozems and Luvisols; on ignimbrites: Leptosols, Andosols and (Vitric) Umbrisols, Alisols and Histosols; on granitic rocks: Leptosols and Umbrisols.

The area belongs to the Neotropical alpine grassland zone of the Jalca, which is seen as a transition between the wet Páramo in the north and the dry Puna in the south (Sánchez Vega et al., 2005). The most important grass species in the grasslands is especially *Calamagrostis tarmensis* Pilger, and *Calamagrostis trichopylla*, but also *Festuca huamachucensis* Infantes, *Agrostis tolucensis* Kunth and *Cortaderia sp.*. Land use is dominated by grazing of Jalca grasslands, small arable fields with regularly barley and wheat at lower locations and potatoes and potato-like crops (ocas) at higher positions, and some planted patches with pine (mostly *Pinus patula* and some *Pinus radiata*) and eucalypt (*Eucalyptus sp.*), which are exotic species, as well as replanting of *Polylepus racemosa* (endemic species). In this region, agriculture is shifting upwards with altitude because of climate change and population growth (Tovar et al., 2013). The land use of the agriculture fields is dynamic as it shows a rotation of cultivation, abandonment and grazing. Usually, the land is ploughed and cultivated for 2 years, followed by grazing or fallow for at least 1–5 years.

2.2. Sampling procedures

Fig. 2.1 shows the distribution of 69 sampling plots along three transect lines. The selection of the transect zones was based on lithology and altitude, with each zone containing contrasting bedrocks and wide ranges of altitude, as well as land use, grazing intensity, slope position and slope angle. Within the units the sample locations were selected at random. Lithology was classified into the classes of calcareous bedrocks (limestone and marl with thin shale intercalations) and acid bedrocks (granite, ignimbrite and quartzite). Land use was classified into 5 categories: grassland, cultivation, abandoned cultivation, cultivated grassland and forest, following the recommendation of Sánchez Vega et al. (2005). Grazing

intensity was estimated in the field and was ranked into 4 levels: none, low, medium and high. The criteria to rank grazing intensity were based on the presence of physical indications of grazing, plant density, as well as the replacement of tall native tussock grasses (e.g. Carex sp.) with shorter invasive grass species and matted herbs including Rumex sp. as also applied by Verweij and Budde (1992). Slope position was classified into 3 groups: top, slope and valley bottom. Furthermore, slope angle and altitude were measured and recorded as numeric variables.

We took one complete soil profile per sampling point and divided these into sections of 10 cm, starting from the top until the C or R horizon was reached. Soil depth was defined from the ground level to the top of the C or R horizon and measured below the ground level. Undisturbed samples were collected from the representative layers with Kopecky rings (100 cm^{-3}) in order to determine bulk density using the core method (Blake and Hartge, 1986). Afterwards, all samples were weighted and transferred into sealed plastic bags before transportation.

2.2.3. Laboratory analysis

Soil bulk density was measured by weighing the intact ring samples after oven-drying at 105 °C, and calculated with the volume of 100cm^3. Field moisture contents were measured by weighing ring samples before and after oven-drying. pH values were measured using a glass electrode with H_2O (w/v=1:5) following the standard protocol of Bates (1973). Total carbon, nitrogen and inorganic carbon contents were measured with a VarioEL Elementar analyzer (Elementar, Germany) with an extension for inorganic carbon. Total organic carbon concentrations were calculated by subtracting inorganic carbon concentrations from total carbon concentrations. Total SOC stocks were calculated by adding SOC stocks every 10 cm of the soil profile from the surface down to the C horizon using the equation:

$$SOC\ stock = \sum_{i=1}^{i=k} B_i C_i D_i$$

In which, B_i = bulk density (g cm^{-3}) of the layer i, C_i = C content (%) of the layer i; D_i = the thickness (cm) of layer i. Total SOC stocks and bulk densities were not corrected for gravel contents and gravel was negligible in most of the soil profiles.

- SOC stocks controlled by lithology and soil depth

2.2.4. Statistics

Linear models were used to test the effect of the SFE factors (lithology, land use, grazing intensity, slope position, altitude and slope angle) on total SOC stocks and SOC stocks of the upper 10 cm. We consider the soil properties (soil depth, moisture and pH) as potential conditional variables, because they may be important predictors for SOC stocks, although the SFE factors rather than soil properties are the focus of our study. The conditional variables were selected from soil properties, based on the criteria that the variables should be significantly related to SOC stocks and also be independent of the SFE factors. The criterion of independence aimed to avoid difficulties in interpretation that are introduced by interactions between the conditional variables and the SFE factors. The linear models were applied to identify the conditional variables (soil properties) that are linearly related to the SOC stocks and independent from the SFE factors. When the conditional variables were selected, we applied the linear models with all conditional variables and only one additional SFE factor to predict SOC stocks. These models are aimed at investigating the effects of individual SFE factors and to make comparisons with the linear models without conditional variables. We also conducted model selections by testing all combinations of conditional variables and SFE factors with up to 5 predictors included, and we selected the best model sets. Models with $\Delta AICc<2$ from the lowest AIC value were selected and presented with averaged standardized coefficients (Beta), R^2 and R^2 changed.

Table 2.1 Descriptions of SOC stocks, slope angles, altitudes and soil properties of the 69 sampling plots.

	Unit	Mean	Max	Min	SD	SE	95% confidence interval for means
SOC stocks total	Mg ha^{-1}	215	663	17	172	21	174-257
SOC stocks 10cm	Mg ha^{-1}	63	190	14	31	4	55-70
SOC stocks 40cm	Mg ha^{-1}	172	581	17	123	15	143-202
Slope angle	°	12	42	1	10	1	10-15
Altitude	m	3611	3901	3373	99	12	3588-3635
Soil depth	cm	41	132	5	25	3	35-47
pH Ave.		5.58	7.80	4.53	0.73	0.09	5.41-5.76
pH 10 cm		5.55	7.93	4.17	0.80	0.10	5.35-5.75
Moisture Ave.	g kg^{-1}	208	495	27	110	13	181-234
Moisture 10 cm	g kg^{-1}	206	654	27	136	17	173-239

pH Ave: average pH value, pH 10 cm: pH value of upper 10 cm, Moisture Ave.: average moisture content, Moisture 10cm: moisture content of upper 10 cm. Sampling size n=69 for each variable except for pH 10cm (n=66)

- SOC stocks controlled by lithology and soil depth

For each of the models that appeared as a suitable model (Based on AIC and significance of coefficients), a thorough visual check of the assumptions underlying the linear model was conducted (normality, homoscedasticity, independence of errors and absence of structural deviations from each of predictors and the response variable) and any apparent violations were reported with the other model results. The selection of best linear model sets was performed in R (R Core Team, 2017) using the MuMIn package (Barton, 2016), whereas other statistical analyses were performed with SPSS 22.0 (SPSS Inc., USA).

2.3. Results

2.3.1. Soil organic carbon (SOC) stocks and soil properties

Total SOC stocks ranged from 16.7 to 662.7 Mg ha^{-1} with a mean value of 215 ± 21 Mg ha^{-1} (mean ± SE), whereas SOC stocks of upper 10 cm and upper 40 cm had means values of 63 ± 4 and 172 ± 15 Mg ha^{-1}. Total SOC stocks were not significantly ($P > 0.05$) different between any SFE factors, whereas SOC stocks of the upper 10 cm were significantly higher ($P < 0.05$) in calcareous bedrocks than in acidic bedrocks, and higher in medium grazing intensity than in other high grazing intensity (Fig. 2.2). Soil depth varied from 5 to 132 cm with a mean value of 41 ± 3 cm, whereas mean soil pH value was 5.58 ± 0.09 and mean soil moisture was 207.74 ± 13.26 g kg^{-1} (Table 2.1).

2.3.2. Factors controlling soil organic carbon (SOC) stocks

Table 2.2 shows the linear models using only one SFE factor to predict the total SOC stocks and the SOC stocks of the upper 10 cm. No model predicting the total SOC stocks was significant ($P > 0.05$), although in the models with land use as the predictive variable (Table 2.2) soils under forest had significantly higher ($P = 0.010$) total SOC stocks than soils under cultivation. In contrast, models predicting SOC stocks of the upper 10 cm were significant, when lithology, grazing intensity and altitude were the predictive variables in the models (Table 2.2). SOC stocks of the upper 10 cm were significantly higher with calcareous bedrocks than with acidic bedrocks ($P = 0.001$, Table 2.2), and were also

➢ SOC stocks controlled by lithology and soil depth

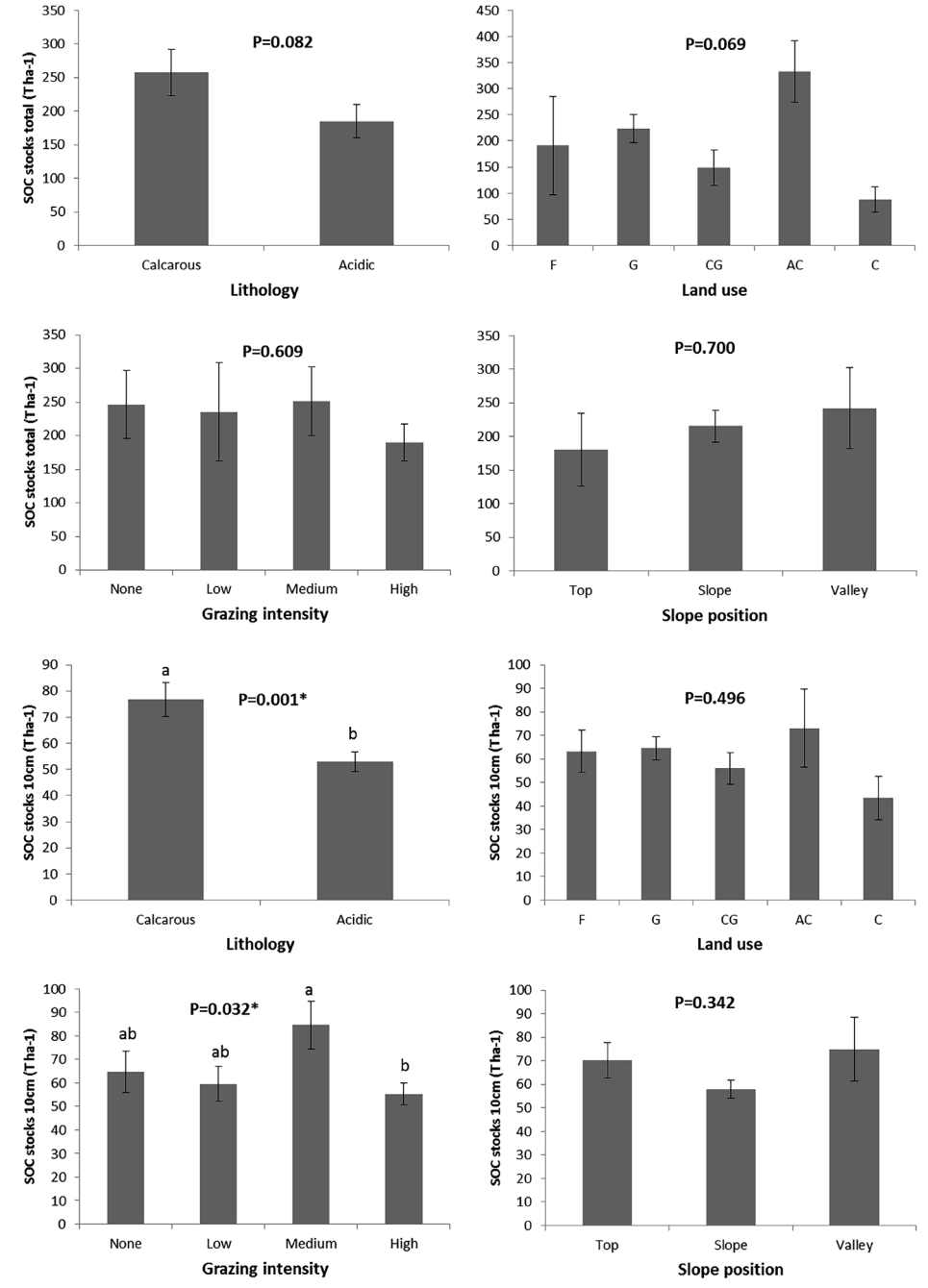


Fig. 2.2 Means and standard errors of total SOC stocks and SOC stocks of the upper 10cm with different types of lithology, land use, grazing intensity and slope position. *Means were compared using linear models (independent T-tests for lithology and one-way ANOVA for land us, grazing intensity and slope position) at a*

significance level of 0.05. F: forest, G: grassland, CG: cultivated grassland, AC: abandoned cultivation, C: cultivation.

significantly lower with high grazing intensity than with medium grazing intensity (P = 0.032, Table 2.2). Furthermore, altitude was a significant predictive variable that had a positive relationship with SOC stocks of the upper 10 cm (P=0.007, Table 2.2). The model with lithology as the predictive variable explained the largest variation of SOC stocks of the upper 10 cm compared to other models (adjusted R^2 = 0.130, Table 2.2). Fig. 2.3 and Table 2.3 give information about the selection of conditional variables from soil depth, soil moisture and pH (see Section 2.2.4). Soil depth was positively related to the total SOC stocks (P < 0.001) and explained 53.6% variation of the total SOC stocks individually. Average soil moisture had a positive relationship with total SOC stocks (P < 0.001) and explained 35.8% variation of the total SOC stocks (Fig. 2.3). Furthermore, soil moisture of the upper 10 cm also explained 37.0% variation of SOC stocks of the upper 10 cm with a positive linear relationship (Fig. 2.3). Soil depth and moisture were independent of all SFE factors, except for a significant relation between average soil moisture and altitude (Table 2.3). In contrast, soil pH was found to be dependent on lithology and land use (Table 2.3). Based on the criteria in Section 2.2.4, soil depth and average soil moisture were selected as conditional variables for total SOC stocks, whereas soil moisture of the upper 10 cm was the only conditional variables for SOC stocks of the upper 10 cm.

Table 2.4 gives the linear models with the conditional variables and only one SFE factor. Compared with linear models without conditional variables (Table 2.2), all models were highly significant (P < 0.001) and had higher values of R^2 and adjusted R^2 (Table 2.4). Within these models, lithology became the only significant SFE factor to predict the total SOC stocks when soil depth and average soil moisture were involved as the conditional variables (Table 2.4). The model with lithology and the conditional variables also explained the majority of the variation of the total SOC stocks (Table 2.4, adjusted R^2 = 0.658). For SOC stocks of the upper 10 cm, lithology, medium grazing intensity and altitude were significant SFE factors, when soil moisture of the upper 10 cm was involved as the conditional variable (Table 2.4). These models gave similar results as the linear models without the conditional variable (Table 2.2). The model with lithology and soil moisture of the upper 10 cm explained the largest part of the variation of the SOC stocks of the upper 10 cm (Table 2.4, adjusted R^2 = 0.456).

Table 2.2 Relation between SOC and single soil formation or environmental variable through linear regression, without any soil depth or moisture involved as conditional variable. The table lists standardized coefficients (Beta) with associated significance (P). Coefficients with P<0.05 are shown in bold. The variable level within brackets under each soil formation or environmental variable means the category with Beta=0. The P-values in the last column give the significance of the total model (i.e. resulting from an ANOVA of the regression model).

	Categorical variable										Numeric variables		R^2	Adjusted R^2	P value of the model
	Lithology (acid)	Land use (F)				Grazing intensity (none)			Slope position (top)		Altitude	Slope Angle			
	calcareous	G	CG	AC	C	Low	Medium	High	Slope	Valley					
SOC stocks total															
Beta	0.21												0.045	0.030	0.082
P	0.082														
Beta		0.09	-0.08	0.33	**-0.37**								0.125	0.071	0.669[1]
P		0.655	0.627	0.109	**0.010**										
Beta						-0.02	0.01	-0.16					0.028	-0.017	0.609
P						0.907	0.941	0.318							
Beta									0.10	0.14			0.011	-0.019	0.699
P									0.562	0.400					
Beta											0.11		0.011	-0.004	0.386
P											0.386				
Beta												-0.19	0.037	0.023	0.113
P												0.113			
SOC stock 10cm															
Beta	**0.38**												**0.143**	**0.130**	**0.001**
P	**0.001**														
Beta		0.02	-0.08	0.13	-0.25								0.051	-0.009	0.496
P		0.924	0.662	0.555	0.095										
Beta						-0.04	0.25	-0.15					**0.125**	**0.085**	**0.032[2]**
P						0.745	0.097	0.331							
Beta									-0.19	0.06			0.054	0.025	0.161
P									0.257	0.717					
Beta											**0.32**		**0.102**	**0.089**	**0.007**
P											**0.007**				
Beta												-0.16	0.025	0.010	0.198
P												0.198			

F: forest, G: grassland, CG: cultivation-grassland, AC: abandoned cultivation, C: cultivation. [1]Soils under cultivation have significantly lower total SOC stocks than soils under forest, although the regression model as a whole is not significant. [2]The multiple comparison shows that SOC stocks 10cm are significantly different

Table 2.3 Effects of soil formation or environmental factors on soil depth, moisture and pH using linear models (univariate regression). Significant factors (P<0.05) are shown in bold.

	Categorical variable								Numeric variable			
	Lithology		Land use		Grazing intensity		Slope position		Slope angle		Altitude	
	R^2	P	R^2	P	R^2	P	R^2	P	R^2	P	R^2	P
Soil depth	0.002	0.692	0.087	0.204	0.007	0.931	0.052	0.175	0.002	0.733	0.043	0.089
Moisture Ave.	0.044	0.082	0.089	0.197	0.089	0.105	0.004	0.866	0.029	0.163	**0.094**	**0.010**
Moisture 10cm	0.010	0.424	0.047	0.532	0.072	0.182	0.024	0.671	0.028	0.168	0.049	0.069
pH Ave.	**0.338**	**<0.001**	**0.175**	**0.014**	0.030	0.577	0.021	0.492	0.001	0.770	0.044	0.085
pH 10cm	**0.287**	**<0.001**	0.118	0.101[(1)]	0.050	0.359	0.053	0.183	<0.001	0.900	0.053	0.062

pH Ave: average pH value, pH 10cm: pH value of the upper 10cm, Moisture Ave.: average moisture content, Moisture 10cm: moisture content of upper 10 cm. [(1)] For this case the assumption of homogeneity of the variance is violated. A non-parametric analysis with a Kruskal-Wallis test leads to a significant effect of land use on pH 10cm (P=0.035).

Table 2.5 Best linear models to predict SOC stocks with soil formation or environmental variables and soil properties. The table lists model-averaged standardized coefficients (Beta) with associated significance (P). The bracket under each soil formation or environmental variable means the category with Beta=0. Coefficients with P<0.05 are shown in bold. Averaging was done over the models that were within a ΔAICc value of 2 from the best model (all-subsets regression up to five predictors). R^2 denotes the range of R^2 values for the models used in the averaged model. ΔR^2 denotes the range of explained variance by the fixed factors for the models used in the averaged mode.

		Categorical variable						Numeric variable		Conditional variable			
		Lithology (acid)	Grazing intensity (none)			Slope position (top)		Altitude	Slope angle	Soil depth	Soil moisture	R^2	ΔR^2
		Calcareous	Low	Medium	High	Slope	Top						
SOC stocks total	Beta	**0.18**	-	-	-	**-0.20**	-0.14	0.16	-0.11	**0.65**	**0.26**	**0.68 – 0.71**	**0.04-0.07**
	P	**0.014**	-	-	-	**0.033**	0.177	0.098	0.113	**<0.001**	**0.006**		
SOC stocks 10cm	Beta	**0.30**	-0.01	**0.26**	0.02	-0.23	-0.07	0.17	-	-	**0.53**	**0.48 – 0.59**	**0.11-0.22**
	P	**0.001**	0.905	**0.020**	0.844	0.068	0.615	0.117	-	-	**<0.001**		

Table 2.4 Relation between SOC and single soil formation or environmental variable through multiple linear regression, with soil depth and/or moisture involved as conditional variables. The table lists standardized coefficients (Beta) with associated significance (P). Coefficients with a p-value <0.05 are shown in bold. The bracket under each soil formation or environmental variable means the category with Beta=0. The P-values in the last column give the significance of the total model (i.e. resulting from an ANOVA of the regression model).

	Categorical variable										Numeric variable		Conditional variable				
	Lithology (acid)	Land use (F)				Grazing intensity (none)			Slope position (top)		Altitude	Slope Angle	Soil depth	Moisture	R^2	Adjusted R^2	P value
	calcareous	G	CG	AC	C	Low	Medium	High	Slope	Valley							
SOC stocks total																	
Beta	**0.18**												**0.61**	**0.31**	**0.673**	**0.658**	**<0.001**
P	**0.020**												**<0.001**	**<0.001**			
Beta		-0.08	-0.13	-0.06	-0.15								**0.57**	**0.35**	0.675	0.643	**<0.001**
P		0.534	0.217	0.670	0.091								**<0.001**	**<0.001**			
Beta						-0.03	0.06	-0.05					**0.60**	**0.34**	0.654	0.626	**<0.001**
P						0.726	0.517	0.654					**<0.001**	**<0.001**			
Beta									-0.12	-0.02			**0.61**	**0.36**	0.656	0.635	**<0.001**
P									0.240	0.860			**<0.001**	**<0.001**			
Beta											0.15		**0.65**	**0.29**	0.662	0.647	**<0.001**
P											0.071		**<0.001**	**0.002**			
Beta												-0.11	**0.59**	**0.34**	0.656	0.641	**<0.001**
P												0.140	**<0.001**	**<0.001**			
SOC stock 10cm																	
Beta	**0.32**													**0.58**	**0.472**	**0.456**	**<0.001**
P	**0.001**													**<0.001**			
Beta		-0.07	-0.06	-0.04	-0.17									**0.61**	0.399	0.352	**<0.001**
P		0.699	0.689	0.823	0.147									**<0.001**			
Beta						0.02	**0.30**	0.04						**0.59**	**0.447**	**0.413**	**<0.001**
P						0.861	**0.013**	0.739						**<0.001**			
Beta									-0.23	-0.06				**0.60**	0.407	0.380	**<0.001**
P									0.087	0.671				**<0.001**			
Beta											**0.20**			**0.57**	**0.406**	**0.388**	**<0.001**
P											**0.049**			**<0.001**			
Beta												-0.06		**0.60**	0.373	0.354	**<0.001**
P												0.570		**<0.001**			

- SOC stocks controlled by lithology and soil depth

Table 2.5 shows the best linear model sets to predict the total SOC stocks and the SOC stocks of the upper 10 cm with all possible combinations of the SFE factors. The best predictive model for the total SOC stocks included lithology, slope position, altitude, slope angle and the conditional variables (soil depth and moisture), in which lithology, category slope of the slope position were significant predictive variables (Table 2.5). For the SOC stocks of the upper 10 cm, the best model included lithology, grazing intensity, slope position, altitude and the conditional variable (soil moisture), with lithology and medium grazing intensity as significant predictors (Table 2.5). With the SFE factors involved, the best models explained an extra 4% - 7% variation of the total SOC stocks and an extra 11% - 22% variation of SOC stocks of the upper 10 cm, comparing to the cases only conditional variables involved (Table 2.5).

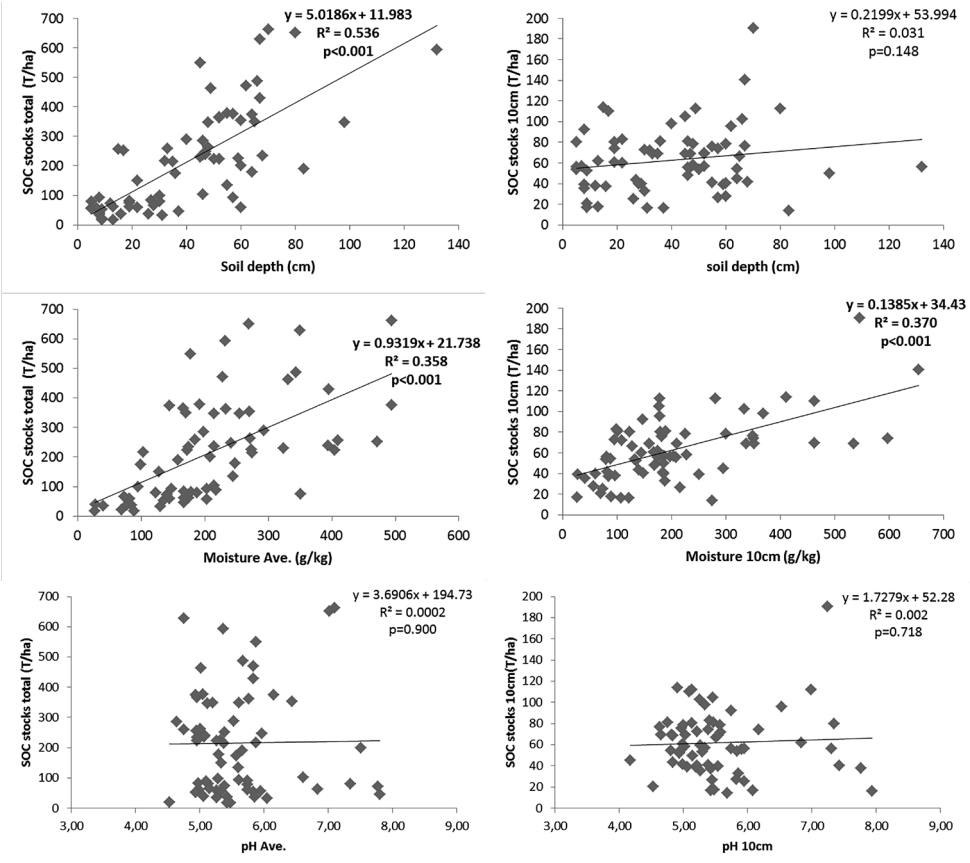


Fig. 2.3 Linear models (univariate linear regression) using soil depth, moisture and pH to predict total SOC stocks and SOC stocks of upper 10 cm. pH Ave: average pH value, pH 10 cm: pH value of upper 10 cm, Moisture Ave.: average moisture content, Moisture 10cm: moisture content of upper 10 cm.

- SOC stocks controlled by lithology and soil depth

2.4. Discussion

2.4.1. Soil organic carbon (SOC) stocks

The SOC stocks in our study area (215 ± 21 Mg ha^{-1} for the whole profiles, on average 41 ± 3 cm deep, Table 2.1) were higher than the global average levels (50 Mg ha^{-1} to 150 Mg ha^{-1} over 1 m; Lal 2004). Our C-rich soils with acidic bedrocks correspond to Andosols, and dark soils with calcareous bedrocks correspond to Chernozems or Phaeozems (WRB, 2006). Batjes (2014) reported that SOC stocks assessed to 50 cm depth are 165 Mg ha^{-1} in Andosols, 86 Mg ha^{-1} in Chernozems and 105 Mg ha^{-1} in Phaeozems. When we compare our soils with acidic bedrocks (185 ± 25 Mg ha^{-1}) to Andosols and soils on calcareous bedrocks (258 ± 34 Mg ha^{-1}) to Chernozems or Phaeozems, our soils had higher average total SOC stocks (Fig. 2.2). Studies in other Andean alpine grassland soils showed either higher or lower SOC stocks compared to our results. Tonneijck et al. (2010) reported SOC stocks reaching 530 ± 40 Mg ha^{-1} in volcanic ash soils in Northern Ecuador, which are higher than our C stocks, due to high SOC concentrations (15 ± 5%) and deep soils (150–200 cm). Sarmiento and Bottner (2002) showed that SOC concentrations of Venezuelan Andean grassland were 10.54 ± 0.07% in the upper 20 cm, which is higher than our SOC concentrations in the upper 10 cm (7.61 ± 0.53%, Supplemental Table 2.1). Farley et al. (2004) showed that carbon stocks in the upper 10 cm soil in an Ecuadorian grassland were 50 Mg ha^{-1}, which is slightly lower than our SOC stocks in the upper 10 cm (63 ± 4 Mg ha^{-1}, Table 2.1). Muñoz García and Faz Cano (2012), Rolando et al. (2017a), Segnini et al. (2011) and Zimmermann et al. (2009) reported lower SOC stocks in Puna grasslands from Bolivia to Central Peru when compared to our results (Table 2.1). Moreover, alpine or subalpine soils outside Andean regions were also reported to have lower SOC stocks compared to our results (Garcia-Pausas et al., 2007; Yang et al., 2008).

2.4.2. Effects of lithology and altitude

Our study area is characterized by heterogeneous parent materials (lithology), which should be distinguished from areas with homogeneous volcanic-ash soils (e.g. Buytaert et al., 2006; Tonneijck et al., 2010). In our results, lithology was the most important factor to predict SOC stocks when soil depth and soil moisture were involved as conditional variables, as indicated by the high Beta values, R^2 and adjusted R^2 compared to other SFE factors (Tables 2.4 and 2.5). Doetterl et al.

(2015) highlighted the importance of soil mineralogy to predict SOC storage. This is consistent with our results, because soil mineralogy is closely related to the lithology. Similarly, Heckman et al. (2009) found that SOC distribution and stabilization is controlled by parent materials and soil mineralogy. Wagai et al. (2008) indicated that the interaction between lithology and climate had effects on the quality of SOC.

The lithology controlled SOC stock patterns can be explained by the lithology related stabilization mechanisms of soil organic matter (SOM). SOC stocks are controlled by the stabilization of SOM, and stabilization of SOM can be further explained by the occlusion of OM in soil aggregates and by the association of OM with the mineral surface (Lehmann and Kleber, 2015; Lützow et al., 2006; Six et al., 2002). The association between OM and mineral surface is considered as a major mechanism contributing to long-term OM stabilization (Mikutta et al., 2006; Schrumpf et al., 2013). The OM-mineral association is largely controlled by soil mineralogy and climate (Breemen and Buurman, 2003). As climate conditions in our study are not much differentiated, lithology, which determines soil mineralogy, becomes a potential factor controlling SOC stocks. Evidence for this explanation is that soil pH values are significantly different between acidic and calcareous bed-rocks ($P < 0.001$, Table 2.3). The differences in pH are potentially related to differences in the type of interaction of SOM with the soil mineral phase. In alkaline and neutral soils, organo-mineral associations are generally formed by polyvalent cation bridges, especially Ca^{2+} bridges; whereas in acidic soils, association of Fe and Al (hydr) oxides with OM and the formation of organo-metallic complexes are major ways for OM stabilization (Lützow et al., 2006; Percival et al., 2000). Furthermore, soils rich in Ca are generally characterized by stable soil aggregates and good soil structure (Bronick and Lal, 2005). In our field observations, we found Iron pans(data not shown), which indicate high contents of iron oxides, in the soils formed on ignimbrite (an acidic bedrock). We also observed that soils with calcareous bedrocks have more stable aggregates and better structure than soils with acidic bedrocks. Our evidence indicates that the lithology related distribution of SOC stocks is in accordance with the consensus of the literature that described mineralogy related OM stabilization mechanisms.

Altitude also had significant effects on SOC stocks of the upper 10 cm, with generally higher SOC stocks at higher altitudes (Tables 2.2 and 2.4). Altitude is

reported as a factor having positive, negative and no relation on SOC stocks (Garcia-Pausas et al., 2007; Leifeld et al., 2005; Schawe et al., 2007; Zimmermann et al., 2009). The positive relations between the altitude and the SOC stocks in our study may be explained by altitude related OM stabilization. de Koning et al. (2003) and Tsai et al. (2010) found amorphous Fe and Al fractions increasingly promote the OM stabilization with increasing altitude. It also can be explained by the low decomposition rate of OM at higher altitude (Du et al., 2014). Places with higher altitude generally have lower temperature, and in our study with high soil moisture contents (Table 2.3). As a result, soils at higher altitudes may have lower OM decomposition rates because of wet and cold climate, compared to soils at lower altitudes.

2.4.3. Effects of land use, grazing intensity and topography

Effects of land use (change) on SOC stocks have been intensively studied. Generally, SOC stocks are higher in grassland and forest soils than in cropland soils, and shifts from grassland or forest to cropland cause depletion of SOC (Guo and Gifford, 2002; Poeplau and Don, 2013). However, the direction and magnitude of the shifts depend on climate factors and soil mineralogy (Powers et al., 2011). Land use had very limited effects on SOC stocks in our study as we only find significant differences of the total SOC stocks between two land use types in a non-significant linear model (Table 2.2). In high Andean soils, Nierop et al. (2007), Rolando et al. (2017a), Tonneijck et al. (2010) and Zimmermann et al. (2009) also reported no differences in SOC stocks between different land use patterns (generally grassland and forest). In our study, the limited effects on land use can be explained by the alternating land use patterns mentioned in the 2.1 site description part. The land use types alternate within a short period, and as a result, the C reserved in soils is likely in a dynamic balance. However, Rolando et al. (2017a) observed shifts in SOC fractions between different land uses in a Peruvian high-Andes grassland, which suggested investigation on SOC fractions can be more effective than on bulk SOC.

Effects of grazing intensity on SOC stocks have been widely studied, in which positive, negative and neutral effects were reported (Cui et al., 2005; Piñeiro et al., 2010; Podwojewski et al., 2002). These inconsistent results can be explained by the variation of vegetation and SFE factors (McSherry and Ritchie, 2013; Piñeiro et al., 2010). Our results showed significant effects of grazing only on SOC stocks of upper 10 cm (Tables 2.2 and 2.4), which suggest that the topsoil may be more

sensitive to grazing. Grazing activities influence SOC, by controlling net primary productivity and C decomposition pathways, and these pathways have more influence on the topsoil than the subsoil (Piñeiro et al., 2010).

SFE factors such as topography (slope position and slope angle) play limited roles in controlling SOC stocks, because we found that (1) slope position acted as a significant predictor only in the best linear model predicting total SOC stocks (Tables 2.2, 2.4 and 2.5); (2) slope angle was not the significant predictive variable (Tables 2.2, 2.4 and 2.5). This may be explained by the tropical location with low latitude (9° S), which indicates relatively homogeneous solar radiation and soil wetness in different aspects. This is supported by the independence of soil moisture from most of the topographical variables (except for altitude and average moisture, Table 2.3). In contrast, topographical factors such as aspect were reported to have strong effects on SOC in regions of higher latitudes with large annual variation of solar radiation (Garcia-Pausas et al., 2007; Schwanghart and Jarmer, 2011; van Hall et al., 2016).

2.4.4. Soil depth and moisture

Our results showed that soil depth was positively related to the total SOC stocks (Fig. 2.3), and explained a large part of variation of the total SOC stocks when compared with soil moisture and SFE variables (R^2=0.536 in Fig. 2.3, large Beta values in Tables 2.4 and 2.5). In addition, including soil depth as a conditional variable can largely improve the linear model to explain more variation of the SOC stocks (comparing R^2 and adjusted R^2 between Tables 2.2 and 2.4). The results indicate the importance of soil depth to predict the total SOC stocks. Similar to our results, Garcia-Pausas et al. (2007 and Zimmermann et al. (2009) also found positive correlations between SOC stocks and soil depth, whereas Yoo et al. (2006) concluded that soil depth is the key factor predicting the spatial SOC patterns. Furthermore, we found no relation between soil depth and SFE factors (Table 2.3), which indicates that soil depth is independent of any SFE factor in our study. Similarly, Garcia-Pausas et al. (2007) found that soil depth cannot be explained by any SFE factor including topographical factors. In contrast, Yoo et al. (2006) found that soil depth is controlled by geomorphic factors, and Zimmermann et al. (2009) found soil depth generally has positive correlations with altitude. The findings underpin the importance of including soil depth to predict SOC stocks, whereas the relation between soil depth and SFE factors need further study.

- SOC stocks controlled by lithology and soil depth

Our results showed that soil profiles with depths of 10 cm and 40 cm (average depths 41 cm) contained 29.3% and 80.0% of the total SOC stocks (Table 2.1). This indicates that sampling constant soil depths instead of the entire soil profiles can cause underestimations of SOC stocks, even assessed with average soil depths. Similarly, Tonneijck et al. (2010) found that the C stocks of Ecuadorian volcanic-ash soils assessed to 200 cm depth were 1.8 to 4.9 times of C stocks assessed to 30 cm depth. As many studies of SOC stock estimation only include soils with constant depths despite large potential SOC stocks in deep soils, SOC stocks can be generally underestimated (Batjes, 2014; Harrison et al., 2011; Wiesmeier et al., 2012). In order to avoid missing the information of the subsoil, SOC stocks are recommended being determined with the entire soil profile up to the C or R horizon, as the composition and stabilization of the deep soil C has distinguishing characteristics when compared to the topsoil C (Schmidt et al., 2011; Wiesmeier et al., 2012). Our results confirm the necessity to include the entire soil profile to avoid bias in the estimation of SOC stocks.

Another problem using constant soil depths, especially when only upper soil layers are involved, is that the effects of the SFE factors on SOC stocks can be overestimated (Harrison et al., 2011; Wiesmeier et al., 2012). Our results showed that models predicting the SOC stocks of the upper 10 cm had higher ΔR^2 values (0.11–0.22) than models predicting the total SOC stocks (0.04–0.07), which indicates SFE factors explained more variation of SOC stocks of the upper 10 cm than of the total SOC stocks (Table 2.5). This suggests the risk of overestimation of the effects of SFE factors when only using the upper soil layers. This can be further substantiated by our linear models without condition variables, which indicates that effects of lithology, grazing intensity and altitude were significant on the SOC stock of the upper 10 cm, but were not significant on the total SOC stocks (Table 2.2). The overestimated effects were also discussed by Poeplau et al. (2011), who found that the subsoil C varied less than the topsoil C with influences of land use change. Furthermore, Podwojewski et al. (2002) found that long-term intensive grazing stimulated soil erosion, which caused destruction of soil structure and C loss from the topsoil rather than the subsoil.

We found that soil moisture was positively related to the SOC stocks, and also explained a large part of the variation of the SOC stocks (Fig. 2.3 and Table 2.4). Other studies also found positive relationships between SOC and soil moisture, and

the positive relationships are often explained by moisture related biodegradation and/or OM stabilization (Farley et al., 2004; Krull et al., 2003; Yang et al., 2008). Based on the Beta values in the linear models, soil moisture explained less variation of total SOC stocks than soil depth, but explains more variation than lithology and grazing intensity (Tables 2.4 and 2.5). However, soil moisture data in our study may have limited power, because of the variation of soil moisture introduced by the cycle of dry and wet seasons. Nevertheless, the climate condition was stable throughout the sampling period, which means the soil moisture data of different plots are comparable.

2.5. Conclusions

Our results showed overall high SOC stocks of Andean grassland soils in the study area, when compared with global average levels as presented by Batjes (2014) and Lal (2004) with similar soil depths and soil groups (WRB, 2006). Total SOC stocks were largely controlled by soil depth, followed by soil moisture. When soil depth and moisture were controlled as conditional variables, lithology became the most important SFE factor for explaining the variation of the total SOC stocks. For SOC stocks of the upper 10 cm, soil moisture, lithology, grazing intensity and altitude were significant factors. Our results indicate that it is important to include the entire soil profile instead of a constant depth to avoid the underestimation of total SOC stocks. Alternatively, when soil samples are only collected from the top or with limited constant depths, effects of the SFE factors on SOC stocks can be overestimated. Therefore, when studying SOC stocks, we recommend sampling the entire soil profile up to the C or R horizon, instead of sampling with a limited constant depth.

In addition to soil depth and moisture, lithology was the most important factor to predict SOC stocks in our study area. As lithology is closely related to mineralogy linked OM stabilizations, further research on mineralogy related mechanisms of SOC sequestration and SOM stabilization may be useful to give applicable information for the management of this region. In addition, intensive grazing activities may be restricted, because these activities may increase risks of SOC loss and erosion induced topsoil material removal. Furthermore, the alternating land use pattern in our study region may be a good example to keep a dynamical balance of high SOC stocks.

- SOC stocks controlled by lithology and soil depth



Chapter 3

Lithology controlled soil organic carbon stabilization in an alpine grassland of the Peruvian Andes

This chapter has been accepted for publication by Environmental Earth Sciences:

Yang, S., Jansen, B., Kalbitz, K., Chunga Castro, F.O., van Hall, R.L., Cammeraat, E.L.H., 2019. Lithology controlled soil organic carbon stabilization in an alpine grassland of the Peruvian Andes. Environmental Earth Science in press.

Abstract

Alpine grasslands of the Neotropical Andes have high soil organic carbon (SOC) stocks and provide crucial ecosystem services. However, stability of the SOC in these grasslands is not well-studied. Having insights into SOC stability contributes to a better understanding of ecosystem vulnerability and maintaining of ecosystem services. The objectives were to get a first insight in organic matter (OM) stabilization in soils from different bedrocks of Andean alpine grasslands near Cajamarca, Peru (7°11" S, 78°35" W) and how this controls SOC stocks. Samples were collected from soils formed on limestone and acid igneous rocks. Stabilization mechanisms of OM were investigated using selective extraction methods separating active Fe, Al and Ca fractions and determined SOC stocks. In both soil types, the results showed important contributions of complexation with and/or adsorption on Fe and Al (oxides) to OM stabilization. Exclusively in the limestone soils, Ca induced OM stabilization by promoting the formation of Ca^{2+} bridges between OM and mineral surfaces. Furthermore, no evidence showed that OM stabilization was controlled by crystalline Fe oxides, clay contents, allophones, Al toxicity or aggregate stability. Limestone soils had significantly higher SOC stocks (405±42 Mg $ha^{-1)}$ compared to the acid igneous rock soils (226±6 Mg ha^{-1}), which is likely explained by OM stabilization related to Ca^{2+} bridges in addition to the stabilization related to Fe and Al (oxides) in the limestone soils. Our results suggest a shift from OM stabilization dominated by Fe and Al (oxides) to that with the presence of Ca-related cation bridges, with increasing pH values driven by lithology.

Keywords: Soil organic matter; Stabilization; Limestone; Acidic igneous bedrocks; Carbon stock

3.1. Introduction

The soil acts as the largest terrestrial carbon (C) pool and plays an important role in global C dynamics (Lal, 2004; Luo et al., 2016). Alpine grassland soils of the Neotropical Andes are characterized by their high soil organic carbon (SOC) stocks and play an important role as the water source for the coastal regions with an arid climate (Buytaert et al., 2011; Rolando et al., 2017b; Tonneijck et al., 2010). However, these grasslands suffer high risks of degradation due to ongoing and future climate change (Gang et al., 2014). To assess the vulnerability of the SOC stocks and the relevant ecosystem services, it is crucial to understand the mechanisms responsible for the stability of the SOC (Buytaert et al., 2011; Rolando et al., 2017b). However, SOC stability is not fully understood, as it is controlled by various environmental and soil formation factors at different scales (Wiesmeier et al., 2019). Most studies on SOC stocks and stabilization in ash soils of the Andean regions focused on the Páramo ecosystem in Ecuador, Colombia, Venezuela and northern Peru (Buytaert et al., 2006b; Hribljan et al., 2016; Tonneijck et al., 2010). However, soils formed on substrates other than volcanic ash, such as soils that occur in the central and southern Peruvian highland, also contain large SOC stocks. These soils have received less attention, especially with respect to the persistence and stability of the SOC (Muñoz-García and Faz-Cano, 2012; Rolando et al., 2017a; Zimmermann et al., 2009)

The dynamics and turnover of SOC are largely controlled by the stabilization of soil organic matter (OM) (Six et al., 2002; Sollins et al., 1996). Recently, we have seen a shift from traditional views of soil OM stabilization based on the 'humification' model and molecular recalcitrance to a new paradigm based on the protection of soil OM by the soil matrix against decomposers (Dungait et al., 2012; Lehmann and Kleber, 2015; Schmidt et al., 2011). In this paradigm, soil physicochemical properties regulate the maximum capacity to stabilize OM (Six et al., 2002). In general, soil OM is considered to be stabilized by: (1) recalcitrance of OM compounds due to their chemical properties, (2) spatial inaccessibility against decomposers because of the protection of soil aggregates, and (3) reduced availability to decomposers as a result of interaction with soil mineral surfaces and metal ions (Lützow et al., 2006). The interaction between OM and the mineral surfaces is considered as a key stabilization mechanism, and controls long-term retention of the OM (Kleber et al., 2015; Schrumpf et al., 2013). In acidic soils, the OM is generally stabilized by ligand exchange with

non-crystalline Fe and Al oxides, as well as complexation with Fe and Al cations. In neutral and alkaline soils, the OM is thought to be stabilized by interaction with the mineral surface through polyvalent cation bridges (e.g. Ca^{2+} bridge) (Lützow et al., 2006; Takahashi and Dahlgren, 2016; Wiesmeier et al., 2019).

Environmental and soil formation factors are considered to play an important role in controlling the persistence and stabilization of soil OM, through complex interactions with other factors including soil minerals, microbes and vegetation (Luo et al., 2016; Schmidt et al., 2011). Recent studies indicate the role of soil mineralogy as a key factor controlling OM stabilization (Doetterl et al., 2015; Heckman et al., 2009). As soil mineralogy is largely determined by the bedrocks and weathering processes, spatial heterogeneity in the bedrocks can induce differences in soil mineralogy and further impact the soil OM stabilization (Wattel-Koekkoek et al., 2003). A previous study in the same area of the present study confirmed that the distribution of SOC stocks depends on lithology (bedrocks)(Yang et al., 2018). The lithology dependent SOC distribution suggests that differences in OM stabilization can be expected to occur for soils with contrasting bedrocks.

The storage, turnover and stabilization of OM can differ substantially between the topsoil and the subsoil (Batjes, 2014; Fontaine et al., 2007; Rumpel and Kögel-Knabner, 2010). Vertical distribution of SOC is related to processed including OM input, decomposition, stabilization and downwards movement. These processed are potentially controlled by pedological processes driven by bedrocks (Kaiser and Kalbitz, 2012; Rumpel and Kögel-Knabner, 2010). Investigating the vertical distribution patterns of OM could yield a better understanding of the SOC distribution as controlled by the spatial distribution of the lithology in the Peruvian Andes.

Our present study aimed to explore the differences in SOC stocks between well-developed limestone soils (LSs) and acid igneous rock soils (ASs) in the Peruvian Andes, and to elucidate potential differences in OM stabilization mechanisms operating in these different lithologies. For this, selective extraction methods were applied in combination with bivariate and partial correlation analysis to identify functional fractions most likely responsible for OM stabilization.

3.2. Methods and materials

3.2.1. Site description

The study area was located to the west of the city of Cajamarca, Peru, with coordinates 7° 11' S, 78° 35' W. The area was on the continental watershed between the Atlantic and the Pacific Ocean, belonging to the Western Cordillera mountain chain of the Andes. The altitudes of our sampling region were between 3500 and 3720 m asl. The annual average temperature and precipitation were estimated as 9 °C and 1100 mm at an altitude of 3500 m asl, based on climate data of Station Porcon 2 (3510 m asl) and Station Cumbe Mayo (3410 m asl). The temperature was characterized by limited seasonal but large daily variations, whereas the majority of the precipitation occurred in wet seasons between October and April (Seijmonsbergen et al., 2010; Sánchez Vega et al., 2006).

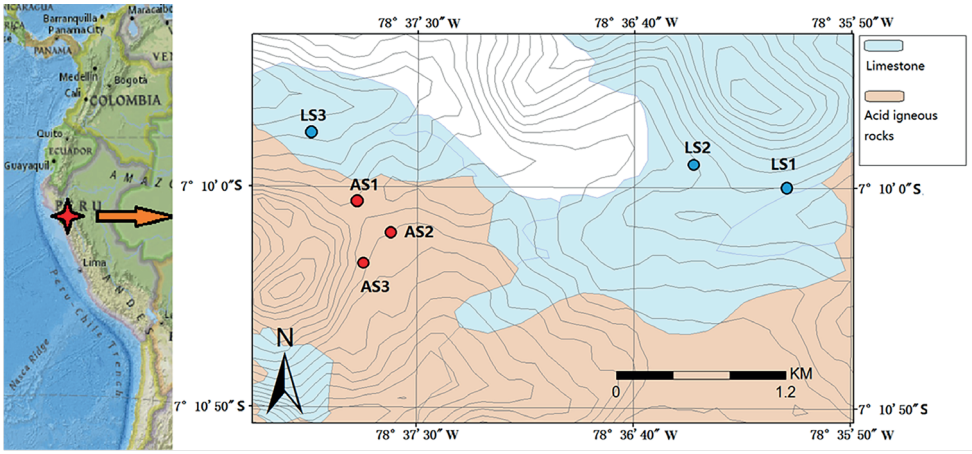
The geological formations consist of a basement of folded Cretaceous marine sediments intruded and overlain by igneous rocks. The sediments include the formations of Cajamarca, Chulec-Calizas, Pariatambo, Farrat and Yumagual, with bedrocks of limestone, shale, marl and quartzite. The igneous bedrocks that belong to the San Pablo formation include intrusive granitic rocks and extrusive ignimbritic rocks (Geo GPS Perú, 2014; Reyes-Rivera, 1980).

The study area belongs to the Jalca (Sánchez Vega et al., 2005) or wet Puna phytoregion (Rolando et al., 2017b), a Neotropical alpine grassland ecosystem as a transition between humid Páramo to the north and dry Puna to the south. This region is characterized by large geodiversity and biodiversity. Significant human activities include cultivation and grazing, which cause land use change and potential degradation of vegetation. The land use pattern is characterized by rotations of cultivation, fallow and grazing, within a period of more than 2 years (Sánchez Vega et al., 2005; Tovar et al., 2013).

3.2.2. Soil sampling and classification

Soil samples were collected in July 2015, the dry season of this region. Fig. 3.1 gives the information of 6 sampling plots characterized by contrasting bedrocks (lithology): 3 limestone plots and 3 acid igneous rock plots, respectively. The plots of acid igneous rocks were located in the transition zone between granite and ignimbrite. In addition to contrasting bedrocks, other factors related to soil

formation were similar for each plot. The sampling plots were selected to meet the following three criteria: 1) located at gentle foot slopes with a stable environment for soil development, 2) having soils directly developed from the bedrocks rather than alluvial materials, and 3) being without crop production or intensive human disturbance. In addition, sampling next to forest patches was avoided to minimize the influence of soil acidification caused by the forest. Soil horizons were diagnosed by field observation. LSs had thick dark A horizons and argic B horizons above the C horizons, whereas ASs had dark vitric A horizons directly above C horizons or weathered bedrocks. Hereby we define the topsoil as A horizons and the subsoil as B horizons. Samples for the SOC stock determination were collected every 10 cm in duplicate with Kopecky rings (100 cm^3) until the C horizons were reached. Samples for soil property analysis and selective extractions were collected in duplicate by diagnostic horizons, with each sample weighing 500-800 g. All samples were transferred into sealed plastic bags before transportation. Soil classification was based on the WRB (2014).



Site	Bedrock	Altitude	Soil depth	Slope angle	Volcanic glass	Phosphate retention	Soil Group
		m	cm	°	%	%	
LS1	Limestone	3716	57	7	n. d.	n. d.	Luvic Phaeozems
LS2	Limestone	3717	66	11	n. d.	n. d.	Haplic Phaeozems (Lixic)
LS3	Limestone	3517	60	10	n. d.	n. d.	Haplic Phaeozems (Lixic)
AS1	Granite/ignimbrite	3583	68	7	50%	59.5%	Umbric Vitric Andosol
AS2	Granite/ignimbrite	3585	45	9	30%	84.8%	Umbric Vitric Andosol
AS3	Granite/ignimbrite	3586	35	14	25%	77.0%	Mollic Vitric Andosol

Fig. 3.1 Sampling site description. *LS: limestone soil, AS: soil on acid igneous rocks, n. d.: not determined*

3.2.3. Soil analysis

Soil samples for the SOC stock determination were freeze-dried. For these samples, soil moisture contents and bulk densities were measured by weighing samples before and after freeze-drying. Sub-samples of 5-10 g were milled to determine carbon (C) and nitrogen (N) concentrations. For samples used for soil property analysis, a porcelain mortar was applied to break large aggregates and passed through a 2 mm sieve, in order to separate fine earth fractions and gravels. The fine earth fractions were used for selective extractions and analyses of C and N contents, silt and clay contents, pH, cation exchange capacity (CEC) and phosphate retention. Total C and N contents were analyzed with an elemental analyzer (vario EL cube, elementar GmbH, Langenselbold, Germany). Inorganic C (carbonate) contents were determined by measuring the produced CO_2 after HCl treatment using the elemental analyzer equipped with a TIC module. As inorganic C contents were negligible in all the samples except for the C horizon of the profile LS2, the total C contents were equal to the OC concentrations. For the sample containing inorganic C (3.1 % inorganic C, data not shown), the organic C content was calculated by subtracting the inorganic C content from the total C content. Silt plus clay (S+C) contents were determined using wet sieving through a 0.063 mm sieve after soil dispersion and OM removal using an H_2O_2 solution for 3 days. The S+C fractions obtained were further used for the clay contents determination using a Sedigraph system (Sedigraph III Plus, Micromeritics, Norcross, USA). Soil pH was determined with a glass electrode in suspensions of soil material in demi-water (w:v=1.5). Phosphate retention was measured using the colorimetry method mentioned by (Blakemore et al. (1987). The percentage of volcanic glass was evaluated from the sand fractions by counting of glass particles using a 40× microscope (Leica M420, macroscope, Leica, Wetzlar, Germany).

Total SOC stocks were calculated by addition of the SOC stocks determined every 10 cm until the C horizon, using the equation:

$$SOC\ stock = \sum_{i=1}^{i=k} BD_i \times C_i \times (1 - S_i) \times D_i$$

In this equation, BD_i = bulk density (g cm^{-3}) of the layer i, C_i = SOC concentration (%) of the layer i, S_i = stoniness (%) of layer i, D_i= thickness (cm) of layer i.

A 0.2 M ammonium oxalate solution was used to extract poor-crystalline Fe and Al (Fe_o and Al_o) at pH=3, using the procedure mentioned by Schwertmann (1964). A 0.1 M sodium pyrophosphate solution was applied to extract Fe, Al and C (Fe_p, Al_p and C_p) from organo-metallic and organo-mineral complexes with minor Al from non-crystalline oxides (Kaiser and Zech, 1996; Kögel-Knabner et al., 2008; Wada, 1989). A citrate-dithionite solution was applied to extract pedogenic Fe (Fe_d) fractions, and the crystalline Fe was calculated by subtracting Fe_o from Fe_d (Holmgren, 1967). A solution of 0.125 M $BaCl_2$ was applied to determine the exchangeable cation contents (Ca_{ex}, Mg_{ex}, Al_{ex}, etc.) and calculate the CEC and the base saturation (BS) (Hendershot and Duquette, 1986). Concentrations of Fe and Al in extracts of citrate-dithionite and pyrophosphate were determined with an Perkin Elmer AAnalist 400 Atomic Absorption Spectrometer (Perkin Elmer, Waltham, USA). Fe, Si and Al concentrations in the ammonium oxalate extracts and Na, K, Ca, Mg, Al, Fe and Mn concentrations in the $BaCl_2$ extracts were determined with a Perkin Elmer Optima-8000 ICP OES (Perkin Elmer, Waltham, USA). In the $BaCl_2$ extracts, the acidity was determined by titration with a 1.0 M NaOH solution, and the NH_4 concentrations were measured by colorimetry at 670 nm with the hypochlorite and salicylate solutions (Krom, 1980). The organic C concentrations in the pyrophosphate extracts were determined with a TOC-VCPH analyzer (Shimadzu Corporation, Kyoto, Japan).

The mean weight diameter (MWD) was determined using the dry-sieving method. Briefly, air-dried soil samples (<16 mm) were fractionated with 4 sieves (5, 2, 0.25 and 0.063 mm) for 20 s at 20 Hz using a horizontal shaker. All fractions >2 mm were corrected for gravel contents. Bulk soil samples and the 5 sieved fractions were weighed, and the MWDs were calculated using the equation:

$$MWD = \sum_{i=1}^{i=5} \left(x_{i\,max} + x_{i\,\min}\right)/2 \times w_i$$

In this equation, $x_{i\,max}$ = maximum diameter (mm) of the fraction i, $x_{i\,min}$ = minimum diameter (mm) of the fraction i, w_i = weight percent of the fraction i.

Macroaggregate stability was determined using a wet sieving method following a modified procedure of Amézketa (1999). Briefly, 5 g air-dried (40 °C) aggregates (>2 mm) were placed on a 2 mm sieve with a horizontal shaker. The aggregates were fast-wetted by water showers and shaken at 20 Hz for 5 min. Materials remaining on the 2 mm sieve were air-dried at 40 °C. The weight percentages of

the remaining materials to the original materials were used as the measure of macroaggregate stability. Microaggregate stability was measured using a particle size detector combined with an ultrasonic disperser (Amézketa, 1999). Briefly, the size distribution of water stable microaggregates (<0.25 mm) was determined using a sedigraph (Sedigraph III Plus, Micromeritics, Norcross, USA) with and without ultrasonic dispersion (10 s, 20 W) applied. The differences of microaggregate size distribution between dispersion and non-dispersion were used as the measure of microaggregate stability. The following equations were used to calculate respectively macroaggregate and microaggregate stability:

$$Stability(MA) = W_{2mm}/W_{all} \times 100\%$$

$$Stability(MI) = MWD_o - MWD_s = \sum_{i=1}^{i=k} x_{o\,i} \times w_{o\,i} - \sum_{i=1}^{i=k} x_{s\,i} \times w_{s\,i}$$

In the equations, *Stability (MA)* = macroaggregate stability, W_{2mm} = weight of fraction >2mm after wet sieving (g), W_{all} = weight of fraction before wet sieving (g), *Stability (MI)* = microaggregate stability, $x_{o\,i}$ = average diameter (mm) of the fraction i without sonication, $w_{o\,i}$ = weight percent of the fraction i without sonication, $x_{s\,i}$ = average diameter (mm) of the fraction i with sonication , $w_{s\,i}$ = weight percent of the fraction i with sonication.

3.2.4. Statistics

All soil samples from A and B horizons were used for the statistical analyses. A principal component analysis (PCA) was performed to get an overview of the characteristics of LSs and ASs. The reliability of the PCA (sampling adequacy and sphericity) were checked using the Kaiser-Meyer-Olkin test and the Bartlett's test before the PCA applied. One-way ANOVAs were applied to compare differences in soil properties between LS-A horizons, LS-B horizons and AS-A horizons. For the post hoc comparison, a Fisher's Least Significant Difference (LSD) test was used. Pearson correlations were applied to test for bivariate correlations between different soil properties. Pearson partial correlations were applied to test correlations between two variables when the effects of one or more other variables (covariates) were removed. The objectives of using partial correlation were to compare potential differences in correlation patterns before and after: (1) the effects of the covariates removed (zero-order and partial correlations); (2) effects between A and B horizons in the LSs removed.

When the assumption of data normality (checked by the Shapiro-Wilk test) was not met, a Kruskal–Wallis H test and Spearman (partial) correlations were applied to correspond to the one-way ANOVA and the Pearson (partial) correlations. When the assumption of variance homogeneity was violated, a Welch robust test and a Games-Howell test were applied instead of the one-way ANOVA and the LSD test. Results of these tests were reported together with original results (e.g. one-way ANOVA) as additional information. All statistical analyses were performed with SPSS 24.0 (SPSS Inc., USA). To reduce the probability of a Type II error, a significance level of $P<0.1$ was used in addition to the commonly used levels of $P<0.05$ and $P<0.01$.

3.3. Results

3.3.1. Soil classification and soil organic carbon (SOC) stocks

The LSs were characterized by dark mollic A horizons, followed by underlying lighter B horizons with clay accumulation. In contrast, the ASs had dark A horizons directly above C horizons, with the presence of volcanic glass, high phosphate retention and $Al_o+1/2Fe_o$ contents under 2 % (Fig. 3.1). Combined with the pH, CEC and BS data, the LSs can be classified as either Haplic or Luvic Phaeozems, and the ASs were classified as Vitric Andosols (Fig. 3.1).

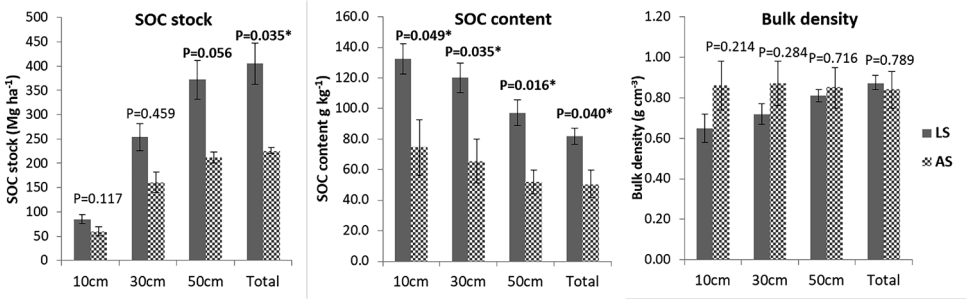


Fig. 3.2 Independent T-tests of SOC stocks, SOC contents and bulk densities accessed to different soil depths and the entire soil profiles. *Bulk density data was revised by gravel contents. LS: limestone soil, AS: acid igneous rock soil, SOC: soil organic carbon, * indicate the significant levels of P<0.05.*

Total SOC stocks were significantly higher ($P<0.05$) in the LSs (405±42 Mg ha^{-1}) compared to the ASs (226±6 Mg ha^{-1}, Fig. 3.2). The LSs had slightly higher SOC stocks compared to the ASs when accessed to 10 cm ($P>0.1$), 30 cm ($P>0.1$) and

50 cm (P<0.1) (Fig. 3.2). The SOC contents accessed to all depths were significantly (P<0.05) higher in the LSs compared to the ASs (P<0.05), whereas soil bulk densities were not significantly different between the two soil types (Fig. 3.2). In addition, soil depths were larger in the LSs (61 cm) compared to the ASs (49 cm, Fig. 3.1).

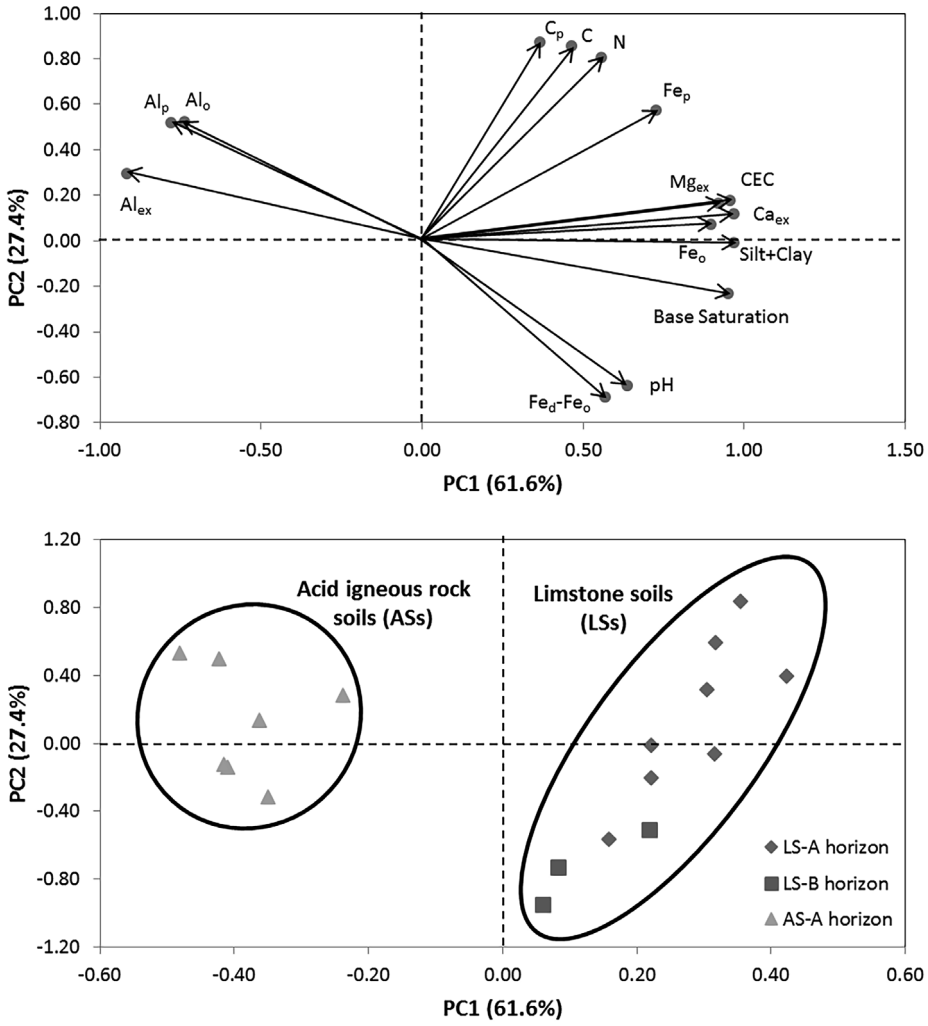


Fig. 3.3 Principal component analysis (PCA) for each soil horizon. *Figure above gives the factor loadings on the principal component 1 (PC1) and principal component 2 (PC2); Figure below shows factor scores of horizons in limestone soils and acid igneous rock soils on the PC1 and PC2. Sampling adequacy and sphericity were checked using the Kaiser-Meyer-Olkin test (0.616) and the Bartlett's test (P<0.001), which confirm the reliability of the PCA.*

3.3.2. Overview of soil properties

Principal component 1 (PC1) and principal component 2 (PC2) explained 61.6% and 27.4% of the total variance in the PCA (Fig. 3.3). PC1 was positively loaded by exchangeable base cations, base saturation, pH, Fe fractions and silt plus clay contents, and was negatively loaded by Al fractions. PC2 had positive contributions from OM-related variables (C, C_p and N) and negative loadings of crystalline Fe oxides and pH (Fig. 3.3). LSs and the ASs were clearly separated along PC1. The LSs were associated with higher Fe fractions, exchangeable Ca and Mg, pH, CEC and base saturation, whereas the ASs were characterized by higher Al fractions (Fig. 3.3).

Table 3.1 Comparisons of soil properties related to OM stabilization in A and B horizons between limestone soils (LSs) and acidic igneous rock soils(ASs).

		LS-A horizon n=8		**LS-B horizon n=3**		**AS-A horizon n=7**		
Soil property	**Unit**	**Mean**	**SE**	**Mean**	**SE**	**Mean**	**SE**	**P value**
C	g kg^{-1}	99.5 ^{a}	12.9	28.4 ^{b}	4.5	59.5 ^{b}	10.6	**0.008****
N	g kg^{-1}	8.1 ^{a}	1.1	2.8 ^{b}	0.6	4.4 ^{b}	0.7	**0.007****
C/N		12.41 ^{a}	0.29	10.37 ^{b}	0.67	13.01 ^{a}	0.46	**0.008****
C_p	g kg^{-1}	58 ^{a}	6	18 ^{b}	0.2	39 ^{b}	6	**0.007****
C-C_p	g kg^{-1}	41 ^{a}	8	10 ^{b}	3	20 ^{ab}	5	**0.038***
C_p/C		61.4 ^{a}	4.4	66.1 ^{a}	3.7	67.3 ^{a}	4.9	0.627
Fe_o	g kg^{-1}	11.73 ^{a}	1.00	8.85 ^{ab}	3.15	2.53 ^{b}	0.13	**<0.001****
Al_o	g kg^{-1}	3.40 ^{b}	0.23	2.46 ^{b}	0.42	8.14 ^{a}	1.19	**0.001****
Fe_p	g kg^{-1}	4.52 ^{a}	0.42	2.07 ^{b}	0.19	2.03 ^{b}	0.17	**<0.001****
Al_p	g kg^{-1}	2.03 ^{b}	0.29	0.94 ^{c}	0.10	7.50 ^{a}	1.22	**<0.001 (0.001)** **
Fe_d-Fe_o	g kg^{-1}	9.96 ^{a}	1.84	17.67 ^{ab}	3.24	1.52 ^{b}	0.14	**<0.001****
Fe_p/Fe_o		40.08 ^{b}	4.43	30.37 ^{b}	10.55	79.88 ^{a}	3.42	**<0.001****
Al_p/Al_o		58.26 ^{b}	4.73	39.57 ^{c}	4.24	91.33 ^{a}	2.49	**<0.001****
mol Fe_p+Al_p	mmol kg^{-1}	156.1 ^{b}	16.5	72.1 ^{c}	7.1	314.6 ^{a}	48.1	**0.001****
mol C/(Fe_p+Al_p)		52.6 ^{a}	4.5	32.4 ^{b}	1.8	16.2 ^{c}	2.1	**<0.001****
Ca_{ex}	mmol kg^{-1}	314.5 ^{a}	24.0	199.8 ^{a}	30.4	19.5 ^{b}	4.4	**<0.001****
Mg_{ex}	mmol kg^{-1}	14.28 ^{a}	1.874	10.48 ^{ab}	2.694	2.09 ^{b}	0.62	**<0.001****
Al_{ex}	mmol kg^{-1}	0.30 ^{b}	0.12	0.07 ^{b}	0.004	11.65 ^{a}	1.56	**<0.001 (0.001)** **
CEC	cmol kg^{-1}	33.40 ^{a}	2.55	21.37 ^{ab}	3.39	6.33 ^{b}	0.66	**<0.001 (0.001)** **
Ca_{ex}/CEC		94.2 ^{a}	0.579	93.7 ^{a}	0.5	29.7 ^{b}	4.2	**<0.001****
Silt+Clay	%	89.9 ^{a}	2.1	85.6 ^{a}	6.0	44.1 ^{b}	2.5	**<0.001****
Clay	%	19.5 ^{a}	1.9	40.6 ^{ab}	9.3	5.8 ^{b}	0.9	**<0.001****
pH		5.97 ^{a}	0.18	6.56 ^{a}	0.21	5.09 ^{b}	0.09	**<0.001 (0.003)** **
MWD	mm	5.68 ^{b}	0.39	8.34 ^{a}	0.21	3.46 ^{c}	0.18	**<0.001****

*LS: limestone soil, AS: soil on acid igneous rocks, * and ** indicate the significant levels of P<0.05 and 0.01. Superscript letters indicate the significant levels of the post hoc analysis. When the assumption of normality is violated, and P values of the non-parametric test are given in the bracket. For mol (Fe_p+Al_p), the assumption of variance homogeneity is violated, the Welch test gave P values of 0.150 and <0.001.*

The LSs had significantly higher SOC and C_p contents compared to the ASs in A horizons (P<0.05, Table 3.1). The LSs also had higher Fe fractions (Fe_p, Fe_o, Fe_d-Fe_o), exchangeable base cations (Ca_{ex} and Mg_{ex}), clay contents and silt plus clay

contents than the ASs, but had lower Al fractions (Al_p, Al_o and Al_{ex}), Si_o contents and molar contents of Fe_p+Al_p (Table 3.1). Additionally, the LSs had significantly lower ratios of Fe_p/Fe_o and Al_p/Al_o but higher molar ratios of $C/(Fe_p+Al_p)$ compared to the ASs ($P<0.05$, Table 3.1). For other soil properties, the LSs were characterized by higher CEC and pH values as well as larger aggregates sizes compared to the ASs ($P<0.05$, Table 3.1). Furthermore, the LSs had more than 90% of the CEC comprised of Ca_{ex}, whereas the ASs had Al_{ex} contents lower than 2.0 cmol kg^{-1} (Table 3.1). For the LSs, A horizons had significantly higher SOC, C_p, C-C_p, Fe_p, Al_p and molar ratios of $C/(Fe_p+Al_p)$ compared to B horizons, whereas B horizons were characterized by coarser aggregates (larger) MWD compared to A horizons ($P<0.05$, Table 3.1).

3.3.3. Correlations between variables in limestone soils (LSs)

The SOC and C_p contents were positively correlated to Fe_p, Al_o, Al_p, Ca_{ex} and silt plus clay contents, but were negatively correlated to Fe_d-Fe_o and clay contents ($P<0.1$ for clay, $P<0.05$ for others, Fig. 3.4). The mean weight diameters (MWDs) of aggregates were negatively correlated to OM-related variables (C, C_p and C-C_p), pyrophosphate fractions (Fe_p and Al_p), exchangeable cations (Ca_{ex} and Mg_{ex}) and clay contents ($P< 0.1$, Table 3.2). Macroaggregate stability was not correlated to OM-related variables or extracted fractions (Table 3.2), whereas microaggregate stability was negatively correlations with C_p, Al_p and silt plus clay contents ($P<0.1$, Table 3.2).

When correlations with Ca_{ex} were removed, OM-related variables (C, C_p and C-C_p) were positively correlated to Fe_p and Al_p, except for the correlation between C-C_p and Al_p ($P<0.05$, Table 3.3). When correlations with Fe_p and Al_p were removed, OM-related variables lost their correlations to Mg_{ex}, Al_{ex} and silt plus clay contents (Table 3.3). In contrast, C and C_p were still positively correlated to Ca_{ex} (Table 3.3). When correlations with horizon were removed, correlations patterns between OM-related variables and other soil variables were not clearly changed compared to the zero-order correlations, except for correlations of C-C_p with Ca_{ex}, Al_p and Al_{ex}, as well as correlations of clay contents with C and C_p (Table 3.3). In addition, correlation patterns between OM-related variables and aggregate related variable (MWD and macroaggregate stability) were also not clearly changed when correlations with horizons were removed (Table 3.2).

➢ SOM stabilization controlled by lithology

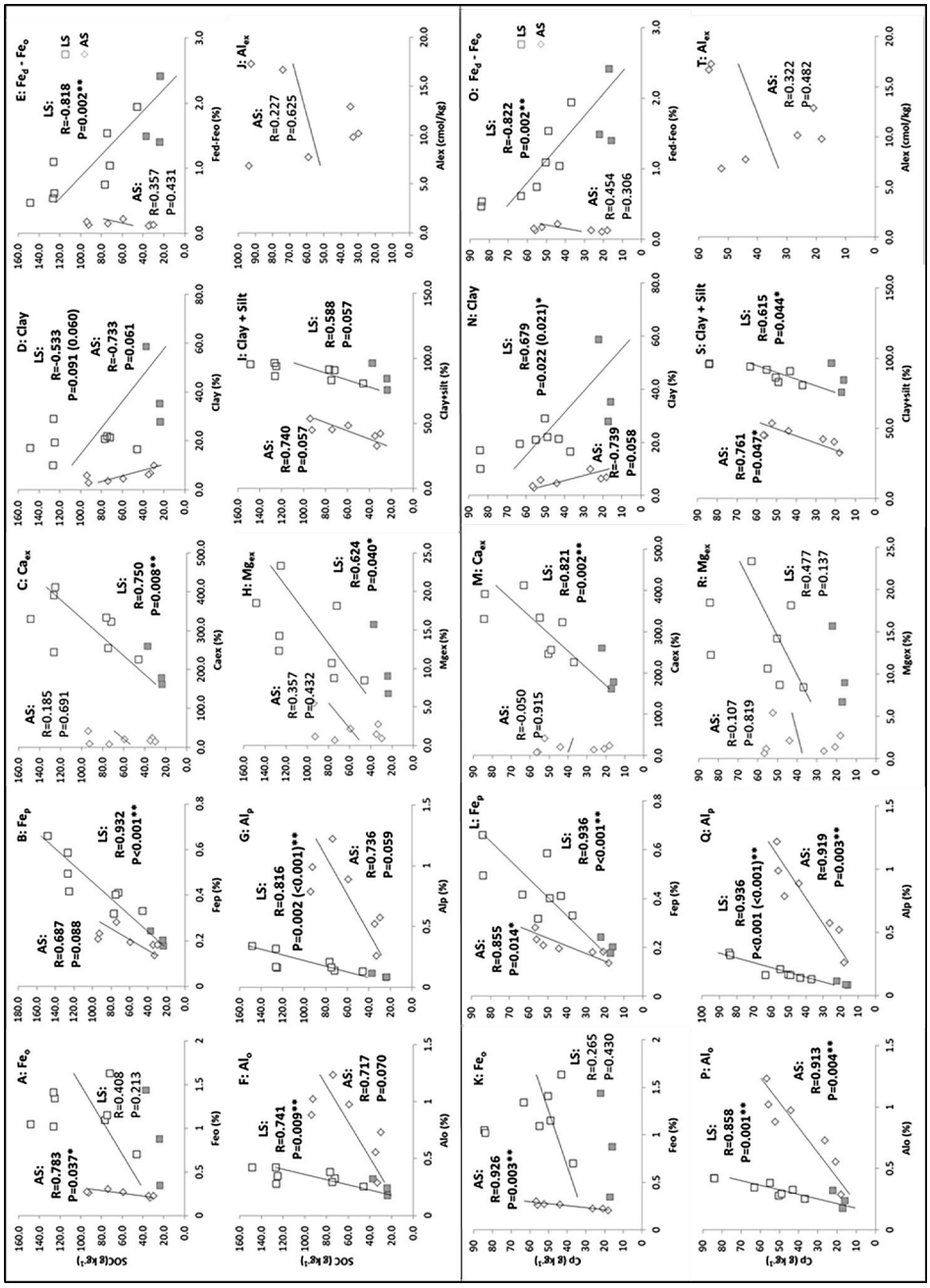


Fig. 3.4 Correlations of soil organic carbon (SOC) and pyrophosphate extracted C (C_p) with extracted Fe, Al, Ca and Mg fractions, clay and silt plus clay contents. *From A to J: correlations between SOC and soil fractions, from K to T: correlations between C_p and soil fractions, Blue hollow square: LS-A horizons, blue solid square: LS-B horizons, red diamond: AS-A horizon. * and ** indicate the significant levels of P<0.05 and 0.01, and P values between 0.05 and 0.1are shown **in bold** without *. When the assumption of normality is violated, and P values of the non-parametric test are given in the bracket.*

Table 3.2 (Partial) correlations between aggregate stability related variables and soil properties related to OM stabilization.

		C	C_p	C-C_p	Fe_p	Al_p	Ca_{ex}	Mg_{ex}	Silt + Clay	Clay
LSs n=11 Zero-order										
MWD	R	**-0.884**	**-0.866**	**-0.779**	**-0.768**	**-0.668**	**-0.804**	**-0.549**	-0.493	**0.583**
	P	**<0.001****	**0.001****	**<0.001****	**0.006****	**0.025 *(iv)**	**0.002****	**0.080**	0.123	**0.060 (ii)**
Stability (MA)	R	0.304	0.144	0.416	0.311	0.248	-0.097	0.066	0.166	0.220
	P	0.363	0.673	0.203	0.351	0.461(i)	0.777	0.847	0.625	0.515(i)
Stability (MI)	R	-0.756	**-0.908**	-0.247	-0.564	**-0.892**	-0.513	-0.154	**-0.828**	0.699
	P	0.140	**0.033***	0.689	0.322	**0.042 ***(i)	0.376	0.805	**0.084**	0.189 (i)
LSs (A vs. B horizon removed) n=11										
MWD	R	**-0.728**	**-0.646**	**-0.632**	-0.426	-0.400	**-0.616**	-0.490	-0.458	-0.053
	P	**0.017***	**0.044***	**0.050***	0.219	0.253 (i)	**0.058**	0.151	0.183	0.885 (i)
Stability (MA)	R	0.570	0.367	0.598	0.595	0.392	-0.034	0.110	0.208	0.212
	P	0.085	0.296	0.068	0.069	0.263 (ii)	0.926	0.761	0.565	0.556 (i)
Stability (MI)	R	N.A.	N.A.	N.A.	N.A.	N.A.	N.A.	N.A.	N.A.	N.A.
	P	N.A.	N.A.	N.A.	N.A.	N.A.	N.A.	N.A.	N.A.	N.A.
ASs n=7 Zero-order										
MWD	R	-0.582	**-0.761**	-0.246	**-0.706**	**-0.824**	0.522	0.382	-0.288	**0.788**
	P	0.170	**0.047***	0.594	**0.076**	**0.023***	0.230	0.398	0.531	**0.035***
Stability (MA)	R	0.544	0.399	0.619	0.209	0.269	0.261	0.389	0.203	**-0.800**
	P	0.207**(ii)**	0.375 (i)	0.138 **(iii)**	0.653(i)	0.559 (i)	0.572 (i)	0.388 **(ii)**	0.662**(ii)**	**0.031* (i)**
Stability (MI)	R	0.359	0.428	0.203	0.026	0.274	0.310	0.346	0.452	-0.162
	P	0.430	0.338	0.662	0.956	0.553	0.499	0.448	0.309	0.729

*LS: limestone soil, AS: soil on acid igneous rocks. * and ** indicate the significant levels of P<0.05 and 0.01, and P values between 0.05 and 0.1 are shown **in bold** without *.Partial correlations with horizon removed are for only LSs. When the assumption of normality is violated, P values of the non-parameter correlations are presented as: (i) P>0.1, (ii) 0.05<P<0.1, (iii) 0.01< P<0.05 and (iv) P<0.01.*

3.3.4. Correlations between variables in acid igneous rock soils (ASs)

The SOC content was positively correlated to Fe_o, Fe_p, Al_o, Al_p and silt plus clay content at the significant level of P<0.1, whereas C_p had positive correlations with the same soil properties at the significant level of P<0.05 (Fig. 3.4). SOC and C_p were negatively correlated to clay content (P<0.1), and were not correlated to Ca_{ex}, Al_{ex} and Fe_d-Fe_o contents (Fig. 3.4). For soil aggregation, MWD was negatively correlated to C_p , Fe_p and Al_p, and had a positive relationship with clay content (Table 3.2). In addition, aggregate stability had poor correlations with OM-related variables and other soil variables, with an exception of positives correlation between macroaggregate stability and clay content (Table 3.2).

Table 3.3 Partial correlation of OM related variables (C, N, C_p and C-C_p) with exchangeable cations (Ca_{ex}, Mg_{ex} and Al_{ex}) and silt plus clay fractions, with effects of Fe_p , Al_p and Ca_{ex} removed for all samples and also effects of horizon removed for only LSs.

		Zero-order							**Fe_p & Al_p removed**				**Ca_{ex} removed**	
		Ca_{ex}	Mg_{ex}	Al_{ex}	Silt+clay	Clay	Fe_p	Al_p	Ca_{ex}	Mg_{ex}	Al_{ex}	Silt+clay	Fe_p	Al_p
LSs n=11														
C	R	**0.750**	**0.624**	**0.705**	**0.588**	**-0.533**	**0.932**	**0.816**	**0.722**	0.577	-0.196	-0.379	**0.937**	**0.635**
	P	**0.008****	**0.040***	**0.015*(iv)**	**0.057**	**0.091(ii)**	**<0.001****	**0.002**(iv)**	**0.028***(i)	0.104(i)	0.613(i)	0.315(i)	**<0.001****	**0.049*(iv)**
C_p	R	**0.821**	0.477	**0.750**	**0.615**	**-0.679**	**0.846**	**0.936**	**0.820**	0.401	-0.384	-0.177	**0.821**	**0.908**
	P	**0.002****	0.137	**0.008**(iv)**	**0.044***	**0.022*(iii)**	**0.001****	**<0.001**(iii)**	**0.007**(iii)**	0.284(i)	0.307**(ii)**	0.650(i)	**0.004****	**<0.001**(iv)**
C-C_p	R	**0.578**	**0.679**	**0.563**	0.481	-0.319	**0.885**	**0.586**	0.470	0.543	-0.021	-0.415	**0.831**	0.327
	P	**0.062**	**0.022***	**0.071(iv)**	0.135	0.339(i)	**<0.001****	**0.058(iii)**	0.202(i)	0.131**(ii)**	0.957(i)	0.267(i)	**0.003****	0.357**(ii)**
LSs (A vs. B horizon removed) n=11														
C	R	0.522	**0.586**	**0.704**	**0.581**	0.051	**0.849**	**0.694**	**0.745**	0.598	-0.129	0.407	**0.925**	**0.597**
	P	0.122	**0.075**	**0.023*(iii)**	**0.078**	0.888(i)	**0.002****	**0.026*(iii)**	**0.034***(i)	0.117(i)	0.761(i)	0.317(i)	**<0.001****	**0.089 (iii)**
C_p	R	**0.653**	0.360	**0.813**	**0.652**	-0.219	**0.633**	**0.939**	**0.773**	**0.640**	0.033	0.375	**0.730**	**0.946**
	P	**0.041***	0.308	**0.004**(iii)**	**0.041***	0.544(i)	**0.050***	**<0.001**(iii)**	**0.024*(iii)**	**0.088**(i)	0.937**(ii)**	0.360(i)	**0.025***	**<0.001**(iv)**
C-C_p	R	0.313	**0.629**	0.471	0.402	0.241	**0.828**	0.363	**0.687**	0.543	-0.200	0.399	**0.836**	0.258
	P	0.379	**0.051**	0.169**(iii)**	0.249	0.502(i)	**0.003****	0.303(i)	**0.060**(i)	0.165(i)	0.635(i)	0.327(i)	**0.005****	0.502(i)
ASs n=7														
C	R	0.185	0.357	0.227	**0.740**	**-0.733**	**0.687**	**0.736**	0.698	0.793	-0.210	0.500	**0.843**	**0.869**
	P	0.691	0.432	0.625	**0.057**	**0.061**	**0.088**	**0.059**	0.190	0.110	0.734	0.391	**0.035***	**0.024***
C_p	R	-0.050	0.107	0.322	**0.761**	**-0.739**	**0.855**	**0.919**	0.720	0.809	-0.306	0.494	**0.912**	**0.964**
	P	0.915	0.819	0.482	**0.047***	**0.058**	**0.014***	**0.003****	0.170	0.097	0.617	0.398	**0.011***	**0.002****
C-C_p	R	0.443	0.599	0.065	0.571	-0.583	0.344	0.365	0.667	0.763	-0.156	0.489	0.632	0.618
	P	0.320	0.155	0.890	0.181	0.169	0.451	0.421	0.219	0.134	0.803	0.403	0.178	0.191

*LS: limestone soil. AS: soil on acidic igneous bedrocks. * and ** indicate the significant levels of P<0.05 and 0.01, and P values between 0.05 and 0.1 are shown **in bold** without *. Horizon is controlled for only LSs. When the assumption of normality is not assumed, P values of the non-parameter correlations are presented as: (i) P>0.1, (ii) 0.05<P<0.1, (iii) 0.01< P<0.05 and (iv) P<0.01.*

Contents of C and C_p were positively correlated to silt plus clay content and pyrophosphate fractions (Fe_p and Al_p) (P<0.1, Table 3.3). However, when correlations with Fe_p and Al_p were removed, C and C_p had no correlation with silt plus clay content. In contrast, when correlations with Ca_{ex} was removed, C and C_p were still positively correlated with Fe_p and Al_p (P<0.05, Table 3.3).

Table 3.4 Correlations between soil pH and soil properties related to OM stabilization.

	C	C_p	C-C_p	Fe_p	Al_p	Ca_{ex}	Mg_{ex}	Silt+Clay	Clay
LS & AS n=18									
pH	-0.210	-0.229	-0.161 (i)	0.063 (i)	**-0.704 (iv)**	**0.532**	**0.447**	**0.652 (iii)**	**0.638 (iv)**
	0.403	0.360	0.523	0.805	**0.001****	**0.023***	**0.063**	**0.003****	**0.004****

*LS: limestone soil. AS: soil on acidic igneous bedrocks. * and ** indicate the significant levels of P<0.05 and 0.01, and P values between 0.05 and 0.1 are shown **in bold** without *. When the assumption of normality is not assumed, P values of the non-parameter correlations are presented as: (i) P>0.1, (ii) 0.05<P<0.1, (iii) 0.01< P<0.05 and (iv) P<0.01.*

3.3.5. Correlations between soil pH and other properties

Correlation between soil pH and other soil properties are presented in Table 3.4. Soil pH was positively correlated to Ca_{ex}, Mg_{ex}, silt plus clay contents and clay contents (P<0.1 for Mg_{ex}, P<0.05 for others), but was negatively correlated to Al_p only (Table 3.4). In contrast, no correlation was found between soil pH and OM-related variables (C, C_p and C-C_p, Table 3.4).

3.4. Discussion

3.4.1 OM stabilization in acid igneous rock soils (ASs)

The results indicate that OM in the ASs is stabilized by complexation and/or adsorption with/on Fe and Al (oxides), as underpinned by: (1) a large pyrophosphate extracted C fraction (high C_p/C ratios, Table 3.1), combined with (2) positive correlations of the pyrophosphate fractions (Fe_p and Al_p) with OM-related variables (C, C_p and C-C_p) (Fig. 3.4 and Table 3.3). Our interpretation is further supported by the robust correlations of Fe_p and Al_p with OM-related variables after correlations with Ca_{ex} and/or horizon were removed (Table 3.3). Similarly, soil OM stabilization in Andean soils is reported to be controlled by soil mineral adsorption through the formation of Fe/Al-OM complexes and/or Fe/Al oxides-OM associations in acid volcanic soils (Buytaert et al., 2006b;

Podwojewski et al., 2002; Tonneijck et al., 2010), as well as in soils formed on sedimentary rocks including limestones (Egashira et al., 1997).

It is unlikely that OM is stabilized by adsorption on clay minerals, given the negative correlations of clay content with SOC and C_p contents (Fig. 3.4D and 3.4N). This can be attributed to the overall coarse soil texture that leaves only a small clay fraction (Table 3.1 and Table A3.1). Similarly, Tonneijck et al. (2010) also reported that OM stabilization was not controlled by clay contents in the Ecuadorian volcanic soils. Aggregate size or aggregate stability was not the factor controlling OM stabilization because of the negative correlations between OM-related variables and MWD and the absence of correlations between OM-related variables and aggregate stability (Table 3.2). Heckman et al. (2014) also found that OM stabilization was not controlled by aggregate stability. They further explained this by the lack of relationship between aggregate stability and capability of aggregates to protect OM (Heckman et al., 2014). Again, the poor controls of soil aggregates on OM stabilization can be explained by the coarse texture and low clay contents in the ASs (Table 3.1), which inhibit aggregate formation (Bronick and Lal, 2005). Ca^{2+} and Mg^{2+} bridges were not found to be OM stabilization agents, as indicated by their poor correlations with OM-related variables, which can be attributed to the low pH in the ASs (Table 3.1 and Fig. 3.4). In acidic volcanic soils, OM is reported to be stabilized by adsorption on the surfaces of allophane and allophane-like minerals, as well as by limited microbial activities due to Al toxicity (Parfitt, 2009; Takahashi and Dahlgren, 2016; Tonneijck et al., 2010). However, no evidence indicates that OM was stabilized by adsorption on allophane or allophane-like minerals in the ASs. This is supported by the high ratios of Al_p/Al_o (Table 3.1) that indicate the ASs are non-allophanic soils (Dümig et al., 2008). In addition, Al toxicity is not likely to promote OM stabilization in the studied soils since the Al_{ex} contents always remained under the toxic level of 2 cmol kg^{-1}. This is further corroborated by the poor correlations between Al_{ex} and OM-related variables (Fig. 3.2 and Table 3.1).

3.4.2 OM stabilization in limestone soils (LSs)

Similar to the ASs, our results suggest that OM stabilization in the LSs is also controlled by complexation and/or adsorption with/on Fe and Al (oxides). This is supported by the positive correlations between the pyrophosphate fractions and OM-related variables (Fig. 3.4 and Table 3.3), as well as their robust correlations

after the correlations with Ca_{ex} and/or horizon removed (Table 3.3). The OM stabilization in the LSs is unlikely explained by crystalline Fe (Fe_d-Fe_o) or clay contents because of their negative correlations (Fig. 3.4). Furthermore, the OM-related variables lost their negative correlations with clay contents after correlations with horizon were removed (Table 3.3). This suggests that the negative correlations might be explained by the effects of soil depths. Surprisingly, no or a negative correlation was observed between aggregate stability and OM-related variables, and between MWD and OM-related variables, although the LSs have high Ca_{ex} contents and larger aggregates (Table 3.1). This suggests that aggregate size or aggregate stability is not likely to control OM stabilization in the LSs.

In addition to Fe and Al (oxides), Ca-related stabilization mechanisms likely play a significant role in OM stabilization in the LSs. This observation is supported by: (1) the high Ca_{ex}/CEC ratios (0.94) in the LSs (Table 3.1), (2) the positive correlations between Ca_{ex} and OM-related variables (Fig. 3.4), and (3) robust correlations between Ca_{ex} and OM-related variables after correlations with Fe_p, Al_p and horizon were removed (Table 3.3). The proposed Ca-related stabilization mechanisms are: (1) Ca^{2+} bridges between mineral surface and OM (Lützow et al., 2006; Wiesmeier et al., 2019), and (2) improved soil structure through the presence of Ca^{2+} bridges, which can potentially stabilize OM by physical protection within aggregates (Bronick and Lal, 2005; Muneer and Oades, 1989). As no clear evidence suggests that aggregation promotes OM stabilization in the LSs as previously explained (Table 3.2), the adsorption of OM on mineral surfaces via Ca^{2+} bridges is likely an important OM stabilization mechanism in the LSs.

The OM stabilization controlled by Ca^{2+} bridging is further corroborated by the observed molar ratios of C/(Fe_p+Al_p) (Table 3.1). In general, complexation and adsorption sites on the Fe and Al (oxides) have a maximum capacity to stabilize OM. The maximum capacity can be quantified using an indicator of molar ratios of C/(Fe_p+Al_p). Summarized from different studies, molar ratios of C/(Fe_p+Al_p) between 5 and 10 were reported as indicative of saturation of the complexation and adsorption sites on the Fe and Al (oxides) (Boudot et al., 1989; Jansen et al., 2011; Masiello et al., 2004; Oades, 1989; Schwesig et al., 2003). The LSs had much higher C/(Fe_p+Al_p) ratios (52.6 and 32.4 for A and B horizon, Table 3.1) compared to the saturation level (5-10), which suggests Fe and Al (oxides) are not

likely the only stabilization agents. As OM associated with mineral surfaces is the major fraction of bulk soil OM (Cerli et al., 2012; Golchin et al., 1994), Ca^{2+} bridges are likely important to stabilize the OM that is not stabilized by Fe and Al (oxides). This can be further supported by that the LSs have lower ratios of Fe_p/Fe_o and Al_p/Al_o than the ASs (Table 3.1). The lower ratios in the LSs suggested less saturated complexation or adsorption sites on Fe and Al (oxides) (Kögel-Knabner et al., 2008), and the less saturated sites are likely to be explained by Ca^{2+} bridges also contributing to the OM stabilization. In contrast, the ASs had lower ratios of $C/(Fe_p+Al_p)$ (16.3) and higher ratios of Fe_p/Fe_o and Al_p/Al_o compared to the LSs (Table 3.1), which suggests that Fe and Al (oxides) dominate the OM stabilization in the ASs.

Unlike the ASs, the LSs are characterized by a B horizon underlying A horizons in each plot. However, OM stabilization mechanisms were not clearly different between A and B horizons, as indicated by (1) similar ratios of Fe_p/Fe_o, C_p/C and Ca_{ex}/CEC between the A and B horizons, and (2) similar (partial) correlation patterns before and after the correlations with horizon were removed (Table 3.1 and 3.3). Although A and B horizons of the LSs share similar OM stabilization mechanisms, Fe_p, Al_p and Ca_{ex} contents decreased with soil depth (Table 3.1 and Table A3.1). The decreased Fe_p, Al_p and Ca_{ex} contents together with declined C input with soil depth, occurrence of microbial degradation and downwards movement of the OM regulate the vertical distribution of SOC contents and C/N ratios in the LSs (Fontaine et al., 2007; Kaiser and Kalbitz, 2012; Rumpel and Kögel-Knabner, 2010).

3.4.3 SOC stocks explained by OM stabilization

The SOC stocks in both LSs and ASs were also higher compared to the global average SOC stocks reported by Batjes (2014) and Lal (2004). For other alpine Andean soils, Farley et al. (2004) and Tonneijck et al. (2010) reported higher SOC stocks in Ecuadorian grasslands with wetter climate compared our soils. In contrast, lower SOC stocks were reported in Bolivia and Southern Peru with drier climate (Muñoz et al., 2016; Rolando et al., 2017a; Zimmermann et al., 2009). When compared to other alpine soils, our soils also have higher SOC stocks (e.g. Garcia-Pausas et al., 2007; Zhu et al., 2015).

The results showed higher total SOC stocks in the LSs compared to the ASs (Fig. 3.2). The higher total SOC stocks can be explained by the higher SOC contents

and deeper soil profiles for the LSs (Fig. 3.1 and 3.2). In contrast, bulk densities were not significantly different between LSs and ASs (Fig. 3.2), which indicates that the differences in SOC stocks are not likely controlled by soil bulk density. The higher SOC contents in the LSs is likely attributed to LSs having OM stabilization mechanisms related to Ca^{2+} bridges in addition to stabilization related to complexation with and/or adsorption on Fe and Al (oxides) that occurs in both LSs and ASs. More specifically, if Fe and Al (oxides) are assumed to be the only OM stabilization agents, the LSs should have lower SOC contents due to their smaller molar Fe_p+Al_p contents compared to the ASs (Table 3.1). Obviously, this does not match the higher SOC stocks and contents in the LSs (Fig. 3.2 and Table 3.1). Thus, the higher SOC stocks in the LSs can be explained by their higher SOC contents induced OM stabilization controlled by Ca^{2+} bridges. This is supported by that: (1) Ca^{2+} bridges are not an OM stabilization agent in the ASs, and (2) OM stabilization in the LSs is poorly controlled by clay contents, crystalline Fe oxides, aggregate size or aggregate stability. In contrast, the small SOC stocks and contents in the ASs are likely restricted by OM stabilization being controlled by interactions with Fe and Al (oxides) only. This is further corroborated by their higher ratios Fe_p/Fe_o and Al_p/Al_o (Table 3.1), which indicate their more-saturated adsorption and/or complexation sites of the Fe and Al (oxides) compared to the LSs (Kögel-Knabner et al., 2008). The adsorption and/or complexation sites of the ASs, which can stabilize less OM compared to the LSs, are likely to be more saturated with OM under similar C input levels compared to the LSs due to their similar vegetation.

3.4.4 OM stabilization driven by soil pH

In our study, although SOC contents are not clearly controlled by soil pH, the underlying OM stabilization mechanisms are clearly regulated by soil pH. This is supported by the lack of correlations between pH and OM-related variables, and the correlations between pH and Fe_p, Al_p and Ca_{ex} fractions (Table 3.4). The positive correlations between pH and Ca_{ex} and the negative correlation between pH and Al_p (Table 3.4) suggests that Ca^{2+} bridges are more important in OM stabilization at higher pH while Al (oxides) is more important at lower pH. The shifts in OM stabilization mechanisms between LSs and ASs coincide with the general view that soil pH plays a fundamental role in controlling soil OM stabilization mechanisms (Clarholm and Skyllberg, 2013; Rowley et al., 2018). In general, the formations of Fe- and Al-OM complexation as well as Al^{3+} toxicity

are reported as the dominant OM stabilization mechanisms in soils with low pH (Dümig et al., 2008; Takahashi and Dahlgren, 2016; Tonneijck et al., 2010). For neutral or alkaline soils, Fe and Al oxides, and base cation bridges are reported as stabilization mechanisms (Kaiser et al., 2011; Masiello et al., 2004; Porras et al., 2017). Similar to our results, Heckman et al. (2009), Kaiser et al. (2011) and Masiello et al. (2004) reported a shift in soil OM stabilization mechanisms from controlled by Fe and Al (oxides) to that controlled by Ca-related mechanisms due to increasing soil pH. Consistent with these studies, our results highlight the shift from OM stabilization dominated by interacting with Fe and Al (oxides) to that controlled by Ca^{2+} bridges with increasing soil pH values.

Clarholm and Skyllberg (2013) reported soil pH values between 6.2-6.8 as a 'window of opportunity', in which OM stabilization controlled by Fe, Al and Ca is not strong. The 'window of opportunity' allows for weak OM stabilization and higher OM degradation. However, our results do not support the 'window of opportunity' because the LSs fall into the window but have highly stabilized OM. A possible explanation is that the OM stabilization is still controlled by OM association with Fe oxides when the LSs falls into the window. The explanation is supported by the robust correlations between OM-related variables and Fe_p in the LSs (Fig. 3.4 and Table 3.3). The findings suggest that more research is needed to unravel the effects of soil pH on OM stabilization controlled by Fe, Al and Ca.

3.5. Conclusions

The results indicate that lithology is the key factor controlling soil OM stabilization mechanisms in the studied soils of the Northern Peruvian Andes. In the ASs, OM stabilization is dominated by OM complexation and/or adsorption with Fe and Al (oxides). In the LSs, OM stabilization is controlled by OM adsorption on mineral surfaces through Ca^{2+} bridges in addition to interactions of OM with Fe and Al (oxides). The LSs had significantly higher SOC stocks than the ASs, which can be explained by their higher SOC contents due to the presence of Ca-related OM stabilization mechanisms. Our results highlighted that the shifts in OM stabilization mechanisms from interacting with Fe and Al (oxides) to interacting with Ca^{2+} bridges are controlled by increasing soil pH values. This suggests that the OM stabilization mechanisms controlled by soil pH in the Peruvian Andes are similar to the general findings in other soils.

- SOM stabilization controlled by lithology

The study indicates that lithology has to be considered for further studies on SOC stocks and the underlying OM stabilization in the Peruvian Andes, because of its important role in controlling OM-mineral interactions. However, it is surprising that OM-related variables were not positively correlated to aggregate parameters in the LSs, which have good soil structure and high Ca_{ex} contents. Further studies could apply methods like density fractionation with ultrasonic treatments and incubation with aggregate destruction to unravel the role of aggregates in soil OM stabilization in the Peruvian Andes.



- Soil aggregation and SOC stability affected by lithology and precipitation

Chapter 4

Lithology and climate controlled soil aggregate size distribution and organic carbon stability in the Peruvian Andes

This chapter has been accepted for publication by SOIL:

Yang, S., Jansen, B., Absalah, S., van Hall, R., Kalbitz, K., Cammeraat, E., 2019. Lithology and climate controlled soil aggregate size distribution and organic carbon stability in the Peruvian Andes. SOIL in press.

- Soil aggregation and SOC stability affected by lithology and precipitation

Abstract

Recent studies indicate that climate change influences soil mineralogy by altering weathering processes, and thus impacts soil aggregation and organic carbon (SOC) stability. Alpine ecosystems of the Neotropical Andes are characterized by high SOC stocks, which are important to sustain ecosystem services. However, climate change in the form of altered precipitation patterns can potentially affect soil aggregation and SOC stability with potentially significant effects on the soil's ecosystem services. This study aimed to investigate the effects of precipitation and lithology on soil aggregation and SOC stability in the Peruvian Andean grasslands, and assessed whether occlusion of organic matter (OM) in aggregates controls SOC stability. For this, samples were collected from soils on limestone and soils on acid igneous rocks from two sites with contrasting precipitation levels. We used a dry-sieving method to quantify aggregate size distribution, and applied a 76-day soil incubation with intact and crushed aggregates to investigate SOC stability in dependence on aggregation. SOC stocks ranged from 153±27 to 405±42 Mg ha^{-1}, and the highest stocks were found in the limestone soils of the wet site. We found lithology rather than precipitation to be the key factor regulating soil aggregate size distribution, as indicated by coarse aggregates in the limestone soils and fine aggregates in the acid igneous rock soils. SOC stability estimated by specific SOC mineralization rates decreased with precipitation in the limestone soils, but minor differences were found between wet and dry sites in the acid igneous rock soils. Aggregate destruction had a limited effect on SOC mineralization, which indicates that occlusion of OM in aggregates played a minor role in OM stabilization. This was further supported by the inconsistent patterns of aggregate size distribution compared to the patterns of SOC stability. We propose that OM adsorption on mineral surfaces is the major OM stabilization mechanism controlling SOC stocks and stability. The results highlight the interactions between precipitation and lithology on SOC stability, which are likely controlled by soil mineralogy in relation to OM input.

Keywords: soil organic matter; stabilization; precipitation; limestone; acid igneous rock; aggregate destruction

- Soil aggregation and SOC stability affected by lithology and precipitation

4.1. Introduction

Soil organic carbon (SOC) is the largest terrestrial carbon (C) pool and plays an important role in global C dynamics (Carvalhais et al., 2014; Lal, 2004). However, the distribution of SOC at a global scale is highly variable (Batjes, 2014; Lal, 2004). Alpine grasslands of the Andes are characterized by large SOC stocks, especially for the Ecuadorian and Peruvian Andes (Muñoz-García and Faz-Cano, 2012; Rolando et al., 2017b; Tonneijck et al., 2010). The Andean grasslands play a crucial role in agricultural production, water provision and sustaining the high biodiversity (Buytaert et al., 2011; Rolando et al., 2017b). The large SOC stocks contribute to crucial ecosystem services, and act as a potential C sink or source for atmospheric CO_2 in the context of global change (Buytaert et al., 2011). However, the studied region, the Andes in Northern Peru, is characterized by heterogeneity in climate, vegetation, agricultural activities and geological formations (Buytaert et al., 2006a; Rolando et al., 2017b), which potentially introduces spatial variability in SOC storage and stability.

Recent views on SOC persistence have shifted from chemical recalcitrance of soil organic matter (OM) to progressive decomposition of soil OM dependent on the surrounding biotic and abiotic environment (Lehmann and Kleber, 2015; Schmidt et al., 2011). Specifically, SOC persistence and stabilization are controlled by: (1) OM adsorption on mineral surfaces that controls long-term stabilization, and (2) physical occlusion of OM within soil aggregates that regulates intermediate-term stabilization with heterogeneous OM composition and residential time (Lützow et al., 2006; Schrumpf et al., 2013). Adsorption of OM on mineral surfaces was reported as an important stabilization mechanism for soil OM underlying the large SOC stocks in the Peruvian and Ecuadorian Andes (Buytaert et al., 2006b; Tonneijck et al., 2010; Yang et al., 2019b). However, studies focusing on aggregate-controlled OM stabilization in relation to climate in the Andes are rare (e.g. Rolando et al., 2017b). Aggregates promote soil OM stabilization against decomposition by regulating the availability of oxygen and water as well as the accessibility of OM itself (Kong et al., 2005). Thus, the formation and turnover of soil aggregates are crucial for SOC storage and OM stabilization (Six et al., 2004; Six and Paustian, 2014). As soil aggregates are formed with monomers of clay minerals, polyvalent cations and OM, their formation and the underlying OM stabilization largely depend on various biotic and abiotic factors (e.g. climate and lithology) (Bronick and Lal, 2005; Doetterl et al., 2015).

- Soil aggregation and SOC stability affected by lithology and precipitation

Lithology is the key factor controlling soil OM stabilization and soil aggregation, mainly attributed to its controls on soil mineralogy and texture (Angst et al., 2018a; Homann et al., 2007; Wiesmeier et al., 2019). In soils formed on acidic bedrocks, OM is generally considered to be stabilized by ligand exchange with non-crystalline Fe and Al oxides, whereas in soils formed on alkaline-rich bedrocks, OM is thought to be stabilized by interaction with the mineral surface through polyvalent cation bridges (e.g. Ca^{2+}) (Lützow et al., 2006). Soil texture also has effects on OM stabilization because OM-mineral association is dominantly controlled by clay-sized minerals (Kaiser and Guggenberger, 2003; Kleber et al., 2007). In addition, soil mineralogy and texture are crucial factors for soil aggregation (Bronick and Lal, 2005). In soils developed on base-rich or calcareous materials, the high clay and calcium (Ca) contents promote the formation of large-sized aggregates. In soils developed on sand-rich or acidic materials, the lack of alkaline cations (e.g. Ca^{2+}) and the coarse texture hinder the formation of coarse aggregates (Bronick and Lal, 2005; Six et al., 2004). The differences in aggregation can potentially affect soil OM stabilization as controlled by occlusion of OM within aggregates (Lützow et al., 2006).

Climate factors, comprising temperature and precipitation, act as the primary drivers regulating SOC storage and OM stabilization by controlling OM input and decomposition (Schmidt et al., 2011; Wiesmeier et al., 2019). Recent studies indicated that climate factors also control OM persistence by regulating soil mineralogy (Chaplot et al., 2010; Doetterl et al., 2015, 2018). The soil mineralogy and OM persistence controlled by climate can be dependent on lithology due to their inherent properties (Jenny, 1941; Wagai et al., 2008). Given the importance of climate and lithology, the heterogeneity in precipitation and lithology in the Andes can potentially cause spatial variation in OM stabilization and consequently SOC stocks. In addition, shifts in e.g. precipitation patterns as a result of global change may impact SOC stocks in different parts of the Andes in different ways.

The objectives of our study were to assess the controls of precipitation and lithology on SOC stocks and stability in the Peruvian Andes. Specifically, we aimed to investigate whether the effects of precipitation and lithology on SOC stability are through the controls of OM stabilization governed by aggregate occlusion and/or mineral adsorption. For this, we applied a combination of aggregate-size fractionation with a 76-day incubation for soil samples collected

from the Peruvian Andes with two contrasting bedrocks and two precipitation levels.

4.2. Materials and methods

4.2.1. Site description

Basic information of the sampling sites is shown in Fig. 1.1. The study areas belong to the Neotropical alpine grassland of the Andes, corresponding to the grassland ecosystem commonly referred as wet Puna or Jalca that is present between the tree line (3500 m asl) and the ice-covered region, having an annual precipitation over 500 mm (Rolando et al., 2017b). Two sampling sites were selected with similar altitudes but with different lithologies and precipitation levels. The wet site is located in the western Cordillera mountain chain of the Peruvian Andes, to the west of Cajamarca, Peru (7°11` S, 78°35` W). The altitudes of the sites range from 3500 m to 3720 m asl. The temperature shows a large daily variation and minor seasonal variation, with an estimated annual mean of 11°C. The sites receive 1100mm precipitation per year and have a wet season between October and April (Sánchez Vega et al., 2005). The dry site is located in the mountain chain of the Cordillera Blanca, to the northeast of Carhuaz (9°22` S, 77°59` W), with altitudes ranging between 3490 and 3700 m asl. The annual temperature and precipitation were estimated as 11 °C and 680 mm, and had similar annual and daily variations as the wet site (Merkel, 2017). Typical land use in both sites is grassland with human activities including cultivation, grazing and plantation of pine trees and eucalyptus (Rolando et al., 2017b; Sánchez Vega et al., 2005). The vegetation in the wet site is a typical disturbed wet Puna (or Jalca) vegetation with dominant grass species *Calamagrostis sp.,* but also *Festuca and Agrostis sp. as well as Rumex sp.* on fallow land. Similarly, the vegetation in the dry site is also a typical disturbed wet Puna (or Jalca) vegetation with *Calamogrostis sp., Stipa and Festuca sp. and Rumex sp.* on fallow land.
For the wet site, the geology consists of a basement of Cretaceous sedimentary formations, which is composed of limestone, marl, shale and quartzite. Neogene igneous bedrocks consisting of granite and ignimbrite intrude or cover parts of the basement (Reyes-Rivera, 1980). For the dry site, intrusive igneous rocks (mainly granodiorite) belonging to the Neogene Cordillera Blanca batholith are present in the western part of the Cordillera Blanca (Coldwell et al., 2011; Portes et al.,

2016). The foot slopes consist of fluvio-glacial and glacial sediments partly covering andesitic ignimbritic rocks of the Neogene Yungay Formation, as well as the sedimentary Cretaceous Carhuaz and Santa formations that are dominated by folded limestones, sandstones and shales (Coldwell et al., 2011). Soils developed on the limestone were classified as Phaeozems or Umbrisols, whereas soils on acid igneous rocks were classified as Andosols and Umbrisols (WRB, 2014).

4.2.2. Sampling procedures

For both the wet and dry sites, we selected three soil sampling plots from limestone and three plots on acid igneous rocks. For limestone soils (LSs) in both sites and acid igneous rock soils (ASs) in the wet site, all soils were directly developed on the bedrock. For ASs in the dry site, one sampling site was directly developed on granodiorite, whereas the other two sites were located on the glacier deposits on lateral moraines with a granodioritic composition. As a previous study in the study area showed that SOC stocks are not significantly controlled by land use (Yang et al., 2018), all sampling sites were selected based on the criteria of (1) grassland, grassland with shrubs or abandoned cropland, (2) gentle slopes, (3) no intensive human activities, and (4) similar soil development status.

For the determination of bulk density and calculation of SOC stocks through the soil profile, samples were collected every 10 cm in duplicate to the depth of the C horizon using Kopecky rings (100 cm^3). For the determination of basic soil properties, aggregate-size fractionation and incubation, soil samples were collected per horizon in triplicate (e.g. A_{h1}, A_{h2} and B_{tg} horizons). To minimize aggregate destruction during transportation, soil samples were transferred into sealed plastic bags and protected by hard plastic boxes.

4.2.3. Laboratory analyses

Soil samples collected every 10 cm were freeze-dried to determine bulk densities and SOC stocks. Soil bulk densities were measured by weighing samples after freeze-drying. Afterward, gravels (>2 mm) were removed from the samples. The rest of the samples was used to determine OC contents and to calculate SOC stocks. Soil samples collected per horizon were air-dried, followed by taking 5-10 g of sub-samples milled for the determination of basic soil properties. For these samples, total C and N contents were analyzed using a VarioEL Elementar

analyzer (Elementar, Germany). As inorganic C contents were negligible in all the samples, the total OC contents were equal to total C contents. Soil pH was determined with a glass electrode in suspensions of soil material in demi-water (w:v = 1:5, Bates, 1973).

Total SOC stocks were calculated using the following equation:

$$SOC\ stock = \sum_{i=1}^{i=k} BD_i \times C_i \times (1 - S_i) \times D_i$$

In which, BD_i = bulk density (g cm^{-3}) of the layer i (including gravels), C_i = SOC content (%) of the layer i (excluding gravels), S_i = stoniness (gravimetric) of layer i, D_i= thickness (cm) of layer i.

Dry-sieving was applied to fractionate soil samples into 5 aggregate-size groups: >5mm, 2-5mm, 0.22-2 mm, 0.063-0.25 mm and <0.063 mm, respectively. Briefly, 170-230 g sub-samples (<16 mm) of each horizon were fractionated using 4 mesh sieves (5, 2, 0.25 and 0.063 mm) by shaking for 20 s at 30 Hz at a horizontal shaker. For all fractions larger than 2 mm, gravels were separated by sieving (2 mm) a subsample of the fraction after breaking aggregates. The gravel content (gravimetric) of each fraction was calculated using the gravel weight divided by the sum of the fraction weight plus the gravel weight. For each fraction, fraction weights as well as total C and N contents were determined.

The mean weight diameter (MWD) of the bulk soil was calculated by:

$$MWD = \sum_{i=1}^{i=5} \frac{x_{i\,max} + x_{i\,min}}{2} \times w_i$$

In which, $x_{i\,max}$ = maximum diameter (mm) of the fraction i, $x_{i\,min}$ = minimum diameter (mm) of the fraction i, w_i = weight percent (excluding gravels) of the fraction i (Klute and Dinauer, 1986).

Sample materials collected from different horizons were used for the incubation. All materials from individual A horizons in the same soil profile were merged (e.g. Ah1 and Ah2 horizons merged to A horizon), based on the weight distribution of the horizons as estimated by their bulk densities and depths. Original B horizons were used because each soil profile only had a single B horizon. Prior to the incubation, all samples were fractionated into large

macroaggregates (LM, >2 mm), small macroaggregates (SM, 0.25-2 mm) and microaggregates (Mi, <0.25 mm), following the dry-sieving procedure (30 Hz for 20 s). The LM and SM fractions were used for the incubation with intact and crushed aggregates. The finer fractions (<0.25 mm) were by far less abundant, and thus were not incubated. The variation in SOC mineralization between intact and crushed aggregates was used as a measure of C stabilization by occlusion within aggregates (Goebel et al., 2009). Aggregates were destructed by crushing the fractions using a porcelain mortar, and all crushed materials could pass a 0.125 mm sieve (Wang et al., 2014). Before incubation, intact and crushed fractions were rewetted at pF 2.0 for 10 days to activate soil microbes. Approximate 10 g dry-weight equivalent fractions were incubated for 76 days at 20 °C in sealed glass jars (120ml). All soil fractions were incubated in duplicate. The headspace of incubating jars was sampled on days 1, 2, 6, 9, 13, 20, 28, 48 and 76. During the sampling period, CO_2-free air was injected into the jars to maintain pressure and avoid too high CO_2 concentrations. The CO_2 concentration was analyzed using a gas chromatograph with a flame ionization detector (GC-FID, Thermo Scientific, Trace GC Ultra) with packed columns (RESTEK Packed Column, Part Nbr: PC7130, Serial Nbr: C34216-01, HayeSep Q, 1/8" 80/100 2m and HayeSep Q, 1/8" 80/100 1m). A methanizer was situated in front of the FID, as the detector can only measure hydrocarbons instead of CO_2. Specific SOC mineralization rates (g CO_2-C g^{-1} C), which were normalized for OC contents, were used as an indicator of the C stability of the soil fractions.

4.2.4. Statistics

Statistical comparisons of soil properties and SOC stocks were made using a one-way ANOVA. *Post hoc* analyses were conducted using the Fisher's Least Significant Difference (LSD) test. Principal component analysis (PCA) was applied to investigate potential differences between different soil profiles and horizons. Before conducting the PCA, Kaiser-Meyer-Olkin tests and Bartlett's tests were used to guarantee that sampling adequacy and the sphericity were suitable for the analysis. Linear regressions were applied to investigate relationships of specific SOC mineralization rates with SOC and C/N ratios. An independent *t*-test was applied to check effects of precipitation, lithology, soil horizon, aggregate size and aggregates destruction on SOC mineralization rates.

Before the *t*-test and the one-way ANOVA, data normality and variance

homogeneity were examined using a Shapiro-Wilk test and a Levene's test. When the assumption of normality was violated, the Kruskal-Wallis H test was applied instead of the one-way ANOVA, while the Mann-Whitney U-test was used instead of the *t*-test. When the homogeneity of the variance could not be assumed, the Robust Welch test was used for the one-way ANOVA. All analyses were conducted using SPSS 24.0 (SPSS Inc., USA).

4.3. Results

4.3.1. Soil properties

Average soil depths were 61 cm for limestone soils (LSs) in both wet and dry sites, and 49 cm and 51 cm for acid igneous rock soils (ASs) in the wet and the dry sites (Fig. 1.1). SOC stocks were highest in LSs of the wet site (wet-LSs, 405.3 ± 41.7 Mg ha^{-1}), followed by ASs of the wet site (wet-ASs), ASs of the dry site (dry-ASs) and dry-LSs. SOC stocks in the wet-LSs were significantly higher compared to other soils (Fig. 4.1). SOC contents in the A horizons were significantly higher in the wet-LSs both with regard to bedrock and precipitation. No significant differences were present for the ASs with regard to precipitation (Fig. 4.1). The LSs had no significant difference in C/N ratios compared to the ASs for the A horizons in the wet sites, however, the LSs had significantly lower C/N ratios in the dry site (Fig. 4.1). With decreasing precipitation, C/N ratios significantly decreased in the LSs and increased in the ASs (Fig. 4.1). The pH values were significantly higher in the LSs compared to the ASs in the wet site, but were not significantly different in the dry site (Fig. 4.1). In addition, significantly lower pH values with lower precipitation were only found in the LSs (Fig. 4.1). With regard to the differences between horizons in the LSs, B horizons were characterized by significant lower SOC contents, lower C/N ratios and higher pH compared to A horizons, except for SOC contents and pH values in the dry sites (Fig. 4.1).

➢ Soil aggregation and SOC stability affected by lithology and precipitation

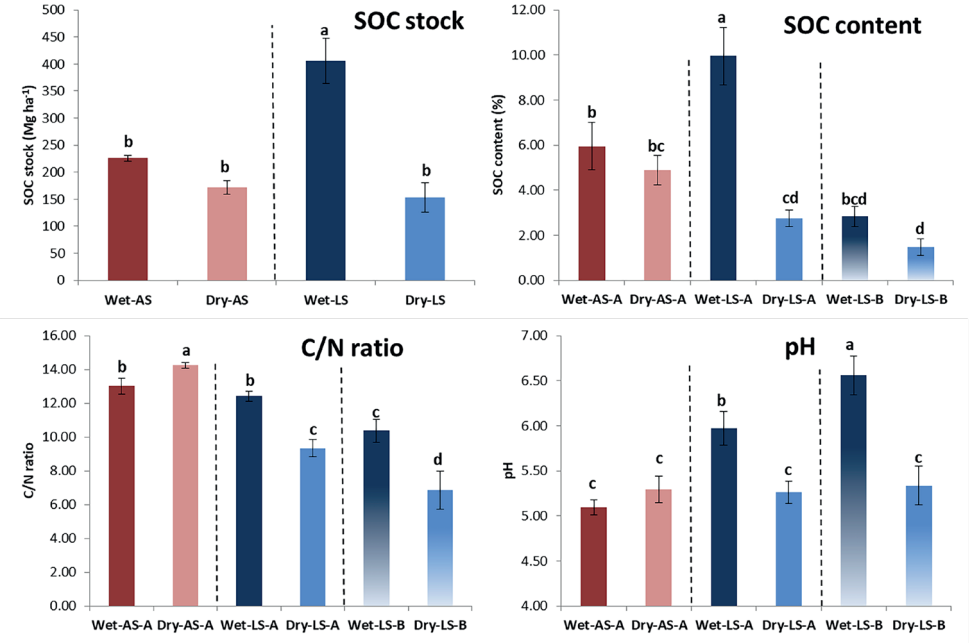


Fig. 4.1 Soil organic carbon stocks in the whole soil profile and soil properties in diagnostic horizons (Mean±SE). Wet: the wet site, Dry: the dry site, LS: limestone soil, AS: acid igneous rock soil, A: A horizons, B: B horizons

4.3.2. Aggregate-size fractionation

The weight distribution of the aggregate-size fractions is shown in Fig 3A and 3C. The LSs had larger aggregate sizes than the ASs in both wet and dry sites, as indicated by that LSs had more LM fraction (> 60%) and less Mi fraction (< 10%) when compared to the AS (Fig 4.2A and 4.2C). When comparing the wet and dry sites, the aggregate-size distribution was not clearly different in the LSs. In contrast, the wet-ASs had larger aggregate sizes (more LM fraction) than the dry-ASs (Fig. 4.2A and 4.2C). When comparing the A and B horizons in the LSs, B horizons had larger aggregates sizes compared to A horizons for both wet-LSs and dry-LS (Fig. 4.2A and 4.2C). The SOC distribution in different fractions is similar to the weight distribution as shown in Fig. 4.2B and 4.2D. The LSs had more SOC located in large-sized aggregates than the ASs , whereas the wet-ASs had more SOC distributed in large aggregates than the dry-ASs. For the LSs, B horizons had more SOC distributed in large-sized aggregates when compared to A horizons (Fig 4.2A-4.2D).

➢ Soil aggregation and SOC stability affected by lithology and precipitation

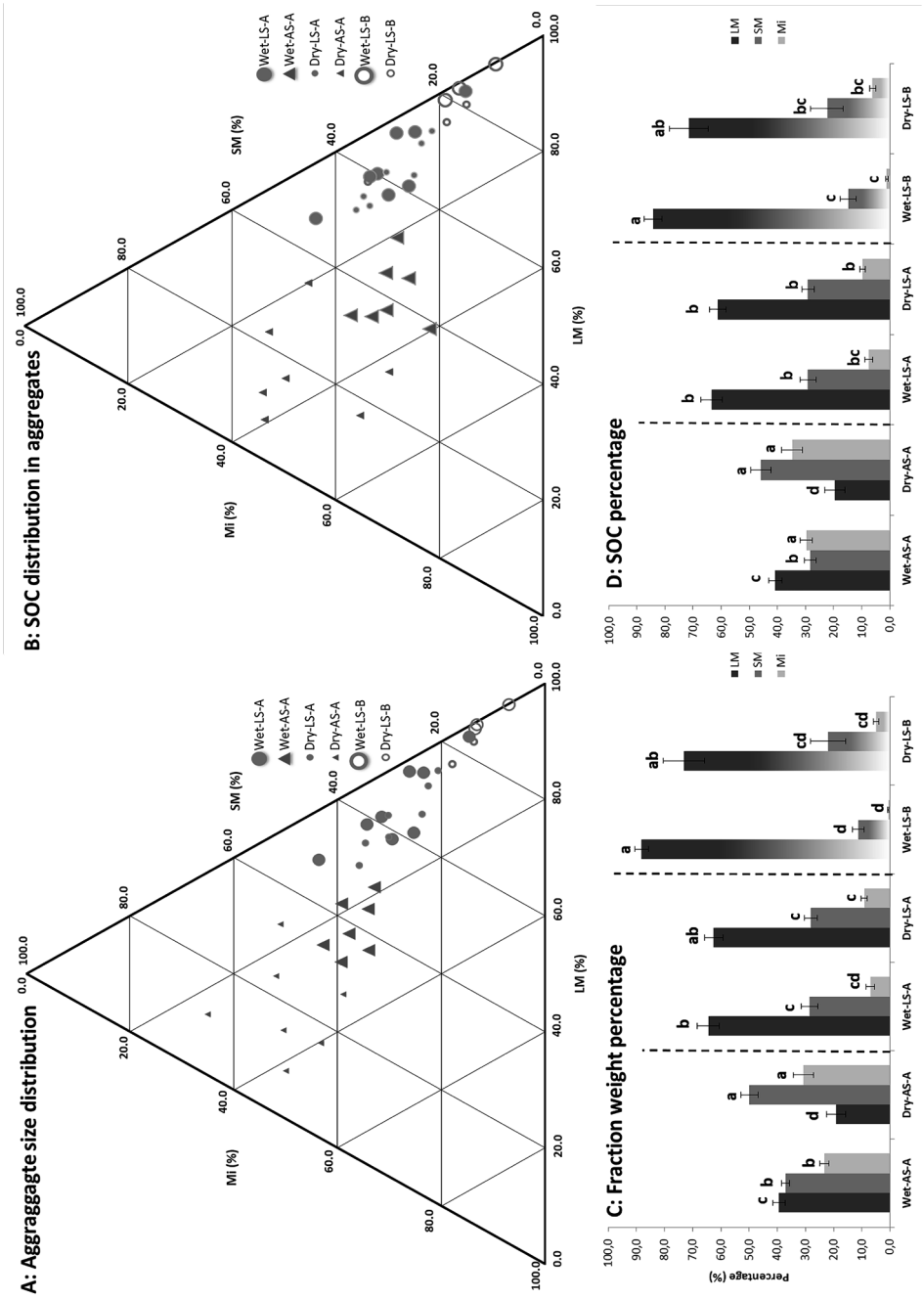


Fig. 4.2 Distribution of fraction weight and soil organic carbon in aggregate size fractions. A: Fraction weight distribution in aggregate size fractions, B: SOC distribution in aggregate size fractions, C: percentages of fraction weights in soil horizons (Mean±SE), D: SOC percentage in soil horizons (Mean±SE). Wet: the wet site, Dry: the dry site, LS: limestone soil, AS: acid igneous rock soil, A: A horizons, B: B horizons, LM: large macroaggregates (>2 mm), SM: small macroaggregates (0.25-2 mm), Mi: microaggreagtes (<0.25 mm)

➢ Soil aggregation and SOC stability affected by lithology and precipitation

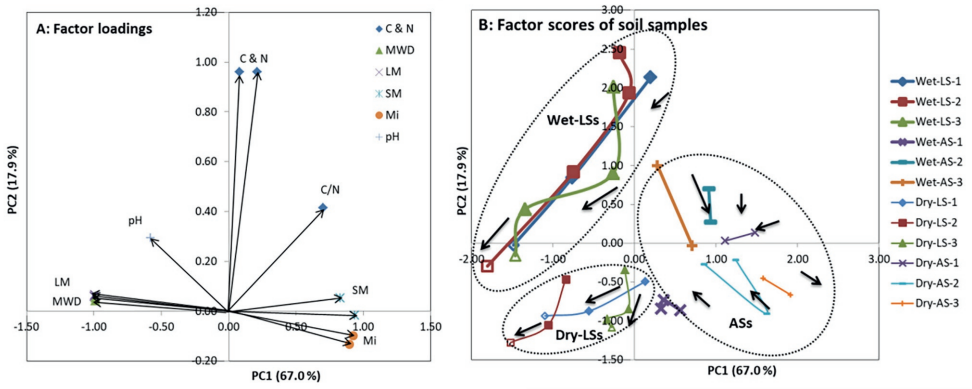


Fig. 4.3 Principal component analysis (PCA) indicating vertical distribution of aggregate-related soil properties in both limestone soils (LSs) and acid igneous rock soils (ASs). Solid points are A horizons, and hollow points are B horizons. Black arrows are pointing to the direction of soil horizons with increasing soil depth. Wet: the wet site, Dry: the dry site, LS: limestone soil, AS: acid igneous rock soil, MWD: mean weight diameter, C: SOC content, N: total nitrogen content, C/N: C/N ratio, LM: large macroaggregates, SM: small macroaggregates, Mi: microaggregates.

Soil properties of different horizons are shown in Fig. 4.3. PC1 and PC2 explained 67.0% and 17.9% of the total variation. PC1 had positive contributions of the SM and Mi fractions and negative loadings of the LM fractions and MWD, whereas PC2 had positive contributions of C and N contents. The LSs were separated from the ASs as indicated by coarser aggregates, higher pH values and lower C/N ratios (Fig. 4.3). In addition, wet-LSs were separated from dry-LSs by higher C and N contents, whereas ASs were not clearly separated by precipitation (Fig. 4.3). The LSs were characterized by increasing coarse aggregate fractions and decreasing C and N contents as well as C/N ratios with increasing soil depth, whereas the ASs had no clear pattern in soil property change with increasing depth (Fig. 4.3).

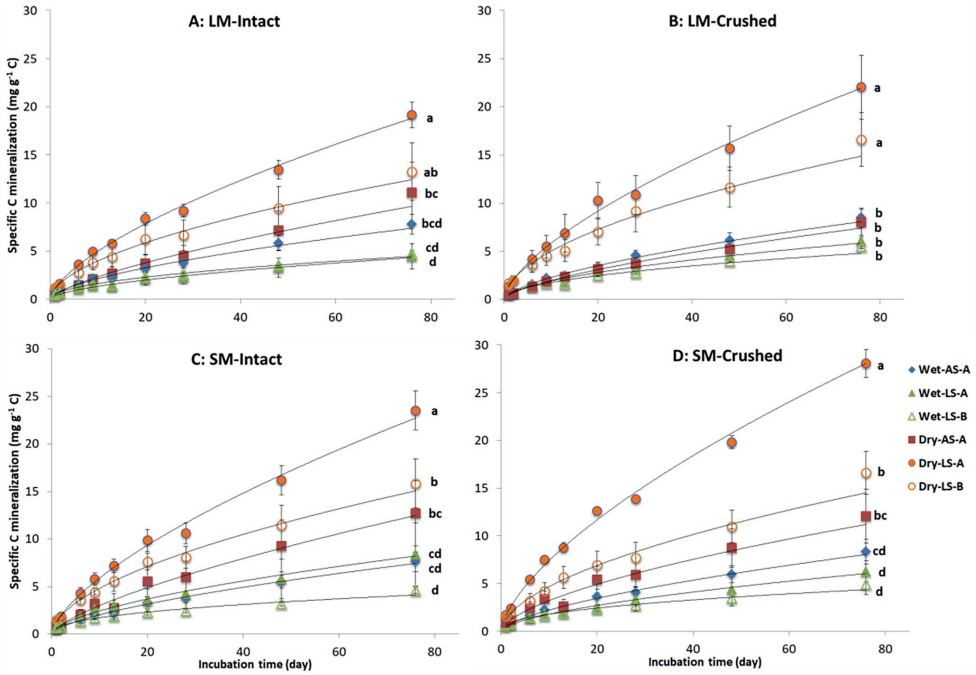


Fig. 4.4 SOC mineralization in the large macroaggregats (LM) and small macroaggregates (SM) in a period of 76-day incubation, with aggregate intact and crushed (Mean ± SE). Letters on the right of each plots indicate significant differences of cumulative C mineralization between different groups on Day 76. LM: large macroaggregates (>2 mm), SM: small macroaggregates (0.25-2 mm), Intact: incubation with aggregates intact, Crushed: incubation with aggregates crushed, Wet: the wet site, Dry: the dry site, AS-A: acid igneous rock soil - A horizon, LS-A: limestone soil - A horizon, LS-B: limestone soil - B horizon.

4.3.3. SOC mineralization

After the 76-day incubation, specific SOC mineralization rates were the highest in A and B horizons of the dry-LSs, when compared to the other soil horizons (Fig. 4.4A-4.4D). For comparisons between two lithologies, SOC mineralization rates were not significantly different in the wet site, but were generally higher in the LSs compared to the ASs in A horizons of the dry site (Table 4.1). For effects of precipitation, SOC mineralization rates were significantly higher in the dry site compared to the wet site for the LS-A horizons in most sampling days, but were not significantly different for the AS-A horizons (Table 4.1). For comparisons between A and B horizons in the LSs, SOC mineralization rates were not significantly different in the wet site. In the dry site, A horizons had significantly higher SOC mineralization rates than B horizons only in the aggregate-crushed SM fraction (Table 4.1).

- Soil aggregation and SOC stability affected by lithology and precipitation

Table 4.1 Comparison in SOC mineralization rates between bedrock, precipitation and horizon with combinations of aggregate sizes and aggregate destruction. Abbreviations in the table indicating the group with significant higher SOC mineralization than the other group.

Day	A horizon: LS vs. AS				A horizon: Wet vs. Dry				LS: A vs. B horizon			
	LM-In	LM-Cr	SM-In	SM-Cr	LM-In	LM-Cr	SM-In	SM-Cr	LM-In	LM-Cr	SM-In	SM-Cr
	Wet				**LS**				**Wet**			
1	n.s.	n.s.	n.s.	n.s.	**Dry****	**Dry***	**Dry***	**Dry****	n.s.	n.s.	n.s.	n.s.
2	n.s.	n.s.	n.s.	n.s.	**Dry****	**Dry***	n.s.	**Dry****	n.s.	n.s.	n.s.	n.s.
6	n.s.	n.s.	n.s.	n.s.	**Dry***	n.s.	n.s.	**Dry****	n.s.	n.s.	n.s.	n.s.
9	n.s.	n.s.	n.s.	n.s.	**Dry****	n.s.	n.s.	**Dry****	n.s.	n.s.	n.s.	n.s.
13	n.s.	n.s.	n.s.	n.s.	**Dry***	n.s.	**Dry***	**Dry****	n.s.	n.s.	n.s.	n.s.
20	n.s.	n.s.	n.s.	n.s.	**Dry***	n.s.	**Dry***	**Dry****	n.s.	n.s.	n.s.	n.s.
28	n.s.	**AS***	n.s.	n.s.	**Dry****	n.s.	**Dry***	**Dry****	n.s.	n.s.	n.s.	n.s.
48	n.s.	n.s.	n.s.	n.s.	**Dry****	**Dry***	**Dry***	**Dry****	n.s.	n.s.	n.s.	n.s.
76	n.s.	n.s.	n.s.	n.s.	**Dry****	**Dry***	**Dry***	**Dry****	n.s.	n.s.	n.s.	n.s.
	Dry				**AS**				**Dry**			
1	**LS***	n.s.	**LS***	n.s.	n.s.	n.s.	n.s.	n.s.	n.s.	n.s.	n.s.	n.s.
2	**LS***	**LS***	**LS***	n.s.	n.s.	n.s.	n.s.	n.s.	n.s.	n.s.	n.s.	n.s.
6	**LS***	n.s.	n.s.	**LS***	n.s.	n.s.	n.s.	n.s.	n.s.	n.s.	n.s.	**A***
9	**LS***	n.s.	n.s.	**LS***	n.s.	n.s.	n.s.	n.s.	n.s.	n.s.	n.s.	**A***
13	n.s.	n.s.	**LS***	**LS****	n.s.	n.s.	n.s.	n.s.	n.s.	n.s.	n.s.	**A****
20	n.s.	**LS***	n.s.	**LS***	n.s.	n.s.	n.s.	n.s.	n.s.	n.s.	n.s.	**A***
28	n.s.	n.s.	n.s.	**LS****	n.s.	n.s.	n.s.	n.s.	n.s.	n.s.	n.s.	**A****
48	n.s.	**LS***	n.s.	**LS****	n.s.	n.s.	n.s.	n.s.	n.s.	n.s.	n.s.	**A****
76	n.s.	**LS***	n.s.	**LS****	n.s.	n.s.	n.s.	n.s.	n.s.	n.s.	n.s.	**A****

LS: limestone soil, AS: acid igneous rock soil, LM: large macroaggregates (>2 mm), SM: small macroaggregates (0.25-2 mm), MA: macroaggregates (>0.25 mm), A: A horizon, In: aggregate intact, Cr: aggregate crushed, Wet: the wet site, Dry: the dry site, *: P<0.05 **: P<0.01, n.s.: not significant.

SOC mineralization rates were slightly stimulated (up to 19.4%) when aggregates were crushed compared to that when aggregates were intact, with exceptions of the LM fraction in dry-AS-A horizons and the SM fraction in dry-AS-A horizons and wet-LS-A horizons (Fig 4.5A and 4.5B). However, the stimulation caused by aggregate destruction was never significant (Fig. 4.5A and 4.5B). In addition, no significant difference in SOC mineralization rates was found between LM and SM fractions. Exclusively, slightly higher SOC mineralization rates (not significant) were found in the SM fraction compared to LM fraction in A horizons of the wet-LS, the dry-LSs and the dry-ASs (Fig. 4.5C and 4.5D).

➢ Soil aggregation and SOC stability affected by lithology and precipitation

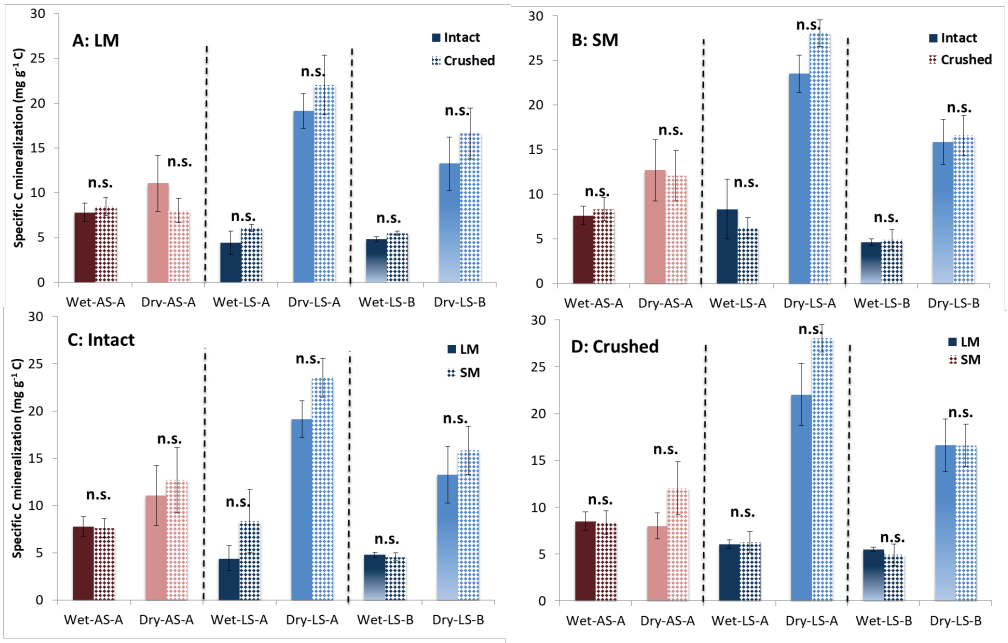


Fig. 4.5 Effects of aggregate destruction and aggregate size on specific SOC mineralization rates in the sampling day 76 (Mean ± SE). A: comparing aggregates intact and crushed in large macroaggregates, B: comparing aggregate intact and crushed in small macroaggregates, C: comparing large and small aggregates with aggregates intact, D: comparing large and small aggregates with aggregates crushed. LS: limestone soil, AS: acid igneous rock soil, LM: large macroaggregates (>2 mm), SM: small macroaggregates (0.25-2 mm), Intact: incubation with aggregates intact, Crushed: incubation with aggregates crushed, A: A horizon, Wet: the wet site, Dry: the dry site, n.s.: not significant.

Overall, SOC mineralization rates had significant negative relationships with SOC contents and C/N ratios, and the negative relationships did not differ between intact and crushed aggregates (Fig. 4.6A and 4.6B). Exclusively for the dry-LSs, positive relationships were found between SOC mineralization rates and SOC contents when aggregates were intact and crushed, and between SOC mineralization rates and C/N ratios when aggregates were crushed (Fig. 4.6C-4.6F). In the dry-LSs, SOC contents and C/N ratios explained 38.2% and 24.9% of the variation of specific SOC mineralization rates when aggregates were intact. When aggregates were crushed, SOC contents and C/N ratios explained 48.0% and 33.3% of the total variation (Fig. 4.6C-4.6F).

➢ Soil aggregation and SOC stability affected by lithology and precipitation

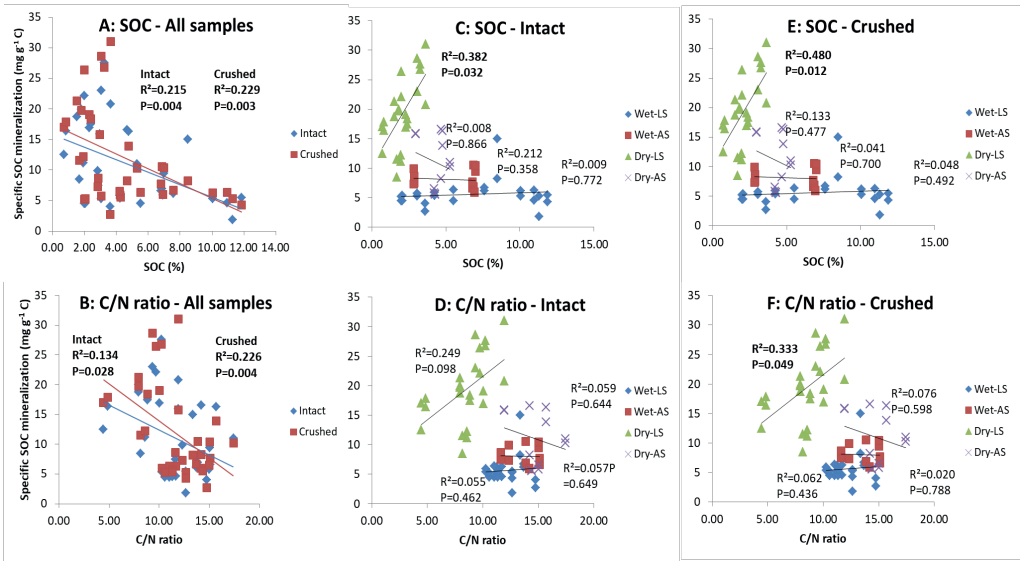


Fig. 4.6 Relationships of specific C mineralization rates (Day 76) with organic carbon contents and C/N ratios when soil aggregates were intact and crushed. Wet: the wet site, Dry: the dry site, LS: limestone soil, AS: acid igneous rock soils, SOC: soil organic carbon content.

4.4. Discussion

4.4.1. Aggregate size distribution

Lithology is the key factor controlling soil aggregate-size distribution in our soils, as indicated by larger aggregates in the LSs when compared to the ASs (Fig. 4.2). The larger aggregates in the LSs are consistent with the literature (Bronick and Lal, 2005; Six et al., 2004). The lithology-controlled aggregate-size distribution can be further supported by the physicochemical properties of aggregate fractions (Fig. A4.1). Compared to the LSs, the ASs had higher C/N ratios in all fractions than the LSs and had a larger increase in OC contents with decreasing fraction size when aggregate size was smaller than 2 mm (Fig. A4.1). Furthermore, increasing aggregate sizes with soil depth were found in the LSs exclusively (Fig. 4.3), which can be explained by the better aggregation promoted by clay illuviation in deep soils. In contrast, no clear vertical differences in the ASs may be related to the lack of the clay fraction in the ASs (Yang et al., 2019b).

- Soil aggregation and SOC stability affected by lithology and precipitation

Unlike lithology, precipitation plays only a minor role in the soil aggregate size distribution for our soils. This is indicated by small differences in properties related to soil aggregation between the wet and the dry sites for the same bedrock types (Fig. 4.2, Fig. 4.3 and Fig. A4.1). Although precipitation potentially controls the OM input and further affects soil aggregation (Bronick and Lal, 2005; Wiesmeier et al., 2019), similar vegetation between wet and dry sites (see *4.2.1 site description*) might alleviate the controls of precipitation on OM input and soil aggregation. In addition, the effects of precipitation might be superimposed by the strong effect of lithology in our study.

Notably, the dry-ASs had smaller aggregates than the wet-ASs (Fig. 4.2). This is probably attributed to their greater gravel contents in the dry-ASs (Fig. 4.1 and Table A4.1) because abundant gravels occupy the space and hinder the formation of large-sized aggregates. Furthermore, gravel contents may affect soil aggregation by controlling root distribution, OM input or soil biological activity. The greater gravel contents in the dry-ASs are likely to be attributed to the terrain conditions (steep mountains and glacial deposits) rather than (Portes et al., 2016). Although aggregate-size distribution is controlled by gavel contents, the physicochemical properties of each aggregate fraction were not clearly affected. This is corroborated by: (1) no clear differences in vertical distribution of aggregate-related soil properties between wet-ASs and dry-ASs (Fig. 4.3), and (2) no clear differences in properties of aggregate fractions between wet-ASs and dry-ASs (Fig. A4.1). An important reason for this is that gravels were always removed from all fractions >2 mm. Thus, analyses conducted for aggregates fractions (e.g. SOC mineralization) are not biased by gravel contents.

4.4.2. SOC stocks and stability

SOC stocks were controlled by interactions between lithology and precipitation, as indicated by increased stocks with precipitation in the LSs and no significant changes in the ASs (Fig. 4.1). Lithology had significant effects on SOC stocks in the wet sites (Fig. 4.1), which is consistent with the findings of Yang *et al.* (2018) showing that lithology is the key factor controlling SOC stocks. In the wet site, the high SOC stocks in the LSs compared to the ASs can be explained by deeper soils and higher SOC contents in A horizons (Fig. 1.1 and 4.1). In the dry site, no difference in SOC stocks between the LSs and the ASs can be explained by that the LSs had lower SOC contents but deeper profiles (Fig. 1.1 and 4.1).

- Soil aggregation and SOC stability affected by lithology and precipitation

Precipitation had significant effects on SOC stocks of the LSs, as indicated by the wet-LSs having greater SOC stocks than the dry-LSs (Fig. 4.1). This is consistent with the consensus that SOC stocks generally increase with precipitation (Homann et al., 2007; Wiesmeier et al., 2019). The higher SOC stocks in the wet-LSs can be also explained by SOC contents because of (1) similar soil depths in the wet-LSs and the dry-LSs (Fig. 1.1) and (2) lower soil bulk densities in the wet-LSs (Table A4.2). Hence, patterns of SOC stocks controlled by lithology and precipitation are mainly explained by SOC contents.

The negative correlations between SOC contents and SOC mineralization rates (Fig. 4.6A and 4.6B) reflect SOC contents controlled by SOC stability. The SOC stability is significantly controlled by precipitation and lithology (Table 4.1) rather than soil horizon, aggregate size or aggregate destruction (Fig. 4.5). For horizons, although SOC stability was different between A and B horizons in the crushed SM fraction of the dry-LSs (Table 4.1), the small contribution of the SM fraction (Fig. 4.2) suggest that horizon is not an important factor controlling the SOC stability.

4.4.3. Organic matter stabilization mechanisms

SOC stability is largely controlled by two mechanisms: (1) OM adsorption on the mineral surfaces and (2) physical occlusion of OM within soil water-stable aggregates (Lützow et al., 2006; Six et al., 2002). In general, OM occluded in water-stable aggregates is isolated using wet-sieving followed by density fractionation plus sonication (Cerli et al., 2012; Moni et al., 2012). However, these methods were not applicable for our ASs because the application of ultrasound caused severe dispersion of OM into the dense solution (i.e. NaPT). The dispersed OM was difficult to be separated from the solution and thus occluded OM could not be isolated. A similar situation has been reported and a potential explanation is that Na^+ in the solution interacted with Al-OM complexes in the ASs and produced a stable suspension (Kaiser and Guggenberger, 2007). As the problem could not be solved, we applied an alternative method, which has been conducted by Goebel et al. (2009) and Wang et al. (2014), to estimate aggregate-occluded OM using a combination of dry-sieving and incubating intact versus crushed aggregates.

Overall, aggregate-occlusion is not a major OM stabilization mechanism in our soils, as indicated by no or insignificant stimulation in SOC mineralization after

aggregate destruction (Fig. 4.5). The minor role of aggregate-occlusion is further supported by the minor changes in correlation patterns of SOC mineralization rates with SOC contents and C/N ratios, when aggregates were intact and crushed (Fig. 4.6A and 4.6B). The limited effects of OM occlusion in aggregates are not consistent with the general view of aggregate-controlled OM stabilization (Lehmann and Kleber, 2015; Wiesmeier et al., 2019), as well as other studies revealing aggregate-protected OM using similar aggregate destruction methods (Mueller et al., 2012; Wang et al., 2014). However, Goebel *et al.* (2009) and Juarez *et al.* (2013) reported limited roles of soil aggregates in protecting OM from decomposition. For the ASs, the limited role of aggregate-occlusion in OM stabilization can be explained by the lack of large-sized aggregates (Fig. 4.2), which suggest the restricted formation of microaggregates within macroaggregates. This potentially weakens the OM protection controlled by occluded in aggregates (Six et al., 2002; Six and Paustian, 2014). For the LSs, the minor contribution of aggregates might be related to the strong adsorption of OM on less-saturated mineral surfaces (Yang et al., 2019b). Because of the limited contribution of OM occlusion in aggregates, OM adsorption on mineral surfaces is most likely the dominant stabilization mechanism. Similar to our results, mineral-controlled OM stabilization mechanisms have been reported in other studies in alpine grassland soils of the Andes (Buytaert et al., 2006b; Rolando et al., 2017a; Tonneijck et al., 2010; Yang et al., 2019b).

Lithology is an important factor for OM stabilization related to mineral surfaces. (Yang et al., 2019b) found that OM stabilization in the wet-LSs was controlled by OM complexed and/or adsorbed with Fe and Al (oxides) as well as by Ca^{2+} bridges. In contrast, OM stabilization in the wet-ASs was only controlled by Fe and Al (oxides) complexation (Yang et al., 2019b). In the wet site, SOC stability between LSs and ASs was not significantly different (Table 4.1). This may be attributed to the mineral surfaces in both LSs and ASs having a large capability for OM stabilization, although their OM stabilization mechanisms are slightly different. In the dry site, lower SOC stability in the LSs compared to the ASs (Table 4.1) suggests the lower capacity of the mineral surfaces to stabilize OM in the LSs. Similarly, Heckman *et al.* (2009) found lower SOC stocks and stability in LSs compared to soils formed on felsic and basaltic igneous rocks, in a region with similar temperature and precipitation to our dry site. They explained this by a lack of active Fe and Al fractions to stabilize OM (Heckman et al., 2009), which might be an explanation for the less stable SOC in our dry-LSs as well.

- Soil aggregation and SOC stability affected by lithology and precipitation

Precipitation is also an important factor to explain the low SOC stability in the dry-LSs, as precipitation has a potential effect on soil mineralogy by controlling weathering processes (Doetterl et al., 2018, 2015b; Wiesmeier et al., 2019). Compared to the wet-LSs, the lower pH values in the dry-LSs indicate that a part of exchangeable base cations (e.g. Ca^{2+}) are replaced by exchangeable H^+. The replacement results in a lower adsorption capacity of the mineral surfaces because H^+ is a monovalent cation that does not promote OM stabilization (Jenny, 1941; Lützow et al., 2006). In addition, positive correlations between SOC mineralization rates and SOC contents, and between SOC mineralization and C/N ratios in the dry-LSs (Fig. 4.6) indicate that SOC mineralization is dominantly dependent on SOC contents and quality. This also suggests a lower sorption capacity of the mineral adsorption sites. Similarly, Wagai et al. (2008) reported positive correlations between SOC mineralization and C/N ratios, and used the positive correlations as an indication of inert mineral surfaces. Furthermore, the lowest C/N ratios in the dry-LSs (Fig. 4.1) indicate a depletion of plant-derived C and a rapid SOC decomposition process (Moni et al., 2012), which suggest the low SOC stability and the low capacity of mineral surfaces to stabilize OM.

4.4.4. Interactions between precipitation and lithology

The effects of precipitation and lithology on SOC stocks and stability are unlikely through the controls of soil aggregation, which is supported by the weak controls of OM stabilization via occlusion in aggregates (Fig. 4.5 and 4.6) and inconsistent patterns of aggregate size distribution compared to the patterns of SOC stability (Fig. 4.2, Fig. 4.3 and Table 4.1). In contrast, the interactions between precipitation and lithology on SOC stocks and stability are likely explained by soil mineralogy. This is supported by (1) the contrasting OM stabilization mechanisms controlled mineral surfaces between the wet-LS and the wet-AS (Yang et al., 2019b), and (2) shifts in pH values, C/N ratios and correlations between SOC mineralization rates and SOC contents that suggest variations in properties of the mineral surfaces (Fig. 4.1 and Fig. 4.6).

Recent studies indicate that controls of climate factors and soil mineralogy are crucial to the persistence and stabilization of soil OM (Chaplot et al., 2010; Doetterl et al., 2015b; Homann et al., 2007). For the LSs, we proposed that the lower SOC stability in the dry site is explained by the weaker interactions between OM and mineral surfaces due to the lower pH when compared to the wet

site. However, the lower pH in the dry-LSs is not consistent with the general soil formation process. The lower pH in the dry-LSs might be explained by soil acidification induced by higher belowground OM input compared to the wet-LSs. The higher OM input in the dry-LSs is supported by (1) more abundant α, ω-dioic acids, ω-hydroxyl alkanoic acids and long-chain fatty acids, especially in B horizons (Fig. A4.2), and (2) low stability of these compounds against decomposition in the dry-LSs (Fig. A4.3). As these compounds are mainly derived from root input (Kögel-Knabner, 2002), the lower pH in the dry-LSs can be explained by the higher belowground OM input because plants need more developed root systems for the low precipitation. By contrast, no clear difference is found between the wet-ASs and the dry-ASs (Fig. 4.1 and Table 4.1). This may be attributed to the limited acidification induced by OM input because the bedrocks are already acidic. Notably, our statement on OM input is based on estimation because quantification of OM input in Andean grasslands is difficult and only a few studies have addressed this (Oliveras et al., 2014).

Similar to our results, Wagai et al. (2008) reported that the controls of altitude (temperature and precipitation) on OM stoichiometry (indicating mineral surface activity) are dependent on soil bedrocks. Furthermore, Doetterl et al. (2015, 2018) indicated that climate factors in relation to soil mineralogy control the potential of soil matrix to stabilize OM. Our findings also support their views that the OM persistence is controlled by climate factors and soil mineralogy. We further propose that the interactions between precipitation and lithology on OM stabilization in our study are through the controls of soil mineralogy in relation to OM input.

4.5. Conclusion

Our findings highlighted (1) SOC stocks and stability controlled by interactions between precipitation and lithology, and (2) soil aggregate size distribution controlled by lithology only. We did not find an important effect of precipitation on aggregation, which was probably superimposed by the effect of lithology. As the assumption that aggregate occlusion contributes to OM stabilization is not supported by our data, we conclude that OM adsorption on mineral surfaces is the major OM stabilization mechanism in these soils. We propose that the controls of

precipitation and lithology on SOC stocks and OM stabilization are through the controls of soil mineralogy in relation to OM input.

Further studies are required for more lithology types and more precipitation levels. In addition, primary effects of precipitation on OM dynamics are not limited to the controls of soil mineralogy. Potential effects of precipitation on quantity and quality of input OM suggest that investigations in OM molecular composition may contribute to a better understanding of the processes governing SOC sequestration in the Neotropical grasslands of the Andes.

- Soil aggregation and SOC stability affected by lithology and precipitation


SHARO

- Carbon chain length and double bonds control fatty acid stability

Chapter 5

Selective stabilization of soil fatty acids related to their carbon chain length and presence of double bonds in the Peruvian Andes

This chapter has been submitted as:

Yang, S., Jansen, B., Absalah, S., Kalbitz, K., Cammeraat, E., 2019. Selective stabilization of soil fatty acids related to their carbon chain length and presence of double bonds in the Peruvian Andes. Revised version submitted to Geoderma.

- Carbon chain length and double bonds control fatty acid stability

Abstract

Recent studies show increasing evidence for perseveration of soil organic matter (SOM) controlled by interactions with the soil matrix (i.e. mineral surfaces and aggregates) rather than chemical recalcitrance of the SOM. However, a consensus is still absent for potential controls of SOM chemical composition on SOM stabilization and persistence. Soil fatty acids (FAs), which form an important SOM component, can be used to investigate the effects of chemical properties on SOM stabilization because they are easily degraded by microorganisms but can be stabilized by the soil matrix against decomposition. Here we investigated whether inherent molecular properties of FAs control their stability in soils and their interactions with the soil matrix. Soil samples were collected from alpine grasslands of the Peruvian Andes (Andosols, Umbrisols and Phaeozems), as they are characterized by high carbon stocks, abundant aliphatic compounds. We applied pyrolysis - gas chromatography / mass spectrometry analyses assisted by tetramethylammonium hydroxide (TMAH-pyrolysis-GC/MS) to determine the chemical composition of bulk SOM and FAs before and after a 76-day incubation experiment, comparing a situation with intact versus crushed soil aggregates. The results showed that the TMAH-pyrolysis-GC/MS yielded more than 60% FA-derived compounds in detected compounds, with a major contribution of free FAs. FA stability was controlled by the presence of double bonds (unsaturated vs. saturated FAs) and carbon chain length. Unsaturated FAs significantly ($P<0.05$) predicted soil organic carbon mineralization rates and were more depleted after the incubation compared to saturated FAs. The depletion of unsaturated FAs is likely explained by their easier degradation compared to saturated FAs. The easier degradation might be explained by the less extent of stabilization through association with mineral surfaces and/or chemical properties rather than stabilization through occlusion in aggregates. In terms of carbon chain length, FA stability decreased from short-chain to long-chain FAs. A possible explanation for this is that short-chain FAs received more protection by occlusion in aggregates compared to long-chain FAs. We also observed the microbial transformation of FAs during the incubation. Such microbial transformation has limited effects on the prediction of FA stability using double bonds and carbon chain length. However, we observed that soil types and horizons did influence the controls of double bonds and carbon chain length on FA stability . This suggests more studies are needed before generalizing the findings to other soils. Our results corroborate the hypothesis that the inherent properties of soil FAs control their interactions with the soil matrix and indirectly govern their stabilization and persistence in the Peruvian Andean soils under study.

Keywords: Soil organic matter; lipids; TMAH-pyrolysis- GC/MS; unsaturated; saturated; incubation

- Carbon chain length and double bonds control fatty acid stability

5.1. Introduction

The persistence of soil organic matter (SOM) is crucial to sustaining the large soil organic carbon (SOC) pool in the context of global change. New-emerging paradigms indicate a shift from SOM persistency controlled by chemical recalcitrance of SOM due to the bond strength between C atoms to that controlled by decreased SOM bioavailability due to interactions between SOM and soil matrix (Lehmann and Kleber, 2015; Schmidt et al., 2011). The underlying mechanisms of the interactions are specified as (1) SOM occlusion in soil aggregates to decrease the accessibility of microbial decomposers, and (2) formation of organo-mineral associations by functional groups of SOM molecules and mineral surfaces (Lützow et al., 2006; Wiesmeier et al., 2019). Although chemical recalcitrance of SOM is considered to be less-important to SOM persistence than previously assumed (Dungait et al., 2012; Kleber, 2010), the consensus on the effects of SOM chemical characteristics on SOM persistency is still absent (Kögel-Knabner, 2017). An important reason is that influences of SOM molecular composition on interactions between organic matter (OM) and the soil matrix are still not well-understood.

Soil lipids are one of the significant SOM fraction, and are increasingly applied as the molecular proxy to investigate the origins of SOM and to reconstruct changes in vegetation, climate and human activities (Jansen and Wiesenberg, 2017; Wiesenberg et al., 2008). In general, soil lipids are separated into: (1) free-lipids that are derived from wax esters of plants, (2) bound-lipids that are part of macromolecules like cutin and suberin, and (3) phospholipid fatty acids that originate from membrane structures of microorganisms (Frostegård and Bååth, 1996; Jansen and Wiesenberg, 2017). The reliability of the application of lipids as molecular proxy for the origins of SOM is largely dependent on persistence and preservation of lipids, which is further controlled by their interactions with the soil matrix (i.e. mineral surfaces and aggregates) (Lützow et al., 2006). However, it is still poorly understood whether inherent properties of lipids, including lipid types, carbon chain length and free vs. bound lipids, have significant influences on the interaction with the soil matrix and further impact compound preservation (e.g. Angst et al., 2018).

Fatty acids (FAs), which originate from both plant materials and microorganisms, are one of the most abundant lipid fractions in soils (Jandl et al., 2004; Kögel-

Knabner, 2002). In general, FAs in soils are vulnerable to decomposition based on both residential time (Jansen and Wiesenberg, 2017; Schmidt et al., 2011) and decomposition experiments (Angst et al., 2016; Moucawi et al., 1981). In addition, FAs are usually used as energy sources because of their higher energy density (38 kJ g^{-1}) than carbohydrates and proteins (17 kJ g^{-1}) subjected to biotic oxidation (Sadava et al., 2008). The decomposition of FAs in soils is controlled by β-oxidation, an intercellular enzyme-dependent process in which FAs are totally decomposed into CO_2 and H_2O (H. Dinel et al., 1990; Rustan and Drevon, 2005). Although soil FAs are common energy sources, they are reported to accumulate in some soils in alpine grasslands and in Antarctica (Matsumoto et al., 1981; Nierop et al., 2007, 2006). The persistence of FAs in soils can be controlled by different mechanisms; especially interaction with mineral surfaces and occlusion in aggregates have been observed to be of importance (Lützow et al., 2006). The amphiphilicity of FA molecules, characterized by a hydrophilic carboxyl group and a hydrophobic methyl group, is crucial for their interaction with soil mineral surfaces (Lützow et al., 2006). The carboxyl groups of the FAs can interact with charged mineral surfaces via ligand exchange and polyvalent cation bridges, whereas the methyl groups can promote the formation of hydrophobic zones (Kleber et al., 2015; Lützow et al., 2006). This is further corroborated by the models of the OM-mineral interaction, in which FAs play an important role in the formation of OM-mineral associations due to their amphiphilicity (Kleber et al., 2007; Wershaw, 1993). In addition, FAs can be stabilized by physical protection of soil aggregates (Angst et al., 2018b; Lehmann et al., 2007). Because aggregate-protected OM is reported to have distinguished chemical properties compared to other fractions (Golchin et al., 1994; Wagai et al., 2009), aggregate-protected FAs can be potentially controlled by their inherent chemical properties.

Soils in alpine grasslands of the Andes accumulate large quantities of SOC. SOC stocks of the entire soil profiles are reported to range from 118±15 to 215±21 Mg ha^{-1} in the Peruvian puna grassland (e.g. Yang et al., 2018; Zimmermann et al., 2009), and up to 530±40 Mg ha^{-1} in the Ecuadorian páramo grassland (Tonneijck et al., 2010). In the Andean grasslands, SOC is preserved by SOM adsorbed on mineral surfaces (Rolando et al., 2017a; Tonneijck et al., 2010), which is further controlled by environmental factors like precipitation and lithology (Yang et al., 2019a). These soils received limited studies on the molecular composition of

SOM, which show a large contribution of lipids to the bulk SOM (Muñoz-García and Faz-Cano, 2012; Nierop and Jansen, 2009).

Table 5.1 Sampling site description and basic soil properties.

	Site 1	Site 2	Site 3	Site 4
Site description				
ID	Wet-LS	Wet-AS	Dry-LS	Dry-AS
Location	7.16° S, 78.61° W	7.17° S, 78.63°W	9.25° S, 77.59°W	9.19° S, 77.60° W
Precipitation (mm)	1100 mm	1100 mm	680 mm	680 mm
Temperature (°C)	11	11	11	11
Altitude (m a.s.l.)	3510-3720	3570-3590	3520-3580	3490-3670
Lithology	Limestone	Granite or ignimbrite (rhyodacitic composition)	Limestone	Granodiorite or glacier material rich in granodiorite
Land use	Grassland/abundant cultivation	Grassland/abundant cultivation	Grassland/abundant cultivation	Grassland
Number of replicates	2	2	2	2
Soil properties				
Soil classification (WRB 2014)	Phaeozems	Andosols	Phaeozems	Andosols/Umbrisols
Soil horizons	Ah-Btg-C	Ah-C	Ah-Btg-C	Ah-C
Soil depth (cm)	61±3	49±10	61±6	51±5
SOC stock (Mg ha^{-1})	405±42	226±6	153±27	172±13
SOC content (%)	A horizons: 9.95±1.29 B horizons: 2.84±0.45	A horizons: 5.95±1.06	A horizons: 2.75±0.37 B horizons: 1.48±0.37	A horizons: 4.88±0.65
pH	A horizons: 5.97±0.18 B horizons: 6.56±0.22	A horizons: 5.09±0.09	A horizons: 5.26±0.12 B horizons: 5.34±0.21	A horizons: 5.29±0.15

Mean ± SE, n = 3. SOC: soil organic carbon, Wet: the wet site, Dry: the dry site, LS: limestone soil, AS: acid igneous rock soil. Data of SOC stocks, SOC contents and pH originate from Yang et al. (2019a). Soil classification was based on field observation.

The paradox that FAs are common energy sources yet able to interact with the soil matrix to gain protection against decomposition suggests that we need a better understanding of soil FA persistence and the underlying mechanisms. The lipid-rich soils in the Andes give an opportunity to investigate the potential relationships between soil FA persistence and their molecular structures. For this, we applied a combination of a pyrolysis-GC/MS analysis assisted by tetramethylammonium hydroxide (TMAH-pyrolysis-GC/MS) and a 76-day incubation of soil aggregates (intact and crushed) to address the stability of FAs in relation to their chemical properties and the soil matrix. The objectives of this study were to investigate (1) whether inherent properties (e.g. carbon chain length and double bonds) of the FAs control their stability in soils, and (2) whether the potential controls of FA stability can be explained by the chemical recalcitrance of the FAs or their interactions with the soil matrix.

- Carbon chain length and double bonds control fatty acid stability

5.2. Materials and methods

5.2.1. Site description and soil sampling

The study area was located in alpine grasslands of the Peruvian Andes, corresponding to the ecosystem of the Jalca or the wet Puna (Rolando et al., 2017b). Sampling sites have an altitudinal ranging from 3490 to 3720 m a.s.l. and an annual average temperate around 11 °C. Major land use type in this region is grassland together with cultivation, grazing and plantation of pine trees and eucalyptus (Rolando et al., 2017b; Sánchez Vega et al., 2005). The sampling sites were selected based on the combination of two bedrock types (limestone and acid igneous rocks) and two precipitation levels (1100 mm and 680 mm). Soils developed on the limestone have dark A horizons above argic B horizons, and are classified as Phaeozems (WRB, 2014). Soils on acid igneous rocks have vitric or umbric A horizons overlaying C horizons, and correspond to Andosols or Umbrisols (WRB, 2014). Detailed soil properties are presented in Fig. 5.1 and Table 5.1.

Soil samples were collected by horizons from two replicated profiles in each combination of bedrock types and precipitation levels. Soil samples were transferred in sealed plastic bags with the protection of hard plastic boxes for the transportation. All soil samples were air-dried at 40 °C before laboratory analyses. Materials from different A sub-horizons were merged to one A horizon (e.g. Ah1, Ah2 and Ah3 merged to Ah horizon) based on the weight distribution of each horizon. Limestone soils (LSs) had one merged A horizon and one B horizon, whereas acid igneous rock soils (ASs) only had one merged A horizon.

5.2.2. Soil properties and incubation

Soil samples from different horizons (n = 12) were fractionated by aggregate sizes using a dry-sieving method. Briefly, 170-230 g air-dried bulk soil samples were sieved into 3 fractions using 2 mesh sieves (diameter 2 and 0.25 mm) on a horizontal shaker (30 Hz for 20 s). All fractions were named by size as large macroaggregate (LM, >2 mm), small macroaggregate (SM, 0.25-2 mm) and microaggregates (Mi, <0.25 mm). For each fraction, weight was determined by weighing materials, while total C contents were measured using a Vario EL Elementar Analyzer (Elementar, Germany). As carbonate was absent in all

samples (Yang et al., 2019a), total C contents were equal to organic carbon (OC) contents.

A 76-day incubation experiment was applied for both LM and SM fractions to investigate potential changes in SOM molecular composition after a short-term microbial decomposition. Intact and crushed aggregates were used for the incubation. Aggregates were crushed by grinding the fractions using a porcelain mortar and passing through a 0.125 mm sieve. Ten-gram materials (dry-weight equivalent) were rewet at pF=2.0 for 10 days and incubated at 20 °C for 76 days in sealed jars (120 cm^3). CO_2 concentrations of the headspace were measured to calculate SOC mineralization rates at the days of 1, 2, 6, 9, 13, 20, 28, 48 and 76. The CO_2 concentrations were analyzed using a gas chromatography with a flame ionization detector (GC-FID, Thermo Scientific, Trace GC Ultra) with a methanizer in front of the FID and packed columns. SOC mineralization rates (mg CO_2-C g^{-1} SOC) with intact aggregates were used to estimate the SOM stabilization controlled by association with mineral surfaces and occlusion in aggregates, whereas SOC mineralization rates with crushed aggregates were to estimate the SOM stabilization controlled by association with mineral surfaces only. The differences in SOC mineralization rates between intact and crushed aggregates were used as measures of the stability of aggregate-occluded SOM (Wang et al., 2014). After the incubation, all samples were dried at 40 °C for molecular analyses using a TMAH-pyrolysis-GC/MS.

5.2.3. TMAH-Pyrolysis-GC/MS

Three grams of dried subsamples before and after incubation were homogenized for TMAH-pyrolysis-GC-MS analyses. Between 20 and 50 mg of samples were weighed depending on the SOC contents. The samples were subsequently mixed with 20-60 µl of the derivatizing reagent (25% tetramethylammonium hydroxide (TMAH) in water). A small amount of the mixture for each sample was spread on a ferromagnetic wire and dried under a halogen lamp for the pyrolysis. The pyrolysis was performed using a Curie-point pyrolyzer (Horizon Instruments; 600 °C; 5 s), which was coupled to a ThermoQuest Trace GC gas chromatograph (Waltham, USA). Helium was used as the carrier gas. The initial temperature of the oven was 40°C for 1 min and heated to 320 °C with a rate of 7.0 °C min-1 and a hold time of 10 minutes. The analytes were separated on a ZB1-MS column (Phenomenex: 30 m, 0.25 mm i.d, 0.50 µm df). The column was connected to a

Finnigan Trace MS mass spectrometer (Waltham, USA; m/z: 47–500, ionization energy: 70 eV, cycle time: 0.45 s).

5.2.4. Data analyses and statistics

Peak identification was based on retention times and mass spectra using the NIST library (Gaithersburg, USA), as well as the information from Brock et al. (2019), Buurman et al. (2007) and Nierop et al. (2007). A peak was identified as a compound when the ratio of signal to noise is larger than three and when the spectra of the target compound can be clearly identified from the peak. The sum of peak areas of all identified compounds was set to 100 % and the relative abundance (RA) of each compound was calculated. Relative abundance shifts (for Fig. 5.2) were calculated by subtracting RAs after the incubation from RAs before the incubation. Changes in compound relative abundances after the incubation of intact aggregates (RACIn) and crushed aggregate (RACCr) were used to estimate the compound stability against decomposition. Increased relative abundances indicated that the compounds were stable against decomposition or produced during incubation, whereas decreased relative abundances indicated that the compounds were depleted and labile against decomposition. Differences in changes in the relative abundance between intact and crushed aggregates (RACr-In) were used to evaluate how much the compounds were likely protected by aggregates. The RAC_{In}, RAC_{Cr} and $RAC_{Cr\text{-}Or}$ were calculated by the following equation:

$$RAC_{In} = (RA_{In}\text{-}RA_{Or}) / RA_{Or} \times 100\ \% \qquad \text{Equation 1}$$

$$RAC_{Cr} = (RA_{Cr}\text{-}RA_{Or}) / RA_{Or} \times 100\ \% \qquad \text{Equation 2}$$

$$RAC_{Cr\text{-}In} = (RA_{Cr}\text{-}RA_{In}) / RA_{Or} \times 100\ \% \qquad \text{Equation 3}$$

In the equation, RAC_{In} = change in relative abundance after incubation of intact aggregates, RAC_{Cr} = change in relative abundance after incubation of crushed aggregates, $RAC_{Cr\text{-}In}$ = difference in change in relative abundance between intact and crushed aggregates after incubation, RA_{Or} = original relative abundance, RA_{Cr} = relative abundance after incubation of crushed aggregates, RA_{In}= relative abundance after incubation of intact aggregates.

An independent t-test was applied to identify differences in relative abundances of compounds and SOC mineralization rates between different aggregate sizes, and

between intact and crushed aggregates. When data normality could not be assumed (checked using a Shapiro-Wilk test), a Mann-Whitney U test was used instead of the t-test. Linear regressions were applied to find significant predictors for the SOC mineralization rates from different compounds. Univariate linear regressions were applied to predict SOC mineralization rates using relative abundance (shifts) of individual FAs. Principal component regressions (PCR) were applied to predict SOC mineralization rates using relative abundance (shifts) of all FAs. The application of PCR instead of multiple linear regression was to solve the problem of collinearity. Briefly, principal component analyses were firstly conducted to create up to 12 orthogonal principal components (PCs). These PCs were used as independent variables to predict SOC mineralization rates using multiple linear regressions. All significant PCs were included in the models and regression coefficients of all significant PCs and all FAs were calculated. The analysis of covariance (ANCOVA) was applied to predict relative abundance changes (RAC) using the presence of double bonds and carbon chain length of the FAs. The ANCOVA models were conducted when all FAs were included and when microbial-produced FAs were removed. Through this we aimed to investigate whether the microbial transformation of FAs during the 76-day incubation had clear effects on our prediction of RAC. The microbially produced FAs were selected based on publications (Barré et al., 2018; Jansen and Wiesenberg, 2017; Kaneda, 1991) and our observation (C16:0 and C18:0, see section 5.4.4). All statistical analyses were performed using SPSS 24.0 (SPSS Inc., USA).

5.3. Results

5.3.1. Incubation and chemical composition of SOM

Data on aggregate-size distribution and SOC mineralization originated from (Yang et al., 2019a). The LM and SM fractions accounted for 61.3 % and 26.5 % of bulk soil samples by weight respectively, whereas the microaggregate fraction was only 12.2 % of the bulk soil (Fig. 5.1). After the 76-day incubation, 1.0 % to 1.3 % of the SOC was mineralized into CO_2 (Fig. 5.1). No significant difference in SOC mineralization rates was observed between LM and SM fractions or between intact and crushed aggregates (Fig. 5.1).

- Carbon chain length and double bonds control fatty acid stability

The TMAH-pyrolysis-GC/MS analyses yielded compounds derived from fatty acids (FAs), α,ω-diacids (DAs), ω-hydroxy alkanoic acids (ω-HAs), *n*-alkanes, *n*-alkenes, esters, lignin, polysaccharides and N-containing compounds, as well as other unspecified compounds (Fig. 5.2). Compounds derived from lipids (sum of FAs, DAs, ω-HAs, *n*-alkanes, *n*-alkenes and esters) were more abundant than compounds derived from polysaccharides, lignin and N-containing compounds (Fig. 5.2). Relative abundances of compounds derived from fatty acids (FAs) were 62.4±4.7 % for the LM fraction and 61.5±2.9 % for the SM fraction (Fig. 5.2). After the 76-day incubation, compounds derived from DAs, ω-HAs, *n*-alkenes, *n*-alkanes and esters were depleted except for ω-HAs in the SM fraction (Fig. 5.2).

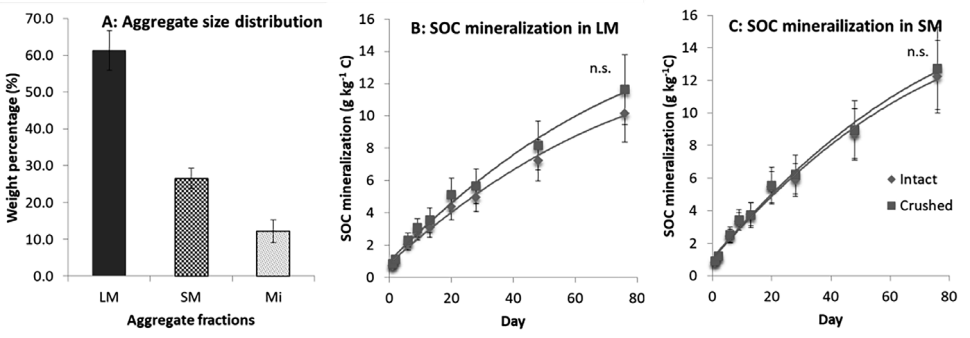


Fig. 5.1 Soil aggregate size distribution (A) and specific soil organic carbon (SOC) mineralization rates in a 76-day incubation (B, C) (*n* = 12, mean ± SE). LM: large macroaggregates (>2 mm), SM: small macroaggregates (0.25–2 mm), Mi: microaggregates (<0.25 mm), Intact: intact aggregates, Crushed: crushed aggregates, n.s.: not significant. Data originate from Yang et al. (2019a)

5.3.2. Changes of fatty acids after incubation

FAs were the most abundant compound type in lipids and in all detected compounds (Fig. 5.2). Twenty-seven different FAs were identified with carbon chain length ranging from 12 to 32. FAs with a carbon chain length of 16 (C16) were the most abundant, followed by compounds with a carbon chain length of 18. Most of the FAs were saturated, except for FAs of C16:1, C18:1 and cyclopropane C19:0 (Fig. 5.3).

In general, relative abundances of unsaturated FAs (C16:1 and C18:1) and long-chain FAs (C>25) declined after the incubation, whereas saturated FAs of C12:0, C16:0 and C18:0 accumulated after the incubation (Fig. 5.3). After the incubation, crushed aggregates generally were less abundant in short-chain FAs (e.g. C16:0

and C17:0) and more abundant in long-chain FAs (e.g. C29:0 and C30:0) compared to intact aggregates (Fig. 5.3).

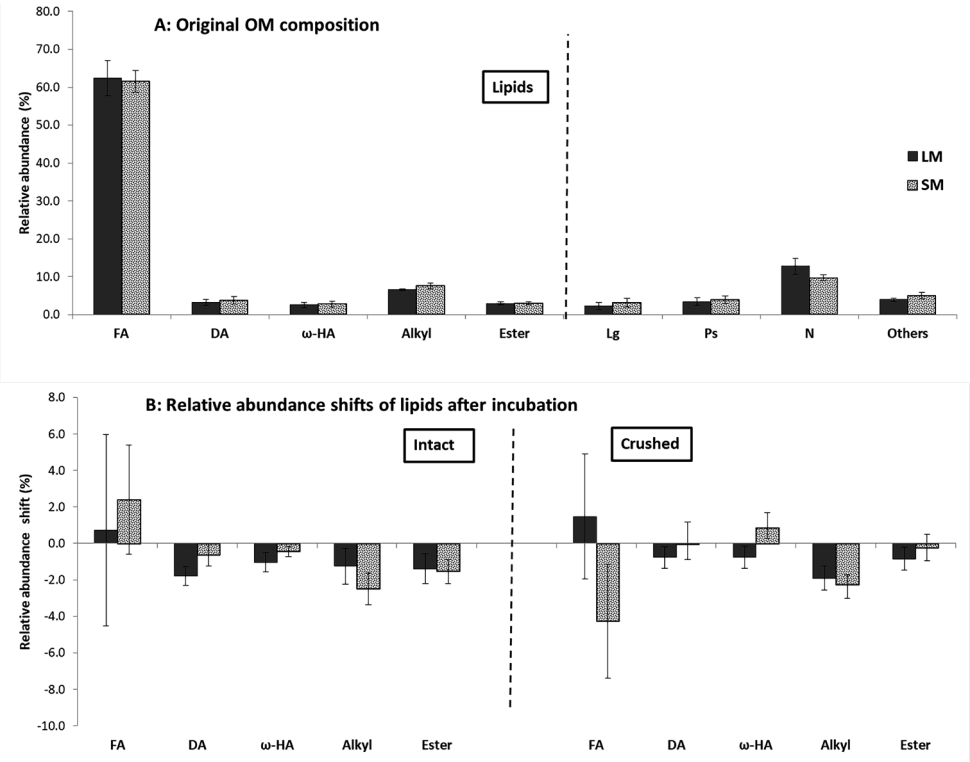


Fig. 5.2 Relative abundances of detected compounds before the incubation and relative abundance shifts for lipids after the incubation (n = 12, mean ± SE). LM: large macroaggregates, SM: small macroaggregates. Intact: incubating intact aggregates, Crushed: incubating crushed aggregates, FA: fatty acids, DA: α,ω-dioic acids, ω-HA: ω-hydroxy alkanoic acids, Alkyl: *n*-alkanes and *n*-alkenes, Lg: lignin-derived and aromatic compounds, Ps: polysaccharide-derived compounds, N: nitrogen-containing compounds.

The PCR models explained 23.4% to 45.0% of the total variation for intact and crushed aggregates (Fig. 5.4A and 5.4B). When using relative abundances before incubation to predict SOC mineralization rates, unsaturated FAs (C16:1 and C18:1) as well saturated FAs of C20:0 and C22:0 were significant predictors that had positive relationships with SOC mineralization rates (Fig. 5.4A and 5.4B). In addition, they had higher regression coefficients (2.39-5.12) than other FAs in the PCR models (Fig. 5.4A and 5.4B). When using relative abundance shifts after the incubation to predict SOC mineralization rates, unsaturated FAs (C16:1 and C18:1) and saturated FAs of C31:0 and C32:0 were significant predictors that had negative correlations with SOC mineralization rates (Fig. 5.4C and 5.4D). They

also had the lowest regression coefficients compared to other FAs (Fig. 5.4C and 5.4D). In contrast, C16:0 and C18:0 were significant predictors having positive regression coefficients to predict SOC mineralization rates (Fig. 5.4C and 5.4D). Notably, the prediction models, for both PCR and linear regressions, had no clear differences in significant predictors between intact and crushed aggregates (Fig. 5.4). In contrast, R^2 values of the PCR models were higher for intact aggregates crushed aggregates (Fig. 5.4).

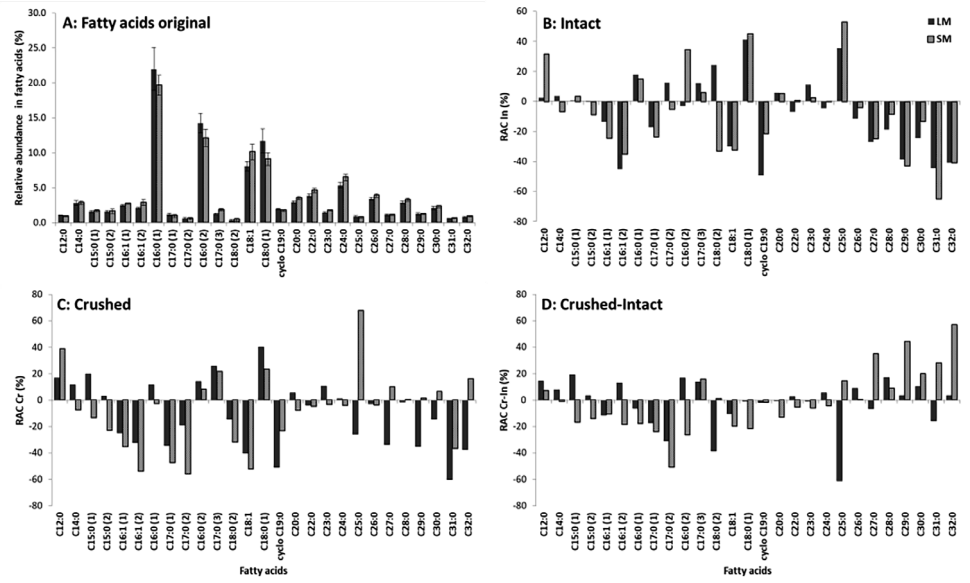


Fig. 5.3 Relative abundances and changes in relative abundances (RAC) of fatty acids after the 76-day incubation (means of n = 12). RAC In: change in relative abundances after incubation of intact aggregates, RAC Cr: change in relative abundances after incubation of crushed aggregates, RAC Cr-In: difference in change in relative abundances after incubation between crushed and intact aggregates (indication of protection of fatty acids by occlusion in aggregates) , LM: large macroaggregates, SM: small macroaggregates, cyclo C19:0: the fatty acid of C19:0 cyclopropanated form.

5.3.3. Predictions of relative abundance changes of fatty acids

Table 5.2 illustrates the prediction of relative abundance changes (RAC) after the incubation for both averaged RACs and RACs of different soil samples, using double bonds and carbon chain lengths of FAs as the predictors. For the overall situation (averaged RACs), unsaturated FAs significantly predicted low RAC_{In} and RAC_{Cr} in both LM and SM fractions ($P<0.05$). In contrast, they were not significant predictors for $RAC_{Cr\text{-}In}$ (Table 5.2). Long-chain FAs were significant predictors for low RAC_{In} in both LM and SM fractions, for low RAC_{Cr} in the LM

fraction, and for high $RAC_{Cr\text{-}In}$ in the SM fraction (Table 5.2). When microbial FAs were removed, significant predictors were not changed in the ANCOVA models, whereas R^2 values slightly increased ($\Delta R^2 = 0.049 \pm 0.029$, Table 5.2).

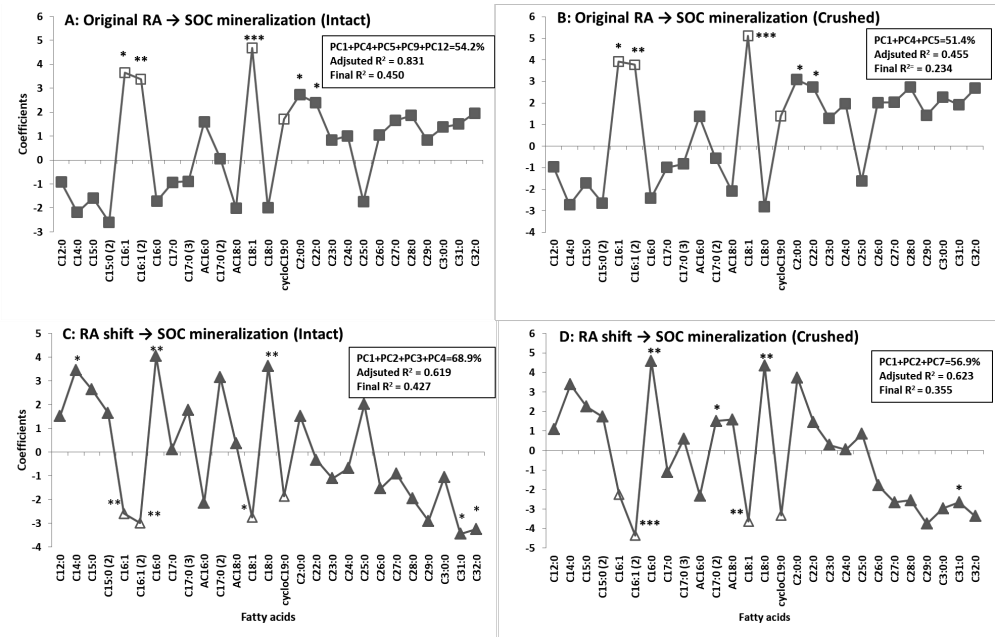


Fig. 5.4 Soil organic carbon (SOC) mineralization rates predicted by relative abundances (RA) of fatty acids and relative abundance shifts after the incubation using principal component regressions (PCR) and linear regressions. Regression coefficients of the PCRs are present as the values of Y axis. The box on the right of each graph presents principal components (PCs) used as the significant predictors and the total variation explained by them. In addition, the box gives information of adjusted R^2 when using PCs to predict SOC mineralization rates and final R^2 when using all fatty acids to predict SOC mineralization rates. The *, ** and*** for each compound present the significant levels of 0.05, 0.01 and 0.001 when SOC mineralization rates are predicted by individual fatty acids using univariate linear regressions. For graphs A and B, high coefficients indicate that the compounds have higher contribution to the SOC mineralization. For graphs C and D, positive coefficients suggest that the compounds are accumulated or produced after the incubation; negative coefficients suggest the compounds are depleted after the incubation. The significant level of each fatty acid was estimated by predicting SOC mineralization rates using only one fatty acid (univariate linear regressions). n = 24, RA: relative abundance, PC: principal component, intact: incubation of intact aggregates, crushed: incubation of crushed aggregates.

When comparing different soil samples and horizons, general findings were that: (1) the presence of double bonds was not a significant predictors ($P<0.05$) for $RAC_{Cr\text{-}In}$ for all soils; (2) long-chain FAs significantly predicted low RAC_{In} and RAC_{Cr} except for B horizons of the wet-LSs; and (3) short-chain FAs were significant predictors for low $RAC_{Cr\text{-}In}$ except for B horizons of the wet-LSs (Table 5.2). In addition, Table 5.2 shows that the R^2 values only slightly changed

($\Delta R^2 = 0.057 \pm 0.018$) after the removal of microbial FAs (see section 5.4.4). However, differences in predictive models were found between soil samples and horizons. The presence of double bonds were more important predictors for the A

Table 5.2 Changes in relative abundances (RAC) of fatty acids after the incubation predicted by the presence of double bonds (DB) and carbon chain length (CCL) using the ANCOVA models. For significantly predictors, the types (i.e. Uns, LC, and SC) corresponding to lower RAC values (more vulnerable) were presented. Microbial-produced FAs are C15:0 (1), C15:0 (2), C16:0 (1), C17:0 (1), C17:0 (2), C17:0 (3), C18:0 (1) and cyclo C19:0. Averaged RACs of all soil samples were used as dependent variables in the ANCOVA models for overall situation.

		Overall			Wet-AS-A			Dry-AS-A			Wet-LS-A			Dry-LS-A			Wet-LS-B			Dry-LS-B		
		DB	CCL	R^2	DB	CCL	R^2	DB	CCL	R^2	DB	CCL	R^2	DB	CCL	R^2	DB	CCL	R^2	DB	CCL	R^2
		(1) All FAs																				
RAC In	**LM**	**Uns****	**LC****	0.523	**Uns****	**LC****	0.456	n.s	n.s	0.042	n.s	**LC****	0.432	**Uns***	n.s	0.325	n.s	**SC****	0.727	n.s	n.s	0.216
	SM	**Uns***	**LC****	0.337	n.s	n.s	0.163	n.s	n.s	0.029	n.s	n.s	0.135	**Uns***	n.s	0.224	n.s	**LC***	0.233	n.s	n.s	0.204
RAC Cr	**LM**	**Uns****	**LC****	0.554	**Uns****	n.s	0.336	**Uns****	n.s	0.239	n.s	**LC****	0.524	**Uns****	n.s	0.304	n.s	n.s	0.045	n.s	n.s	0.049
	SM	**Uns***	n.s	0.249	**Uns****	n.s	0.366	n.s	n.s	0.115	n.s	n.s	0.048	**Uns****	**LC***	0.357	n.s	**SC****	0.46	n.s	n.s	0.218
RAC Cr-In	**LM**	n.s	n.s	0.006	n.s	n.s	0.164	n.s	n.s	0.038	n.s	n.s	0.008	n.s	**SC****	0.265	n.s	**LC****	0.713	n.s	**SC****	0.493
	SM	n.s	**SC****	0.531	n.s	**SC***	0.231	n.s	n.s	0.108	n.s	**SC***	0.262	n.s	n.s	0.042	n.s	**SC****	0.773	n.s	n.s	0.063
		(2) Microbial FAs removed																				
RAC In	**LM**	**Uns****	**LC****	0.476	**Uns***	**LC***	0.403	n.s	n.s	0.037	n.s	**LC****	0.534	n.s	n.s	0.191	n.s	**SC****	0.712	n.s	n.s	0.021
	SM	**Uns***	**LC***	0.387	n.s	**LC***	0.299	n.s	n.s	0.023	n.s	**LC***	0.265	**Uns****	n.s	0.486	n.s	**LC***	0.389	**Uns***	**LC***	0.348
RAC Cr	**LM**	**Uns****	**LC****	0.635	**Uns****	n.s	0.456	n.s	n.s	0.239	n.s	**LC****	0.660	n.s	n.s	0.165	n.s	n.s	0.095	n.s	n.s	0.226
	SM	**Uns***	n.s	0.415	**Uns****	n.s	0.617	n.s	n.s	0.121	n.s	n.s	0.174	**Uns****	**LC****	0.750	n.s	**SC***	0.373	**Uns***	n.s	0.341
RAC Cr-In	**LM**	n.s	n.s	0.009	n.s	n.s	0.150	n.s	n.s	0.008	n.s	n.s	0.126	n.s	n.s	0.197	n.s	**LC***	0.691	n.s	**SC***	0.494
	SM	n.s	**SC****	0.574	n.s	**SC****	0.491	n.s	n.s	0.147	n.s	n.s	0.240	n.s	n.s	0.091	n.s	**SC****	0.758	n.s	n.s	0.187

n = 27 (27 fatty acids). Wet: the wet site, Dry: the dry site, LS: limestone soil, AS: acid igneous rock soil, A: A horizon, B: B horizons, In: intact aggregate, Cr: crushed aggregates, Cr-In: differences between intact and crushed aggregates, LM: large macroaggregates, SM: small macroaggregates, DB: double bounds, CCL: carbon chain length, Uns: unsaturated fatty acids, LC: long-chain fatty acids, SC: short-chain fatty acids, *: $P < 0.05$, **: $P < 0.01$, n.s.: not significant.

horizons of the wet-ASs and the dry-LSs (Table 5.2). For the B horizons of the wet-LSs, short-chain FAs significantly predicted low RAC_{In} and RAC_{Cr}, whereas long-chain FAs were a significant predictor for low $RAC_{Cr\text{-}In}$ (Table 5.2).

5.4. Discussion

5.4.1. Chemical composition

It is important to note that the OM molecular composition yielded by TMAH-pyrolysis-GC/MS does not necessarily reveal the quantitative composition of bulk SOM because the methodology is not fully quantitative. Nevertheless, it is still possible to compare our results to those of other studies using the same methodology under similar conditions. When compared to other studies using TMAH-pyrolysis-GC/MS (e.g. Barré et al., 2018; Brock et al., 2019; Nierop and Verstraten, 2003), our results highlighted a large proportion of lipid-derived compounds and a small proportion of lignin- and polysaccharide-derived compounds (Fig. 5.2). This suggests that lipids are selectively preserved in the Peruvian Andean soil under study. Similar to our results, Matsumoto et al. (1981) found a large contribution of fatty acids (FAs) in Antarctic soils, whereas Nierop et al. (2007) reported lipid-rich and lignin-depleted soils in the Andean grassland of Northern Ecuador. As Nierop et al. (2007) found poor relationships between SOM molecular composition and vegetation (i.e. grassland vs. forest), the selective preservation of lipids is unlikely to be attributed to SOM input related to the vegetation. The small proportions of compounds derived from lignin and polysaccharides in our soils agree with the results of Nierop et al. (2007), who found lignin- and polysaccharide-depleted soils in the Andean grasslands of Ecuador. In contrast, soils in other systems have larger amounts of lignin- and polysaccharide-derived compounds than our soils (Barré et al., 2018; Brock et al., 2019; Nierop and Verstraten, 2003). This suggests that compounds considered in former times as recalcitrant do not always persist in soils, which corroborates the emerging view that long-term SOM stabilization is not regulated by chemical recalcitrance per se (Dungait et al., 2012; Schmidt et al., 2011).

- Carbon chain length and double bonds control fatty acid stability

Soil lipids are separated into free lipids derived from leaf wax, bound lipids derived from macromolecules (e.g. cutin and suberin) and lipids derived from microorganisms (Jansen and Wiesenberg, 2017). The results allow for an estimation of soil lipids of plant origins. In general, α-, ω-dioic acids and ω-hydroxyl alkanoic acids are mostly derived from bound lipids as part of macromolecules (Feng et al., 2010; Nierop et al., 2006). The small proportions of α-, ω-dioic acids and ω-hydroxyl alkanoic acids in our soils (Fig. A5.2) suggest a minor contribution of bound lipids. This is further supported by (1) the absence of cutin or suberin biomarkers (e.g. 9,10,ω-trihydroxy alkanoic acids and x,ω-dihydroxy alkanoic acids), and (2) the depletion of α-, ω-dioic acids and ω-hydroxyl alkanoic acids after the incubation (Fig. 5.2 and A5.2). Thus, free lipids derived from plants rather than bound lipids are particularly important in our soils. The preferential accumulation of free lipids in our soils can be explained by the chemical properties of free lipids (not part of macromolecules), which make them easier to interact with the soil matrix compared to bound lipids (Angst et al., 2018b). In addition, differences in functional groups (e.g. carboxyl groups vs. ester groups) between free and bound lipids can also affect their interactions with the soil matrix and further control their stability (Kleber et al., 2007; Lützow et al., 2006). Because of the abundant FAs and the major contribution of free FAs, the following discussions on FA stabilization are representative for free FAs.

5.4.2. Unsaturated and saturated fatty acids (FAs)

The results indicated that unsaturated FAs were more depleted than saturated FAs after the incubation (Fig. 5.3, Fig. 5.4 and Table 5.2). This is consistent with the general view that unsaturated FAs are less persistent than saturated FAs (Ayala et al., 2014). The depletion of unsaturated after the incubation might be attributed to: (1) microbial decomposition and (2) association with mineral surfaces or macromolecules and being undetectable. We propose that microbial decomposition most likely causes the depletion of unsaturated FAs because the SOC mineralization rates were significantly predicted by the abundances of unsaturated FAs before the incubation and the changes of unsaturated FAs during the incubation (Fig. 5.4). In addition, it is logical that microbes utilize unsaturated FAs when other energy sources (e.g. carbohydrates in our soils) are rare. The depletion of unsaturated FAs is unlikely explained by the association with mineral surfaces or incorporation into macromolecules because: (1) TMAH-pyrolysis-GC/MS is capable to break macromolecules into monomers (e.g. Brock et al.,

2019; Nierop et al., 2007); (2) natural soils should reach balances of the interactions of OM with minerals and macromolecules; and (3) the balances were unlikely to have been significantly shifted during the 76-day incubation. Thus, unsaturated FAs were less stable against microbial decomposition compared to saturated FAs with similar carbon chain length. Similar to our results, Moucawi et al. (1981) found higher decomposition rates for oleic acid (C18:1) compared to stearic acid (C18:0) in acid soils only, whereas Dent et al. (2004) reported the accumulation of saturated FAs and the depletion of unsaturated FAs during the necromass decomposition in soils.

The stabilization of both unsaturated and saturated FAs in soils is controlled by: (1) FAs occluded in aggregates, (2) FAs association with mineral surfaces, and (3) chemical recalcitrance of the FAs (Lehmann and Kleber, 2015; Lützow et al., 2006). Occlusion within aggregate is unlikely the explanation for the vulnerability of unsaturated FAs compared to saturated FAs, because the presence of double bonds was not a significant predictor for the $RAC_{Cr\text{-}In}$ (Table 5.2). This suggests that the unsaturated FAs are protected by aggregates to a similar extent as the saturated FAs with similar carbon chain length. Alternatively, FAs associated with mineral surfaces and/or their chemical properties are potential explanations for the depletion of unsaturated FAs. Considering chemical properties, the unsaturated FAs are more vulnerable to lipid peroxidation than saturated FAs due to their double bonds. Briefly, the unsaturated FAs are susceptible to the attack of reactive radicals at the position of double bonds and are vulnerable to biotic and abiotic rancidification. These processes allow for easier degradation of unsaturated FAs as compared to saturated FAs (Ayala et al., 2014; Gardner, 1989). In addition, incorporation within macromolecules may also control the bioavailability of FAs in the early stages of decomposition (Schmidt et al., 2011). This may also affect the stability of unsaturated and saturated FAs in our study because the incubation was conducted for 76 days. For the association with mineral surfaces, unsaturated and saturated FAs might have different affinities to the association sites of mineral surfaces. Saturated FAs are straight molecules, whereas unsaturated FAs generally have one or multiple bent structures as cis-double bonds have an angle of 120° (Rustan and Drevon, 2005). In the models of OM-mineral association, straight FAs and compounds with similar structures are important with respect to interaction with mineral surfaces and the formation of hydrophobic zones (Kleber et al., 2007; Wershaw, 1993). If the saturated FAs were replaced by unsaturated FAs, unsaturated FAs are unable to pack as tightly

as saturated FAs due to the bent structures introduced by their cis configuration (Rustan and Drevon, 2005). This can potentially weaken the association of unsaturated FAs with minerals when compared to saturated FAs. However, this situation might not be applicable for soils in which OM complexation with Fe and Al is the dominant stabilization mechanism (e.g. Andosols).

5.4.3. Carbon chain length

In general, carbon chain length is a significant predictor for changes in relative abundances, and short-chain FAs were more stable than long-chain FAs except for the B horizons of wet-LSs (Table 5.2). To our knowledge, only a few studies have investigated the stability of soil FA related to carbon chain length. Moucawi et al. (1981) reported that long-chain FAs were more stable than short-chain FAs, which is not consistent with our results. Notably, they estimated FA stability by adding new FAs in soils and determining their decomposition rates (Moucawi et al., 1981), which suggests that the FA stability in their study is more related to chemical recalcitrance of the FAs rather than FA stabilization controlled by the soil matrix. Mueller et al. (2013) and Otto and Simpson (2007) found that carbon chain length is crucial to soil lipids distribution, however, the stability of the lipids against decomposition was not investigated. Otto and Simpson (2007) also found more contribution of free-lipids in long-chain lipids, which might affect the stability of FAs with different chain length in our soils. However, the influences are probably limited in our soils because of the minor contribution of bound-FAs (see discussion 5.4.1).

In general, the declined FA stability with increasing carbon chain length might be related to: (1) the affinity of FAs to the mineral surfaces, (2) the possibility that FAs were stabilized by occluded in aggregates, and (3) chemical recalcitrance (Lützow et al., 2006; Wiesmeier et al., 2019). We observed that short-chain FAs were consistently preferentially stabilized by occlusion in aggregates except for B horizons of wet-LS, as indicated by short-chain FAs corresponding to lower $RAC_{Cr\text{-}In}$ values (more likely protected by aggregates, Table 5.2). Thus, the selective stabilization of short-chain FAs by occlusion in aggregates is a possible explanation for their higher stability compared to long-chain FAs for our results. This might be attributed to the fact that long-chain FAs are generally distributed in large-sized aggregates (Lützow et al., 2006). As large-sized aggregates can only provide weak protection and can have high microbial activities (Six et al.,

2004, 2000), long-chain FAs are potentially easily decomposed. In contrast, small-size aggregates provide OM with strong and long-term protection (Six et al., 2004, 2000) that allows for short-chain FAs more stable than long-chain FAs.

5.4.4. Microbial transformation

During the incubation, microbial transformation of FAs generally occurs in addition to the mineralization of FAs. In our study, soil microbes are likely to mineralize unsaturated FAs into CO_2 and H_2O to gain energy through β-oxidation coupled with the tricarboxylic acid cycle, meanwhile, they metabolize microbial (short-chain) FAs to maintain cell structures (Dinel et al., 1990; Rustan and Drevon, 2005). As these

It is important to know whether the microbial transformation of FAs affects the prediction of FA stability using the presence of double bonds and carbon chain length. When these microbial FAs (C16:0, C18:0, cyclopropane C19:0 and isomers of C15:0 and C17:0) were removed from the ANCOVA models, the unchanged or slightly changed significance of predictors (Table 5.2) suggested that the removal of microbial FAs does not clearly affect the prediction of FAs stability. This is further supported by the fact that R^2 values were only slightly changed after the removal of microbial FAs (Table 5.2). Thus, although the microbial transformation of FAs occurred during the incubation, it has a limited impact on our estimation of FA stability using the presence of double bonds and carbon chain length.

5.4.5. Differences between soil samples

When comparisons were made between different soils, we could propose conclusions that are applicable to all our soil samples. Unsaturated FA stabilization is unlikely controlled by occlusion in aggregates, as indicated by the fact that $RAC_{Cr\text{-}In}$ was never significantly predicted by the presence of double bonds (Table 5.2). Short-chain FAs were preferentially stabilized by occlusion in aggregates, as indicated by short-chain FAs significantly predicting lower $RAC_{Cr\text{-}In}$ except for the B horizons of wet-LSs (Table 5.2).

However, the differences between soil samples (Table 5.2) indicated that we must be careful when we generalize our findings to soils with different bedrocks, climate conditions and horizons. For example, the B horizons in wet-LSs showed

higher stability of long-chain FAs, which is not consistent with the situations in other soils of our study (Table 5.2). A possible explanation is the high clay contents in the B horizons of wet-LSs (40 %) due to clay illuviation promoting the formation of a massive sticky structure in which OM is not protected effectively by occlusion in aggregates (Yang et al., 2019b). With regard to unsaturated FAs, the significant control of RAC by double bonds was mainly observed in the wet-ASs and the dry-LSs (Table 5.2). This might be attributed to the abundant of unsaturated FAs in the dry-LSs and the wet-ASs and their higher depletion after the incubation (Fig. A5.3). In addition, the dry-LSs had the lowest SOC stability (Yang et al., 2019a) and the highest abundances of unsaturated FAs compared to other soils (Fig. A5.3). This is consistent with our findings and the general view that unsaturated FAs were less stable compared to saturated FAs (Ayala et al., 2014).

5.4.6. Implications to bulk soil organic matter

The results indicate an accumulation of free lipids and FAs as well as a minor contribution of bound lipids and FAs (see section 5.4.1). The selective preservation of free FAs suggests the origins of FAs are crucial to FA persistency. Our results also give direct evidence that chemical properties of the FAs control their interaction with the soil matrix and indirectly influence their persistence in soils. This addresses the current discussion on the importance of SOM chemical properties on SOM persistence in soils (Dungait et al., 2012; Schmidt et al., 2011), and is supported by recent findings that SOM chemical properties control the interaction with the soil matrix and further influence OM stabilization (Angst et al., 2018b, 2017). As our study showed a large proportion of FAs when compared to other studies using similar methods (Fig. 5.2), the findings highlight that chemical properties of SOM are also important factors controlling SOM persistence and stabilization in the Peruvian Andes. When applied to SOM turnover in general, we should pay attention to soil properties. Our results showed clear differences in the effects of double bonds and carbon chain length on relative abundance changes of FAs between different soil profiles and horizons (Table 5.2). As these soil profiles and horizons had large differences in soil mineralogy and aggregate (Yang et al., 2019b, 2019a), the differences can be potential factors regulating the interactions between SOM composition and SOM stability.

- Carbon chain length and double bonds control fatty acid stability

5.5. Conclusions

The TMAH-pyrolysis-GC/MS analyses of the soils under study revealed large relative abundances of FAs, with a major contribution of free FAs. Our results highlighted that the presence of double bonds and carbon chain length are key factors controlling FA stability in the Peruvian soils under study. Unsaturated FAs were depleted after the incubation and this is likely explained by their easier decomposition by soil microbes when compared to saturated FAs. The easy degradation of unsaturated FAs is likely explained by their less stabilization controlled by association with mineral surfaces and/or chemical properties rather than that controlled by occlusion in aggregates. In terms of carbon chain length, FA stability decreased from short-chain to long-chain FAs. A possible explanation for this is that short-chain FAs received more protection by occluded in aggregates compared to long-chain FAs. Our results also suggest the microbial transformation of FAs during the incubation. However, the transformation has limited effects on the controls of double bonds and carbon chain length on FA stability. Finally, the controls of double bonds and carbon chain length on FA stability were different between soil samples and horizons.

Our study provides direct evidence that chemical properties of the FAs influence their interaction with the soil matrix, which supports the view that the chemical composition of SOM has an impact on SOM stabilization controlled by the soil matrix. However, more studies are needed before generalizing our findings to other soils because of the differences between soil samples and horizons. Our results were insufficient to explain whether the differences in stability between unsaturated and saturated FAs are attributed to chemical recalcitrance or interactions with mineral surfaces. Thus, future research should compare the affinity to mineral surfaces between unsaturated and saturated FAs through sorption experiments.


MountTol 55+5L

Chapter 6

Synthesis

The large soil organic carbon (SOC) stocks in the alpine grasslands of the Peruvian Andes are crucial to ecosystem services and global carbon (C) dynamics. However, few studies have focused on how soil formation and environmental factors affect SOC stocks and the underlying mechanisms controlling the SOC stability in the Peruvian Andes. To address these knowledge gaps, the objectives of this thesis were: (1) to quantify the SOC stocks and to find key factors controlling the SOC spatial patterns, (2) to have insights into the underlying mechanisms of soil organic matter (SOM) stabilization, (3) to investigate SOM stabilization controlled by aggregates as affected by precipitation and lithology, and (4) to investigate potential relationships between SOM molecular composition and SOM stabilization in the studied alpine grasslands of the Peruvian Andes. Major conclusions on SOC stocks and SOM stabilization are synthesized in this chapter. Implications and possible future research are presented in the final part of this chapter.

6.1. Main conclusions

6.1.1. SOC stocks and significant predictors

In the wet site, the SOC stocks estimated using 69 samples were 215 ± 21 Mg ha^{-1} (Chapter 2), which is higher than the global average level reported by Lal (2004). In the wet site, the SOC stocks were 405 ± 42 for the limestone soils (LSs) and 226 ± 6 Mg ha^{-1} for the acid igneous rock soils (ASs). In the dry site, the SOC stocks were 153 ± 27 for the LSs and 172 ± 13 Mg ha^{-1} for the ASs. The LSs and the ASs in both wet and dry sites had higher SOC stocks when compared to corresponding soil groups (Batjes, 2014). When compared to other alpine grasslands of the Andes, SOC stocks are higher in Páramo soils of the Ecuadorian and Venezuelan Andes with higher precipitation rates (Sarmiento and Bottner, 2002; Tonneijck et al., 2010). In contrast, SOC stocks are lower in Southern Peru and Bolivia with drier climate conditions (Muñoz-García and Faz-Cano, 2012; Rolando et al., 2017a; Zimmermann et al., 2009). When compared to soils from

other alpine grasslands (Garcia-Pausas et al., 2007; Yang et al., 2008), our soils also have higher SOC stocks.

These findings suggest that precipitation drives SOC accumulation in Andean soils. This is further supported by our observation that SOC stocks were higher in the wet site when compared to the dry site for both LSs and ASs (Chapter 4). This trend coincides with the general observation that SOC stocks are high in cool and humid environments (Wiesmeier et al., 2019). The observed SOC stock pattern indicates that precipitation is crucial to the distribution of SOC stocks in the Andean region. In general, precipitation controls SOC sequestration through primary productivity, OM input and microbial decomposition (Wiesmeier et al., 2019). In addition, precipitation can also influence OM stabilization by controlling soil mineralogy through weathering processes (Doetterl et al., 2015b; Homann et al., 2007). Lithology is a key factor controlling the SOC stocks, as lithology became the significant predictor when soil depth and moisture were controlled as conditional variables (Chapter 2). The effects of lithology on SOC stocks can be explained by differences in soil mineralogy, which affect OM stabilization related to soil aggregates and mineral surfaces (Kleber et al., 2015; Lützow et al., 2006).

Compared to precipitation and lithology, other soil formation and environmental factors were less important to predict the SOC stock patterns (Chapter 2). It is surprising that land use was not a significant predictor for SOC stocks. This may be closely related to the special land use strategy in which a rotation in the order of cultivation, land set-aside and grazing were repeated every 3-5 years. This type of land use pattern keeps SOC stocks in a dynamic balance (Chapter 2). Grazing intensity only had significant effects on the SOC stock of the top 10cm, which suggests that its impacts on the SOC input and decomposition processes might be more severe for the topsoil than for the subsoil (Piñeiro et al., 2010). SOC stocks of the top 10cm were stimulated by increasing altitudes (Chapter 2), which can be explained by declined microbial decomposition due to lower temperatures (Du et al., 2014). The limited importance of topographical factors (slope position and slope angle) might be attributed to the homogeneous solar radiation and soil wetness for different aspects as the results of the tropical latitude (9 °S) of the study area.

6.1.2. OM stabilization mechanisms

OM occluded in aggregates had a limited contribution to SOM stabilization in our studied soils, as indicated by (1) limited stimulation of SOC mineralization after the incubation with crushed aggregates compared to intact aggregates, (2) unclear correlations between aggregate stability and SOC contents and stability, and (3) inconsistent patterns between aggregate-size distribution and SOC stability (Chapter 4). For the ASs, the limited contribution of aggregates in SOM stabilization can be explained by the lack of large-sized aggregates. For the LSs, it might be a consequence of the strong adsorption of OM on mineral surfaces. As OM occlusion in aggregates only had a minor contribution to OM stabilization, OM adsorption on mineral surfaces is proposed to be the dominant stabilization mechanism (Chapter 4).

In the wet site, the stabilization mechanisms of SOM were different between LSs and ASs, although their SOC stability was not significantly different. In the wet-ASs, SOM was stabilized by complexation with and/or adsorption on Fe and Al (oxides) rather than clay contents, allophanes or Al toxicity (Chapter 3). In the wet-LSs, OM stabilization was promoted by Ca-induced cation bridges in addition to interactions between OM and Fe and Al (oxides). Similar to our results, SOM has also been reported to be stabilized by Fe and Al (oxides) in alpine grasslands of the Andes (Buytaert et al., 2006b; Podwojewski et al., 2002; Tonneijck et al., 2010). The wet-LSs had significantly higher SOC stocks than the wet-ASs, which can be explained by OM stabilization being exclusively controlled by Ca^{2+} bridges in the wet-LSs (Chapter 3). Our results suggest a shift in OM stabilization from adsorption on Fe and Al (oxides) to the presence of Ca^{2+} bridges, with increasing pH values driven by lithology (Chapter 3). Similar shifts in OM stabilization mechanisms with changes in lithology and pH have been widely reported in other soils (e.g. Heckman et al., 2009; Kaiser et al., 2011; Masiello et al., 2004).

In the dry site, the LSs had lower SOC stocks and lower SOC stability compared to the ASs (Chapter 4). The lower SOC stability in the dry-LSs might be explained by the weak adsorption of SOM on mineral surfaces due to low pH values (Heckman et al., 2009). The lower pH suggests the weak interaction between OM and mineral surfaces through polyvalent cation bridges because Ca^{2+} is replaced by H^+ with lower pH values (Jenny, 1941). Furthermore, the positive correlations between SOC mineralization rates and C/N ratios exclusively found

in the dry-LSs suggest that the decomposition of OM in the dry-LSs was more dependent on OM quality in comparison to other soils.

6.1.3. Effects of precipitation and lithology

When precipitation levels decreased, SOC stocks and stability decreased in the LSs but did not clearly change in the ASs. The different responses between LSs and ASs might be attributed to differences in soil mineralogy (calcareous vs. acidic bedrock) related to weathering processes and OM input that is driven by precipitation (Chapter 4). By contrast, aggregate-size distribution was largely controlled by lithology rather than by precipitation. This suggests that soil aggregation is mainly regulated by soil mineralogy in our studied area (Chapter 4).

We observed lower SOC stability and lower soil pH values with lower precipitation amounts in the LSs. Although the lower pH values in the dry-LSs compared to the wet-LSs are not common from a pedogenetic point of view, they coincide with the higher belowground OM input in the dry-LSs. This is supported by: (1) the larger contributions of α, ω-dioic acids, ω-hydroxyl alkanoic acids and long-chain fatty acids, and (2) the depletion of these compounds after the incubation (Chapter 4). The higher belowground OM input in the dry-LSs caused more intensive acidification and lower pH values when compared to the wet-LSs. This further weakens the capacity of mineral surfaces to stabilize OM in the dry-LSs. A potential explanation for the higher OM input is that plants need more developed root systems to adapt to the lower precipitation in the dry-LSs. In contrast, the ASs had no clear difference in pH values between wet and dry sites. This might be explained by an absence of the effects of OM input on soil acidification in soils formed on the already acidic bedrocks.

Recent studies indicated that climate factors, including precipitation, control OM stabilization by regulating soil mineralogy through weathering processes (Chaplot et al., 2010; Doetterl et al., 2018, 2015b). Our results support this view and suggest that interactions between precipitation and lithology are crucial for the stabilization of OM. Furthermore, OM input controlled by precipitation might play an important role in regulation weathering process in the LSs rather than in the ASs.

6.1.4. Molecular composition of SOM

Although the method of TMAH-pyrolysis-GC/MS does not yield quantitative data, we can still compare our results with other studies using similar methods. We observed large fractions of lipid-derived compounds, which are consistent with the results of Nierop et al. (2007) in alpine grassland soils in the Ecuadorian Andes. In contrast, soils outside alpine grasslands of the Andes had smaller fractions of lipid-derived compounds (Barré et al., 2018; Brock et al., 2019; Nierop and Verstraten, 2003). In addition, we found smaller fractions of pyrolysis products derived from lignin and polysaccharides (<10%) in most of our soil samples (Chapter 5). This is consistent with the study of Nierop et al. (2007) conducted in alpine grasslands of the Ecuadorian Andes. After a 76-day incubation, unsaturated FAs were depleted, whereas short-chain saturated FAs (e.g. C16:0 and C18:0) accumulated. In addition, the depletion of unsaturated FAs was strongly correlated to SOC mineralization rates. This suggests that depletion of unsaturated FAs is likely attributed to the microbial mineralization.

The results indicated that double bonds (saturated vs. unsaturated) and carbon chain length are two major factors controlling FA stability against decomposition. Unsaturated FAs were more vulnerable than saturated FAs, which is unlikely explained by their stabilization by occlusion in aggregates. Instead, the vulnerability might be explained by their chemical recalcitrance and/or association with mineral surfaces (Chapter 5). Long-chain FAs had lower stability than short-chain FAs. A possible explanation for this is that short-chain FAs received more protection by occlusion in aggregates compared to long-chain FAs. Only a few other studies have examined the effects of double bonds and carbon chain length on FA stabilization in soils (e.g. Dent et al., 2004; Moucawi et al., 1981). Microbial transformation of FAs was observed during the 76-day incubation. However, the microbial transformation had no significant effect on the controls of double bonds and carbon chain length on the stability of FAs.

Although chemical recalcitrance is recently considered less important in SOM stabilization than previously believed (Lehmann and Kleber, 2015; Schmidt et al., 2011), the chemical composition of SOM can potentially affect their stabilization by interacting with the soil matrix (Angst et al., 2018b, 2017). For this, our results provided evidence to support that the chemical properties of FAs influence their interactions with the soil matrix and further control their stabilization. Finally, our results also indicate that soil types and soil horizons also influence the effects of double bonds and carbon chain length on FA stabilization. This suggests that

more studies are required before generalizing our findings to other soils (Chapter 5).

6.2. Implications

6.2.1. Implications for SOC sequestration in the Andes

Land use change is well-known to affect SOC stocks. A change from cropland to grassland generally causes SOC accumulation, whereas the opposite results in SOC depletion (Poeplau et al., 2011). A possible explanation is that aggregates, which promote SOM stabilization, are destroyed by agricultural activities such as cultivation and tillage (Guo and Gifford, 2002). However, our results showed no significant differences in SOC stocks between different land use types. Similar results have been reported in the Peruvian Andes by Rolando et al. (2017b) and Zimmermann et al. (2009). A possible explanation is that the aggregation had a limited role in SOM stabilization in our study (Chapter 4). Thus, SOC stocks were not significantly affected by aggregate destruction caused by agricultural activities. A second explanation is that the local land use pattern, in which a rotation in the order of cultivation, land set-aside and grazing was applied every 3-5 years, might keep the SOC stocks at a high level and in a dynamical balance. This applied land use pattern might give a potential solution for how to sustain high SOC stocks in alpine grassland of the Peruvian Andes with intensive agriculture productions.

SOC stocks and SOC stability in the LSs were more sensitive to precipitation changes when compared to the ASs. We previously assumed that the SOC stocks in the ASs were more vulnerable to the potential change in precipitation compared to the LSs because the LSs had better soil structure. However, this assumption is not supported by our data because SOM stabilization was not clearly controlled by soil aggregation. Our findings suggest that the LSs may lose more SOC stocks than the ASs when the climate becomes drier. This suggests that lithology should be considered when evaluating potential feedbacks of SOC storage and stability to global change, as well as when making management plans to sustain ecosystem services in the Peruvian Andes.

6.2.2. Implications for SOC stocks estimation

The results of Chapter 2 highlighted the importance of using the entire soil profile to estimate SOC stocks instead of using a constant soil depth. In general, SOC stocks are estimated using constant soil depths (e.g. Doetterl et al., 2015; Du et al., 2014). However, this increases the risk of inaccurate estimations of SOC stocks and potential effects of environmental factors on SOC stocks, because (1) deep soils may also contain large SOC stocks, and (2) SOC stability may be different between topsoil and subsoil (Batjes, 2014; Wiesmeier et al., 2012). Our results showed that SOC stocks were underestimated and the effects of soil formation and environmental factors on SOC stocks were overestimated when using a constant soil depth (Chapter 2). Thus, we confirm the necessity to include the entire soil profile to avoid bias in the estimation of SOC stocks.

6.2.3. Implications for SOM stabilization mechanisms

The results of this thesis indicated that SOM stabilization in the Andean grasslands was controlled both by lithology and precipitation in relation to SOM input. The lower SOC stocks and stability in the dry-LSs, when compared to the wet-LSs, were explained by the weaker interaction between OM and mineral surfaces via Ca^{2+} bridges as controlled by lower pH values (Chapter 4). The lower pH values were likely further controlled by intensive soil acidification caused by larger belowground OM input. Doetterl et al., (2015b, 2018) reported that SOC stability is controlled by soil mineralogy, which is further governed by climate factors. In addition to the mineralogical control, our results suggest that OM input from the vegetation might also play an important role. Thus, it is important to consider the effects of biotic factors like vegetation and OM input for future research on mineral-controlled SOM stabilization due to the interactions between biotic factors and weathering processes. However, a very limited number of studies have reported OM input in the alpine Andes (e.g. Oliveras et al., 2014).

When compared with other studies using the TMAH-pyrolysis-GC/MS, our results suggest that it is likely that soils of the Andean highland, including soils in our study, have higher aliphatic compounds and lower contributions of lignin and polysaccharides (Barré et al., 2018; Brock et al., 2019; Nierop et al., 2007; Nierop and Verstraten, 2003). Thus, an open question remains whether the large SOC stocks in the Andean highland are associated with the chemical composition of SOM. It is important to understand the underlying mechanisms related to SOM

input, decomposition and stabilization that controlled by biotic and abiotic factors.

Recently, chemical recalcitrance is considered less-important in SOM stabilization than previously thought. Instead, increasing evidence indicates that SOM stabilization is controlled by the interactions between OM molecules and the soil matrix that reduce OM decomposition rates (Dungait et al., 2012; Lehmann and Kleber, 2015; Schmidt et al., 2011). However, to the author's point of view, this does not necessarily mean that the molecular composition of SOM is not important for SOM persistence. Molecular composition not only determines the chemical recalcitrance of SOM but also affects the interactions between SOM and the soil matrix. Based on the SOM adsorption models, molecular composition largely controls the affinity of SOM to the association sites of mineral surfaces (Kleber et al., 2007). Recent studies also indicated that SOM composition had influences on SOM stabilization by interacting with the soil matrix (Angst et al., 2018b, 2017). Furthermore, the results of Chapter 5 showed direct evidence for this and gave better insights into the effects of SOM molecular composition on SOM persistence. Thus, SOM composition may still be important because of the potential effects of molecular composition on SOM stabilization by interacting with the soil matrix.

6.3. Future research

The research involved in this thesis has improved the understanding of mechanisms and processes affecting the storage, distribution, stabilization and molecular composition of SOM in the studied areas of the Peruvian Andes. However, more studies are needed to gain further understanding of SOC sequestration and stabilization in the Peruvian Andes and in general.

With regard to SOC sequestration, very few studies have focused on C input of the Andean grasslands (e.g. Oliveras et al., 2014). As C input is an important factor for the SOC sequestration (Wiesmeier et al., 2019), studies focusing on the quality and quantity of input C may help understand SOC sequestration better in the Andean alpine grasslands. Furthermore, future studies could focus on the application of the knowledge highlighted in this thesis to improve the soil

management and to sustain the ecosystem services in the alpine grasslands of the Peruvian Andes.

For SOM stabilization controlled by occlusion in soil aggregates, we found a small contribution of aggregates in SOM stabilization, even in LSs with good soil structure. The small contribution of aggregates needs further investigation. Future studies can also gain insights into the microbial activity, SOM decomposition and SOM stabilization in soil aggregates.

For the chemical composition of SOM, more open questions can be studied. One question is why the soils in alpine grasslands of the Andes have larger abundances of lipids compared to soils from other regions (e.g. Barré et al., 2018; Brock et al., 2019; Nierop and Verstraten, 2003). The underlying mechanisms of the selective preservation of lipids can be an interesting research focus. In addition, the results of Chapter 5 cannot explain whether the vulnerability of unsaturated FAs compared to saturated FAs is attributed to the differences in chemical recalcitrance or in the interactions between FAs and mineral surfaces. Further studies can apply a combination of adsorption and decomposition experiments to investigate the affinity of saturated and unsaturated FAs to the mineral surfaces and their stability against decomposition. Finally, as we found that soil types and horizons have influences on the controls of FA properties on their stabilization, more studies are needed before generalizing our findings to other soils.



Appendices

Table A1.1 Soil profile description

Wet-LS1			
Location: 7.16744 S, 78.60119 W; Altitude: 3716m Marly limestone, land use: fallow, ploughed last year, potato cereals			
Horizon	**Depth**	**Color**	**Description**
Ap	0-20	10YR 1.7/1	Silt loam, fine to medium crumbly structure, medium aggregate, silty sticky, friable consistency. High root content, high biological activities. Many fine and coarse pores. Mollic or umbric
Ah2	20-37	10YR 1.7/1	Silt loam coarse sub-angular blocky structure, silty sticky, friable consistency. Medium roots, many macro-pores, vitric property. Mollic or umbric
Btg	37-57	2.5Y 2/1	Silty clay loam to clay; coarse angular blocky structure. Many curtains, slightly hard consistence, slightly sticky. Few roots many macro-pores.
C/R	>57	2.5Y 4/2	Slightly stony, silty clay loam to clay. Slightly hard consistency, medium sub-angular blocky structure. Sticky, no roots, humid shiny pads. Stony with weathered stone.

Wet-LS2			
Location: 7.16519 S, 78.60631 W; Altitude: 3717m Land use: recently ploughed, before cereals, marly limestone			
Horizon	**Depth**	**Color**	**Description**
Ap	0-14	10YR 2/1	Sandy loam, fine crumbly structure, marked of earth-worm excrements. Hard consistency , lots of roots, many micro- and macro-pores. Mollic or umbric
Ah2	14-40	10YR 1.7/1	Sandy loam, medium sub-angular blocky structure, slightly hard consistency, common roots, many micro- and macro-pores. Mollic/umbric
Ah3	40-55	10YR 1.7/1	Silt loam, medium to coarse angular blocky structure, slightly hard consistency, normal sticky, hardly roots, common macro pores. Mollic/ umbric
Btg	55-66	2.5Y 5/2	Silty clay loam, coarse angular blocky structure, curtans, slightly stony, less macro-pores pseudo clay mottled (pseudo clay properties). Argic, pseudo gleyic properties.
C	>66	2.5Y 7/4	Silt loam, poor/no structure, coarse angular structure, weathered rock fragments, slightly hard consistency, slightly sticky, no root, vague-mottled. Weathered bedrock at 80 cm deep.

Wet-LS3			
Location: 7.16361 S, 78.63176 W; Altitude: 3517m Land use: allow field, cereals, slightly sloping concave, having a limited outcrop			
Horizon	**Depth**	**Color**	**Description**
Ah1	0-12	2.5Y 3/2	Silty loam to dandy loam, medium sub-angular blocky, very hand consistency, few shrinkage cracks, abundant roots, glass fragments common strong micro-aggregates many macro-pores, high biological activities.
Ah2	12-37	2.5Y 3/1	Silty loam, coarse angular blocky structure, hard consistency, many large shrinkage cracks, common roots, common marcro-pores, strong micro-aggregation, high biological properties. Vertic properties
Ah3	37-47	2.5Y 3/1	Silty loam, course sub-angular blocky, moderate roots, slightly hard to friable consistency (moist), common macro-pores, mediate biological activities, common glass.

Btg	47-60	2.5Y 4/2	Clay loam with weathered rock fragments, mixture of organic matter coatings/clay coatings on structural elements; coarse/medium angular blocky structure, very sticky, compact signs of biological activity many macro-pores, but no roots, no glass.
C	60-80	2.5Y 7/4	Clay loam, many weathered rock fragments, also exotic, not argic, stagnic colors, massive "structure", sticky almost no roots, no glass.

Wet-AS1

Location: 7.16771 S, 78.62878 W; altitude: 3583 m
Grassland, terraced, AC profile

Horizon	Depth	Color	Description
Ah1	0-20	10YR 3/2	Loamy sand, very few gravel, high glass content, coarse crumbly structure, lots of excrements, slightly hard consistency, common roots, abundant biological activities, few macro-pores, many micro-pores. Umbric
Ah2	20-45	10YR 3/2	Sandy loam, slightly gravel(very fine), high glass content, strongly weathered gravel, medium sub-angular blocky, moderate structure, friable consistency, few to common roots, few macro- and micro-pores low biological activities. Umbric
Ah3	45-68	2.5Y 4/1	Loamy sand, medium to fine sub-angular blocky structure(weak), slightly hard consistency, high glass content, few macro-pores, many micro-pores, very few roots, few biological activities. Rock fragments(slightly weathered) up to 5 cm. Umbric (boundary vary irregularly)
C/R	>68	7.5Y 8/3	Weathered granite, with thin OM in between, 70-80 with seams of A materials, below 80 is weathered granite

Wet-AS2

Location 7.16970 S, 78.62797 W; altitude: 3585 m
Grassland, terraced, at foot slope

Horizon	Depth	Color	Description
Ap	0-20	10YR 2/2	Sandy loam, lose crumb to medium crumbly structure, friable consistency, lots of excrements, abundant of roots, high macro- and micro-pores, high biological activities, vitric
Ah2	20-45	10YR 3/1	Sandy loam, few rock fragments, very few fine gravel, medium to coarse sub-angular blocky structure, friable consistency, many excrements. Vitric property.
C/R	45-55	5Y 7/3	Vivid boundary between CR and A_2, with pockets of A material into C/R. Bedrock is weathered granite.

Wet-AS3

Location: 7.17114 S, 78.62864 W; Altitude: 3586
Grass/ploughed along road, low slope angle

Horizon	Depth	Color	Description
Ah1	0-15	2.5Y 3/2	Sandy loam, fine-medium crumbly structure, elements of excrement, slightly hard consistency abundant roots, common macro-pores, high biological activities. Vitric
Ah2	15-35	2.5Y 3/2	Slightly cravenly sandy loam, fine to medium sub-angular structure, slightly hard consistency, common roots, common macro-pores, vivid regular boundary with pocket, sub biological activity. Vitric property.
C	>35	2.5Y 7/4	Gravelly loamy sand with weathered rock fragments, with ignimbrite/granite.

Dry-LS1

Location: 9°15.213`S, 77°35.27`W, 3573m, clear weather
Slope angle 22°, aspect: WSW, straight slope, limestone, abandoned farmland.
Surface crust, small path nearby, grazing intensity: 1, moisture statue A horizon: 2, root depth: 55cm, gravels top 30cm: <5%
Vegetation: evenly, shrubs 10%, grass 85%,bare rock 5%.

Horizon	Depth	Color	Description
Ah1	0-22	2.5Y 5/3	Silty loam, sub-angular blocky, worm cast, no gravel, common root, friable to firm consistency, slightly sticky, common fine pores
Ah2	22-42	2.5Y 7/4	Silty clay loam, sub-angular blocky, very few gravel, few roots, slightly sticky, firm consistency, few fine pores
Btg	42-56	2.5Y 6/4	Silty clay, sub angular blocky, very few gravels, very few roots, firm consistency, sticky , very few fine pores,
BC	56-63	2.5Y 7/6	Silty clay, wavy boundary with B_t horizon, many fine gravels, no structure, very few fine roots, firm consistency, sticky, very few fine pores.
R	>63	2.5Y 5/3	

Dry-LS2

Location: 9°15.248`S, 77°35.288`W, 3532m, clear
Slope angle 20°, aspect WSW, straight slope, limestone, abandoned farmland
No surface crust, grazing intensity: 1, moisture Ah: 2, gravel top 30cm: 5%, root depth 50 cm
Vegetation: evenly, shrub 15%, grass 85%

Horizon	Depth	Color	Description
Ah1	0-21	2.5Y 6/4	Loam, sub-angular blocky, worm cast, few fine to medium gravels, common fine to medium roots, firm consistency, not sticky, common fine to medium poles.
Ah2	21-34	2.5Y 6/4	Loam to sandy loam, sub angular blocky, few medium to coarse gravels, few roots, firm consistency, few fine pores, slightly sticky
Bt	34-54	2.5Y 7/6	Silty clay, massive to sub-angular blocky, clay coating, firm to very firm consistency, sticky, very few roots, very few pores.
BCt	>54	10YR 7/6	Clay to silty clay, no structure, sticky, few fine gravels, mottles, no roots.

Dry-LS3

Location: 9°15.246`S, 77°35.26`W, 3560m, clear
Slope angle 21°, aspect WSW, straight slope, limestone, abandoned farmland
Surface crust, grazing intensity: 1, moisture Ah 1, gravles top 30cm: 2%, root depth 68 cm
Vegetation: evenly, 15% shrubs, 82% grass, 3% bare stone.

Horizon	Depth	Color	Description
Ah1	0-21	2.5Y 6/4	Loam, sub-angular blocky, common roots, few fine gravels, friable to firm consistency, not sticky, common fine to medium pores, worm cast.
Ah2	21-42	2.5Y 6/4	Loam to silty loam, sub-angular blocky, common roots, few fine gravels, firm consistency, not sticky, few to common pores, animal cast.
Ah3	42-62	2.5Y 6/4	Silty loam, sub-angular blocky, few roots, few fine gravels, few fine pores, slightly sticky, firm consistency.
Btg	62-73	2.5Y 7/4	Silty clay, sub-angular blocky, few roots, few to common gravels, few fine pores, sticky, clay illuviation
C/R	>73	2.5Y 7/4	Clay, weathered parent materials, no structure, very sticky, no roots.

Dry-AS1

Location: 9°11.305` S, 77°35.982` W, 3667m, sunny with few clouds.
Slope angle 29°, aspect SW, straight slope, granodiorite, directly on the bedrock, abandoned farmland for years.
Surface crust, embedded stone, grazing intensity(0-2): 0, moisture of A horizon: 3 (0-5), root depth 60 cm, % gravel top 30: 20%.
Vegetation: evenly with bare spots, Shrubs 40%, grass 40%, bare soil 5%, bare rock 5%.

Horizon	Depth	Color	Description
Ah1	0-19	10YR 3/2	Silty loam, crumbly, moderate to common medium gravels, many fine roots, animal crust, medium porosity, friable consistency, not sticky
Ah2	19-44	10YR 3/1	Sandy loam, sub-angular blocky, common fine to medium gravels, common medium roots, few porosity, friable consistency, not sticky
C	44-69	7.5Y 6/1	Sandy loam to loamy sand, no structure, many medium to coarse gravel, no root, slightly sticky, not sticky, waving boundary to Ah2.
R	>69	-	Sand, no structure, no root.

Dry-AS2

Location: 9°11.612`S, 77°35.906`W, 3521 m, few clouds
Slope angle: 26°, aspect: SE, convex slope, sub-glacier till with >90% granodiorite and <5% composition of pyrite containing sandstones, lateral moraine, abandoned farmland.
Surface crust, embedded stones, >5 boulders(>20 cm),grazing intensity: 1, proximity stream(irrigation canal), A horizon moisture: 3-4, root depth: 60 cm, % gravels top 30cm: 5-10%.
Vegetation: evenly, shrubs 30%, grass 65%, bare soil & rock 5%

Horizon	Depth	Color	Description
Ah1	0-10	10Y 4/2	Loam to sandy loam, crumbly structure, few fine gravels, common fine to medium roots, many animal crust, few fine pores, friable consistency, not sticky
AC	10-15	2.5Y 4/2	Loamy sand, sub-angular blocky/granular, abundant medium to coarse gravels(40-50%), few fine to medium roots, common fine pores, friable consistency, not sticky
2Ahb	15-60	10YR 3/3	Sandy loam, sub-angular blocky, few fine gravels, common fine to medium roots, few to common fine pores, friable consistency, not sticky.
2B/Cw	>60	2.5Y 8/3	Sand, no structure, no roots

Dry-AS3

Location: 9°11.756`S, 77°36.091`W ,3495m, sunny with few clouds
Slope angle 29°, aspect SE, straight slope, sub-glacier till, with >90% granodiorite and <5% composition of pyrite containing sandstones, lateral moraine, abandoned farmland.
Surface crust, road cut, > 5 boulders, grazing level: 1, moisture status of A horizon: 2, root depth 55cm, % gravel top 30cm: 5%.
Vegetation: trees 5%, shrubs 10%, grass 80%, bare soil+rock 5%.

Horizon	Depth	Color	Description
Ah1	0-19	10YR 3/3	Sandy loam, crumbly, few to common fine gravels, abundant roots, many animal crust, common fine to medium pores, friable consistency, not sticky
Ah2	19-50	10YR 3/3	Loam to sandy loam, sub-angular blocky, few fine to medium gravels, common roots, few fine pores, friable consistency, not sticky.
B/Cw	50-90	2.5Y 8/4	Sandy, no structure, no roots, hard consistency, granular, yellow-redish spots, percentage of spots decrease with depth, not sticky.
C/R	>90		Technique hard materials, sandy, few spots

The unit of depth is cm; Munsell Color is determined using air-dried soils.

Table A2.1 Information of soil formation and environmental factors and soil properties in all soil profiles.

Soil class	Soil Formation and Environmental factors (Predictive variables)							Soil properties									SOC stocks (Responding variables)		
	Lithology	Lithology type	Land use	Grazing	Slope position	Slope angle	Altitude	Soil depth	SOC Ave.	SOC 10cm	BD Ave.	BD 10cm	Moisture Ave.	Moisture 10cm	pH Ave.	pH 10cm	SOC stock total	SOC stock 10cm	SOC stock 40cm
						°	m	cm	%	%	g cm^{-3}	g cm^{-3}	g kg^{-1}	g kg^{-1}			Mg ha^{-1}	Mg ha^{-1}	Mg ha^{-1}
Luvisol/Lixisol	marl	CAL	CG	H	T	6	3681	46	2.96	5.81	0.90	0.82	215	169	6.61	n.d.	103	48	103
Luvisol/Lixisol	shale	CAL	AC	M	V	3	3602	70	11.72	22.15	0.99	0.86	495	546	7.10	7.24	663	190	581
Phaeozem	marl	CAL	G	M	S	17	3637	40	8.56	13.39	0.89	0.73	293	368	5.52	5.33	289	98	289
Phaeozem	marl	CAL	G	L	S	1	3687	52	6.64	7.85	0.94	0.72	233	187	5.76	7.30	362	57	273
Leptosol	shale	CAL	G	N	T	1	3901	15	13.67	12.53	0.94	0.91	410	410	4.95	4.91	256	114	256
Leptosol	limestone	CAL	G	N	S	30	3877	17	12.15	10.71	1.04	1.03	471	462	5.39	5.09	252	110	252
Umbrisol	shale	CAL	G	M	S	20	3840	49	9.82	12.90	0.96	0.87	331	281	5.02	5.13	463	112	422
Umbrisol	shale	CAL	C	L	S	17	3755	19	10.31	10.31	0.72	0.72	351	351	5.38	5.38	74	74	74
Andosol	granite	CAL	G	M	S	8	3621	55	7.34	9.93	0.89	0.76	192	182	5.05	4.97	378	75	283
Andosol	shale	CAL	G	H	V	1	3506	62	8.21	11.13	0.97	0.86	229	178	5.83	6.53	471	96	338
Leptosol	marl	CAL	G	M	S	30	3563	5	7.84	7.84	1.02	1.02	123	123	7.34	7.34	80	80	80
Luvisol	limestone	CAL	G	H	V	8	3505	47	4.94	6.12	1.01	0.91	242	208	5.97	5.90	248	56	218
Leptosol	limestone	CAL	G	H	V	10	3490	13	6.82	6.82	0.91	0.91	174	174	6.83	6.83	62	62	62
Luvisol	limestone	CAL	G	H	S	2	3527	80	7.80	11.11	1.06	1.01	269	178	7.02	6.99	652	112	388
Leptosol	ignimbrite	ACI	G	H	S	9	3658	16	3.17	3.17	1.17	1.17	85	85	5.43	5.43	37	37	37
Acrisol/Alisol	ignimbrite	ACI	G	H	S	12	3593	57	1.82	3.23	0.87	0.82	203	216	5.61	5.45	93	26	74
Luvisol	marl	CAL	AC	H	S	5	3577	37	2.18	1.56	1.04	1.03	167	122	7.80	7.93	45	16	45
Regosol	ignimbrite	ACI	CG	H	S	18	3543	30	3.36	3.51	0.92	0.93	188	187	5.75	5.85	79	33	79
Umbrisol	ignimbrite	ACI	C	N	S	18	3498	31	1.61	1.63	1.04	1.01	130	108	6.05	6.08	33	17	33
Andosol	granite	ACI	G	H	S	18	3581	132	6.34	7.53	0.98	0.75	233	197	5.37	5.74	593	56	243
Acrisol/Alisol	granite	ACI	G	H	S	6	3560	52	8.43	10.83	0.67	0.64	404	462	4.96	4.65	224	69	224
Leptosol	granite	ACI	F	M	S	31	3512	19	11.15	11.15	0.72	0.72	179	179	5.13	5.13	80	80	80
Andosol	granite	ACI	F	N	S	31	3517	19	8.44	8.44	0.72	0.72	167	167	4.99	4.99	61	61	61
Andosol	granite	ACI	G	H	V	18	3373	83	2.66	1.61	1.07	0.87	158	274	5.66	5.68	190	14	141
Regosol	granite	ACI	G	H	V	1	3390	13	2.31	2.31	0.76	0.76	89	89	5.48	5.48	18	18	18
Leptosol	limestone	CAL	G	M	T	1	3685	8	9.59	9.59	0.96	0.96	147	147	5.74	5.74	92	92	92
Luvisol	limestone	CAL	CG	H	T	15	3655	36	5.61	7.85	1.03	1.03	99	102	5.56	5.47	174	81	174
Leptosol	shale	CAL	CG	H	S	12	3530	5	6.16	6.16	0.91	0.91	80	80	5.95	5.95	56	56	56
Leptosol	shale	CAL	G	H	T	10	3687	22	8.43	9.64	0.89	0.86	128	98	5.33	5.41	149	83	149
Phaeozem	limestone	CAL	CG	H	T	5	3714	32	5.85	8.58	0.95	0.84	103	109	5.87	5.58	216	72	216
Luvisol/Lixisol	limestone	CAL	G	H	V	1	3543	45	9.28	10.68	0.99	0.98	178	177	5.87	5.46	550	105	366
Histosol	ignimbrite	ACI	G	H	V	4	3611	67	10.42	21.90	0.96	0.64	395	654	5.83	n.d.	429	140	415
Leptosol	ignimbrite	ACI	G	L	T	10	3659	8	3.89	3.89	1.01	1.01	28	28	5.06	5.06	39	39	39
Leptosol	ignimbrite	ACI	G	M	V	4	3606	22	5.68	5.68	1.05	1.05	145	145	5.26	5.26	60	60	60
Regosol	quartzite	ACI	F	H	V	30	3599	30	4.22	6.36	1.18	1.14	95	95	5.28	5.21	98	73	98
Umbrisol	quartzite	ACI	G	N	S	12	3629	52	6.33	8.36	1.04	0.82	166	210	4.96	4.83	365	69	225
Umbrisol	quartzite	ACI	G	H	S	4	3614	48	8.03	11.56	0.91	0.68	255	225	5.20	5.00	348	79	305
Leptosol	quartzite	ACI	G	H	V	2	3559	5	6.55	6.55	0.82	0.82	80	80	5.83	5.83	54	54	54
Umbrisol	quartzite	ACI	AC	H	S	8	3590	64	5.42	6.40	0.97	0.85	145	89	4.94	4.80	375	54	192
Umbrisol	quartzite	ACI	G	M	S	22	3715	46	6.26	9.78	0.93	0.83	198	189	4.64	4.75	285	81	252

Table A2.1 Information of soil formation and environmental factors and soil properties in all soil profiles (Continued).

Soil class	Soil Formation and Environmental factors (Predictive variables)							Soil properties									SOC stocks (Responding variables)		
	Lithology	Lithology type	Land use	Grazing	Slope position	Slope angle	Altitude	Soil depth	SOC Ave.	SOC 10cm	BD Ave.	BD 10cm	Moisture Ave.	Moisture 10cm	pH Ave.	pH 10cm	SOC stock total	SOC stock 10cm	SOC stock 40cm
						°	m	cm	%	%	g cm^{-3}	g cm^{-3}	g kg^{-1}	g kg^{-1}			Mg ha^{-1}	Mg ha^{-1}	Mg ha^{-1}
Leptosol	quartzite	ACI	F	N	S	18	3707	9	2.84	2.84	0.72	0.72	70	70	4.53	4.53	20	20	20
Leptosol	ignimbrite	ACI	G	H	S	25	3648	8	3.01	3.01	1.17	1.17	41	41	5.26	5.26	35	35	35
Andosol	ignimbrite	ACI	C	N	S	18	3675	27	4.19	4.32	0.99	1.01	167	140	4.98	4.83	83	44	83
Acrisol/Alisol	ignimbrite	ACI	AC	H	S	16	3650	48	5.77	6.23	0.91	0.93	272	228	5.00	5.02	263	58	216
Acrisol/Alisol	ignimbrite	ACI	AC	H	S	11	3638	46	5.29	6.82	0.91	0.81	214	175	5.07	4.97	235	55	199
Acrisol /Alisol	ignimbrite	ACI	C	N	S	11	3642	64	2.93	5.55	0.94	0.81	248	295	5.29	4.17	178	45	140
Leptosol	ignimbrite	ACI	G	M	S	10	3660	9	4.47	4.47	1.17	1.17	135	135	4.94	4.94	52	52	52
Acrisol/Alisol	ignimbrite	ACI	G	H	S	4	3675	59	4.12	3.88	0.94	1.01	274	250	5.32	5.19	225	39	138
Acrisol/Alisol	ignimbrite	ACI	G	H	T	1	3691	29	4.48	3.96	0.99	1.01	218	186	5.10	5.21	88	40	88
Leptosol	ignimbrite	ACI	G	H	T	2	3693	7	4.87	4.87	1.17	1.17	204	204	5.33	5.33	57	57	57
Acrisol/Alisol	ignimbrite	ACI	F	N	T	8	3688	67	16.05	17.39	0.68	0.44	350	349	4.76	4.63	628	77	399
Histosol	ignimbrite	ACI	G	M	V	6	3520	47	6.00	10.80	0.87	0.64	394	535	5.08	n.d.	240	69	206
Andosol	ignimbrite	ACI	CG	H	S	4	3488	60	2.62	3.40	0.85	0.81	81	57	5.74	5.82	60	28	60
Andosol	ignimbrite	ACI	CG	H	V	10	3496	28	4.03	4.87	0.82	0.81	73	60	5.15	5.54	66	39	66
Umbrisol	ignimbrite	ACI	F	N	S	10	3526	33	7.10	8.42	0.92	0.82	185	159	4.75	4.81	259	69	259
Luvisol/Lixisol	limestone	CAL	G	H	S	2	3423	55	2.11	3.96	1.08	1.03	245	184	5.60	5.38	135	41	101
Acrisol/Alisol	ignimbrite	ACI	G	L	S	36	3475	98	4.23	5.33	0.98	0.93	215	186	5.12	5.14	347	50	140
Phaeozem	limestone	CAL	AC	M	S	24	3672	65	5.68	6.46	1.02	1.03	170	128	5.61	5.51	349	67	255
Phaeozem	shale	CAL	G	H	S	16	3632	50	5.19	7.42	0.89	0.72	172	133	5.26	5.29	223	53	190
Phaeozem	shale	CAL	AC	N	S	42	3602	60	3.08	4.05	1.10	1.00	209	149	7.51	7.42	200	40	160
Leptosol	limestone	CAL	C	H	S	21	3632	12	3.53	3.66	1.03	1.03	141	97	7.77	7.76	72	38	72
Andosol	ignimbrite	ACI	G	H	S	30	3634	26	1.99	2.73	0.92	0.93	77	73	5.86	5.95	37	25	37
Leptosol	shale	CAL	G	H	S	18	3634	9	1.67	1.67	1.00	1.00	27	27	5.43	5.43	17	17	17
Phaeozem	limestone	CAL	AC	N	S	7	3716	57	8.91	14.69	0.82	0.51	494	597	6.15	6.17	375	74	285
Phaeozem	limestone	CAL	AC	N	S	11	3717	66	8.47	13.72	0.97	0.75	343	333	5.67	5.25	488	103	389
Phaeozem	limestone	CAL	CG	L	S	10	3517	60	7.17	11.33	0.91	0.71	271	299	6.44	5.57	353	78	279
Andosol	granite	ACI	G	M	S	7	3583	68	3.27	3.84	1.10	1.16	175	82	4.96	4.99	233	42	162
Andosol	granite	ACI	CG	H	S	9	3585	45	6.21	8.97	0.85	0.78	324	337	4.99	5.03	229	69	225
Andosol	granite	ACI	G	H	S	14	3586	35	5.68	9.57	0.88	0.73	274	351	5.38	5.54	215	69	209
						12	3612	41	6.04	7.61	0.95	0.88	208	206	5.59	5.55	215	63	172
						10	99	25	3.06	4.37	0.12	0.16	110	138	0.73	0.80	172	31	123
						1	12	3	0.37	0.53	0.01	0.02	13	17	0.09	0.10	21	4	15

SOC stocks total: total soil organic carbon stocks, SOCS 10 cm: soil organic carbon stocks of the upper 10 cm, SOC Ave.: average soil organic carbon concentration, SOC 10 cm: soil organic carbon concentration of the upper 10 cm, SN Ave. : average soil total nitrogen, SN 10cm: soil total nitrogen in top 10 cm, Moisture Ave.: average moisture content, Moisture 10cm: moisture content of upper 10 cm, BD Ave.: average bulk density, BD 10cm: bulk density of the upper 10 cm; CAL: calcareous bedrocks, AIC: acidic bedrocks; C: cultivation, G: grassland, AC: abandoned cultivation, CG: cultivated grassland, F: forest; N: none, L: low, M: medium, H: high; T: top, S: slope, V: valley bottom. Soils with an argic horizon have been classified based on their base saturation as expected from their pH in either Luvisol/Lixisol or Alisol/Acrisol.

Table A3.1 Soil properties of diagnostic horizons in limestone soils (LSs) and acidic igneous rock soils (ASs).

Site	Horizon	depth	C	N	C_p	Fe_o	Si_o	Al_o	Fe_p	Al_p	Fe_d-Fe_o	Ca_{ex}	Mg_{ex}	Al_{ex}	CEC	BS	pH	Mol C/ (Fe_p+ Al_p)	MWD	Silt+ clay	Clay	Stability (MA)	Stability (MI)
		cm	g kg^{-1}	g kg^{-1}	g kg^{-1}	g kg^{-1}	g kg^{-1}	g kg^{-1}	g kg^{-1}	g kg^{-1}	g kg^{-1}	mmol kg^{-1}	mmol kg^{-1}	mmol kg^{-1}	cmol kg^{-1}	%			mm	%	%	%	%
LS1	Ap	20	125.1	11.0	63	13.39	0.56	3.47	4.17	1.60	6.13	412.2	23.34	0.25	44.16	99.6	6.17	77.8	4.22	94.2	19.4	75.3	19.7
	Ah2	37	72.0	6.4	43	16.31	0.65	3.25	4.10	1.39	10.37	323.0	18.12	0.18	34.58	99.7	6.07	48.0	6.42	91.0	21.3	66.9	n.d.
	Bt	57	37.3	4.0	22	14.35	0.75	3.22	2.43	1.15	14.88	259.9	15.70	0.08	28.09	99.6	6.22	36.0	7.99	96.5	58.6	79.4	n.d.
	C/R		26.8	3.6	12	10.83	0.75	2.72	1.68	0.85	21.89	222.0	13.72	0.06	24.12	99.5	6.47	36.3	n.d.	95.3	18.4	n.d.	n.d.
LS2	Ap	14	148.4	12.1	84	10.46	0.38	4.22	6.60	3.39	4.70	330.4	18.48	1.07	36.07	97.9	5.25	50.7	5.33	95.7	17.0	96.8	15.0
	Ah2	40	126.5	10.1	84	10.18	0.45	4.21	4.94	3.18	5.35	390.6	12.29	0.45	40.89	99.2	5.50	51.0	4.80	96.4	10.0	72.1	12.9
	Ah3	55	76.7	6.0	55	10.90	0.71	3.81	3.18	2.08	7.46	333.7	10.67	0.12	34.75	99.7	5.98	47.6	6.37	91.8	20.9	88.4	n.d.
	Btg	66	24.1	2.4	16	8.75	0.95	2.38	2.02	0.83	14.00	178.1	9.00	0.07	18.98	99.7	6.49	30.0	8.72	84.5	35.2	92.0	n.d.
	C [a)]		8.3	1.4	4	4.05	1.34	2.20	0.88	0.40	16.10	113.6	8.42	0.04	12.43	99.8	7.11	23.3	n.d.	94.5	32.3	n.d.	n.d.
LS3	Ap	12	126.3	10.1	50	14.08	0.43	2.78	5.85	1.66	10.94	245.2	14.22	0.13	26.78	98.3	5.57	63.3	5.64	86.3	29.0	95.3	19.0
	Ah2	37	74.7	5.7	49	11.50	0.46	2.94	4.02	1.62	15.33	255.4	8.71	0.09	26.81	99.6	6.42	47.1	4.97	83.2	22.0	82.6	23.0
	Ah3	47	45.9	3.4	37	7.02	0.36	2.52	3.31	1.30	19.42	225.9	8.44	0.08	23.73	99.8	6.84	35.6	7.66	80.7	16.5	59.2	n.d.
	Bt	60	23.7	2.0	17	3.45	0.29	1.77	1.77	0.85	24.13	161.4	6.73	0.06	17.11	99.7	6.97	31.2	8.30	75.7	27.8	75.8	n.d.
	Cg		8.7	1.4	3	2.07	0.53	1.90	0.35	0.37	24.43	143.5	8.60	0.06	15.62	99.7	7.33	36.2	n.d.	73.6	27.4	n.d.	n.d.
AS1	Ap	20	33.0	2.8	18	2.06	0.15	2.90	1.37	2.62	1.32	24.2	2.74	9.82	6.28	47.1	4.99	22.6	3.76	32.8	6.9	91.7	15.5
	Ah2	45	34.6	2.9	21	2.26	0.65	5.57	1.83	5.23	1.15	17.1	1.44	12.91	6.11	34.3	4.90	12.7	4.00	40.7	6.3	87.1	6.9
	Ah3	68	29.7	2.6	26	2.27	1.14	7.32	1.82	5.77	1.30	14.8	0.96	10.18	5.43	32.7	5.00	10.0	3.80	42.5	9.9	21.2	15.6
	C/R		5.3	0.6	2	0.17	0.09	0.71	0.03	0.26	0.49	n.d.	n.d.	n.d.	n.d.	n.d.	5.54	43.4	n.d.	n.d.	n.d.	n.d.	n.d.
AS2	Ap	20	92.4	6.7	56	2.62	0.77	10.22	2.34	9.92	1.29	9.7	1.19	17.28	5.06	34.9	5.03	18.8	2.89	45.0	3.0	93.9	15.9
	Ah2	45	73.8	5.2	57	3.04	1.35	12.36	2.82	12.22	1.55	7.6	0.68	16.70	6.10	18.2	4.96	12.2	2.93	45.4	3.6	90.6	14.2
	C/R		4.8	0.4	7	0.57	3.71	9.64	0.18	2.97	0.77	n.d.	n.d.	n.d.	n.d.	n.d.	5.16	3.5	n.d.	n.d.	n.d.	n.d.	n.d.
AS3	Ah1	15	93.8	6.6	52	2.76	1.17	8.84	2.10	7.88	1.78	42.2	5.47	6.89	10.27	66.8	5.54	23.7	3.79	54.0	5.9	98.4	18.0
	Ah2	35	59.0	4.3	44	2.67	1.56	9.75	1.96	8.91	2.25	21.2	2.19	7.78	5.37	50.0	5.26	13.5	3.08	48.5	4.7	96.8	23.0
	C		4.8	0.6	5	2.63	2.25	7.65	0.90	3.00	2.31	10.1	1.93	2.60	2.56	56.4	5.36	3.2	n.d.	46.6	9.8	n.d.	n.d.

LS: limestone soil. AS: soil on acidic igneous bedrocks. CEC: cation exchange capacity. BS: base saturation; n.d.: not determined. [a)] The sample contains inorganic C.

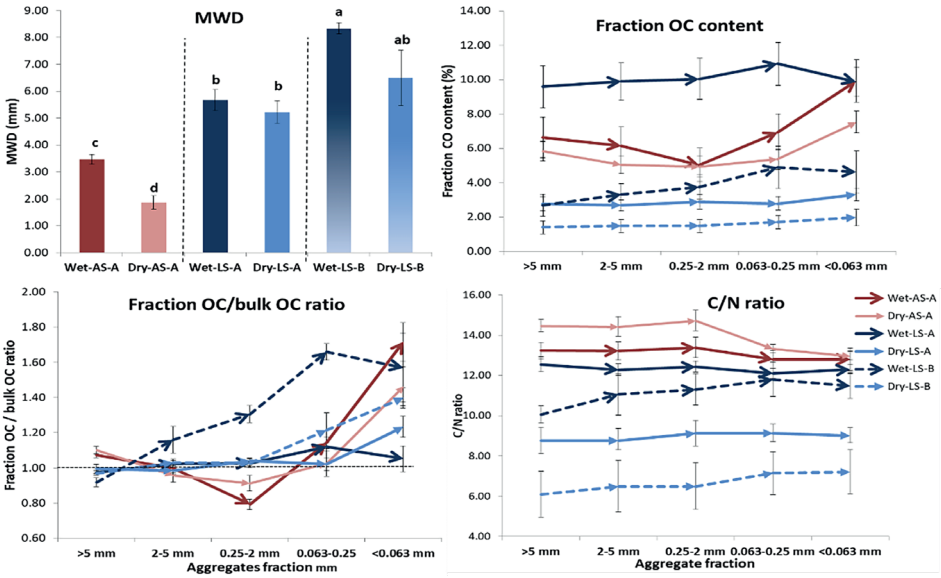


Fig. A4.1 Mean weight diameters (MWD) of soil horizons and properties of aggregate size fractions. Arrows indicate decreasing aggregate sizes**.** Wet: the wet site, Dry: the dry site, LS: limestone soil, AS: acid igneous rock soil, A: A horizons, B: B horizons, fraction OC content: organic carbon contents of aggregate-size fractions.

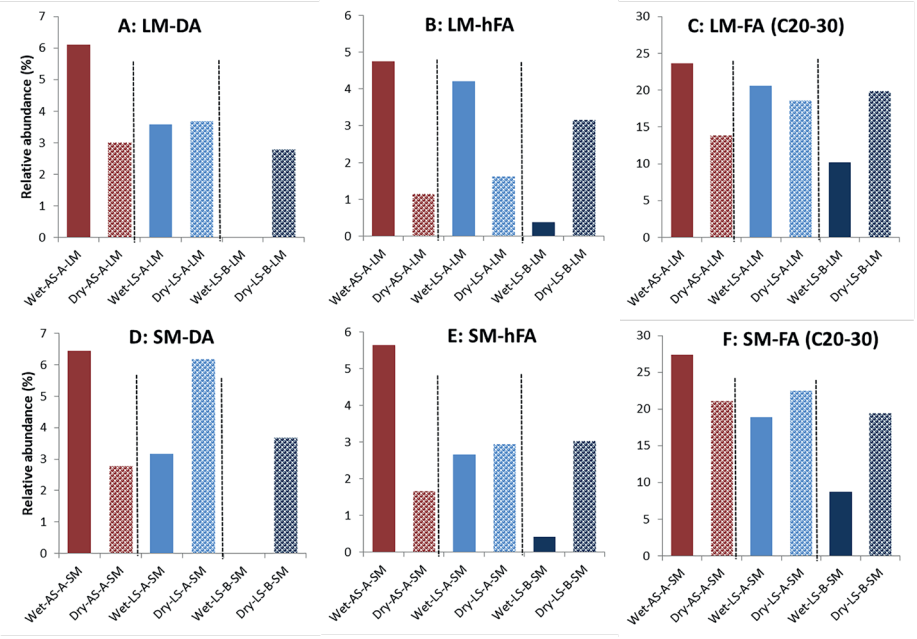


Fig. A4.2 Relative abundances of α, ω-dioic acids (DA), hydroxyl alkanoic acid (hFA) and long-chain fatty acids (FA) in aggregate fractions before the incubation. Wet: the wet site, Dry: the dry site, LS: limestone soil, AS: acid igneous rock soil, A: A horizons, B: B horizons, LM: large macroaggregates (>2 mm), SM: small macroaggregates (0.25-2 mm).

Table A4.1 Bulk soils properties and distribution of fraction weights, C and N in aggregate-size fractions.

Site	Horizon	Depth	C	N	pH	MWD	Gravels in LM	W5	W4	W3	W2	W1	C5	C4	C3	C2	C1	N5	N4	N3	N2	N1
		cm	%	%		mm	%	%	%	%	%	%	%	%	%	%	%	%	%	%	%	%	%
Wet (Cajamarca)																						
LS1	A_{h1}	20	12.51	1.10	6.17	4.22	0.00	29.2	18.6	43.5	7.9	0.7	11.94	11.73	12.25	13.59	12.23	1.06	1.05	1.06	1.24	1.07
	A_{h2}	37	7.20	0.64	6.07	6.42	0.75	51.6	20.2	26.2	2.0	0.0	6.67	8.39	8.05	9.37	10.58	0.61	0.74	0.72	0.83	0.87
	B_t	57	3.73	0.40	6.22	7.99	18.91	68.9	17.4	13.2	0.5	0.0	3.96	4.53	5.19	7.38	6.91	0.40	0.46	0.50	0.68	0.64
LS2	A_{h1}	14	14.84	1.21	5.25	5.33	0.29	41.1	20.4	25.2	8.9	4.1	14.22	14.25	14.66	15.42	11.64	1.15	1.18	1.18	1.27	0.95
	A_{h2}	40	12.65	1.01	5.50	4.80	0.00	34.4	24.0	29.5	9.2	2.9	12.15	12.46	12.60	13.58	10.58	0.95	1.00	1.01	1.11	0.87
	A_{h3}	55	7.67	0.60	5.98	6.37	0.00	50.7	22.3	23.4	3.4	0.2	7.44	8.24	8.34	9.26	7.22	0.57	0.65	0.67	0.73	0.58
	B_{tg}	66	2.41	0.24	6.49	8.72	18.43	77.1	15.6	7.1	0.2	0.0	2.11	2.44	2.90	3.69	2.67	0.22	0.24	0.27	0.33	0.24
LS3	A_p	12	12.63	1.01	5.57	5.64	0.00	44.8	16.3	31.4	6.0	1.3	12.21	11.66	12.43	13.25	12.40	0.99	0.97	0.99	1.10	1.05
	A_{h2}	37	7.47	0.57	6.42	4.97	0.00	36.1	22.4	34.3	6.1	1.0	7.52	7.32	7.17	7.78	8.25	0.57	0.57	0.55	0.63	0.65
	A_{h3}	47	4.59	0.34	6.84	7.66	0.14	65.3	18.2	14.7	1.6	0.3	4.55	5.12	4.81	5.19	5.99	0.32	0.37	0.35	0.40	0.45
	B_{tg}	60	2.37	0.20	6.97	8.30	0.62	73.7	11.6	13.6	1.1	0.0	1.98	2.98	3.17	3.59	4.27	0.18	0.23	0.25	0.27	0.34
AS1	A_p	20	3.30	0.28	4.99	3.76	11.16	29.2	7.9	34.0	23.2	5.6	3.77	3.70	2.32	4.48	6.78	0.30	0.30	0.18	0.39	0.60
	A_{h2}	45	3.46	0.29	4.90	4.00	4.96	29.3	14.8	34.1	17.0	4.8	3.83	3.79	2.82	4.19	7.48	0.32	0.32	0.25	0.36	0.65
	A_{h3}	68	2.97	0.26	5.00	3.80	17.00	26.4	16.1	39.3	14.0	4.2	3.06	2.83	2.21	3.47	5.93	0.25	0.24	0.19	0.30	0.55
AS2	A_p	20	9.24	0.67	5.03	2.89	9.14	18.4	13.9	39.2	21.1	7.0	9.82	9.70	7.53	8.77	14.28	0.68	0.69	0.52	0.63	1.01
	A_{h2}	45	7.38	0.52	4.96	2.93	18.10	17.7	15.9	42.8	19.3	4.3	8.01	7.52	6.81	9.24	12.68	0.56	0.52	0.47	0.68	0.88
AS3	A_{h1}	15	9.38	0.66	5.54	3.79	9.26	24.4	23.9	32.8	14.1	4.4	10.83	9.83	8.34	10.43	12.28	0.78	0.68	0.58	0.74	0.91
	A_{h2}	35	5.90	0.43	5.26	3.08	43.10	18.6	19.4	37.7	17.3	6.9	7.15	5.67	5.16	7.95	10.01	0.52	0.42	0.37	0.60	0.72
Dry (Carhuaz)																						
LS1	A_{h1}	22	3.62	0.33	5.21	3.72	8.95	21.8	28.9	35.6	9.8	3.6	4.35	3.59	3.87	3.27	3.85	0.39	0.34	0.34	0.32	0.37
	A_{h2}	42	2.34	0.25	5.11	5.99	7.18	48.8	16.9	23.7	8.1	2.5	2.15	2.33	2.39	2.43	2.60	0.26	0.27	0.27	0.27	0.28
	B_t	56	1.99	0.24	5.02	7.35	10.48	63.4	13.9	17.9	4.0	0.9	1.82	1.96	1.95	2.05	2.61	0.27	0.25	0.26	0.25	0.30
LS2	A_{h1}	21	2.95	0.32	5.85	6.18	9.53	49.1	22.0	22.5	5.0	1.3	2.86	3.07	3.11	3.01	3.82	0.33	0.34	0.35	0.34	0.44
	A_{h2}	34	1.39	0.20	5.58	6.72	7.13	55.3	19.3	20.5	3.7	1.1	1.22	1.35	1.34	1.45	1.92	0.21	0.21	0.22	0.20	0.27
	B_{tg}	54	0.77	0.17	5.74	7.70	0.00	66.2	17.0	13.7	2.3	0.8	0.64	0.71	0.72	0.94	1.01	0.17	0.18	0.17	0.19	0.20
LS3	A_{h1}	21	4.29	0.40	5.02	5.00	6.89	37.2	21.2	30.0	9.0	2.4	3.98	3.77	4.69	4.67	4.70	0.39	0.37	0.44	0.45	0.48
	A_{h2}	42	2.62	0.27	4.95	4.43	15.21	29.9	25.4	34.6	7.7	2.4	2.79	2.60	2.71	2.58	3.48	0.31	0.29	0.28	0.26	0.38
	A_{h3}	62	2.05	0.24	5.11	4.52	11.89	28.6	33.6	30.2	5.8	1.8	2.03	2.02	2.05	2.11	2.70	0.25	0.26	0.24	0.26	0.31
	B_{tg}	73	1.69	0.22	5.25	4.44	22.56	28.3	30.7	34.1	5.4	1.4	1.72	1.74	1.74	2.09	2.27	0.23	0.23	0.22	0.25	0.30
AS1	A_{h1}	19	7.27	0.54	5.49	1.62	57.95	7.3	9.2	43.1	27.5	12.8	7.18	6.97	5.62	7.69	8.97	0.46	0.51	0.43	0.63	0.76
	A_{h2}	44	6.66	0.48	5.26	2.43	44.45	14.4	12.6	38.8	21.2	12.9	6.32	5.25	4.41	6.26	8.93	0.47	0.40	0.33	0.49	0.70
AS2	A_{h1}	10	4.62	0.32	5.63	2.03	55.76	8.3	15.3	51.6	20.8	3.6	5.83	5.41	5.96	5.74	6.45	0.40	0.38	0.38	0.42	0.50
	AC	15	1.98	0.14	5.82	1.20	80.25	1.0	9.6	64.9	18.5	6.0	2.69	2.52	1.93	2.80	4.69	0.20	0.19	0.14	0.20	0.35
	$2A_{bh}$	60	4.40	0.31	5.24	2.90	31.46	16.3	16.8	50.9	13.6	2.3	5.40	4.31	4.10	5.66	6.41	0.38	0.30	0.29	0.42	0.49
AS3	A_{h1}	19	4.81	0.32	4.83	1.90	33.58	10.9	4.2	50.2	24.2	10.0	6.27	5.60	5.63	4.29	8.96	0.42	0.33	0.35	0.31	0.65
	A_{h2}	50	4.40	0.30	4.78	1.01	77.88	1.6	6.7	49.8	27.9	13.7	7.11	5.17	6.98	5.04	8.24	0.47	0.35	0.43	0.37	0.63

LS: limestone soil, AS: acid igneous rock soil, Wet: the wet site, Dry: the dry site, MWD: mean weight diameter, LM: large macroaggregates (>2 mm), W: weight percentage, C: organic carbon content, N: nitrogen content, -5: fractions >5 mm, -4: fraction 2-5 mm, -3: fraction 0.25-2 mm, -2: fraction 0.063-0.25 mm, -1: fraction <0.063 mm.

Table A4.2 SOC concentrations and bulk densities every 10 cm.

Depth cm	SOC content %	BD g cm^{-1}	BDG g cm^{-1}	Depth cm	SOC content %	BD g cm^{-1}	BDG g cm^{-1}	Depth cm	SOC content %	BD g cm^{-1}	BDG g cm^{-1}
Wet-LS1				**Wet-LS2**				**Wet-LS3**			
10	14.69	0.51	0.51	10	13.72	0.75	0.75	10	11.33	0.71	0.71
20	13.46	0.58	0.58	20	14.41	0.78	0.78	20	9.56	0.78	0.78
30	10.18	0.76	0.75	30	11.43	0.84	0.84	30	9.33	0.76	0.75
40	6.48	0.89	0.88	40	8.99	0.87	0.87	40	6.22	0.89	0.89
50	5.29	1.02	1.01	50	6.45	0.99	0.98	50	4.31	1.06	1.05
60	3.33	1.14	1.10	60	3.28	1.19	0.70	60	2.25	1.28	1.27
				70	1.00	1.37	1.32				
Ave.	8.91	0.82	0.81	Ave.	8.47	0.97	0.89	Ave.	7.17	0.91	0.91
Wet-AS1				**Wet-AS2**				**Wet-AS3**			
10	3.84	1.16	1.09	10	8.97	0.78	0.77	10	9.57	0.73	0.71
20	3.34	1.15	1.13	20	8.81	0.75	0.75	20	7.43	0.80	0.72
30	3.93	1.09	1.09	30	7.37	0.85	0.78	30	5.70	0.87	0.82
40	4.11	0.99	0.99	40	4.97	0.83	0.65	40	5.14	0.84	0.77
50	3.23	1.16	0.91	50	0.95	1.05	0.50	50	0.55	1.16	1.09
60	2.74	1.08	1.01								
70	1.67	1.05	0.85								
Ave.	3.27	1.10	1.01	Ave.	6.21	0.85	0.69	Ave.	5.68	0.88	0.82
Dry-LS1				**Dry-LS2**				**Dry-LS3**			
10	4.95	0.96	0.94	10	4.08	1.08	0.97	10	5.05	0.95	0.92
20	2.56	1.01	0.97	20	2.14	1.07	1.02	20	3.34	1.08	1.05
30	2.32	0.99	0.96	30	1.51	1.16	1.09	30	2.78	1.09	1.05
40	2.17	1.08	1.08	40	0.99	1.29	1.21	40	2.38	1.07	1.03
50	1.96	1.04	1.01	50	0.57	1.28	1.28	50	2.11	1.11	1.08
60	1.47	1.22	1.19	60	0.66	1.25	1.25	60	2.09	1.16	1.09
								70	1.69	1.19	1.15
Ave.	2.57	1.05	1.03	Ave.	1.66	1.19	1.14	Ave.	2.78	1.09	1.05
Dry-AS1				**Dry-AS2**				**Dry-AS3**			
10	6.88	0.74	0.48	10	5.19	0.73	0.68	10	4.88	0.99	0.85
20	5.46	0.87	0.64	20	2.78	1.13	0.89	20	4.77	0.70	0.62
30	5.37	0.78	0.74	30	3.48	1.04	0.74	30	4.88	0.72	0.69
40	2.29	0.96	0.75	40	4.31	0.81	0.73	40	5.45	0.78	0.69
50	0.91	1.21	1.18	50	4.08	0.84	0.78	50	4.48	1.09	0.77
60	0.98	1.28	1.25	60	4.59	1.03	0.77				
				70	0.51	1.59	1.25				
Ave.	3.65	0.97	0.84	Ave.	3.56	1.03	0.83	Ave.	4.89	0.86	0.72

Wet: the wet site, Dry: the dry stie, LS: limestone soil, AS: acidic igneous bedrock soils

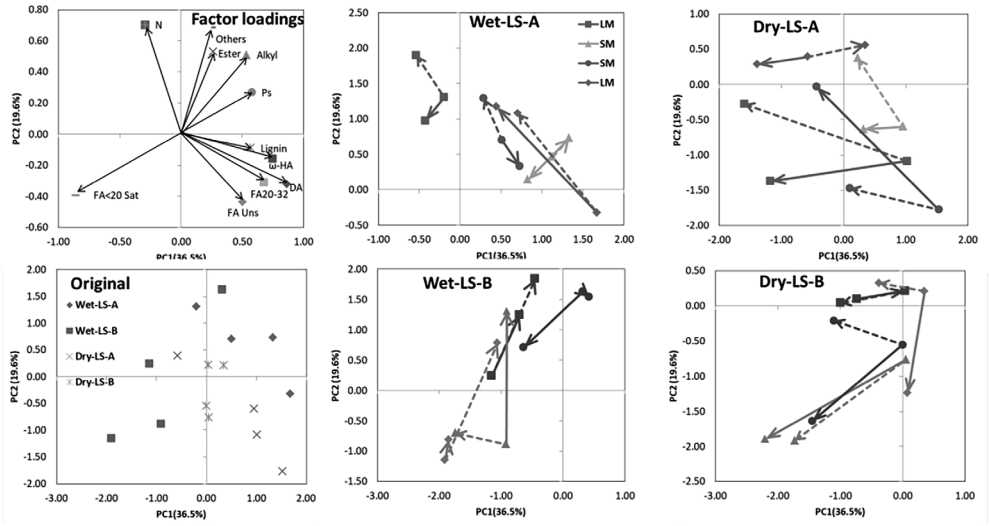


Fig. A4.3 Principal component analysis indicating changes in organic matter chemical composition after a 76-day incubation. DA: α, ω-dioic acid, ω-HA: ω-hydroxyl alkanoic acid, Alkyl: *n*-alkanes and *n*-alkenes, Ps: polysaccharides, N: nitrogen containing compounds, FA<20 Sat: saturated fatty acids with <20 carbon atoms, FA Uns: unsaturated fatty acids, FA20-32: saturated fatty acids with 20-32 carbon atoms, Wet: the wet site, Dry: the dry site, LS: limestone soil, AS: acid igneous rock soil, A: A horizon, B: B horizon. Arrows in solid line mean relative abundance change after incubation of intact aggregates; arrows in dotted line mean relative abundance change after incubation of crushed aggregates. Pyrolysis-gas chromatography / mass spectrometry (GC/MS) analysis was applied for the organic matter molecular composition. The analysis is described in Fig. S2.

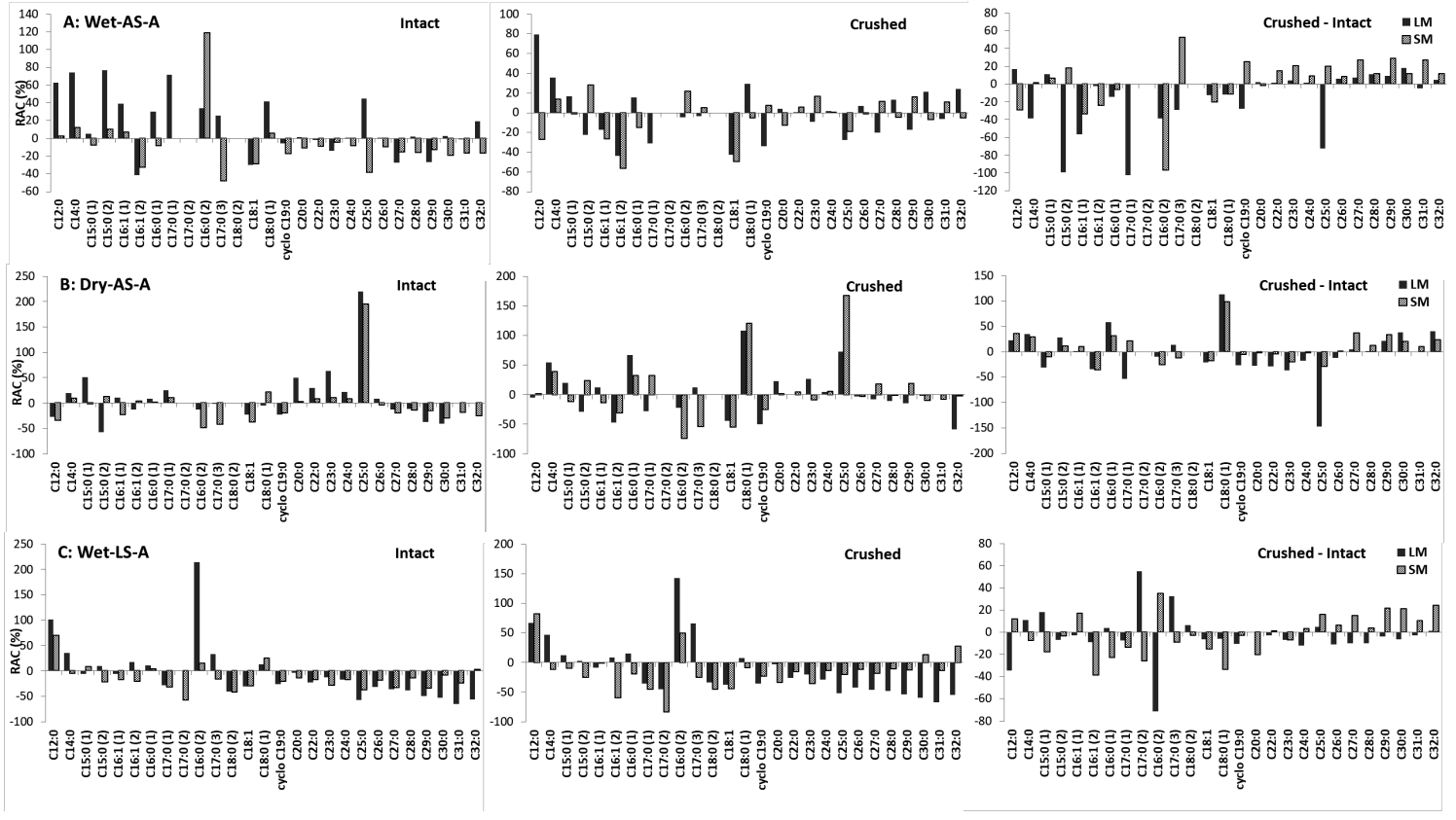


Fig. A5.1 Changes in relative abundances (RAC) of fatty acids for different soil samples after the 76-day incubation (means of $n = 2$). RAC change in relative abundances after the incubation, Intact: incubation of intact aggregates, Crushed: incubation of crushed aggregates, Crushed - Intact: differences between intact and crushed aggregates, LM: large macroaggregates, SM: small macroaggregates, Wet: the wet site, Dry: the dry site, LS: limestone soil, AS: acid igneous rock soil, A: A

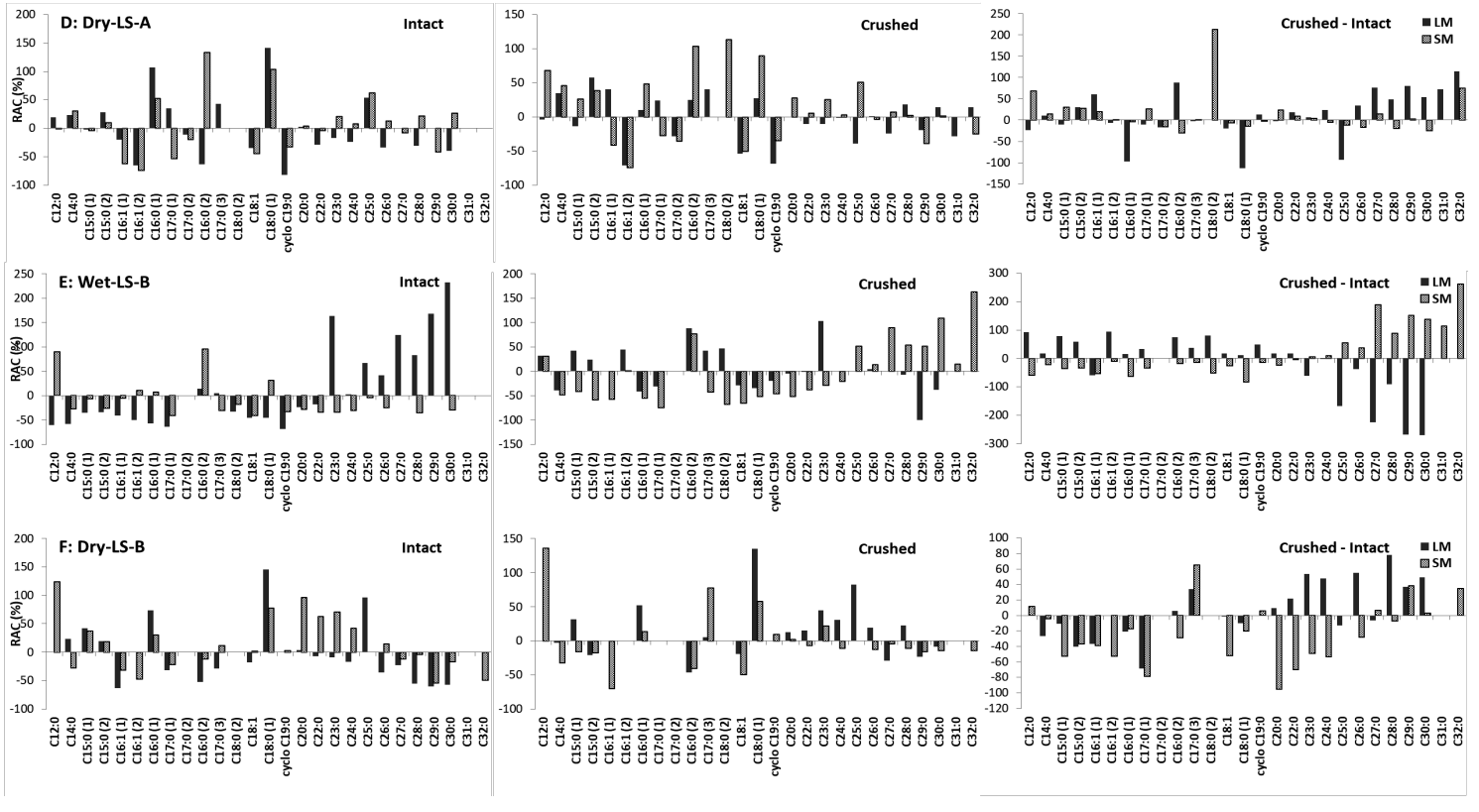


Fig. A5.1 Continue.

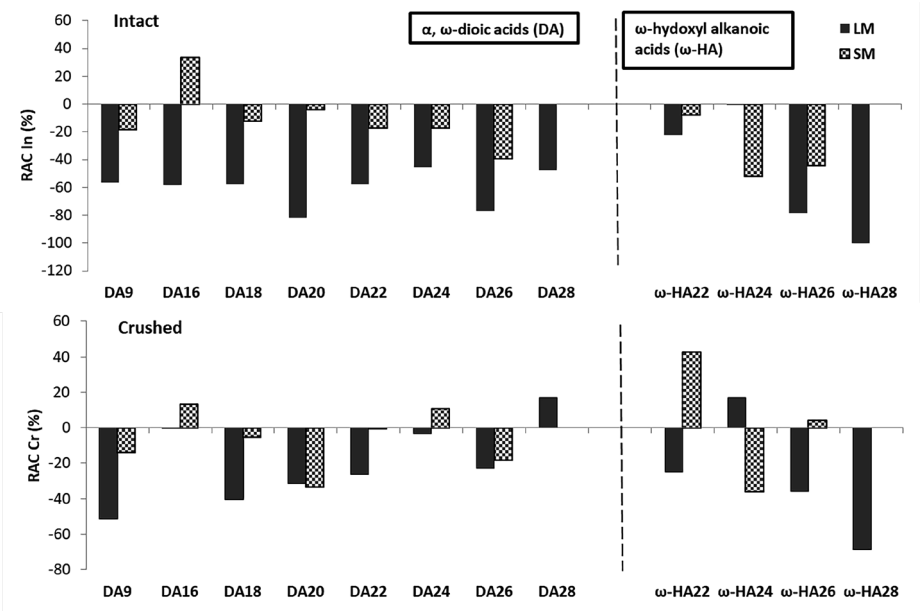


Fig. A5.2 Changes in relative abundance of α-, ω- diacids (DA), ω-hydroxyl alkanoic acids (ω-HA) after the 76-day incubation (means of *n* = 24). RAC In: relative abundance change after incubation with aggregate intact, RAC Cr: relative abundance change after incubation with aggregates crushed, LM: large macroaggregates, SM: small macroaggregates.

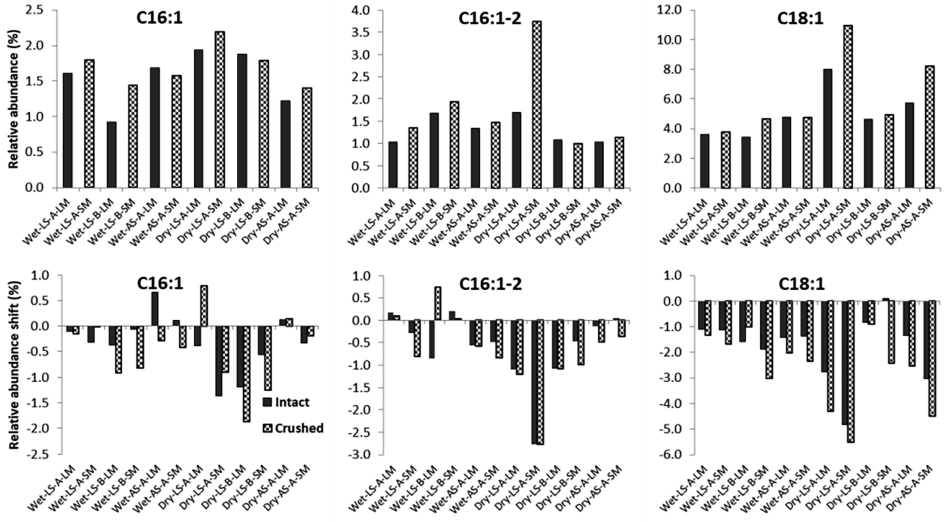


Fig. A5.3 Relative abundances of unsaturated fatty acids and their relative abundance shifts for different soil samples after the 76-day incubation (means of *n* = 2). RAC change in relative abundances after the incubation, Intact: incubation of intact aggregates, Crushed: incubation of crushed aggregates, LM: large macroaggregates, SM: small macroaggregates, Wet: the wet site, Dry: the dry site, LS: limestone soil, AS: acid igneous rock soil, A: A horizon, Btg: B horizon.

Table A5.1 Major compounds detected in the pyrolysis-GC/MS analyses

Compounds	RT (min)	Fragment ions/M+	Compounds	RT (min)	Fragment ions/M+	Compounds	RT (min)	Fragment ions/M+	Compounds	RT (min)	Fragment ions/M+
Fatty acids			Dioic acids & ω-hydroxyl alkanoic acids			*n*-alkanes & *n*-alkenes			Lignin and aromatic compounds		
C12:0	21.16	74/83/143	DA9	21.40	55/74/83/111/152/185	C16:1	22.52	55/57/83/97/111	G1	13.72	123/138
C14:0	24.47	74/83/143	DA16	31.67	74/98/112/283	C16:0	22.64	57/71/85/99/113	P3	14.27	119/134
C15:0(1)	25.47	74/83/143	DA18	34.07	74/98/112/297/311	C17:1	24.13	55/57/83/97/111	P4	15.31	92/135/136
C15:0(2)	25.59	74/83/143	DA20	36.29	74/98/112/226/339	C17:0	24.26	71/85/99/113	G2	15.76	137/152
C16:1(1)	27.16	55/69/97	DA22	38.33	74/98/112/293/367	C21:1	29.73	55/57/83/97/111	S1	17.01	153/168
C16:1(2)	27.29	55/69/97	DA24	40.26	74/98/112/395	C22:1	31.18	55/57/83/97/111	P6	17.92	135/166
C16:0(1)	27.5	74/83/143	DA26	42.17	74/98/112/207/423	C24:1	33.59	55/57/83/97/111	G3	18.28	91/149/164
C17:0(1)	28.11	74/83/143	DA28	44.59	74/98/112/451	C24:0	33.66	57/73/85/99/113	$C_{10}H_{14}O_4$	19.64	140/183/198
C17:0(2)	28.37	74/83/143				C25:1	34.66	55/57/83/97/111	G4	20.58	151/165/166
C16:0(2) [1]	28.70	60/73/129	ω-HA22	37.39	55/74/98/143/352/369	C25:0	34.8	71/85/99/113	G21	20.81	163/178
C17:0(3)	28.89	74/83/143	ω-HA24	39.36	55/74/98/143/348/380	C26:1	35.82	55/57/83/97/111	$C_{10}H_{10}O_4$	21.19	135/163/194
C18:0(1)	28.97	74/87/143	ω-HA26	41.21	55/74/98/143/112/408	C26:0	35.88	281/309/366	G5	22.22	137/165/180
C18:1	29.86	55/69/97	ω-HA28	43.32	55/74/98/143/207/437	C27:1	36.85	55/57/83/97/111	G6	22.33	165/181/196
C18:0(2)	30.21	74/83/143				C27:0	36.95	57/71/85/113	S4	22.55	125/181/196
C19:1	31.32	55/69/97				C28:1	37.9	55/57/83/97/111	G7	22.90	151/179/194
C20:0	32.7	74/83/143				C28:0	38.03	69/81/95/113	G10+11	23.26	165/193/208
C22:0	35.08	74/83/143				C29:0	38.92	57/71/85/113	S5	23.74	139/195/210
C23:0	36.09	74/83/143				C31:0	40.78	57/71/85/99/113	P17	23.90	133/161/192
C24:0	37.12	74/83/143				C33:0	42.72	57/71/85/99/113	S6	24.39	195/211/226
C25:0	38.14	74/83/143							G13	24.85	91/177/208
C26:0	39.12	74/83/143							S7	25.27	181/209/224
C27:0	40.06	74/83/143							G17+18	26.96	191/207/222
C28:0	40.98	74/83/143									
C29:0	41.92	74/83/143									
C30:0	43.01	74/83/143									
C31:0	44.24	74/83/143									
C32:0	45.66	74/83/143									

[1] This is the unsuccessfully methylated C16:0 fatty acid. DA: Dioic acids, ω-HA: ω-hydroxyl alkanoic acids. RT: retention time. G1: 1,2-dimethoxybenzene, P3: methoxystyrene, P4: 4-methoxybenzaldehyde, G2: 3,4-dimethoxytoluene, S1: 1,2,3-trimethoxybenzene, P6: 4-methoxybenzoic acid methyl ester, G3: 3,4-dimethoxystyrene, $C_{10}H_{14}O_4$: 1,2,3,4-tetramethoxybenzene, G4: 3,4-dimethoxybenzaldehyde, G21: 1-(3,4-dimethoxyphenyl)-1-propene, $C_{10}H_{10}O_4$: 1, 4-Benzenedic arboxylc acid, dimethylester, G5: 3,4-dimethoxyacetophenone, G6: 3,4-dimethoxybenzoic acid methyl ester, S4: 3,4,5-trimethoxybenzaldehyde, G7: cis-1-(3,4-dimethoxyphenyl)-2-methoxyethylene, G10: cis-1-(3,4-dimethoxyphenyl)-1-methoxy-1-propene, G11: trans-1-(3,4-dimethoxyphenyl)-1-methoxy-1-propene, S5: 3,4,5-trimethoxyacetophenone, P17: cis-3-(4-methoxyphenyl)-3-propenoic acid methyl ester, S6: 3,4,5-trimethoxybenzoic acid methyl ester, G13: trans-1-(3,4-dimethoxyphenyl)-3-methoxyprop-1-ene, S7: cis-1-(3,4,5-trimethoxyphenyl)-2-methoxyethylene, G17: cis-3-(3,4-dimethoxyphenyl)-3-propenoic acid methyl ester, G18: trans-3-(3,4-dimethoxyphenyl)-3-propenoic acid methyl ester.

Table A5.1 Continue.

Compounds	RT (min)	Fragment ions/M+	Compounds	RT (min)	Fragment ions/M+	Compounds	RT (min)	Fragment ions/M+	Compounds	RT (min)	Fragment ions/M+
Esters			Polysaccharides			Nitrogen compounds			Others		
Ester1[(2)]	35.16	57/71/149/167	Ps1	8.77	67/96	N1	6.83	53/94	1,3,5-Triazine, hexahydro-1,3,5-trimethyl-	10.59	57/86/129
C28	39.6	57/97/257/424	Ps2	9.23	67/95/110	N2	8.31	72	Benzoic acid, hydrazide	12.79	51/77/105/136
C30	41.3	57/83/97/257/452	Ps3	12.01	81/109/124	N3	13.26	54/108/139	poly-hydroxyl fatty acid[(3)]	20.62	75/101/129/161
C32	43.4	57/83/97/257/480	Ps4	14.1	69/71/101	N4	13.65	122	Hexanoic acid, 2-ethyl-, anhydride	36.00	57/99/127/270/327
C34	46.15	57/71/97/257	Ps5	15.56	142	N5	15.7	94/108/134			
			Ps6	18.63	71/101/143	N6	18.99	58/98/141			
						N7	23.1	115/158/172			
						Amide C18	31.85	87/100/114			
						Amide C20	34.3	87/100/114			

[(2)] 1,2-Benzenedicarboxylic acid, mono (2-ethylhexyl) ester, [(3)] 2,4,5,6,7-Pentamethoxyheptanoic acid. RT: retention time, Ps1: 2-Cyclopenten-1-one, 2-methyl-, Ps2: 2-Cyclopenten-1-one, 3,4-dimethyl, Ps3: 2-Cyclopenten-1-one, 2,3,4-trimethyl-, Ps4: Fructofuranose, 2,6-anhydro-1,3,4-tri-O-methyl-, Ps5: 3(2H)-Furanone, 4-methoxy-2,5-dimethyl-, Ps6: 1,5-Anhydro-2,3,4,6-tetra-O-methyl-D-mannitol, N1: 1H-Pyrrole, 2,3-dimethyl-, N2: 2-(N,N-Dimethyl)]-1,2-propanediamine, N3: Methyl 1-methylpyrrole-2-carboxylate, N4: 1H-Pyrrole, 2,3,4,5-tetramethyl-, N5: 2,5-Dimethyl-1-propylpyrrole, N6: 4-Piperidinamine, 2,2,6,6-tetramethyl- , N7: 1,2,3,7-Tetramethylin

References

Amézketa, E., 1999. Soil Aggregate Stability : A Review. Journal of Sustainable Agriculture 14, 83–151. doi:10.1300/J064v14n02

Angst, G., Heinrich, L., Kögel-Knabner, I., Mueller, C.W., 2016. The fate of cutin and suberin of decaying leaves, needles and roots - Inferences from the initial decomposition of bound fatty acids. Organic Geochemistry 95, 81–92. doi:10.1016/j.orggeochem.2016.02.006

Angst, G., Messinger, J., Greiner, M., Häusler, W., Hertel, D., Kirfel, K., Kögel-Knabner, I., Leuschner, C., Rethemeyer, J., Mueller, C.W., 2018a. Soil organic carbon stocks in topsoil and subsoil controlled by parent material, carbon input in the rhizosphere, and microbial-derived compounds. Soil Biology and Biochemistry 122, 19–30. doi:10.1016/j.soilbio.2018.03.026

Angst, G., Mueller, K.E., Kögel-Knabner, I., Freeman, K.H., Mueller, C.W., 2017. Aggregation controls the stability of lignin and lipids in clay-sized particulate and mineral associated organic matter. Biogeochemistry 132, 307–324. doi:10.1007/s10533-017-0304-2

Angst, G., Nierop, K.G.J., Angst, Š., Frouz, J., 2018b. Abundance of lipids in differently sized aggregates depends on their chemical composition. Biogeochemistry 7, 111–125. doi:10.1007/s10533-018-0481-7

Ayala, A., Muñoz, M.F., Argüelles, S., 2014. Lipid peroxidation: Production, metabolism, and signaling mechanisms of malondialdehyde and 4-hydroxy-2-nonenal. Oxidative Medicine and Cellular Longevity 2014. doi:10.1155/2014/360438

Ayoubi, S., Mokhtari Karchegani, P., Mosaddeghi, M.R., Honarjoo, N., 2012. Soil aggregation and organic carbon as affected by topography and land use change in western Iran. Soil and Tillage Research 121, 18–26. doi:10.1016/j.still.2012.01.011

Barré, P., Quénéa, K., Vidal, A., Cécillon, L., Christensen, B.T., Kätterer, T., Macdonald, A., Petit, L., Plante, A.F., van Oort, F., Chenu, C., 2018. Microbial and plant-derived compounds both contribute to persistent soil organic carbon in temperate soils. Biogeochemistry 140, 81–92. doi:10.1007/s10533-018-0475-5

Barton, K., 2016. MuMIn: Multi-Model Inference. In: R Package Version 1.15.6, . https://CRAN.R-project.org/package=MuMIn.

Bates, R.G., 1973. Determination of pH: theory and practice. Journal of The Electrochemical Society 120, 3C–263C.

Batjes, N.H., 2014. Total carbon and nitrogen in the soils of the world. European Journal of Soil Science 65, 1. doi:10.1111/ejss.12120

Blake, G.R., Hartge, K.H., 1986. Methods of soil analysis part 1. Phys. Mineral. Methods

363–375.

Blakemore, L.C., Searle, P.L., Daly, B.K., Bureau, N.Z.S., 1987. Methods for chemical analysis of soils.

Boudot, J.P., Bel Hadj Brahim, A., Steiman, R., Seigle-Murandi, F., 1989. Biodegradation of synthetic organo-metallic complexes of iron and aluminium with selected metal to carbon ratios. Soil Biology and Biochemistry 21, 961–966. doi:10.1016/0038-0717(89)90088-6

Breemen, N. Van, Buurman, P., 2003. Soil Formation, 2nd ed. Springer Science & Business Media, New York, Boston, Dordrecht, London, Moscow. doi:10.1007/0-306-48162-6_2

Brock, O., Kooijman, A., Nierop, K.G.J., Muys, B., Vancampenhout, K., Jansen, B., 2019. Disentangling the effects of parent material and litter input chemistry on molecular soil organic matter composition in converted forests in Western Europe. Organic Geochemistry 134, 66–76.

Bronick, C.J., Lal, R., 2005. Soil structure and management: a review. Geoderma 124, 3–22. doi:10.1016/j.geoderma.2004.03.005

Buurman, P., Peterse, F., Almendros Martin, G., 2007. Soil organic matter chemistry in allophanic soils: a pyrolysis-GC/MS study of a Costa Rican Andosol catena. European Journal of Soil Science 58, 1330–1347. doi:10.1111/j.1365-2389.2007.00925.x

Buytaert, W., Celleri, R., Willems, P., Bièvre, B. De, Wyseure, G., 2006a. Spatial and temporal rainfall variability in mountainous areas: A case study from the south Ecuadorian Andes. Journal of Hydrology 329, 413–421. doi:10.1016/j.jhydrol.2006.02.031

Buytaert, W., Cuesta-Camacho, F., Tobón, C., 2011. Potential impacts of climate change on the environmental services of humid tropical alpine regions. Global Ecology and Biogeography 20, 19–33. doi:10.1111/j.1466-8238.2010.00585.x

Buytaert, W., Deckers, J., Wyseure, G., 2006b. Description and classification of nonallophanic Andosols in south Ecuadorian alpine grasslands (páramo). Geomorphology 73, 207–221. doi:10.1016/j.geomorph.2005.06.012

Carvalhais, N., Forkel, M., Khomik, M., Bellarby, J., Jung, M., Migliavacca, M., Mu, M., Saatchi, S., Santoro, M., Thurner, M., Weber, U., Ahrens, B., Beer, C., Cescatti, A., Randerson, J.T., Reichstein, M., Mu, M., Saatchi, S., Santoro, M., Thurner, M., Weber, U., Ahrens, B., Beer, C., Cescatti, A., Randerson, J.T., Reichstein, M., Mu, M., Saatchi, S., Santoro, M., Thurner, M., Weber, U., Ahrens, B., Beer, C., Cescatti, A., Randerson, J.T., Reichstein, M., 2014. Global covariation of carbon turnover times with climate in terrestrial ecosystems. Nature 514, 213–217. doi:10.1038/nature13731

Cerli, C., Celi, L., Kalbitz, K., Guggenberger, G., Kaiser, K., 2012. Separation of light and heavy organic matter fractions in soil — Testing for proper density cut-off and dispersion level. Geoderma 170, 403–416. doi:10.1016/j.geoderma.2011.10.009

Chaplot, V., Bouahom, B., Valentin, C., 2010. Soil organic carbon stocks in Laos: Spatial variations and controlling factors. Global Change Biology 16, 1380–1393. doi:10.1111/j.1365-2486.2009.02013.x

Chenu, C., Stotzky, G., Huang, P., Bollag, J., 2002. Interactions between microorganisms and soil particles: an overview, in: Interactions between Soil Particles and Microorganisms: Impact on the Terrestrial Ecosystem. pp. 1–40.

Chevallier, P., Pouyaud, B., Suarez, W., Condom, T., 2011. Climate change threats to environment in the tropical Andes: Glaciers and water resources. Regional Environmental Change 11, 179–187. doi:10.1007/s10113-010-0177-6

Clarholm, M., Skyllberg, U., 2013. Translocation of metals by trees and fungi regulates pH, soil organic matter turnover and nitrogen availability in acidic forest soils. Soil Biology and Biochemistry 63, 142–153. doi:10.1016/j.soilbio.2013.03.019

Coldwell, B., Clemens, J., Petford, N., 2011. Deep crustal melting in the Peruvian Andes: Felsic magma generation during delamination and uplift. Lithos 125, 272–286. doi:10.1016/j.lithos.2011.02.011

Cui, X., Wang, Y., Niu, H., Wu, J., Wang, S., Schnug, E., Rogasik, J., Fleckenstein, J., Tang, Y., 2005. Effect of long-term grazing on soil organic carbon content in semiarid steppes in Inner Mongolia. Ecological Research 20, 519–527. doi:10.1007/s11284-005-0063-8

de Koning, G.H.J., Veldkamp, E., López-Ulloa, M., 2003. Quantification of carbon sequestration in soils following pasture to forest conversion in northwestern Ecuador. Global Biogeochemical Cycles 17, n/a-n/a. doi:10.1029/2003GB002099

Dent, B.B., Forbes, S.L., Stuart, B.H., 2004. Review of human decomposition processes in soil. Environmental Geology 45, 576–585. doi:10.1007/s00254-003-0913-z

Dinel, H., Schnitzer, M., Mehuys, G., 1990. Soil lipids: origin, nature, content, decomposition, and effect on soil physical properties, in: Soil Biochemistry.

Dinel, H., Schnitzer, M., Mehuys, G.R., 1990. Soil lipids: origin, nature, content, decomposition, and effect on soil physical properties, in: Soil Biochemistry.

Doetterl, S., Berhe, A.A., Arnold, C., Bodé, S., Fiener, P., Finke, P., Fuchslueger, L., Griepentrog, M., Harden, J.W., Nadeu, E., Schnecker, J., Six, J., Trumbore, S., Van Oost, K., Vogel, C., Boeckx, P., 2018. Links among warming, carbon and microbial dynamics mediated by soil mineral weathering. Nature Geoscience 11, 589–593. doi:10.1038/s41561-018-0168-7

Doetterl, S., Cornelis, J.T., Six, J., Bodé, S., Opfergelt, S., Boeckx, P., Van Oost, K., 2015a. Soil redistribution and weathering controlling the fate of geochemical and

physical carbon stabilization mechanisms in soils of an eroding landscape. Biogeosciences 12, 1357–1371. doi:10.5194/bg-12-1357-2015

Doetterl, S., Stevens, A., Six, J., Merckx, R., Oost, K. Van, Pinto, M.C., Casanova-katny, A., Muñoz, C., Boudin, M., Venegas, E.Z., Boeckx, P., 2015b. Soil carbon storage controlled by interactions between geochemistry and climate. Nature Geoscience 8, 780–783. doi:10.1038/NGEO2516

Du, B., Kang, H., Pumpanen, J., Zhu, P., Yin, S., Zou, Q., Wang, Z., Kong, F., Liu, C., 2014. Soil organic carbon stock and chemical composition along an altitude gradient in the Lushan Mountain, subtropical China. Ecological Research 29, 433–439. doi:10.1007/s11284-014-1135-4

Dümig, A., Schad, P., Kohok, M., Beyerlein, P., Schwimmer, W., Kögel-Knabner, I., 2008. A mosaic of nonallophanic Andosols, Umbrisols and Cambisols on rhyodacite in the southern Brazilian highlands. Geoderma 145, 158–173. doi:10.1016/j.geoderma.2008.01.013

Dungait, J.A.J., Hopkins, D.W., Gregory, A.S., Whitmore, A.P., 2012. Soil organic matter turnover is governed by accessibility not recalcitrance. Global Change Biology 18, 1781–1796. doi:10.1111/j.1365-2486.2012.02665.x

Egashira, K., Uchida, S., Nakashima, S., 1997. Aluminum-Humus Complexes for Accumulation of Organic Matter in Black-Colored Soils under Grass Vegetation in Bolivia. Soil Science and Plant Nutrition 43, 25–33. doi:10.1080/00380768.1997.10414711

Esri. "Topographic" [basemap]. Scale Not Given. "World Topographic Map". June, 2013. http://www.arcgis.com/home/item.html?id=30e5fe3149c34df1ba922e6f5bbf808f. (June, 2019).

Farley, K. a., Kelly, E.F., Hofstede, R.G.M., 2004. Soil organic carbon and water retention after conversion of grasslands to pine plantations in the Ecuadorian Andes. Ecosystems 7, 729–739. doi:10.1007/s10021-004-0047-5

Feng, X., Xu, Y., Jaffé, R., Schlesinger, W.H., Simpson, M.J., 2010. Turnover rates of hydrolysable aliphatic lipids in Duke Forest soils determined by compound specific 13 C isotopic analysis. Organic Geochemistry 41, 573–579. doi:10.1016/j.orggeochem.2010.02.013

Fernández-Romero, M.L., Lozano-García, B., Parras-Alcántara, L., 2014. Topography and land use change effects on the soil organic carbon stock of forest soils in Mediterranean natural areas. Agriculture, Ecosystems & Environment 195, 1–9. doi:10.1016/j.agee.2014.05.015

Field, C.B., 2014. Climate change 2014–Impacts, adaptation and vulnerability: Regional aspects. Cambridge University Press, Cambridge.

Fontaine, S., Barot, S., Barré, P., Bdioui, N., Mary, B., Rumpel, C., 2007. Stability of

organic carbon in deep soil layers controlled by fresh carbon supply. Nature 450, 277–80. doi:10.1038/nature06275

Frostegård, A., Bååth, E., 1996. The use of phospholipidfatty acid analysis to estimate bacterial and fungal biomass in soil. Biology and Fertility of Soils 3, 59–65.

Gang, C., Zhou, W., Chen, Y., Wang, Z., Sun, Z., Li, J., Qi, J., Odeh, I., 2014. Quantitative assessment of the contributions of climate change and human activities on global grassland degradation. Environmental Earth Sciences 72, 4273–4282. doi:10.1007/s12665-014-3322-6

Garcia-Pausas, J., Casals, P., Camarero, L., Huguet, C., Sebastià, M.-T., Thompson, R., Romanyà, J., 2007. Soil organic carbon storage in mountain grasslands of the Pyrenees: effects of climate and topography. Biogeochemistry 82, 279–289. doi:10.1007/s10533-007-9071-9

Gardner, H.W., 1989. Oxygen radical chemistry of polyunsaturated fatty acids. Free Radical Biology and Medicine 7, 65–86. doi:10.1016/0891-5849(89)90102-0

Geo GPS Perú, 2014. GEO GPS PERÚ: Base de datos Perú - Shapefile - *.shp - MINAM - IGN - Límites Políticos [WWW Document]. URL https://www.geogpsperu.com/2013/09/cuadro-de-empalme-de-la-cartografia.html

Goebel, M.O., Woche, S.K., Bachmann, J., 2009. Do soil aggregates really protect encapsulated organic matter against microbial decomposition? Biologia 64, 443–448. doi:10.2478/s11756-009-0065-z

Golchin, A., Oades, J.M., Skjemstad, J.O., Clarke, P., 1994. Study of Free and Occluded Particulate Organic Matter in Soils by Solid state 13C NMR Spectroscopy and Scanning Electron Microscopy 285–309.

Guo, L.B., Gifford, R.M., 2002. Soil carbon stocks and land use change: A meta analysis. Global Change Biology 8, 345–360. doi:10.1046/j.1354-1013.2002.00486.x

Hamkalo, Z., Bedernichek, T., 2014. Total, cold and hot water extractable organic carbon in soil profile: impact of land-use change. Zemdirbyste-Agriculture 101, 125–132. doi:10.13080/z-a.2014.101.016

Harrison, R.B., Footen, P.W., Strahm, B.D., 2011. Deep Soil Horizons : Contribution and Importance to Soil Carbon Pools ... Forest Science 57, 67–76.

Heckman, K., Throckmorton, H., Clingensmith, C., González Vila, F.J., Horwath, W.R., Knicker, H., Rasmussen, C., 2014. Factors affecting the molecular structure and mean residence time of occluded organics in a lithosequence of soils under ponderosa pine. Soil Biology and Biochemistry 77, 1–11. doi:10.1016/j.soilbio.2014.05.028

Heckman, K., Welty-Bernard, A., Rasmussen, C., Schwartz, E., 2009. Geologic controls of soil carbon cycling and microbial dynamics in temperate conifer forests. Chemical Geology 267, 12–23. doi:10.1016/j.chemgeo.2009.01.004

Hendershot, W.H., Duquette, M., 1986. A simple barium chloride method for determining cation exchange capacity and exchangeable cations. Soil Science Society of America Journal 50, 605–608.

Hobley, E., Wilson, B., Wilkie, A., Gray, J., Koen, T., 2015. Drivers of soil organic carbon storage and vertical distribution in Eastern Australia. Plant and Soil 390, 111–127. doi:10.1007/s11104-015-2380-1

Holmgren, G.G., 1967. A rapid citrate-dithionite extractable iron procedure. Soil Science Society of America Journal 31, 210–211.

Homann, P.S., Kapchinske, J.S., Boyce, A., 2007. Relations of mineral-soil C and N to climate and texture: Regional differences within the conterminous USA. Biogeochemistry 85, 303–316. doi:10.1007/s10533-007-9139-6

Hribljan, J.A., Suárez, E., Heckman, K.A., Lilleskov, E.A., Chimner, R.A., 2016. Peatland carbon stocks and accumulation rates in the Ecuadorian páramo. Wetlands Ecology and Management 24, 113–127. doi:10.1007/s11273-016-9482-2

Jandl, G., Leinweber, P., Schulten, H.-R., Eusterhues, K., 2004. The concentrations offatty acids in organo-mineral particle-size fractions ofa Chernozem. European Journal of Soil Science 55, 459–469. doi:10.1111/j.1365-2389.2004.00623.x

Jansen, B., Tonneijck, F.H., Verstraten, J.M., 2011. Selective Extraction Methods for Aluminium, Iron and Organic Carbon from Montane Volcanic Ash Soils. Pedosphere 21, 549–565. doi:10.1016/S1002-0160(11)60157-4

Jansen, B., Wiesenberg, G.L.B., 2017. Opportunities and limitations related to the application of plant-derived lipid molecular proxies in soil science. Soil 3, 211–234. doi:10.5194/soil-3-211-2017

Jenny, H., 1941. Factors of soil formation: a system of quantitative pedology. Courier Corporation.

Juarez, S., Nunan, N., Duday, A.C., Pouteau, V., Schmidt, S., Hapca, S., Falconer, R., Otten, W., Chenu, C., 2013. Effects of different soil structures on the decomposition of native andadded organic carbon. European Journal of Soil Biology 58, 81–90. doi:10.1016/j.ejsobi.2013.06.005

Kaiser, K., Guggenberger, G., 2007. Sorptive stabilization of organic matter by microporous goethite: Sorption into small pores vs. surface complexation. European Journal of Soil Science 58, 45–59. doi:10.1111/j.1365-2389.2006.00799.x

Kaiser, K., Guggenberger, G., 2003. Mineral surfaces and soil organic matter. European Journal of Soil Science 54, 219–236. doi:10.1046/j.1365-2389.2003.00544.x

Kaiser, K., Kalbitz, K., 2012. Cycling downwards – dissolved organic matter in soils. Soil Biology and Biochemistry 52, 29–32. doi:10.1016/j.soilbio.2012.04.002

Kaiser, K., Zech, W., 1996. Defects in estimation of aluminum in humus complexes of

podzolic soils by pyrophosphate extraction. Soil Science 161, 452–458.

Kaiser, M., Berhe, A.A., 2014. How does sonication affect the mineral and organic constituents of soil aggregates? - A review. Journal of Plant Nutrition and Soil Science 177, 479–495. doi:10.1002/jpln.201300339

Kaiser, M., Walter, K., Ellerbrock, R.H., Sommer, M., 2011. Effects of land use and mineral characteristics on the organic carbon content, and the amount and composition of Na-pyrophosphate-soluble organic matter, in subsurface soils. European Journal of Soil Science 62, 226–236. doi:10.1111/j.1365-2389.2010.01340.x

Kaneda, T., 1991. Iso- and Anteiso-Fatty Acids in Bacteria: Biosynthesis, Function, and Taxonomic Significancet. MICROBIOLOGICAL REVIEWS 55, 288–302. doi:10.14743/apem2017.1.239

Kleber, M., 2010. What is recalcitrant soil organic matter? Environmental Chemistry 7, 320. doi:10.1071/EN10006

Kleber, M., Eusterhues, K., Keiluweit, M., Mikutta, C., Mikutta, R., Nico, P.S., 2015. Mineral-Organic Associations: Formation, Properties, and Relevance in Soil Environments, Advances in Agronomy. Elsevier Ltd. doi:10.1016/bs.agron.2014.10.005

Kleber, M., Sollins, P., Sutton, R., 2007. A conceptual model of organo-mineral interactions in soils: self-assembly of organic molecular fragments into zonal structures on mineral surfaces. Biogeochemistry 85, 9–24. doi:10.1007/s10533-007-9103-5

Klute, A., Dinauer, R.C., 1986. Methods of Soil Analysis Part 1. Physical and Mineralogical Methods, 2nd ed. Madison.

Kögel-Knabner, I., 2017. The macromolecular organic composition of plant and microbial residues as inputs to soil organic matter: Fourteen years on. Soil Biology and Biochemistry 105, A3–A8. doi:10.1016/j.soilbio.2016.08.011

Kögel-Knabner, I., 2002. The macromolecular organic composition of plant and microbial residues as inputs to soil organic matter: Fourteen years on. Soil Biology and Biochemistry 34, 139–162. doi:10.1016/S0038-0717(01)00158-4

Kögel-Knabner, I., Guggenberger, G., Kleber, M., Kandeler, E., Kalbitz, K., Scheu, S., Eusterhues, K., Leinweber, P., 2008. Organo-mineral associations in temperate soils: Integrating biology, mineralogy, and organic matter chemistry. Journal of Plant Nutrition and Soil Science 171, 61–82. doi:10.1002/jpln.200700048

Kong, A.Y.Y., Six, J., Bryant, D.C., Denison, R.F., van Kessel, C., 2005. The Relationship between Carbon Input, Aggregation, and Soil Organic Carbon Stabilization in Sustainable Cropping Systems. Soil Science Society of America Journal 69, 1078. doi:10.2136/sssaj2004.0215

Krom, M.D., 1980. Spectrophotometric determination of ammonia: a study of a modified Berthelot reaction using salicylate and dichloroisocyanurate. The Analyst 105, 305–316.

Krull, E.S., Baldock, J.A., Skjemstad, J.O., 2003. Importance of mechanisms and processes of the stabilisation of soil organic matter for modelling carbon turnover. Functional Plant Biology 30, 207–222. doi:10.1071/FP02085

Lal, R., 2004. Soil carbon sequestration impacts on global climate change and food security. Science 304, 1623–1627.

Lehmann, J., Kinyangi, J., Solomon, D., 2007. Organic matter stabilization in soil microaggregates: Implications from spatial heterogeneity of organic carbon contents and carbon forms. Biogeochemistry 85, 45–57. doi:10.1007/s10533-007-9105-3

Lehmann, J., Kleber, M., 2015. The contentious nature of soil organic matter. Nature 528, 60–8. doi:10.1038/nature16069

Leifeld, J., Bassin, S., Fuhrer, J., 2005. Carbon stocks in Swiss agricultural soils predicted by land-use, soil characteristics, and altitude. Agriculture, Ecosystems and Environment 105, 255–266. doi:10.1016/j.agee.2004.03.006

Lineger, H., Weingartner, R., Grosjean, M., 1998. Mountains of the World : Water Towers for the 21 st Century 32.

Luo, Y., Ahlström, A., Allison, S.D., Batjes, N.H., Brovkin, V., Carvalhais, N., Chappell, A., Ciais, P., Davidson, E. a, Finzi, A., Georgiou, K., Guenet, B., Hararuk, O., Harden, J.W., He, Y., Hopkins, F., Jiang, L., Koven, C., Jackson, R.B., Jones, C.D., Lara, M.J., Liang, J., Mcguire, a D., Parton, W., Peng, C., Randerson, J.T., Salazar, A., Sierra, C. a, Smith, M.J., Tian, H., Todd-brown, K.E.O., Torn, M., Groenigen, K.J., Wang, Y.P., West, T.O., Wei, Y., Wieder, W.R., Xia, J., Xu, X., Xu, X., Zhou, T., 2016. Toward more realistic projections of soil carbon dynamics by Earth system models. Global Biogeochemical Cycles 1–17. doi:10.1002/2015GB005239.Received

Lützow, M. V., Kögel-Knabner, I., Ekschmitt, K., Matzner, E., Guggenberger, G., Marschner, B., Flessa, H., 2006. Stabilization of organic matter in temperate soils: mechanisms and their relevance under different soil conditions - a review. European Journal of Soil Science 57, 426–445. doi:10.1111/j.1365-2389.2006.00809.x

Masiello, C.A., Chadwick, O.A., Southon, J., Torn, M.S., Harden, J.W., 2004. Weathering controls on mechanisms of carbon storage in grassland soils. Global Biogeochemical Cycles 18, 1–9. doi:10.1029/2004GB002219

Matsumoto, G., Toriit, T., Hanya, T., 1981. High abundances of long-chain normal alkanoic acids in Antarctic soil. Nature 290, 688–690.

McSherry, M.E., Ritchie, M.E., 2013. Effects of grazing on grassland soil carbon: A global review. Global Change Biology 19, 1347–1357. doi:10.1111/gcb.12144

Merkel, A., 2017. Climate-data [WWW Document]. URL https://en.climate-data.org/south-america/peru-27/

Mikutta, R., Kleber, M., Torn, M.S., Jahn, R., 2006. Stabilization of Soil Organic Matter: Association with Minerals or Chemical Recalcitrance? Biogeochemistry 77, 25–56. doi:10.1007/s10533-005-0712-6

Minasny, B., Malone, B.P., McBratney, A.B., Angers, D.A., Arrouays, D., Chambers, A., Chaplot, V., Chen, Z.S., Cheng, K., Das, B.S., Field, D.J., Gimona, A., Hedley, C.B., Hong, S.Y., Mandal, B., Marchant, B.P., Martin, M., McConkey, B.G., Mulder, V.L., O'Rourke, S., Richer-de-Forges, A.C., Odeh, I., Padarian, J., Paustian, K., Pan, G., Poggio, L., Savin, I., Stolbovoy, V., Stockmann, U., Sulaeman, Y., Tsui, C.C., Vågen, T.G., van Wesemael, B., Winowiecki, L., 2017. Soil carbon 4 per mille. Geoderma 292, 59–86. doi:10.1016/j.geoderma.2017.01.002

Minaya, V., Corzo, G., Romero-Saltos, H., Van Der Kwast, J., Lantinga, E., Galárraga-Sánchez, R., Mynett, A., 2016. Altitudinal analysis of carbon stocks in the Antisana páramo, Ecuadorian Andes. Journal of Plant Ecology 9, 553–563. doi:10.1093/jpe/rtv073

Moni, C., Derrien, D., Hatton, P.-J., Zeller, B., Kleber, M., 2012. Density fractions versus size separates: does physical fractionation isolate functional soil compartments? Biogeosciences 9, 5181–5197. doi:10.5194/bg-9-5181-2012

Moucawi, J., Fuste, E., Jambi, P., 1981. Decomposition of Lipids in Soils : Free and Esterified Fatty Acids , Alcohols and Ketones. Soil Biology and Biochemistry 13, 461–468.

Mueller, C.W., Schlund, S., Prietzel, J., Kögel-Knabner, I., Gutsch, M., 2012. Soil Aggregate Destruction by Ultrasonication Increases Soil Organic Matter Mineralization and Mobility. Soil Science Society of America Journal 76, 1634. doi:10.2136/sssaj2011.0186

Mueller, K.E., Eissenstat, D.M., Müller, C.W., Oleksyn, J., Reich, P.B., Freeman, K.H., 2013. What controls the concentration of various aliphatic lipids in soil? Soil Biology and Biochemistry 63, 14–17. doi:10.1016/j.soilbio.2013.03.021

Muneer, M., Oades, J.M., 1989. The Role of Ca-Organic Interactions in Soil Aggregate Stability. I. Laboratory Studies with 14C-glucose, CaC03 and CaS04.2H20. Aust. J. Soil Res 27, 389–399.

Muñoz-García, M.A., Faz-Cano, A., 2012. Soil organic matter stocks and quality at high altitude grasslands of Apolobamba, Bolivia. Catena 94, 26–35. doi:10.1016/j.catena.2011.06.007

Muñoz, C., Cruz, B., Rojo, F., Campos, J., Casanova, M., Doetter, S., Boeckx, P., Zagal, E., 2016. Temperature sensitivity of carbon decomposition in soil aggregates along a climatic gradient. Journal of Soil Science and Plant Nutrition 16, 461–476. doi:10.4067/S0718-95162016005000039

Myneni, S.C.B., Brown, J.T., Martinez, G.A., Meyer-Ilse, W., 1999. Imaging of humic substance macromolecular structures in water and soils. Science 286, 1335–1337. doi:10.1126/science.286.5443.1335

Nierop, K.G.J., Jansen, B., 2009. Extensive transformation of organic matter and excellent lipid preservation at the upper, superhumid Guandera páramo. Geoderma 151, 357–369. doi:10.1016/j.geoderma.2009.05.002

Nierop, K.G.J., Jansen, B., Hageman, J.A., Verstraten, J.M., 2006. The complementarity of extractable and ester-bound lipids in a soil profile under pine. Plant and Soil 286, 269–285. doi:10.1007/s11104-006-9043-1

Nierop, K.G.J., Tonneijck, F.H., Jansen, B., Verstraten, J.M., 2007. Organic Matter in Volcanic Ash Soils under Forest and Páramo along an Ecuadorian Altitudinal Transect. Soil Science Society of America Journal 71, 1119. doi:10.2136/sssaj2006.0322

Nierop, K.G.J., Verstraten, J.M., 2003. Organic matter formation in sandy subsurface horizons of Dutch coastal dunes in relation to soil acidification. Organic Geochemistry 34, 499–513. doi:10.1016/S0146-6380(02)00249-8

Oades, J.M., 1989. An introduction to organic matter in mineral soils, in: Minerals in Soil Environments Mineralsinsoile. pp. 89–159.

Oliveras, I., Girardin, C., Doughty, C.E., Cahuana, N., Arenas, C.E., Oliver, V., Huaraca Huasco, W., Malhi, Y., 2014. Andean grasslands are as productive as tropical cloud forests. Environmental Research Letters. doi:10.1088/1748-9326/9/11/115011

Otto, A., Simpson, M.J., 2007. Analysis of soil organic matter biomarkers by sequential chemical degradation and gas chromatography - Mass spectrometry. Journal of Separation Science 30, 272–282. doi:10.1002/jssc.200600243

Parfitt, R.L., 2009. Allophane and imogolite: role in soil biogeochemical processes. Clay Minerals 44, 135–155. doi:10.1180/claymin.2009.044.1.135

Percival, H.J., Parfitt, R.L., Scott, N. a., 2000. Factors Controlling Soil Carbon Levels in New Zealand Grasslands. Soil Science Society of America Journal 64, 1623. doi:10.2136/sssaj2000.6451623x

Piñeiro, G., Paruelo, J.M., Oesterheld, M., Jobbágy, E.G., 2010. Pathways of Grazing Effects on Soil Organic Carbon and Nitrogen. Rangeland Ecology & Management 63, 109–119. doi:10.2111/08-255.1

Podwojewski, P., Poulenard, J., Zambrana, T., Hofstede, R., 2002. Overgrazing effects on vegetation cover and properties of volcanic ash soil in the pàramo of Llangahua and al Esperanza (Tungurahua, Ecuador). Management 18, 45–55. doi:10.1079/SUM2001100

Poeplau, C., Don, A., 2013. Sensitivity of soil organic carbon stocks and fractions to different land-use changes across Europe. Geoderma 192, 189–201.

doi:10.1016/j.geoderma.2012.08.003

Poeplau, C., Don, A., Vesterdal, L., Leifeld, J., Van Wesemael, B., Schumacher, J., Gensior, A., 2011. Temporal dynamics of soil organic carbon after land-use change in the temperate zone - carbon response functions as a model approach. Global Change Biology 17, 2415–2427. doi:10.1111/j.1365-2486.2011.02408.x

Porras, R.C., Hicks Pries, C.E., McFarlane, K.J., Hanson, P.J., Torn, M.S., 2017. Association with pedogenic iron and aluminum: effects on soil organic carbon storage and stability in four temperate forest soils. Biogeochemistry 133, 333–345. doi:10.1007/s10533-017-0337-6

Portes, R.D.C., Spinola, D.N., Reis, J.S., Ker, J.C., Costa, L.M. Da, Fernandes Filho, E.I., Kühn, P., Schaefer, C.E.G.R., 2016. Pedogenesis across a climatic gradient in tropical high mountains, Cordillera Blanca - Peruvian Andes. Catena 147, 441–452. doi:10.1016/j.catena.2016.07.027

Poulenard, J., Podwojewski, P., Herbillon, A.J., 2003. Characteristics of non-allophanic Andisols with hydric properties from the Ecuadorian páramos. Geoderma 117, 267–281. doi:10.1016/S0016-7061(03)00128-9

Powers, J.S., Corre, M.D., Twine, T.E., Veldkamp, E., 2011. Geographic bias of field observations of soil carbon stocks with tropical land-use changes precludes spatial extrapolation. Proceedings of the National Academy of Sciences of the United States of America 108, 6318–6322. doi:10.1073/pnas.1016774108

Reyes-Rivera, L., 1980. Geología de los cuadrángulos de Cajamarca, San Marcos y Cajambamba 15-f, 15-g, 16-g-[Boletín A 31].

Rolando, J.L., Dubeux, J.C., Perez, W., Ramirez, D.A., Turin, C., Ruiz-Moreno, M., Comerford, N.B., Mares, V., Garcia, S., Quiroz, R., 2017a. Soil organic carbon stocks and fractionation under different land uses in the Peruvian high-Andean Puna. Geoderma 307, 65–72. doi:10.1016/j.geoderma.2017.07.037

Rolando, J.L., Turin, C., Ramírez, D.A., Mares, V., Monerris, J., Quiroz, R., 2017b. Key ecosystem services and ecological intensification of agriculture in the tropical high-Andean Puna as affected by land-use and climate changes. Agriculture, Ecosystems and Environment 236, 221–233. doi:10.1016/j.agee.2016.12.010

Rowley, M.C., Grand, S., Verrecchia, É.P., 2018. Calcium-mediated stabilisation of soil organic carbon. Biogeochemistry 137, 27–49. doi:10.1007/s10533-017-0410-1

Rumpel, C., Kögel-Knabner, I., 2010. Deep soil organic matter—a key but poorly understood component of terrestrial C cycle. Plant and Soil 338, 143–158. doi:10.1007/s11104-010-0391-5

Rustan, A.C., Drevon, C.A., 2005. Fatty Acids: Structures and Properties. Encyclopedia of Life Sciences 1–7. doi:10.1038/npg.els.0003894

R Core Team, 2017. R: A Language and Environment for Statistical Computing. R

Foundation for Statistical Computing, Vienna, Austria. https://www.R-project.org/.

Sadava, D.E., Heller, H.C., Purves, W.K., Orians, G.H., Hillis, D.M., 2008. Life: The science of biology. MacMillan.

Sánchez Vega, I., Cabanillas Soriano, M., Miranda Leiva, A., Poma Rojas, W., Díaz Navarro, J., Terrones Hernández, F Bazán Zurita, H., 2005. La jalca: el ecosistema frio del noroeste peruano, fundamentos biologicos y ecologicos.

Sánchez Vega, I., Dillon, M.O., 2006. Jalcas. In: Moraes, M., Øllgaard, Kvist, L.P., Borchsenius, F., Balslev, H. (Eds.), Botanica Economica de los Andes Centrales. Universidad Mayor de San Andrés, La Paz, pp. 77–90.

Sarmiento, L., Bottner, P., 2002. Carbon and nitrogen dynamics in two soils with different fallow times in the high tropical Andes: Indications for fertility restoration. Applied Soil Ecology 19, 79–89. doi:10.1016/S0929-1393(01)00178-0

Schawe, M., Glatzel, S., Gerold, G., 2007. Soil development along an altitudinal transect in a Bolivian tropical montane rainforest: Podzolization vs. hydromorphy. Catena 69, 83–90. doi:10.1016/j.catena.2006.04.023

Schmidt, M.W.I., Torn, M.S., Abiven, S., Dittmar, T., Guggenberger, G., Janssens, I.A., Kleber, M., Kögel-Knabner, I., Lehmann, J., Manning, D.A.C., Nannipieri, P., Rasse, D.P., Weiner, S., Trumbore, S.E., 2011. Persistence of soil organic matter as an ecosystem property. Nature 478, 49–56. doi:10.1038/nature10386

Schrumpf, M., Kaiser, K., Guggenberger, G., Persson, T., Kögel-Knabner, I., Schulze, E.-D., 2013. Storage and stability of organic carbon in soils as related to depth, occlusion within aggregates, and attachment to minerals. Biogeosciences 10, 1675–1691. doi:10.5194/bg-10-1675-2013

Schwanghart, W., Jarmer, T., 2011. Linking spatial patterns of soil organic carbon to topography - A case study from south-eastern Spain. Geomorphology 126, 252–263. doi:10.1016/j.geomorph.2010.11.008

Schwertmann, U., 1964. Differenzierung der Eisenoxide des Bodens durch Extraktion mit Ammoniumoxalat-Lösung. Journal of Plant Nutrition and Soil Science 105, 194–202.

Schwesig, D., Kalbitz, K., Matzner, E., 2003. Effects of aluminium on the mineralization of dissolved organic carbon derived from forest floors. European Journal of Soil Science 54, 311–322. doi:10.1046/j.1365-2389.2003.00523.x

Segnini, a., Posadas, a., Quiroz, R., Milori, D.M.B.P., Vaz, C.M.P., Martin-Neto, L., 2011. Soil carbon stocks and stability across an altitudinal gradient in southern Peru. Journal of Soil and Water Conservation 66, 213–220. doi:10.2489/jswc.66.4.213

Seijmonsbergen, a. C., Sevink, J., Cammeraat, L.H., Recharte, J., 2010. A potential geoconservation map of the Las Lagunas area, northern Peru. Environmental Conservation 37, 107–115. doi:10.1017/S0376892910000408

Sierra, C.A., del Valle, J.I., Orrego, S.A., Moreno, F.H., Harmon, M.E., Zapata, M., Colorado, G.J., Herrera, M.A., Lara, W., Restrepo, D.E., Berrouet, L.M., Loaiza, L.M., Benjumea, J.F., 2007. Total carbon stocks in a tropical forest landscape of the Porce region, Colombia. Forest Ecology and Management 243, 299–309. doi:10.1016/j.foreco.2007.03.026

Six, J., Bossuyt, H., Degryze, S., Denef, K., 2004. A history of research on the link between (micro)aggregates, soil biota, and soil organic matter dynamics. Soil and Tillage Research 79, 7–31. doi:10.1016/j.still.2004.03.008

Six, J., Conant, R.T., Paul, E.A., Paustian, K., 2002. Stabilization mechanisms of soil organic matter : Implications for C-saturation of soils 155–176.

Six, J., Elliott, E.T., Paustian, K., 2000. Soil macroaggregate turnover and microaggregate formation: A mechanism for C sequestration under no-tillage agriculture. Soil Biology and Biochemistry 32, 2099–2103. doi:10.1016/S0038-0717(00)00179-6

Six, J., Paustian, K., 2014. Aggregate-associated soil organic matter as an ecosystem property and a measurement tool. Soil Biology and Biochemistry 68, A4–A9. doi:10.1016/j.soilbio.2013.06.014

Sollins, P., Homann, P., Caldwell, B.A., 1996. Stabilization and destabilization of soil organic matter : mechanisms and controls 74, 65–105.

Stevenson, F.J., 1994. Humus Chemistry: Genesis, Composition, Reactions. John Wiley & Sons.

Takahashi, T., Dahlgren, R. a., 2016. Nature, properties and function of aluminum-humus complexes in volcanic soils. Geoderma 263, 110–121. doi:10.1016/j.geoderma.2015.08.032

Tonneijck, F.H., Jansen, B., Nierop, K.G.J., Verstraten, J.M., Sevink, J., De Lange, L., 2010. Towards understanding of carbon stocks and stabilization in volcanic ash soils in natural Andean ecosystems of northern Ecuador. European Journal of Soil Science 61, 392–405. doi:10.1111/j.1365-2389.2010.01241.x

Tovar, C., Seijmonsbergen, A.C., Duivenvoorden, J.F., 2013. Monitoring land use and land cover change in mountain regions: An example in the Jalca grasslands of the Peruvian Andes. Landscape and Urban Planning 112, 40–49. doi:10.1016/j.landurbplan.2012.12.003

Tsai, C.C., Chen, Z.S., Kao, C.I., Ottner, F., Kao, S.J., Zehetner, F., 2010. Pedogenic development of volcanic ash soils along a climosequence in Northern Taiwan. Geoderma 156, 48–59. doi:10.1016/j.geoderma.2010.01.007

van Hall, R.L., Cammeraat, L.H., Keesstra, S.D., Zorn, M., 2016. Impact of secondary vegetation succession on soil quality in a humid Mediterranean landscape. Catena 149, 836–843. doi:10.1016/j.catena.2016.05.021

Verweij, P.A., Budde, P.E., 1992. Burning and grazing gradients in páramo vegetation

initial ordination analyses, in: Páramo: An Andean Ecosystem under Human Influence. Academic Press, London, pp. 177–195.

Wada, K., 1989. Allophane and imogolite. Minerals in Soil Environments Mineralsinsoile 1051–1087.

Wagai, R., Mayer, L.M., Kitayama, K., 2009. Nature of the "occluded" low-density fraction in soil organic matter studies: A critical review. Soil Science and Plant Nutrition 55, 13–25. doi:10.1111/j.1747-0765.2008.00356.x

Wagai, R., Mayer, L.M., Kitayama, K., Knicker, H., 2008. Climate and parent material controls on organic matter storage in surface soils: A three-pool, density-separation approach. Geoderma 147, 23–33. doi:10.1016/j.geoderma.2008.07.010

Wang, X., Cammeraat, E.L.H., Cerli, C., Kalbitz, K., 2014. Soil aggregation and the stabilization of organic carbon as affected by erosion and deposition. Soil Biology and Biochemistry 72, 55–65. doi:10.1016/j.soilbio.2014.01.018

Wattel-Koekkoek, E.J.W., Buurman, P., Van Der Plicht, J., Wattel, E., Van Breemen, N., 2003. Mean residence time of soil organic matter associated with kaolinite and smectite. European Journal of Soil Science 54, 269–278. doi:10.1046/j.1365-2389.2003.00512.x

Wershaw, R.L., 1993. Model for Humus: In Soils and Sediments. Environmental Science and Technology 27, 814–816. doi:10.1021/es00042a603

Wiesenberg, G.L.B., Schmidt, M.W.I., Schwark, L., 2008. Plant and soil lipid modifications under elevated atmospheric CO2 conditions: I. Lipid distribution patterns. Organic Geochemistry 39, 91–102. doi:10.1016/j.orggeochem.2007.09.005

Wiesmeier, M., Spörlein, P., Geuß, U., Hangen, E., Haug, S., Reischl, A., Schilling, B., von Lützow, M., Kögel-Knabner, I., 2012. Soil organic carbon stocks in southeast Germany (Bavaria) as affected by land use, soil type and sampling depth. Global Change Biology 18, 2233–2245. doi:10.1111/j.1365-2486.2012.02699.x

Wiesmeier, M., Urbanski, L., Hobley, E., Lang, B., von Lützow, M., Marin-Spiotta, E., van Wesemael, B., Rabot, E., Ließ, M., Garcia-Franco, N., Wollschläger, U., Vogel, H.J., Kögel-Knabner, I., 2019. Soil organic carbon storage as a key function of soils - A review of drivers and indicators at various scales. Geoderma 333, 149–162. doi:10.1016/j.geoderma.2018.07.026

WRB, I.W.G., 2014. World reference base for soil resources 2014. International soil classification system for naming soils and creating legends for soil maps. FAO, Rome.

WRB, I.W.G., 2006. World reference base for soil resources 2006, World Soil Resources Reports No. 103. FAO, Rome. doi:10.1017/S0014479706394902

Yang, S., Cammeraat, E., Jansen, B., den Hann, M., van Loon, E., Recharte, J., 2018. Soil organic carbon stocks controlled by lithology and soil depth in a Peruvian alpine

grassland of the Andes. Catena 171, 11–21. doi:10.1016/j.catena.2018.06.038

Yang, S., Jansen, B., Absalah, S., van Hall, R., Kalbitz, K., Cammeraat, E., 2019a. Lithology and climate controlled soil aggregate size distribution and organic carbon stability in the Peruvian Andes. SOIL in Press.

Yang, S., Jansen, B., Kalbitz, K., Chunga Castro, F.O., van Hall, R.L., Cammeraat, E.L.H., 2019b. Lithology controlled soil organic carbon stabilization in an alpine grassland of the Peruvian Andes. Environmental Earth Science in Press.

Yang, Y., Fang, J., Tang, Y., Ji, C., Zheng, C., He, J., Zhu, B., 2008. Storage, patterns and controls of soil organic carbon in the Tibetan grasslands. Global Change Biology 14, 1592–1599. doi:10.1111/j.1365-2486.2008.01591.x

Yoo, K., Amundson, R., Heimsath, A.M., Dietrich, W.E., 2006. Spatial patterns of soil organic carbon on hillslopes: Integrating geomorphic processes and the biological C cycle. Geoderma 130, 47–65. doi:10.1016/j.geoderma.2005.01.008

Zhu, P., Chen, R., Song, Y., Liu, G., Chen, T., Zhang, W., 2015. Effects of land cover conversion on soil properties and soil microbial activity in an alpine meadow on the Tibetan Plateau. Environmental Earth Sciences 74, 4523–4533. doi:10.1007/s12665-015-4509-1

Zimmermann, M., Meir, P., Silman, M.R., Fedders, A., Gibbon, A., Malhi, Y., Urrego, D.H., Bush, M.B., Feeley, K.J., Garcia, K.C., Dargie, G.C., Farfan, W.R., Goetz, B.P., Johnson, W.T., Kline, K.M., Modi, A.T., Rurau, N.M.Q., Staudt, B.T., Zamora, F., 2009. No Differences in Soil Carbon Stocks Across the Tree Line in the Peruvian Andes. Ecosystems 13, 62–74. doi:10.1007/s10021-009-9300-2

List of Abbreviations

AS:	acid igneous rock soil	BD:	bulk density
C:	carbon	CEC:	cation exchange capacity
DA:	dioic acid	FA:	fatty acid
LM:	large macroaggregate (>2 mm)	LS:	limestone soil
Mi:	microaggregate (<0.25 mm)	MWD:	mean weight diameter
N:	nitrogen	OC:	organic carbon
OM:	organic matter	PC:	principal component
PCA:	principal component analysis	RA:	relative abundance
RAC:	change in relative abundance	S+C:	silt plus clay
SE:	standard error	SOC:	soil organic carbon
SOM:	soil organic matter	ω-HA:	ω-hydroxyl alkanoic acid

GC/MS: gas chromatography / mass spectrometry

SFE: soil formation and environmental factor

SM: small macroaggregate (0.25-2 mm)

TMAH: tetramethylammonium hydroxide

Publications and Author Contributions

(1) Yang, S., Cammeraat, E., Jansen, B., den Hann, M., van Loon, E., Recharte, J., 2018. Soil organic carbon stocks controlled by lithology and soil depth in a Peruvian alpine grassland of the Andes. Catena 171, 11–21. doi:10.1016/j.catena.2018.06.038

EC, MdH designed the study. MdH, EC and SY contributed to the sample collection and the laboratory experiments. EvL and SY contributed to the data analysis. SY wrote the manuscript and all authors contributed to manuscript revision. EC and BJ supervised the project.

(2) Yang, S., Jansen, B., Kalbitz, K., Chunga Castro, F.O., van Hall, R.L., Cammeraat, E.L.H., 2019. Lithology controlled soil organic carbon stabilization in an alpine grassland of the Peruvian Andes. Environmental Earth Sciences, in press. (ID: ENGE-D-19-01293)

SY, EC, BJ and KK designed the study. EC, FOCC and SY contributed to the sample collection. SY and RvH performed the laboratory experiments. SY wrote the manuscript and all authors contributed to manuscript revision. EC, BJ and KK supervised the project.

(3) Yang, S., Jansen, B., Absalah, S., van Hall, R.L., Kalbitz, K., Cammeraat, E.L.H., 2019. Lithology and climate controlled soil aggregate size distribution and organic carbon stability in the Peruvian Andes. SOIL, in press (ID: soil-2019-40)

SY, EC, BJ and KK designed the study. EC, BJ and SY contributed to the sample collection. SY, SA and RvH performed the laboratory experiments. SY wrote the manuscript and all authors contributed to manuscript revision. EC, BJ and KK supervised the project.

(4) Yang, S., Jansen, B., Absalah, S., Kalbitz, K., Cammeraat, E.L.H., 2019. Selective stabilization of soil fatty acids related to their carbon chain length and presence of double bonds in the Peruvian Andes. Submitted to Geoderma.

SY, EC, BJ and KK designed the study. EC, BJ and SY contributed to the sample collection. SY and SA performed the laboratory experiments. SY, SA and BJ contributed to the data validation. SY wrote the manuscript and all authors contributed to manuscript revision. EC, BJ and KK supervised the project.

Acknowledgements

I am a person who is interested in challenges, who enjoy crazy experiences such as cycling to Tibet, finishing the "Tour du Mont Blanc" trail using a mountain bike and doing a massive fall during an overhanging climbing. For these challenges, I need not only good skills and strong muscles but also enough support from other people. I need support from my friends and the team for the crazy experience of cycling and need a trusted belayer to overcome the fear of falling. I totally believe it is the same for my PhD. Today, I still have a vivid memory of the bit crazy moment when I decided to start my PhD in the Netherlands. Doing a PhD outside China is one of the most challenging decisions in my life. Now, at the end of my PhD, I am convinced that I could not finish my PhD without the kind support from my supervisors, colleagues, friends and family. Thus, I would give my sincere gratitude to all the people who gave me help.

First of all, I would like to express my sincere gratitude to my promotors Erik Cammeraat and Boris Jansen, and my co-promotors Karsten Kalbitz and Franciska de Vries. Without your guidance, I cannot imagine how I could conduct my PhD research. In the beginning, Karsten gave me a great opportunity to start my PhD in Amsterdam. During the 5-year PhD study, it was quite often that Erik and Boris had discussions with me on my research proposal, experimental design and paper writing. In addition, it is very kind of you to extend my stay in the Netherlands several times to guarantee the completion of the PhD study. Furthermore, I would like to thank Karsten for your important suggestions on experiment design and paper writing, as well as Franciska for your input on my thesis. It is also important to show my gratitude to China Scholarship Council and Institute for Biodiversity and Ecosystem Dynamics as they funded my doctoral research.

I would also thank my technical colleagues from the physical-chemical laboratory for your guidance and support for my sample analysis. I could not finish this thesis without your help. For this, I am very grateful to the support from Samira Absalah, Rutger van Hall, Jorien Schoorl, Eva de Rijke, Chiara Cerli, Joke Westerveld, Leo Hoitinga, John Visser, Peter Serné, Rick Helmus and Leen de Lange. Furthermore, I would also especially thank Amedée Wever and Lisa

Boerdam for your contributions to the lab work and the data analysis.

I would never forget my colleagues in the ELD and the previous ESS group. I would give many thanks to Albert Tietema, John Parsons, Elly Morriën, William Gosling, Emiel van Loon, Carina Hoorn, Annemieke Kooijman, Crystal McMichael, Roland Bol, Sebastian de Vet, Julian Campo, Estela Nadal-Romero, Jiajia Gao, Huasheng Huang, Olaf Brock, Thamara Jonkman, Liz Veerman, Thomas Wagner, Baptiste Poursat, Joost Dalmijn, Andrea Carboni, Vittorio Albergamo, Jort Hammer, Xia Meng, Milan Teunissen van Manen, Shixiu Zhang, Mengru Jia, Sofie te Wierik, Xiang Wang and Caixia Wei. Also, the support from IBED secretaries and human resources is also kindly acknowledged for: Tanya Noorlander, Mary Parra Tasayco, Maria Dolorita, Saskia Heijboer and Truc Ngo-Ha. Finally, I would also say thank you to those people who helped me but I forget to mention here.

Furthermore, I would also not forget my friends from the Chinese community of the Netherlands. We cooked delicious food, visited each other's house, went hiking in the black forest, cycled to Germany and Belgium, mountain-biked in so exciting trails and traveled to different countries. For the nice experience, Chao Ding, Xinyi Li, Xiaolong Liu, Juan Xiao, Yiwei Sun, Yuan Gao, Si Wen, Muhe Diao, Zepeng Sun, Xiaoning Zhang, Xing Ji, Ke Gao, Zijian Zhou, Yang Hu, Zhongcheng Pan, Huan Zhou, Guowei Lü, Yifan Chen, Longjian Piao, Chong Wang, Zeya Wei, Jie Fu, Yumei Wang, Yao Li, Wenyang Wu, Shuo Chen, Jiming Li, Ziming Li, Xiaoya Deng, Shaojie Jiang and Mingxiong Huang are gratefully acknowledged. I apologize if I forget to mention your name.

Finally, I would like to give special thanks to my family for their unconditional support and appreciation.

UNIVERSITY OF AMSTERDAM



